

Assessment of the environmental risk
and risk-benefit analysis of the nano-iron based
groundwater remedial agent Carbo-Iron

by

Mirco Weil

from Gießen, Germany

Accepted dissertation thesis for the partial fulfilment of the requirements
for a doctor of natural sciences

- Cumulative thesis -

Fachbereich 7: Natur- und Umweltwissenschaften

Universität Koblenz-Landau

Thesis examiners:

Prof. Dr. Ralf Schulz, University of Koblenz-Landau, Germany

Jun.-Prof. Dr. Mirco Bundschuh, University of Koblenz-Landau, Germany

Date of oral examination: 23. Aug. 2019

Declaration

I hereby declare that I autonomously conducted the work presented in this PhD thesis entitled “Assessment of the environmental risk and risk-benefit analysis of the nano-iron-based groundwater remedial agent Carbo-Iron”. All used assistances and involved contributors are clearly declared. This thesis has never been submitted elsewhere for exam, as a thesis for evaluation in similar context to any department of this university or any scientific institute. I am aware that a violation of the aforementioned conditions can have legal consequences.

Landau in der Pfalz

Place, date

Signature

The following parts of this thesis are published in international peer-reviewed journals and attached to this thesis in the appendices A, B, C and D:

- [A]:** Potthoff, A., Weil, M., Meißner, T., Kühnel, D. (2015). Towards sensible toxicity testing for nanomaterials: proposal for the specification of test design. *Science and Technology of Advanced Materials* 16, 065006. DOI: 10.1088/1468-6996/16/6/065006
- [B]:** Weil, M., Meißner, T., Busch, W., Springer, A., Kühnel, D., Schulz, R., Duis, K. (2015). The oxidized state of the nanocomposite Carbo-Iron® causes no adverse effects on growth, survival and differential gene expression in zebrafish. *Science of The Total Environment* 530–531, 198–208. DOI: 10.1016/j.scitotenv.2015.05.087.
- [C]:** Weil, M., Meißner, T., Springer, A., Bundschuh, M., Hübler, L., Schulz, R., Duis, K. (2016). Oxidized Carbo-Iron causes reduced reproduction and lower tolerance of juveniles in the amphipod *Hyalella azteca*. *Aquatic Toxicology* 181, 94–103. DOI: 10.1016/j.aquatox.2016.10.028.
- [D]:** Weil, M., Mackenzie, K., Foit, K., Kühnel, D., Bundschuh, M., Schulz, R., Duis, K. (2019). Environmental risk or benefit? Comprehensive risk assessment of groundwater treated with nano Fe0-based Carbo-Iron®. *Science of the Total Environment* 677, 156-166. DOI: 10.1016/j.scitotenv.2019.04.360

Acknowledgement

I would like to thank Prof. Dr. Ralf Schulz and Jun.-Prof. Dr. Mirco Bundschuh for their support and professional input in the last years. The way they integrated someone with such limited presence time as myself in the working group “Ecotoxicology and Environment” exceeded my expectations by far. I always felt welcome and taken seriously, thank you.

This work would not have been possible without Dr. Karen Duis, who helped me in nearly every aspect mentioned on this page and which I forgot to mention. Thank you for patiently trying to mentor me to become a really good scientist. Maybe someday...

Special thanks go to Dr. Anja Coors, Dr. Jörg Römbke and Dr. Thomas Knacker for their support.

The German Ministry for Education and Research (BMBF) is acknowledged for funding the project Fe-NANOSIT (FKZ 03X0082 F), within the experimental work of this thesis was performed. Thanks go to the project partners in Fe-NANOSIT, especially Dr. Katrin Mackenzie and Dr. Tobias Meißner for valuable discussions and patient answers to lots of questions.

I would like to acknowledge friends and colleagues at ECT, Daniel Gilberg, Dr. Philipp Egeler and all the others.

Further, thanks go to Dr. Ricki Rosenfeldt, Dr. Jochen Zubrod, Dr. Frank Seitz and Dr. Dominic Englert for welcoming me in the working group “Ecotoxicology and Environment” without much fuzz or any restraint.

Finally, I would like to thank Jasmin for constant support and Emil and Thore for constant distraction.

Content

List of abbreviations.....	1
1 Abstract.....	3
2 Zusammenfassung.....	4
3 Introduction.....	5
3.1 Groundwater.....	5
3.2 Remediation of groundwater.....	7
3.3 Potential environmental risk of nanomaterials.....	8
3.4 Environmental risk assessment.....	9
3.5 Motivation and research questions.....	10
3.6 Thesis layout.....	11
4 Results.....	14
4.1 Strategy for ecotoxicity testing of Carbo-Iron.....	14
4.2 Uptake and ecotoxicity of Carbo-Iron.....	18
4.2.1 Uptake.....	18
4.2.2 Survival.....	19
4.2.3 Sublethal endpoints.....	20
4.3 Environmental risk of Carbo-Iron.....	22
4.3.1 Exposure assessment for Carbo-Iron.....	22
4.3.2 Derivation of a PNEC & environmental risk assessment for Carbo-Iron.....	24
4.4 Comprehensive risk assessment for the remediated site.....	24
5 Discussion.....	27
5.1 Strategy for ecotoxicity testing.....	27
5.2 Ecotoxicity of Carbo-Iron.....	28
5.3 Environmental risk of Carbo-Iron.....	30
5.4 Comprehensive risk assessment for the remediated site.....	32
6 Conclusion and outlook.....	37
7 References.....	40

Appendices	51
[A.1]: Towards sensible toxicity testing for nanomaterials: Proposal for the specification of test design.....	53
[B.1]: The oxidized state of the nanocomposite Carbo-Iron® causes no adverse effects on growth, survival and differential gene expression in zebrafish.....	77
[B.2]: Supplemental information to: The oxidized state of the nanocomposite Carbo-Iron® causes no adverse effects on growth, survival and differential gene expression in zebrafish	109
[C.1]: Oxidized Carbo-Iron causes reduced reproduction and lower tolerance of juveniles in the amphipod <i>Hyalella azteca</i>	117
[C.2]: Supplemental information to: Oxidized Carbo-Iron causes reduced reproduction and lower tolerance of juveniles in the amphipod <i>Hyalella azteca</i>	141
[D.1]: Environmental risk or benefit? Comprehensive risk assessment of groundwater treated with nano Fe ⁰ -based Carbo-Iron®.....	161
[D.2]: Supplemental information to: Environmental risk or benefit? Comprehensive risk assessment of groundwater treated with nano Fe ⁰ -based Carbo-Iron®	189
[E.1]: Curriculum vitae	235

List of abbreviations

cRI:	Chemical risk index
CMC:	Carboxymethyl cellulose
DLS:	Dynamic light scattering
EC _x :	Concentration leading to an effect in x% of organisms (e.g. EC ₅₀)
EDX :	Energy dispersive X-ray microanalysis
EEA:	European Environment Agency
ERA:	Environmental risk assessment
eRI:	Ecotoxicological risk index
Fe ⁰ :	Zero-valent iron
LC _x :	Concentration leading to mortality of x% of organisms (e.g. LC ₅₀)
LOEC:	Lowest observed effect concentration
nFe ⁰ :	Nanoscaled zerovalent iron
NOEC:	No observed effect concentration, i.e. investigated test concentration below the LOEC
OECD:	Organisation for Economic Co-operation and Development
PBS:	Phosphate buffered saline
PCE:	Tetrachloroethene
PEC:	Predicted environmental concentration
PNEC:	Predicted no effect concentration
ROS:	Reactive oxygen species
pRI:	Physico-chemical risk index

sd: Standard deviation of the group of data values used to calculate e.g. a mean

SEM: Scanning electron microscopy

TCE: Trichloroethylene

TEM: Transmission electron microscopy

1 Abstract

Groundwater is essential for the provision of drinking water in many areas around the world. The ecosystem services provided by groundwater-related organisms are crucial for the quality of groundwater-bearing aquifers. Therefore, if remediation of contaminated groundwater is necessary, the remediation method has to be carefully selected to avoid risk-risk trade-offs that might impact these valuable ecosystems. In the present thesis, the ecotoxicity of the *in situ* remediation agent Carbo-Iron (a composite of zero valent nano-iron and active carbon) was investigated, an estimation of its environmental risk was performed, and the risk and benefit of a groundwater remediation with Carbo-Iron were comprehensively analysed.

At the beginning of the work on the present thesis, a sound assessment of the environmental risks of nanomaterials was impeded by a lack of guidance documents, resulting in many uncertainties on selection of suitable test methods and a low comparability of test results from different studies with similar nanomaterials. The reasons for the low comparability were based on methodological aspects of the testing procedures before and during the toxicity testing. Therefore, decision trees were developed as a tool to systematically decide on ecotoxicity test procedures for nanomaterials. Potential effects of Carbo-Iron on embryonic, juvenile and adult life stages of zebrafish (*Danio rerio*) and the amphipod *Hyaletta azteca* were investigated in acute and chronic tests. These tests were based on existing OECD and EPA test guidelines (OECD, 1992a, 2013a, 2013b; US EPA, 2000) to facilitate the use of the obtained effect data in the risk assessment. Additionally, the uptake of particles into the test organisms was investigated using microscopic methods. In zebrafish embryos, effects of Carbo-Iron on gene expression were investigated. The obtained ecotoxicity data were complemented by studies with the waterflea *Daphnia magna*, the algae *Scenedesmus vacuolatus*, larvae of the insect species *Chironomus riparius* and nitrifying soil microorganisms.

In the fish embryo test, no passage of Carbo-Iron particles into the perivitelline space or the embryo was observed. In *D. rerio* and *H. azteca*, Carbo-Iron was detected in the gut at the end of exposure, but no passage into the surrounding tissue was detected. Carbo-Iron had no significant effect on soil microorganisms and on survival and growth of fish. However, it had significant effects on the growth, feeding rate and reproduction of *H. azteca* and on survival and reproduction in *D. magna*. Additionally, the development rate of *C. riparius* and the cell volume of *S. vacuolatus* were negatively influenced.

A predicted no effect concentration of 0.1 mg/L was derived from the ecotoxicity studies based on the no-effect level determined in the reproduction test with *D. magna* and an assessment factor of 10. It was compared to measured and modelled environmental concentrations for Carbo-Iron after application to an aquifer contaminated with chlorohydrocarbons in a field study. Based on these concentrations, risk quotients were derived. Additionally, the overall environmental risk before and after Carbo-Iron application was assessed to verify whether the chances for a risk-risk trade-off by the remediation of the contaminated site could be minimized. With the data used in the present study, a reduced environmental risk was identified after the application of Carbo-Iron. Thus, the benefit of remediation with Carbo-Iron outweighs potential negative effects on the environment.

2 Zusammenfassung

In einem Großteil der Welt wird Grundwasser für die Versorgung von Siedlungen und Agrarflächen genutzt. Organismen, die im Grundwasser leben, erfüllen wichtige Funktionen im Ökosystem und haben positiven Einfluss auf die Grundwasserqualität. Um das Risiko negativer Effekte auf diese wertvollen Ökosysteme zu minimieren muss die entsprechende Sanierungsmethode, im Falle einer Grundwasserbehandlung, mit Vorsicht gewählt werden. In der vorliegenden Thesis wurde das Umweltrisiko von Carbo-Iron untersucht, ein Komposit aus nanoskaligem null-valentem Eisen und Aktivkohle zur *in situ*-Behandlung von Grundwasser. Des Weiteren wurde eine umfassende Beurteilung des Umweltrisikos und des Nutzens einer Grundwasserbehandlung mit Carbo-Iron durchgeführt.

Zu Beginn der Arbeit an der vorliegenden Thesis existierten noch keine Empfehlungen für Untersuchung der Ökotoxizität von Nanomaterialien. Daher bestanden viele Unsicherheiten hinsichtlich geeigneter Methoden. Im Rahmen dieser Thesis wurde eine Entscheidungshilfe entwickelt, um bei der ökotoxikologischen Untersuchung von Nanomaterialien systematisch geeignete methodische Schritte auszuwählen.

Mögliche Effekte von Carbo-Iron wurden in Tests mit embryonalen, juvenilen und adulten Lebensstadien des Zebrafischlings (*Danio rerio*) und juvenilen und adulten Amphipoden (*Hyalella azteca*) untersucht. Die gewählten Testsysteme basierten auf existierenden Testmethoden der OECD und EPA zur ökotoxikologischen Untersuchung von Chemikalien (OECD, 1992a, 2013a, 2013b; US EPA, 2000). Zusätzlich wurde die Aufnahme der Partikel in die genannten Testorganismen untersucht. In Zebrafischembryonen wurden außerdem potentielle Effekte auf die Genexpression mittels Microarrays ermittelt. Die erhaltenen Daten wurden später mit Ergebnissen aus Tests mit dem Wasserfloh *Daphnia magna*, der Alge *Scenedesmus vacuolatus*, Larven der Mücke *Chironomus riparius* und nitrifizierenden Bodenmikroorganismen ergänzt.

In dem Fischembryotoxizitätstest wurde keine Passage der Carbo-Iron-Partikel durch das Chorion in den perivitellinen Raum oder den Embryo beobachtet. Nach der Exposition wurde Carbo-Iron im Darm von *H. azteca* und *D. rerio*, aber keinem anderen Gewebe oder Organen detektiert. Carbo-Iron hatte keine signifikanten Effekte auf die Nitrifikationsrate der Bodenmikroorganismen sowie Überleben und Wachstum des Zebrafischlings. Dennoch wurden signifikant negative Effekte auf Wachstum, Fütterungsrate und Reproduktion von *H. azteca* und auf das Überleben und die Reproduktion von *D. magna* festgestellt. Des Weiteren war die Entwicklungsrate von *C. riparius* und das Zellvolumen von *S. vacuolatus* negativ beeinflusst.

Anhand der durchgeführten Studien wurde basierend auf dem Ergebnis des Reproduktionstests mit *D. magna* und einem *assessment factor* von 10 für Carbo-Iron eine *predicted no effect concentration* von 0,1 mg/L ermittelt. Diese wurde mit modellierten und gemessenen Umweltkonzentrationen von Carbo-Iron verglichen die in einer Studie erhoben wurden, in denen Carbo-Iron zur Behandlung eines mit Chlorkohlenwasserstoffen kontaminierten Aquifers eingesetzt wurde, und Risiko-Quotienten wurden abgeleitet. Zur gesamtheitlichen Betrachtung wurde anschließend ein Schema zur Bewertung des Umweltrisikos vor und nach der Behandlung des Aquifers mit Carbo-Iron entwickelt. Die erhobenen Daten weisen auf ein reduziertes Umweltrisiko nach der Applikation von Carbo-Iron hin. Dementsprechend überwiegen die Vorteile einer Grundwasserbehandlung mit Carbo-Iron die potentiellen negativen Effekte auf die Umwelt.

3 Introduction

3.1 Groundwater

Groundwater constitutes more than 97% of the world's unfrozen fresh water and provides the major source for drinking water in most developed and many developing nations (Gibert et al., 1994). It sustains many aquatic and terrestrial ecosystems, among them springs and wetlands as well as surface waters with their hyporheic and riparian zones (Kløve et al., 2011). The groundwater-bearing aquifers are heterogeneous ecosystems. Considerable differences exist between groundwater with low flow-rates in alluvial sediments and groundwater flowing with a much higher speed through karstic systems (Danielopol et al., 2004). Owing to the heterogeneous habitats and, often, due to the absence of interconnections between different groundwater bodies, a huge diversity of highly specialized microorganisms and invertebrates lives in groundwater communities (Galassi, 2001; Hahn and Fuchs, 2009). These ecosystems provide important services for human welfare, among them the purification of water by microbiological biodegradation of chemical substances and the elimination of pathogens (Griebler and Avramov, 2015). Furthermore, groundwater microorganisms metabolize dissolved organic matter, thereby improving the water quality and keeping aquifer pore spaces open (Danielopol, 1989; Hahn, 2009).

Any contamination of groundwater can, obviously, have negative impacts on groundwater ecology and render the water unusable as drinking water. In Table 3.1, the groundwater pollutants most frequently causing significant risk the EU are shown (data available at European Environment Agency database (EEA, 2018)). While the list of the most abundant pollutants is dominated by compounds that are used in agriculture, contamination of groundwater by chemicals, e.g. from tank leakages and accidental spills (Bartzas et al., 2015; Baun et al., 1999; Compennolle et al., 2014; Kargar et al., 2012; Musolff et al., 2010; Rail, 1989; Stuart et al., 2012) is frequent. Among those, a total of 132 groundwater bodies in the EU are contaminated with the chlorinated alkenes tetrachloroethene (PCE) and/or trichloroethene (TCE). Pollution of groundwater by chlorinated alkenes originates from dry cleaning facilities, refrigeration, lubricants and vapour degreasing (Pant and Pant, 2010; Russell et al., 1992). They are also among the most commonly identified organic chemicals in groundwater outside the EU (Moran et al., 2007), and their removal from groundwater is required due to their toxicity and cancerogenic effects. PCE and TCE are procarcinogens (secondary carcinogens) that are activated in the human liver (Azimi et al., 2017; Henschler and Bonse, 1977; Wang et al., 2002; Weiss, 1995). Degradation of PCE and TCE, either intended or by microbial communities in the groundwater, may result in the production of vinyl chloride which is a known primary carcinogen (Bartsch and Montesano, 1975; Bolognesi et al., 2017).

Table 3.1: Groundwater pollutants in member states of the EU causing significant impairment of human uses and environmental risk (first twenty, ranked by number of contaminated water bodies, and trichloroethylene). Numbers of water bodies (total contaminated and uncontaminated=13,411) affected by pollutants and the respective area (total contaminated and uncontaminated=4.3 million km²) and further data were reported by the member states (total=25) to the EEA by spring 2018. Data were obtained from the database (EEA, 2018), for a brief description see the respective report (Kristensen et al., 2018).

Pollutant	Contaminated water bodies (n)	Contaminated area (km ²)	Affected EU member states (n)
Nitrate	803	613,252	23
Pesticides (Active substances including metabolites)	295	250,861	9
Chloride	231	77,123	13
Ammonium	128	101,089	11
Sulphate	120	76,981	13
Electrical conductivity ¹	106	55,115	10
Arsenic and its compounds	103	58,102	11
Trichloroethene + tetrachloroethene	62	38,877	4
Tetrachloroethene	59	14,105	9
Trichloromethane	73	42,570	2
Nickel and its compounds	60	60,493	9
Lead and its compounds	48	23,611	8
Benzo(a)pyrene	36	25,740	6
Iron and its compounds	30	22,922	5
Dibromochloromethane	28	22,019	1
Cadmium and its compounds	26	13,422	4
Bromodichloromethane	26	22,843	1
Phosphate	24	32,974	4
Zinc and its compounds	24	12,747	4
Chromium	22	5,245	1
Trichloroethene	11	486	6

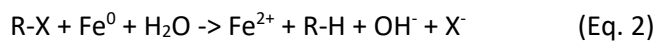
¹: Electrical conductivity is probably attributed to saline intrusions, as only member states with coastal areas reported this parameter (Kristensen et al., 2018).

Besides the contamination with pollutants, the global overexploitation of groundwater, i.e. existing resources cannot sustain under the current use, represents an additional threat to aquifers (Gleeson et al., 2012). This extensive use highlights the dependence of modern civilization on groundwater resources and further indicates the need for groundwater remediation. In the past decades, research for the development of suitable treatment methods therefore intensified (Cundy et al., 2008).

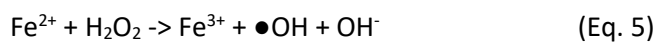
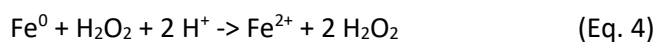
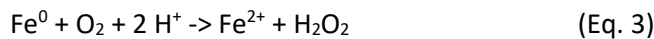
3.2 Remediation of groundwater

A common remediation technique was pump & treat, an *ex situ* treatment of the groundwater. However, due to its limited effectiveness and high costs (Karn et al., 2009), it was increasingly replaced by the technique of permeable reactive barriers. This *in situ* treatment involves the set-up of reactive media barriers perpendicular to the flow of the contaminated groundwater. As the contamination plume migrates through the barrier under the influence of the natural hydraulic gradient, the contaminants in the plume react with the reactive media leading either to their transformation or to their fixation (Obiri-Nyarko et al., 2014).

In the past decades, zero-valent iron (Fe^0) was increasingly used in studies with reactive barriers to treat contaminations with halogenated chlorohydrocarbons, metals and other organic pollutants (Li et al., 2006). Fe^0 has a redox potential of -440 mV and can thus be an effective reductant (Eq.1). It reduces contaminants such as halogenated compounds (R-X) in aqueous media (Eq. 2).



Additionally, in the presence of oxygen in water, Fe^0 can transfer two electrons to oxygen and hydrogen peroxide is produced (Eq. 3). Hydrogen peroxide is reduced to water (Eq. 4) and a hydroxyl radical ($\bullet\text{OH}$) is produced in the Fenton reaction (Eq. 5). This radical has a strong capacity to oxidize various organic compounds (Fu et al., 2014).



In the past decade, studies mainly focused on development of remediation technologies using nanoscaled zero-valent iron (nFe^0) with particle sizes < 100 nm (Corsi et al., 2018; Fu et al., 2014; Gonçalves, 2016). Compared to bulk Fe^0 , the higher ratio of surface to volume in nanoparticles improves the reaction rates by a factor > 25 (Li et al., 2006). However, subsurface mobility of nFe^0 is limited due to its tendency to agglomerate in aqueous media and its clearly higher density (6.7 g/cm^3) than water (Keller et al., 2010; Kocur et al., 2014; Phenrat et al., 2009). To reduce the negative properties of nFe^0 for its use in permeable reactive barriers, various carriers have been employed, e.g. silica (Zheng et al., 2008), polymer resin (Ponder et al., 2000) or active carbon. The active carbon composites are very promising for remediation methods, since the carbon has a high sorption ability for organic pollutants and additionally increases the mobility and thus the efficiency for pollutant removal compared to pure nFe^0 (Busch et al., 2015, 2014; Mackenzie et al., 2012).

Currently, five composites of $n\text{Fe}^0$ and active carbon are commercially available for *in situ* remediation of groundwater (Fan et al., 2017).

3.3 Potential environmental risk of nanomaterials

With the increasing production and use of nano-sized materials in the past decades, concerns on their potential environmental impacts rose (Arnaud, 2010; Boverhof and David, 2010; Davis, 2007; Fairbrother and Fairbrother, 2009; Handy et al., 2008; Hansen et al., 2008a). Existing data from environmental risk assessments are generally available for the bulk materials, but in the nanosized state the surface area of a material is proportionally larger and its reactivity is increased. Concerning their environmental fate, uptake into organisms and ecotoxicity, nanomaterials may thus differ from the respective bulk material (Griffitt et al., 2008; Höss et al., 2015; Hua et al., 2014; Karlsson et al., 2009; Kennedy et al., 2008; Seitz et al., 2014).

The potential ecotoxicity of nanomaterials is influenced by their fate in environmental matrices (Figure 3.1A) and their availability for organisms. In liquid media, it is possible that composites of nano iron and active carbon, which are not within the nanoparticle definition as they have a particle size above 100 nm, release nanoscaled iron particles. Furthermore, the release of iron ions into the liquid is possible. If electrostatic repulsion between the particles is not sufficiently high, they will agglomerate. With increasing size of the agglomerates, sedimentation will occur. The nanomaterial will then no longer be available for pelagic organisms, but sediment-dwelling organisms will be exposed to the agglomerated particles. In environmental matrices, the Fe^0 rapidly reacts with organic molecules and hydrolyses in water. This ageing process is unavoidable and starts immediately after application of the material into the aquifer. Therefore, the environmentally most relevant oxidation states of Fe^0 are Fe^{2+} and Fe^{3+} (e.g. in FeOOH , Fe_3O_4 and Fe_2O_3).

Several mechanisms of toxicity are likely for nanomaterials (Figure 3.1B), based on their size, shape and surface characteristics. While not necessarily applicable to all nanostructured compounds, two mechanisms are considered most relevant (Auffan et al., 2009; Thwala et al., 2016): a) redox modification of the particle surface that can induce oxidative stress in organisms (Auffan et al., 2008; Cullen et al., 2011), and b) dissolution of metallic nanomaterials and the release of ions at neutral (Hoheisel et al., 2012; Hua et al., 2014) or acidic pH (Heinlaan et al., 2011), e.g. in the gut of organisms. The release of ions can then lead to oxidative stress. In case of iron, Fe^0 or Fe^{2+} can generate reactive oxygen species (ROS) via the Fenton reaction described in Eq. 5 (Sevcikova et al., 2011) and possible effects of Fe^0 and Fe^{2+} on the sub-cellular level include DNA damage, lipid peroxidation and oxidation of proteins (Valko et al., 2005). Due to their size, the translocation of nanomaterials through biological membranes cannot be excluded and was observed previously (Mattsson et al., 2016). Additionally, nanoparticles adhering to biological surfaces were shown to

have physical/mechanical impacts, influencing e.g. swimming behaviour (Noss et al., 2013) and moulting of *Daphnia* (Dabrunz et al., 2011). Further, nanoparticles can penetrate cell membranes (Lin et al., 2010; Wild and Jones, 2009), disrupting diffusion processes through the membrane. Depending on the composition of the nanomaterial, a catalytic activity is possible e.g. the photocatalytic activity of nano-TiO₂ (Bundschuh et al., 2011a; Clemente et al., 2014; Hund-Rinke and Simon, 2006), but unlikely for iron-based particles.

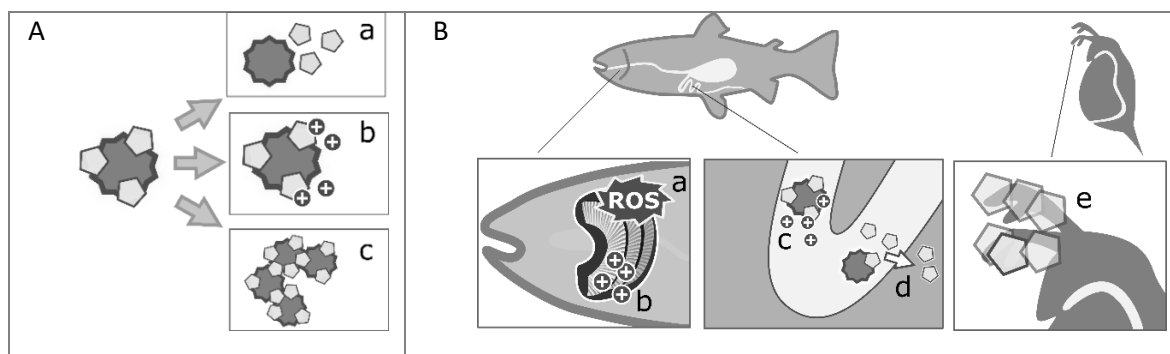


Figure 3.1: **(A):** Potential fate processes of nano-composites most relevant for toxicity assessment in liquid matrices. Nanoparticles break out of the supporting structure (a), ions leach from the metal nanoparticles (b), and/or composites aggregate to larger particles (c). **(B):** Most relevant uptake processes and potential mechanisms of action of nano-composites in organisms. Metal-based nanoparticles can promote oxidative stress by formation of reactive oxygen species that damage sensible structures, e.g. the gills in fish (a). Metal ions leaching from nanoparticles due to dissolution in neutral (b) or acidic pH (c) exhibit toxicity due to their composition and oxidation state. Particles could cross biological membranes (d), translocate to other organs and elicit one or several of the toxic mechanisms mentioned above. Additionally, a physical / mechanical effect can occur after adhesion of particles to biological surfaces, e.g. the antenna of *Daphnia magna* (e), and result in disfunction of the respective structure.

3.4 Environmental risk assessment

Because of the unknown fate and effects of nFe⁰/active carbon-composites in the environment and, especially, in organisms, an environmental risk assessment (ERA) is required. In an ERA, estimated or measured environmental concentrations are compared with predicted no effect concentrations (PNEC; ECHA, 2016). For the determination of these PNEC, effect concentrations are determined with organisms of different trophic levels in ecotoxicity tests. Standard test guidelines are available from the Organisation for Economic Cooperation and Development (OECD). Hazard data generated using such guidelines falls under OECD's system of mutual acceptance of data, which facilitates the international acceptance of information for the regulatory safety assessment of chemicals. However, these guidelines were developed for the testing of chemicals and their suitability for testing the ecotoxicity of nanomaterials was under debate when the work on the present thesis started (Grieger et al., 2009; Kühnel and Nickel, 2014; OECD, 2009; Petersen et al., 2015).

3.5 Motivation and research questions

Contamination of groundwater with chlorinated alkenes is a frequent problem in European groundwater bodies (see section 3.1) and can represent a considerable risk for human health and the environment. Therefore, the remediation of groundwater contaminated with PCE and TCE will be required frequently. Currently, risk-based management of contaminated groundwater sites consists of two stages: risk assessment and decision analysis. If the assessed risk of the contaminated groundwater is not acceptable, potential remedial actions are identified and a decision analysis is performed to choose the best treatment. The best option is selected on the basis of a risk-of-failure – cost - benefit analysis (Khadam and Kaluarachchi, 2003). Existing decision supporting tools for the identification of appropriate remediation methods are focused on human health and do not consider potential impacts of the remedial technique on the groundwater ecosystem (An et al., 2017, 2016; Compennolle et al., 2014; Khadam and Kaluarachchi, 2003; Ren et al., 2017; Yang et al., 2012). This might be caused by the assumption that a severe contamination of the groundwater impedes any living fauna. However, the EU Groundwater Directive (EC, 2006) focuses on the protection and the improvement of the chemical, qualitative (physico-chemical) and quantitative (abundance, abstraction and recharge of groundwater) state of groundwater. The significance of groundwater ecosystems and their protection has been added to the Groundwater Directive (Hahn, 2009).

When using permeable reactive barriers for groundwater treatment, the remediation agent will likely remain in the aquifer for a long time or not be removed at all after the contamination is successfully removed and may have negative impacts on the local or regional scale (Lemming et al., 2010a). While nFe⁰/active carbon-composites are promising remediation agents, there is an urgent need to characterize their risk before introducing them into the environment to avoid a “risk-risk-trade-off”, the substitution of one risk with another (Hansen et al., 2008b). Grieger et al. (2010) highlighted the need for an ERA of nFe⁰, since extensive uncertainties exist regarding their potential environmental risks, particularly in the long-term time scale.

At the beginning of the work on the present thesis, no studies on the environmental risk of nFe⁰ or any nFe⁰-composites were available in the scientific literature. Since then, recommendations for such an assessment were made (Corsi et al., 2018; Hjorth et al., 2017; Patil et al., 2016). However, to the author’s knowledge, no assessment of the environmental risk has been performed so far, although research on nFe⁰ and its use in composites has proceeded (Chen et al., 2017; Ezzatahmadi et al., 2017; Fu et al., 2014; Gonçalves, 2016). In the present thesis, the potential environmental risk of the nFe⁰-active carbon composite Carbo-Iron developed by Mackenzie et al. (2012) was investigated. The overall aim was to evaluate whether the risk or the benefit for the environment

are predominating when remediating a contaminated groundwater with Carbo-Iron. The methods used to reach this goal should be suitable for similar investigations with other nanocomposites or nanoparticles. To reach this objective, a step-wise approach was developed considering the following research questions:

- 1) How should ecotoxicity tests be designed for the determination of the toxicity of Carbo-Iron to generate reproducible data that fulfil the requirements for the risk assessment of nanomaterials?
- 2) What are the effects of Carbo-Iron on environmental organisms of different trophic levels?
- 3) Does Carbo-Iron pose a risk to the environment?
- 4) Does the treatment of a contaminated groundwater with Carbo-Iron increase or reduce the local environmental risk as assessed in a site-specific comprehensive risk assessment?

3.6 Thesis layout

The research questions defined in section 3.5 were investigated in a step-wise approach (Figure 3.2). The results obtained during the investigation of the research questions were described in four peer-reviewed manuscripts [Appendices A, B, C and D].

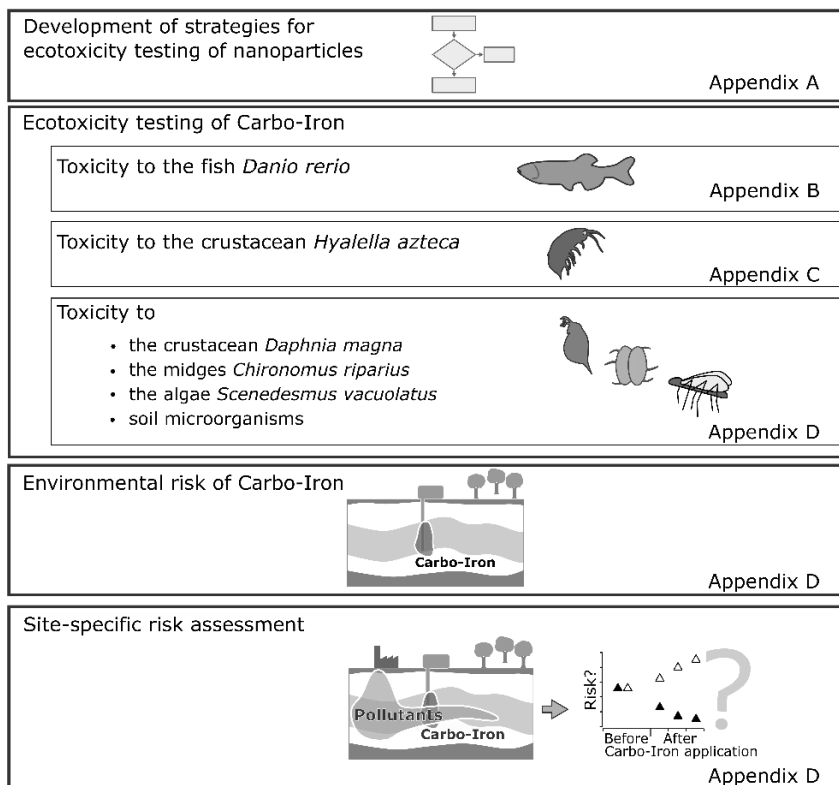


Figure 3.2: Work steps followed in the present thesis to perform a comprehensive risk assessment of the $n\text{Fe}^0$ -composite Carbo-Iron used for remediation of contaminated groundwater.

At the beginning of the experimental work, basic considerations concerning the ecotoxicity testing of nanoparticles and nanocomposites existed (Crane et al., 2008; Handy et al., 2008; Handy et al., 2012), but no clear guidance was available (Kühnel and Nickel, 2014). Thus, testing strategies for various nanoparticles were developed in the present thesis, including decision tools to provide guidance and to promote a harmonization of the ecotoxicity testing of nanoparticles and nanocomposites. Using this guidance, reproducible studies can be performed that are easy to compare with each other [A.1]. Based on this framework, a testing strategy covering appropriate methods for application of Carbo-Iron into test media, selection of test organisms and concentration-metrics, was chosen to investigate the ecotoxicity of Carbo-Iron. To fulfil the requirements for the use in an ERA (see section 3.4), all tests were performed based on available test guidelines from the OECD or US EPA.

The choice of the test systems and test organisms employed in the present thesis was based on the following aspects. For an ERA, the investigation of effects on primary producers (represented by algae), herbivores (represented by aquatic invertebrates) and predators (represented by fish) is required (ECHA, 2008). The algae *Scenedesmus vacuolatus*, the crustacean *D. magna* and the fish *D. rerio* were chosen as test species. Moreover, it seemed relevant to investigate how an accidental spillage or dislocation of the reactive barrier at the site of remediation might affect soil organisms. Considering the depth below ground level, at which a dislocation of the reactive barrier might occur, microorganisms were considered to be the most relevant functional group and a test with nitrifying soil microorganisms was performed. The microbial community in the soil used in the test is considered as a representative indicator of potential bacterial toxicity of Carbo-Iron. Additionally, the bioremediation of the pollution by microorganisms is an important aspect for polluted sites. Autotrophic bacteria, e.g. nitrifying bacteria, can degrade hydrocarbons (Deni and Penninckx, 1999; Rasche et al., 1990). Negative impacts of Carbo-Iron on microorganisms would thus be of high importance.

Under static test conditions in aqueous media, Carbo-Iron agglomerates and precipitates from the water phase during approximately 10 d. Therefore, benthic and epi-benthic organisms were considered as most relevant and thus the amphipod *Hyaella azteca* and larvae of the midge *Chironomus riparius* were chosen as additional test organisms. An additional benefit of choosing *H. azteca* as test organism is its similarity to groundwater inhabiting crustacean: the structure of the nervous system differs between malacostracans, e.g. *H. azteca*, and branchipods, e.g. the standard test organism *D. magna* (Aramant and Elofsson, 1976; Harzsch, 2006). Therefore, to be protective for groundwater-inhabiting crustaceans, tests with organisms from the class Malacostraca should be performed additionally (Schäfers et al., 2001).

In the studies with the fish *D. rerio* [B.1 and B.2] and the amphipod *H. azteca* [C.1 and C.2], effects of Carbo-Iron on survival were assessed in acute exposures (2 to 10 d exposure time), and effects on survival and growth (weight and length) in chronic exposures (21 to 56 d exposure time). In the chronic test with *H. azteca*, reproduction (number of offspring) was assessed during chronic exposures (42 and 56 d) to Carbo-Iron. Additional to these endpoints that are described in the respective test guidelines, potential effects on the gene expression were investigated in fish (*D. rerio*) embryos. After the 34-d exposure of fish early life stages to Carbo-Iron, changes in the morphology of the gut were evaluated. For *H. azteca*, the influence of Carbo-Iron on the feeding rate was investigated in a 7-d exposure and a potential change in sensitivity of the offspring from adults exposed to Carbo-Iron was studied. Since it is a common concern for nanoparticles (see section 3.4), the uptake and potential translocation of Carbo-Iron in *D. rerio* and *H. azteca* was analysed with scanning electron microscopy, transmission electron microscopy and energy dispersive X-ray microanalysis in *D. rerio* and *H. azteca*. As recommended for the testing of nanoparticles, the Carbo-Iron particle size and the concentrations of potentially leaching iron ions were determined at regular intervals during most of the exposures. Carbo-Iron concentrations were determined at regular intervals in the exposure media of the chronic test with early life stages of *D. rerio*.

To complement the data set for the effect assessment of Carbo-Iron, additional ecotoxicity tests with the crustacean *D. magna*, the midge *C. riparius* and the alga *S. vacuolatus* were performed [D.1 and D.2] with a focus on the endpoints described in the respective OECD test guidelines. Additionally, a test with nitrifying soil microorganisms was performed [D.1 and D.2]. Carbo-Iron was spiked into the soil in suspension and as powder to investigate potential impacts of the application on toxicity [described in D.1].

Environmental concentrations of Carbo-Iron were derived from data obtained during the application of Carbo-Iron for remediation of a contaminated groundwater in a field study described by Mackenzie et al. (2016). Using these environmental concentrations and the data from the ecotoxicity tests, the environmental risk of Carbo-Iron was assessed [D.1].

For a comprehensive risk assessment for the treated site, a Triad-based assessment method described by Dagnino et al. (2008) was modified and used with data for the relevant pollutant concentrations and physico-chemical parameters measured in the groundwater from this field study. The environmental risk was estimated for various time points before and during the treatment of the groundwater with Carbo-Iron, integrating chemical, physico-chemical and ecotoxicity data. With these data, the potential benefit or a possible risk-risk trade-off of the application of Carbo-Iron into the groundwater were identified.

4 Results

4.1 Strategy for ecotoxicity testing of Carbo-Iron

When performing ecotoxicity tests with nanomaterials and nanocomposites, either a realistic or a worst-case scenario can be chosen as testing strategy [A.1]. In the realistic scenario, particles are added to the test “as is” and agglomeration of the particles is accepted. In the worst-case scenario, particles are dispersed by energy input to the smallest dispersible unit and dispersant agents can be used to minimize agglomeration in stock suspensions and test media. For the assessment of effects of Carbo-Iron in ecotoxicity tests the worst-case scenario was chosen (Figure 4.1 [A.1]). Carbo-Iron was stabilized with the dispersant carboxymethyl cellulose (CMC) in the stock suspensions. Stock suspensions of Carbo-Iron were prepared with the same method for all experiments: 100 mg Carbo-Iron were added to 100 mL CMC solution and the smallest dispersible unit was created by treatment of the particles in aqueous media with a relatively high energy input of 170 MJ/m³ via an ultra-sonic probe for 7 min (see e.g. A.2, section 2.1 for details). If volumes > 100 mL were needed, this procedure was repeated, and the obtained suspensions were pooled. All tests with aquatic test organisms were performed on the basis of the highlighted successive decisions shown in Figure 4.1.

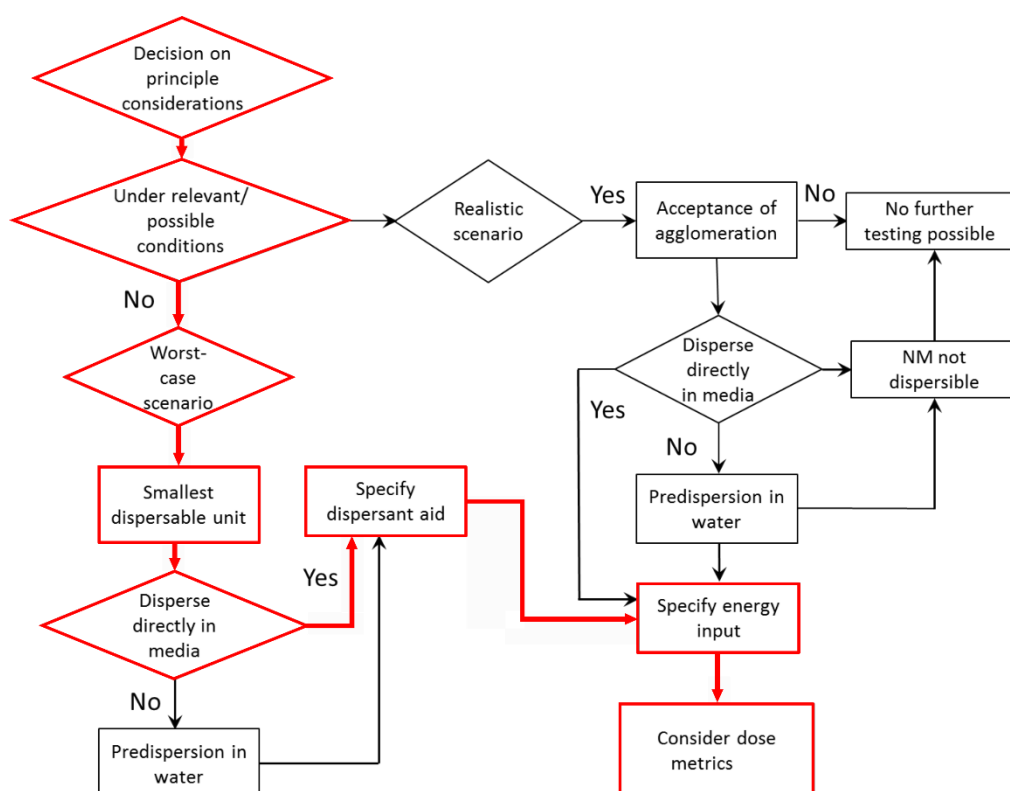


Figure 4.1: Choice of test scenario and application of nanomaterials to liquid media and principal considerations for the testing of nanomaterials [A.1]. In the experiments performed for the present thesis, effects of nanomaterials under worst-case conditions was chosen as general concept.

The consideration of concentration metrics, mentioned in Figure 4.1 is important to interpret the ecotoxicological results and has a high significance in a regulatory context, where effect concentrations and e.g. exposure limits are derived. Therefore, a decision tree was developed (Figure 4.2) integrating the suggestions of available studies (Delmaar et al., 2015; Kühnel and Nickel, 2014; Petersen et al., 2015) for mass-based (e.g. mg particles/L), number-based (e.g. particles/mL) and surface-based (e.g. particles/mm²) concentration metrics. In the present study, the use of mass-based metrics (mg/L and mg/kg) was chosen for all studies. In any case, initial particle properties and characteristics should be determined analytically. The investigation of the particle behaviour in a test, specifically regarding parameters such as agglomeration, dissolution and sedimentation, is highly recommended [A.1]. Therefore, these parameters were investigated in the experiments with *D. rerio* and *H. azteca* as presented in Figure 4.2.

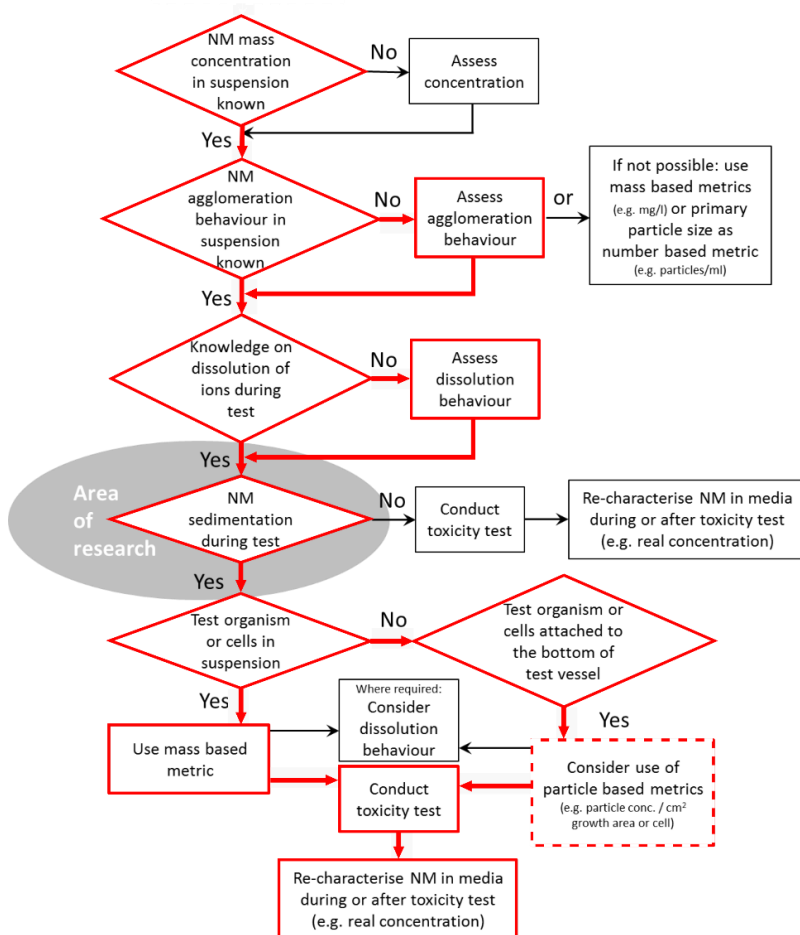


Figure 4.2: Concentration metrics in liquid media. The decision node on sedimentation is marked as 'Area of research', as currently no protocols for a reliable quantification of the amount of nanomaterials settled out during the tests are available. In all test in the present thesis, concentration metrics are based on mass (mg/L) and other suggested concentration metrics (box with dashed frame) are not considered. All tests with aquatic test organisms were performed on the basis of the highlighted successive decisions (red arrows and boxes).

During the assessment of the agglomeration behaviour of Carbo-Iron, as required in Figure 4.2, a mean hydrodynamic diameter of 274 nm was measured in the samples from the stock suspension used for the fish embryo toxicity test. For this test, < 100 mL stock suspension were required. Hydrodynamic diameters measured in stock suspensions used for all other exposures of *D. rerio* and *H. azteca* were in size ranges between 380 to 395 nm and 322 to 395 nm, respectively [B.1, section 3.1 and A.3, section 3.1]. For these experiments, stock suspension volumes > 100 mL were needed and the consecutive preparation of 100 mL aliquots of stock suspension and subsequent pooling of these aliquots was necessary. Apparently, measured Carbo-Iron diameters increased with the volume of the prepared stock suspension. A possible explanation is that the sonication probe became very hot during preparation of the first 100 mL aliquot and did not cool down before starting to prepare the next aliquot, although the stock suspensions were placed on ice during sonication. Additionally, pooling and mixing of the aliquots could have influenced particle size due to the input of mechanical energy. In the test suspensions in the tests with *D. rerio*, measured particle diameters were between 329 and 355 nm in static exposure conditions and between 439 and 486 nm in flow-through exposure conditions [B.1, section 3.1]. The different size ranges may have been caused by the peristaltic pumps used for delivery of the test water from the storage tank to the test vessels, which elicited pressure on the tubing and, thus, the particles in the test suspensions. During the exposure of *D. rerio* in the fish early life stage test, exposure concentrations were measured [B.1, section 2.2.3] as recommended in Figure 4.2. Measured particle concentrations deviated less than 20% from the nominal concentrations. Test suspensions with concentrations ≥ 12.5 mg/L Carbo-Iron in the tests with *H. azteca* were stable for 3 d, and measured Carbo-Iron diameters were between 315.1 ± 9 nm and 575 ± 35 nm.

The analysis of dissolution of iron ions from Carbo-Iron revealed increasing $\text{Fe}^{2+}/\text{Fe}^{3+}$ concentrations with increasing Carbo-Iron concentrations in the tests with *D. rerio* (≤ 68 $\mu\text{g/L}$ at 100 mg/L Carbo-Iron) [B.1, section 3.1]. However, in the water-sediment test with *H. azteca*, $\text{Fe}^{2+}/\text{Fe}^{3+}$ concentrations were between 170 and 280 $\mu\text{g/L}$ in all test vessels and no differences between treatments and controls was found [C.1, section 2.3]. It was assumed that in this test most of the iron had leached from the constituents of the artificial sediment [C.1, section 3.7].

For the investigation of the effects of Carbo-Iron on nitrifying soil microorganisms [D.2, sections 1.1.5 and 2.3.5], the experimental setup was selected based on the specifications in Figure 4.3 [A.1]. Here, particles were applied into the test soil either as powder or in suspension to investigate whether the application had an influence on the effect concentrations. Unfortunately, characterisation of Carbo-Iron in the test soils was not feasible, mainly due to presence of particles in a similar size range as Carbo-Iron and the high background values for the Carbo-Iron components

carbon and iron. Therefore, no data on the influence of the application method on particle behaviour were obtained. Since no effects were observed in the test with the soil microorganisms, the influence of the application method on Carbo-Iron toxicity could not be evaluated.

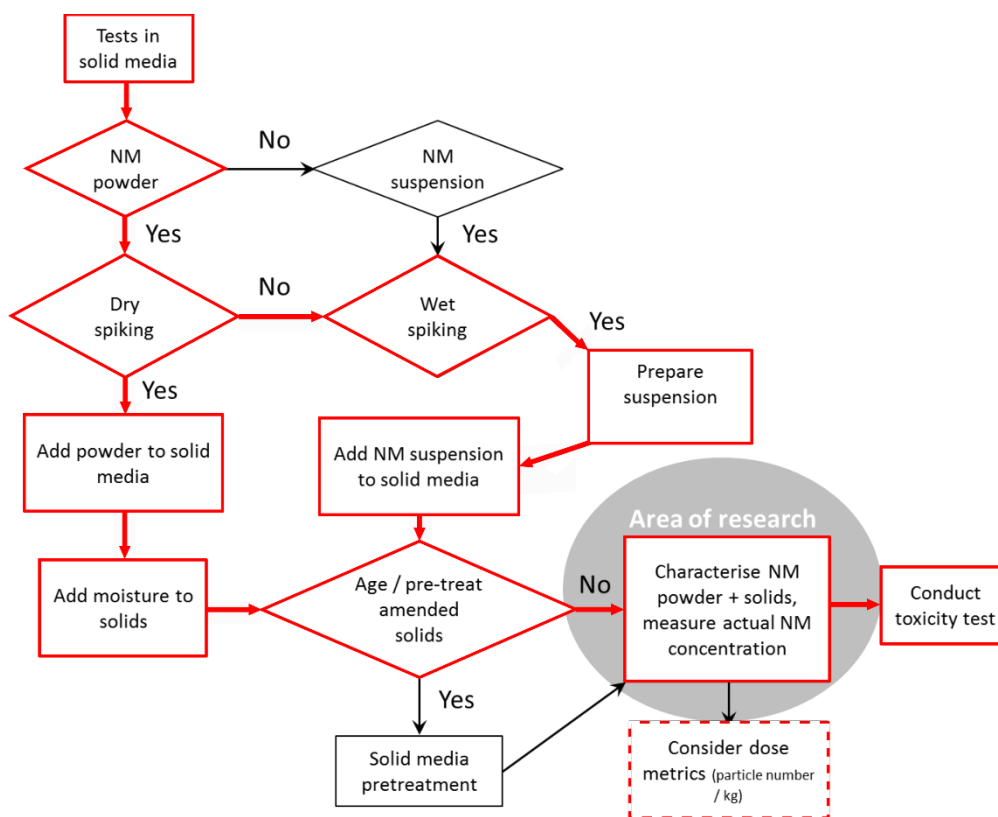


Figure 4.3: Application of nanomaterials to solid test media. The number given in parenthesis relates to the decision tree shown in Figure 4.1. The decision node on characterisation and concentration measurement of nanomaterial in the soil is marked as 'Area of research', as currently no protocols for these quantifications in solid media are available. In all tests in the present thesis, concentration metrics are based on mass (mg/L) and other suggestions on concentration metrics (box with dashed frame) are not considered. The test with soil-inhabiting test organisms was performed on the basis of the highlighted successive decisions (red arrows and boxes).

In order to prove the applicability and correctness of the developed decision trees, a model study on the effects of nanoscale CuO powder (primary particle size of 35 nm) was conducted with the *D. magna* acute immobilization test (OECD, 2004a) [A.1, section 2.2]. In this model study, different scenarios were considered: environmental relevant conditions, i.e. investigation of the particles "as is", and worst-case conditions, i.e. use of dispersant and generation of smallest dispensable unit [A.1, sections 3.3 and 3.4]. The different test conditions had a clear influence on the effect values, with EC₅₀ values for nCuO ranging from 0.44 to 11.23 mg/L [A.1, section 3.7].

4.2 Uptake and ecotoxicity of Carbo-Iron

Ecotoxicity of Carbo-Iron was investigated with the crustaceans *H. azteca* and *D. magna*, the fish *D. rerio*, the algae *S. vacuolatus*, the midge *C. riparius* and nitrifying soil microorganisms. In *D. rerio* and *H. azteca*, uptake of Carbo-Iron into the organisms was investigated. Carbo-Iron elicited no effects on soil microorganisms at concentrations between 500 and 2828 mg/kg soil dry weight. In all other test organisms used in the experimental phase of the present work, lethal and/or sublethal effects were observed in Carbo-Iron concentrations of approx. 1 to 100 mg/L. These results are described in the following sections.

4.2.1 Uptake

At the end of the fish embryo test, the acute toxicity test and the fish early life stage test with *D. rerio* [B.1, sections 2.4, 2.5 and 2.6] and the acute toxicity test with *H. azteca* [C.1, section 2.3.1] all organisms were stored for microscopic analysis. For a detailed investigation of potential uptake of Carbo-Iron into the organisms, scanning electron microscopy (SEM) and transmission electron microscopy (TEM) analyses were performed, and the presence of iron was investigated with elemental digital mapping (EDX).

The chorion, surrounding the fish embryo, is an effective barrier against Carbo-Iron. Although Carbo-Iron attached to the egg [B.1, Fig. 3], no particles were observed in the perivitelline space of the egg (Figure 4.4A). Carbo-Iron was identified in the gut of *D. rerio* (Figure 4.4B) and *H. azteca* (Figure 4.4D), and it adhered to the integument of *D. rerio* larvae (Figure 4.4C). However, it was not detected in any other part of the investigated organisms. Carbo-Iron was excreted from the gut of *D. rerio* during a 4-d post-exposure period in control water [B.1, Fig.6].

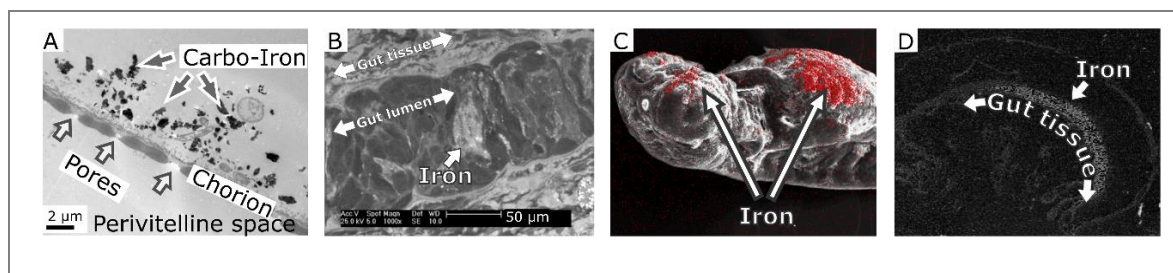


Figure 4.4: (A) Lateral cut (ultrathin section, TEM) through the zebrafish egg shows Carbo-Iron on the outside of the egg (dark particles). The lack of Carbo-Iron particles in the chorion pores and the perivitelline space indicates that the chorion acts as barrier for the uptake of Carbo-Iron. (B) Scanning electron micrograph of the gut of an adult zebrafish (lateral cut) after 96 h of exposure to 100 mg/L of aged Carbo-Iron. The white areas in the lumen of the gut represent iron particles with Carbo-Iron-like morphology. (C) Iron containing particles adhering to the integument of larvae exposed to 2.5 mg/L Carbo-Iron (D) EDX elemental mapping shows distribution of iron as white spots in the gut of *H. azteca* after 10 d of exposure to 100 mg/L Carbo-Iron.

4.2.2 Survival

In the fish embryo test and the acute toxicity test with *D. rerio* [B.1, sections 3.2 and 3.3], no effects on survival were observed in the investigated concentration range up to 100 mg/L. In the acute toxicity test with *H. azteca* (EPA 600/R-99/064 (2000)), a statistically not significant increase in mortality of *H. azteca* was observed after exposure to 100 mg/L Carbo-Iron for 10 d [C.1, section 3.2] and an LC₂₀ of 100 mg/L and LC₅₀ > 100 mg/L was derived (Figure 4.5). Mortality of *D. magna* in the acute toxicity test (OECD 202, 2004a) was increased at concentrations ≥ 10 mg/L, but no clear correlation of the mortality with the Carbo-Iron concentrations was observed [D.1, section 3.1.1]. The LC₁₀ and LC₅₀ of 2.3 and 34 mg/L, respectively, (Figure 4.5) were associated with large confidence intervals [D.2, SI section 2.3.1.2].

In the chronic guideline tests, no effects on survival were observed in the 28-d exposure of *C. riparius* [D.2, section 3.1.3] and the 32-d exposure of *D. rerio* [B.1, section 3.4]. After 42-d and 56-d exposure of *H. azteca* to Carbo-Iron, LC₂₀ values of 57 and 9 mg/L were determined (Figure 4.5).

Effects of Carbo-Iron on *D. magna* and *H. azteca* were additionally investigated with modified exposure scenarios. Compared to the results obtained in the acute test after 2 d of exposure of *D. magna*, the addition of a post-exposure period of 5 d under control conditions led to a clearly lower survival (LC₁₀= 0.6 and LC₅₀=3.4 mg/L) [D.1, section 3.1.1]. Similarly, the use of juvenile *H. azteca* collected from parental animals exposed to Carbo-Iron for 10-d acute toxicity tests according to EPA (2000) [see A.3, section 2.3.5] led to a lower survival than in a test with offspring from unexposed test organisms (Figure 4.5) [C.2, Fig. S1 and C.1, section 3.6]. *H. azteca* collected from exposed parents lead to LC₂₀ values up to factor 14 more sensitive than in the test with previously unexposed test organisms. The acute lethal toxicity determined with *H. azteca* collected from parents exposed to 12.5 mg/L Carbo-Iron for 56 d (LC₂₀=7.1 mg/L) was lower than the chronic lethal toxicity values determined in the 56-d exposure (LC₂₀=8.7 mg/L). In the same way, 10-d exposure of juvenile *H. azteca* collected from parents exposed to Carbo-Iron for 42 d (LC₂₀=9.6 mg/L) lead to lower LC values than the 42-d exposure of *H. azteca* (LC₂₀=56.9 mg/L).

though still slightly lower [B.1, Fig. 7]. Growth of fungi on the chorion was observed with increasing Carbo-Iron concentrations in the fish embryo test [B.1, Fig. 2 and Fig. S3] and the fish early life stage test [B.1, section 3.4], but this had no influence on hatching or any other evaluated endpoint.

For the test with algae *S. vacuolatus*, several deviations from the method described in the respective guideline (OECD, 2011) were necessary, mainly concerning the exposure time and the investigated endpoint. The determination of the commonly used parameters algal biomass or its surrogate endpoints cell number and fluorescence was not possible because Carbo-Iron interfered with the respective measurement methods by covering the algae cells. Thus, the cell volume was assessed after an exposure time of 16 h when the volume of the cells had increased, but the cells had not yet divided [D.1, section 2.1.2]. For this endpoint, an EC₁₀ of 7.2 mg/L was determined [D.1, section 3.1.2]. The reduction of the increase in cell volume was probably caused by shading of the algae by the Carbo-Iron particles, since similar effects were obtained after the exposure of *S. vacuolatus* to active carbon and light intensities in the test vessels were significantly influenced by both particles [D.2, section 2.3.2]. However, it is possible that the sequestration of nutrients from the test media by the active carbon (both as component of Carbo-Iron and as active carbon particle) could additionally have caused nutrient depletion in the culture medium (Bundschuh et al., 2011c) and thus contributed to the observed toxicity.

In the tests with *H. azteca* (Figure 4.6), the most sensitive endpoint was reproduction with a NOEC of 6.3 mg/L after 56 d of exposure to Carbo-Iron [C.1, section 3.5]. In the same test, the endpoint growth was less sensitive (NOEC=12.5 mg/L). These values are lower than NOECs derived after an exposure of *H. azteca* for 42 d [C.1, section 3.4]. The feeding activity of *H. azteca* was significantly reduced by exposure to 100 mg/L Carbo-Iron (NOEC=32 mg/L) [C.1, section 3.3].

Carbo-Iron was applied to the water-sediment study with *C. riparius* via the water phase. The total number of emerging adult midges was not influenced by up to 100 mg/L Carbo-Iron. However, the highest test concentration lead to significantly lower development rate of the midge larvae and a NOEC of 56.2 mg/L was determined (Figure 4.6) [D.1, section 3.2.3].

wells were not measured analytically, since the Carbo-Iron constituents iron and carbon would be unnoticeable in the natural high background values. Therefore, concentrations and distribution of Carbo-Iron in the groundwater were estimated based on information on the time-dependent distribution pattern of Carbo-Iron from soil column studies [D.2, section 2.1]. In the zones Ia, Ib, Ic and I (Figure 4.7B), calculated Carbo-Iron concentrations of 650, 475, 1.3 and 0.5 mg/L, respectively, were obtained. Further information on the site are provided in section 2.2 in A.4.

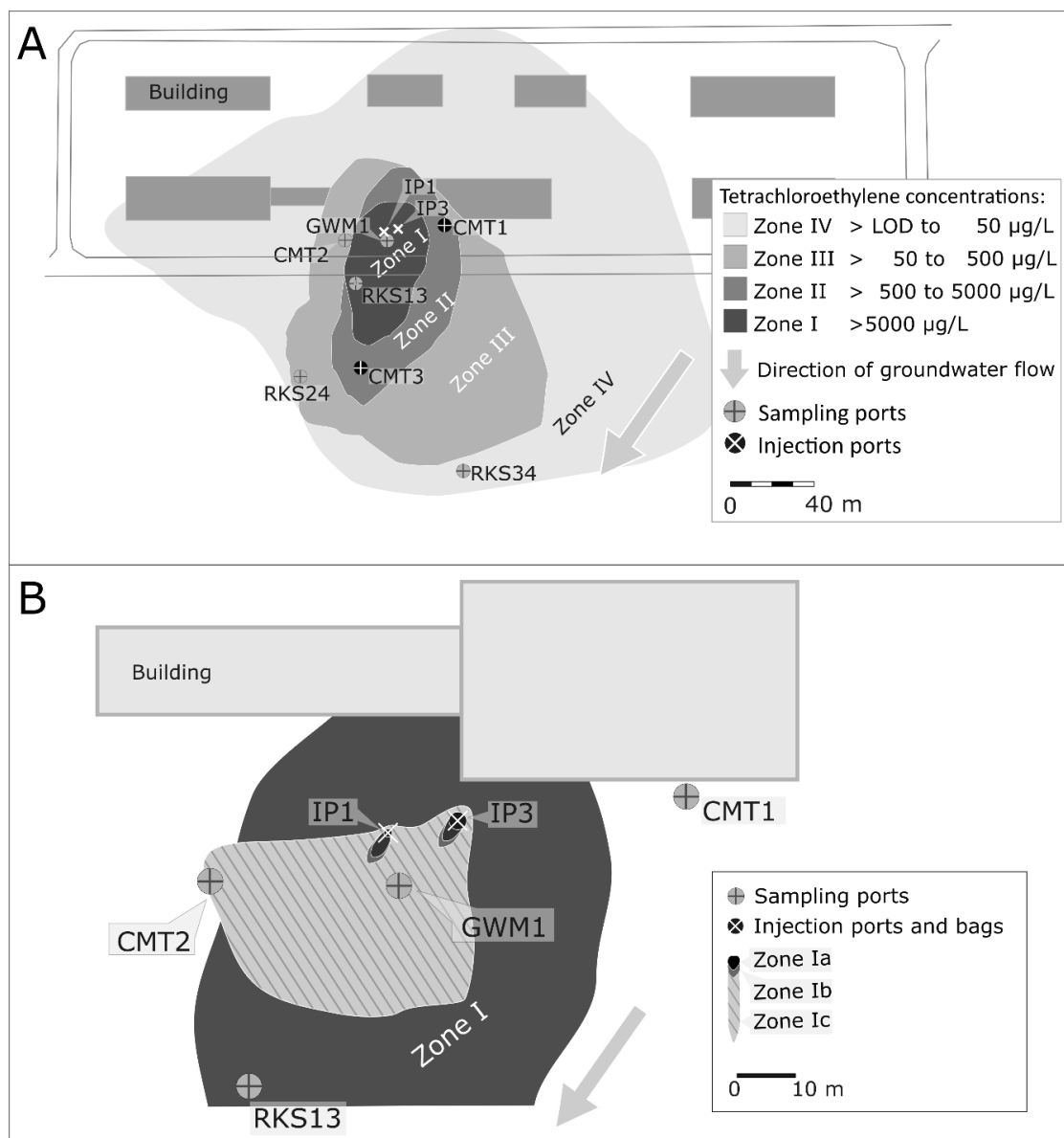


Figure 4.7: Site treated with Carbo-Iron in the pilot study of Mackenzie et al. (2016). Groundwater monitoring well (GWM1) with a sampling depth of 8 m below ground level; continuous monitoring well with multichannel-tubing (CMT1, CMT2, CMT3) with seven ports in depths between 6 and 25 m below ground level; window sampling tubes (RKS 13, RKS 24, RKS 34) with two sampling ports at approx. 6.5 and 8 m below ground level. **A:** Overview of the area and allocation of zones based on measured concentrations of PCE above the analytical limit of detection (LOD=0.5 $\mu\text{g/L}$). **B:** Distribution of Carbo-Iron after injection in zone I. Subdivisions Ia, Ib, and Ic indicate the calculated Carbo-Iron concentrations of 650, 475 and 1.3 mg/L.

4.3.2 Derivation of a PNEC & environmental risk assessment for Carbo-Iron

The most sensitive effect concentration for Carbo-Iron was determined in the reproduction test with *D. magna* (NOEC=1.0 mg/L). For the determination of the environmental risk of Carbo-Iron, an assessment factor of 10 was chosen, as data from chronic tests with at least three functional groups were available (ECHA, 2008, 2017) and a predicted no effect concentration (PNEC) of 0.1 mg/L was calculated. The risk quotient of the predicted environmental concentrations (PEC) and the PNEC indicates the degree of risk expected to be caused by Carbo-Iron in the treated aquifer. A risk quotient of PEC/PNEC below 1 is generally considered acceptable (ECHA, 2016).

The most sensitive effect concentration, an LC₁₀ of 0.64 mg/L, was determined in the acute test with *D. magna* with the 5-d post-exposure period. While the use of effects data that were not obtained in guideline tests is generally possible in the present study this test result was not used for the derivation of a PNEC for Carbo-Iron. This decision is based on the comparability of data used for the risk assessment of the chlorohydrocarbons in the following section 4.4: here, all effects data used for the derivation of the respective PNEC were obtained in guideline tests. Further, in the ERA described in ECHA (2017), the use of a LC₁₀ derived in an acute test is not mentioned but the use of the LC₅₀. The most sensitive effect concentration that is described in a test guideline and the guidelines for the ERA (ECHA, 2017) was determined in the reproduction test with *D. magna*. This NOEC of 1 mg/L was used in the risk assessment of Carbo-Iron. Since results of chronic studies with all three trophic levels are available, an assessment factor of 10 was used and a PNEC of 0.1 mg/L was derived for Carbo-Iron [D.1, section 3.2].

In the pilot study site, the estimated environmental concentration of Carbo-Iron in the area close to the injection points (zone Ia) exceeds the PNEC by a factor of 6500 [D.1, section 3.2]. With increasing distance to the injection point, the risk quotients decrease to 4750 (zone Ib), 13 (zone Ic, sampling well GWM1) and 5 (zone I, sampling well RKS13, approx. 10 m from injection points). The estimated migration of Carbo-Iron through the aquifer is supported by the detection of Carbo-Iron particles in samples from GWM1 on d 30, 57, 92 and 139 after injection, and in samples from CMT2 on d 139 after injection [D.2, Fig. S1 and section 3.2]. Based on the estimated transport data for Carbo-Iron from the column studies [D.1, SI section 3.1], a distribution of Carbo-Iron beyond zone I is unlikely. Hence, the risk quotients in zones II, III and IV can be assumed to be below 1 indicating no risk due to Carbo-Iron application.

4.4 Comprehensive risk assessment for the remediated site

The pilot study site was highly polluted with chlorohydrocarbons [D.2, Table S8] and the potential benefit or a possible risk/risk trade-off of the Carbo-Iron treatment was investigated in a Triad-based ERA. Risk indices were calculated based on the comparison of the measured parameters (e.g.

PCE concentration or pH) per day and well with a target value for these parameters [see A.4, section 2.3.3 for a full description of the calculations]. The risk assessment integrated the following components:

- The chemical component integrates concentrations of the relevant pollutants before and after treatment with Carbo-Iron. The target values were generally taken from Swartjes (1999), who derived intervention values for the assessment of groundwater, and Crommentuijn (2000), who derived maximum permissible concentrations for surface water.
- The ecotoxicological component integrates data for the relevant pollutants as well as for Carbo-Iron. Instead of ecotoxicity tests with groundwater samples, data from single-substance standard ecotoxicity tests were used. To derive target values for this component, available ecotoxicity data for the relevant hydrocarbons were evaluated [D.1, section 2.3.2] to derive PNEC values [D.2, Table S10].
- A physico-chemical component was introduced, since changes in the physico-chemical parameters, among others, redox-potential and pH due to the injection of Carbo-Iron may increase the environmental risk for the groundwater fauna. The physico-chemical component includes parameters that are very likely to change after application of Carbo-Iron into the groundwater. Target values or ranges were taken from the EU directive on the quality of water for human consumption (European Communities, 1998), the aquatic life criteria provided by the US EPA (1999) and derived on data from literature search [D.1, section 2.3.3.3].

With this approach, risk indices for the chemical (cRI), ecotoxicological (eRI) and physico-chemical (pRI) component were calculated. In Figure 4.8, the results of the site-specific ERA are shown for the contamination zones I to IV [D.1, section 3.3]. The desired remedial effect of Carbo-Iron is discernible in the decreasing chemical and ecotoxicological risk indices in all investigated groundwater samples (Figure 4.8) during the first 58 d after Carbo-Iron injection. This effect is most pronounced in samples from the contamination zones Ic and I (wells GWM1 and RKS13) The chemical and ecotoxicological risks increase again after 58 d, possibly due to inflow of chlorohydrocarbon-contaminated groundwater from the non-treated area upstream of the injection wells and depletion of reactive Carbo-Iron. However, on d 190 in zones Ic (GWM1), I (RKS13) and III (RKS24), a strong decline of the chemical and ecotoxicological risk occurred compared to d 93. This was mainly caused by a drop of measured concentrations of PCE and TCE [D.2, Table S8], possibly as a result of a precipitation event. In most investigated zones, the eRI and the cRI reached similar but lower values on d 190 than before the application of Carbo-Iron. Yet, in

zone II (CMT2), the eRI increased on d 93 and d 190 above any previous values and the environmental risk is higher than before the application of Carbo-Iron. The physico-chemical risk was relatively stable in all contamination zones during the 190 d after Carbo-Iron injection. Increased pRI due to a reduced redox potential were visible in zone II (CMT2) on d 190 and zone III (RKS24) on d 31 and d 58. The slightly increased pRI in zone II (well CMT1) on d 93 was caused by an increased conductivity and a lower pH than on the sampling days before [D.2, Table S19].

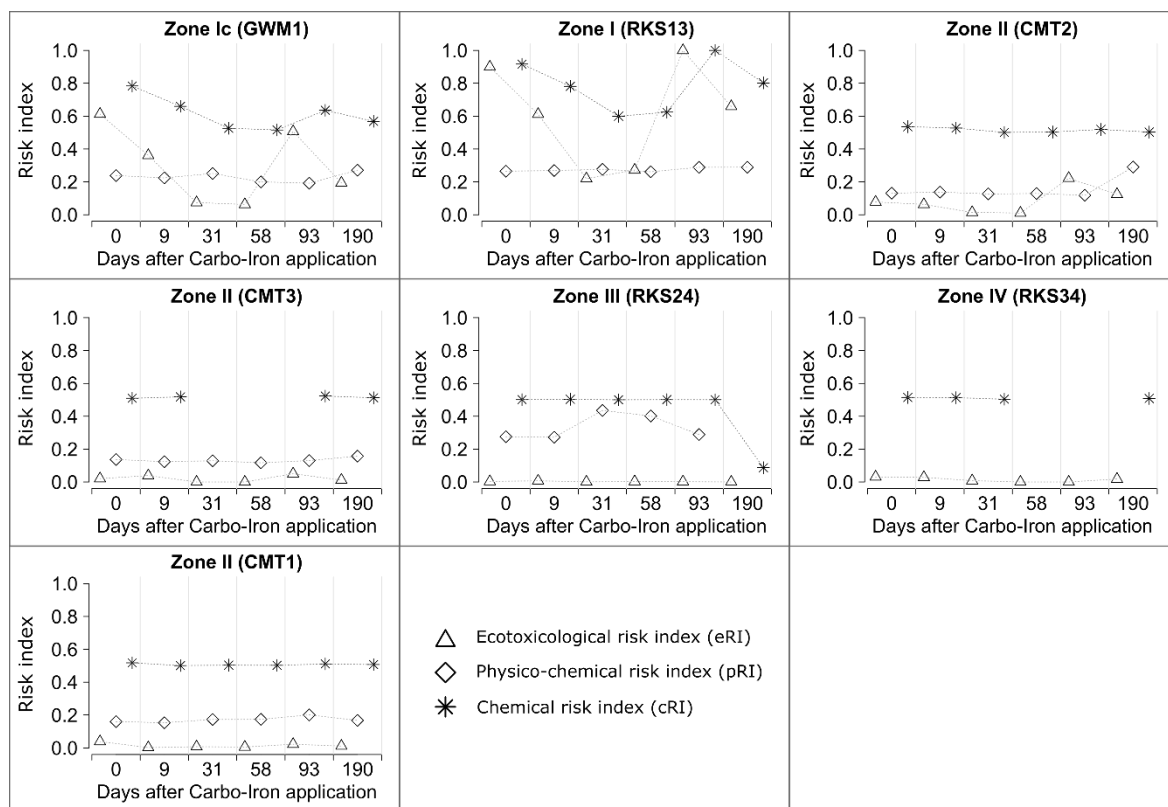


Figure 4.8: Comparison of the calculated risk indices for groundwater contaminated with chlorohydrocarbons during the first 190 d after treatment with Carbo-Iron using a TRIAD-based approach.

5 Discussion

5.1 Strategy for ecotoxicity testing

The requirement for specific test procedures for the ecotoxicity testing of nanomaterials arises from their unique properties and behaviour, which in many aspects differs substantially from that of chemical substances. The design of ecotoxicity tests has to be adapted for nanomaterials and amendments to existing testing protocols need to be implemented (Handy et al., 2012; Kühnel and Nickel, 2014; Nickel et al., 2014; OECD, 2012b; Petersen et al., 2015). The need for clearly defined test conditions was highlighted in the present study by the toxicity data obtained for nanoscaled CuO and *D. magna*, varying by a factor of approx. 20 depending on the chosen exposure scenario [A.1]. When assessing the effects of nanomaterials on environmental organisms, various considerations have to be taken into account, regarding e.g. the test design, the preparation of test suspensions, the test procedure (e.g. in view of the expected behaviour of the nanomaterial in the test media), and data interpretation. In the present thesis, decision trees and flow charts were developed as a tool to support a consistent and structured testing of nanomaterials, and their suitability was evaluated. The decision trees [A.1] provide a stepwise approach, dividing a method or process into crucial steps. Furthermore, they allow the selection of the most appropriate scenario for a specific research question, e.g. investigation of the respective nanomaterial under conditions that are close to realistic environmental conditions or conditions that simulate a worst-case scenario.

In the ecotoxicity tests, which are relevant for the ERA of Carbo-Iron (section 4.2) and were performed based on the developed decision trees, the measured hydrodynamic diameters of Carbo-Iron in the test suspensions differed slightly between the individual tests. However, the variation of Carbo-Iron size in each of the tests was low, indicating that exposure conditions were constant, as required for ecotoxicity effects for an ERA (ECHA, 2016; OECD, 2010). With the flow-through exposure in the fish early life stage test, concentrations of Carbo-Iron in the water phase were stable and with the use of the dispersant CMC, sedimentation was minimized for approx. 10 d in the used aqueous media. Thus, the exposure conditions chosen represented the desired worst-case scenario.

The decision trees were helpful in defining an appropriate test scenario. The developed approach also contributes to a verification of the suitability of existing test guidelines for the testing of nanomaterials, fostering harmonization of nanomaterial testing in the future (Jaworska and Hoffmann, 2010).

5.2 Ecotoxicity of Carbo-Iron

Using semi-static and flow-through conditions for the acute fish test and the fish early life stage test, respectively, sedimentation of the particles from the water phase was minimized and the pelagic *D. rerio* could be exposed to Carbo-Iron. In the acute and chronic tests with the crustaceans *H. azteca* and *D. magna*, the Carbo-Iron particles precipitated to the sediment over time. Since *H. azteca* are epi-benthic and *D. magna* migrates between the water phase and the bottom of the test vessel, they were in contact with the nano-composite, too. The test media in the test with the alga *S. vacuolatus* were aerated, keeping both the algae and the respective particles (Carbo-Iron or active carbon) in suspension. However, in the fish embryo toxicity test exposure of the embryos to Carbo-Iron was reduced, since Carbo-Iron did not cross the chorion (see section 4.2.3). Therefore, it is not surprising that the expression of selected marker genes in zebrafish embryos, usually a very sensitive endpoint (Weil et al., 2009), indicated no changes compared to the control [D.1, section 3.5]. In the water-sediment test with *C. riparius*, larvae were buried in the sediment while Carbo-Iron precipitated from the water phase and covered the sediment surface. Although burrowing activity of the larvae was visible on the surface of the sediment, the exposure of the larvae to Carbo-Iron was limited to those particles ingested by the larvae from the sediment surface into the layers beneath. In the test with nitrifying soil microorganisms, no observation on the behaviour of the particles in the test soil was possible. It is likely that Carbo-Iron quickly adhered to soil particles and that bioavailability was limited (see review by Handy et al. (2012)).

For the investigation of the ecotoxicity of Carbo-Iron, modifications of existing test guidelines, regarding e.g. the preparation of test suspensions, were necessary (section 4.1). Assessing the standard endpoints described in the respective guidelines, significant effects of Carbo-Iron on reproduction and survival of *D. magna* and *H. azteca*, and the development rate of *C. riparius* were determined (Figure 4.5 and Figure 4.6). In *D. rerio*, no impact on the commonly assessed endpoints survival, hatch, swim-up and growth were observed. By investigating the number of microvilli in the gut of *D. rerio* as an additional endpoint, a NOEC of 2.5 mg/L was determined. By modification of the exposure, e.g. addition of a post-exposure period for *D. magna*, the use of pre-exposed *H. azteca* in acute toxicity tests effect levels were up to factor 10 lower compared to the non-modified exposure (Figure 4.5 and Figure 4.6). Higher crustaceans are important groundwater organisms and the increasing sensitivity of juvenile *H. azteca* collected from the exposed parental generation, should thus be considered when assessing a potential environmental risk of Carbo-Iron.

The presence of Carbo-Iron in the gut of *D. rerio* (Figure 4.4A) and *H. azteca* (Figure 4.4D) but not in any other part of their body suggests that (1) ingestion is the major route of uptake, and (2) that Carbo-Iron is not transferred from the intestinal tract to the surrounding tissue. As proposed for

nanomaterials (Figure 3.1A), Carbo-Iron particles are adhering to biological surfaces, covering e.g. zebrafish larvae (Figure 4.4C) or the chorion in the fish embryo test. Carbo-Iron might serve as substrate for the growth of fungi in the fish embryo test [B.1, Fig. 2 and Fig. S3] and the fish early life stage test [B.1, section 3.4]. Yet, no effects of the fungi on the development of the fish larvae were observed. However, it is not clear whether effects are likely in embryos of fish species with longer time to hatch, e.g. the fathead minnow with 4-5 d after fertilization or the rainbow trout with approx. 30 d after fertilization.

In the acute toxicity tests with the crustaceans *H. azteca* and *D. magna*, lethal effect concentrations (Figure 4.5) were in a similar range as sublethal effect concentrations obtained mainly in chronic toxicity tests (Figure 4.6). It seems that this is partly due to the modified exposure scenarios used in the present study, that mainly comprise extended test duration either by use of pre-exposed organisms (*H. azteca*) or by addition of a post-exposure phase (*D. magna*). In this time period, effects of Carbo-Iron that weaken the organism and result e.g. in reduced growth are intensifying and lead to mortality. However, part of the similar sensitivity of the Carbo-Iron concentrations causing lethal effects compared to sublethal effects is simply caused by not including growth as an endpoint in the acute tests or, alternatively, extending the chronic tests by a post-exposure phase. The toxicity of nanocomposites might be caused by toxic effects of ions released from the metal-component of the particle (Figure 3.1B). Therefore, and as recommended in the chosen testing strategy (Figure 4.2), ionic iron (Fe^{2+} and Fe^{3+}) was measured in the test suspensions during the exposure of *D. rerio* and *H. azteca* to Carbo-Iron. Measured concentrations for the sum of Fe^{2+} and Fe^{3+} in Carbo-Iron test media were between 0.068 and 0.28 mg/L [B.1, section 3.1 and A.3, section 2.3]. For the test organisms used for assessment of ecotoxicity in the present study, reported no effect levels for Fe^{2+} and Fe^{3+} are ≥ 0.34 mg/L [C.1, section 3.7]. Thus, the toxicity observed in the tests was most likely not caused by Fe ions leaching from the nFe^0 -component of Carbo-Iron. The formation of reactive oxygen species or release of Fe ions in the gut of the test organisms, potential mechanisms of action for nanomaterials (Figure 3.1B), were not investigated systematically in the present study.

It seems likely that the predominant mechanism of action for Carbo-Iron is related to the attachment of the particles to the gut. A reduced uptake of nutrients is probably the main reason leading to reduced survival and growth of *H. azteca* and *D. magna* exposed to Carbo-Iron. Energy reserves are passed from the parental generation to the eggs and used during the development (Dutra et al., 2007). In juvenile amphipods collected during the 56-d exposure, sensitivity to Carbo-Iron increased with the Carbo-Iron concentrations, to which the parental amphipods were exposed, and with the exposure duration of the parental generation. The poor condition of the juveniles

resulted most likely from the limited provision of the parental *H. azteca* with nutrients. Juveniles collected from test vessels with 25 mg/L Carbo-Iron were unable to recover from their persisting poor condition even after transfer to control conditions. For *D. magna* exposed to Carbo-Iron for 48 h an LC₅₀ of 34 mg/L was determined, but they were unable to recover from this exposure during the 5-d post-exposure and the LC₅₀ decreased to 3.37 mg/L [D.1, section 3.1.1].

D. magna and *H. azteca* ingest Carbo-Iron together with the food. However, Carbo-Iron provides no nutritional value and increased feeding rates would have been necessary to compensate for this. However, feeding rates of *H. azteca* exposed to 100 mg/L Carbo-Iron decreased to 63% of the value in the dispersant control as shown in the feeding activity test with *H. azteca* [C.1, section 3.3]. Due to the need to prolong gut transit time for exploiting the food, nutrient-poor food, as in this case Carbo-Iron, might move slower through the gut than nutrient-rich food (Tirelli and Mayzaud, 2005) and fine material moves slower through the gut of amphipods and *D. magna* than coarse material (Icely and Nott, 1985; Rist et al., 2017). This would slow down excretion of the food and, hence, result in reduced ingestion (i.e. reduced feeding rates) and, consequently, a reduced provision with nutrients. In the fish *D. rerio*, significant effects of Carbo-Iron were observed on the number of microvilli at concentrations ≥ 7.9 mg/L [B.1, Fig. 7]. Microvilli are involved in nutrient absorption and secretion and they are also a functional part of the gut structure in both *D. magna* (Quaglia et al., 1976) and amphipods like *H. azteca* (Icely and Nott, 1985; Storch, 1987). Hence, it is possible that Carbo-Iron had similar effects on the abundance of gut microvilli in the crustacean as in the fish. Similar findings were made in *D. magna* exposed to for micro- and nanoplastic (Rist et al., 2017), carbo-nanotubes (Edgington et al., 2014) and gold-nanoparticles (Lovern et al., 2008).

The sequestration of nutrients from the test media by activated carbon (Bundschuh et al., 2011b), the main component of Carbo-Iron, and subsequent excretion of Carbo-Iron (with the bound nutrients) could have contributed to the assumed nutrient depletion and, hence, to the toxicity of Carbo-Iron.

5.3 Environmental risk of Carbo-Iron

The endpoint used for the ERA of Carbo-Iron was the number of living offspring in the 21 d-exposure of *D. magna* (NOEC=1 mg/L) [D.1, section 3.1.1]. With an assessment factor of 10, a PNEC of 0.1 mg/L (100 µg/L) was derived for Carbo-Iron [D.1, section 3.2]. This PNEC is relatively high when compared to PNEC values obtained for nano-Ag (0.02 µg/L), nano-ZnO (1 µg/L), fullerenes (4 µg/L), nano-TiO₂ (16 µg/L) and carbo-nano tubes (CNT; 56 µg/L) (Coll et al., 2016). This is probably related to the fate of the nanomaterials in aqueous media and, partly, by their mode of action in the organisms: The toxicity of nano-Ag and nano-ZnO is primarily caused by the release of Ag⁺ and Zn²⁺

ions into liquid media (Bundschuh et al., 2018; Cronholm et al., 2013; McShan et al., 2014; Roy et al., 2015; Song et al., 2010). The mode of action of fullerenes is not completely understood. Early studies reported high rates of ROS generation, but Henry et al. (2011) highlighted the minimal potential of fullerenes to produce ROS and attributed the ROS activity in previous studies to the presence of residual tetrahydrofuran used during production of the fullerenes (Henry et al., 2011; Zhang et al., 2009). According to Jovanović and Palić (2012), fullerenes cause inflammation and increase the extracellular lysozyme activity, leading to cell damage. For TiO₂, Coll et al. (2016) suspect that the photocatalytic activity of the anatase form was responsible for the low effect concentrations. The most sensitive endpoint in their dataset was obtained in a study by Bundschuh et al. (2011a) with *Gammarus fossarum* under UV light. In summary, the toxicity of nano-Ag, nano-ZnO, fullerenes and nano-TiO₂ is caused by direct (metal ions) and indirect (photoactivation of nano-TiO₂) reactions on the sub-cellular level, most likely including lipid peroxidation and oxidation of proteins as well as general cell damage. Additionally, the mobility of ions in liquid media is much higher than the mobility of particles while their size is manifold smaller, increasing their bioavailability and thus further contributing to the low PNEC of metal nanomaterials. This is in clear contrast with the described effect of Carbo-Iron on the energy budget of the exposed organisms, which is caused by physically blocking the gut and binding of nutrients. Similarly, the toxicity of CNT is probably mediated by physical interaction of CNT with the organisms (Petersen et al., 2011; Skjolding et al., 2016), comparable to Carbo-Iron. The physical mode of action and the lower bioavailability of Carbo-Iron and CNT are most likely the main factors explaining the high PNEC values for these nanomaterials, which are in a similar range.

The relevant release of the nanomaterials investigated by Coll et al. (2016) into the environment is occurring globally via diffuse routes over the whole product life cycle and predicted environmental concentrations are low. Risk quotients derived for these nanomaterials were ≤ 0.09 for freshwater. In contrast, the release of Carbo-Iron is local, intended and immediate, i.e. a major portion of the produced amounts is pumped into contaminated groundwater. At the site chosen for remediation, the estimated PEC values for Carbo-Iron exceed the PNEC in the area close to the injection ports and risk quotients ≥ 5 are obtained up to a distance of approx. 10 m from the injection ports [D.1, section 3.2]. Beyond this zone, an environmental risk of Carbo-Iron is very unlikely. The environmental risks of any remedial agent need to be assessed prior to their application into an aquifer. Obviously, a remediation method is only suitable, if the environmental risk after application is lower than before the start of the treatment (Lemming et al., 2010a) and it is necessary to assess potential harm to the environment and inform decision makers about possible risks (Grieger et al., 2010).

5.4 Comprehensive risk assessment for the remediated site

To assess whether the environmental risk in the groundwater caused by the chlorinated alkenes can be reduced by treatment with Carbo-Iron, a comprehensive risk assessment was performed. The environmental risk before and after application of Carbo-Iron was assessed, integrating risk indices for the chemical, ecotoxicological and physico-chemical component.

The desired remedial effect of Carbo-Iron is discernible in the decreasing chemical and ecotoxicological risk indices in all groundwater samples investigated [D.1, Figure 5 and D.2, Tables S9 and S12] during the first 58 d after Carbo-Iron injection. This effect is most pronounced in samples from the contamination zone I (wells GWM1 and RKS13). While the chemical and ecotoxicological risk indices decreased during this first post-treatment period, Carbo-Iron caused increased physico-chemical risk indices due to a reduced redox potential (in zone II (CMT2) on d 190 and in zone III (RKS24) on d 31 and d 58) or an increased conductivity and a lower pH (in zone II (CMT1) on d 93) [D.1, section 3.3]. This effect on redox potential can be assumed to be temporary, caused by the reaction of Carbo-Iron with the pollutants and the oxygen in the groundwater, i.e. ceasing with loss of reactivity of Carbo-Iron. However, with the available data it is not possible to verify these assumptions.

The risk indices increased again after the first 58 d of Carbo-Iron application. This was expected, since the amount of Carbo-Iron used in the field study was not sufficient for a complete remediation of the groundwater [D.1, section 3.3]. In most contamination zones, the risk indices reached values slightly lower than before the application of Carbo-Iron. However, in zone II (CMT2), the risk index for the ecotoxicological risk increased on d 93 and d 190 above all previous values and the environmental risk, representing the mean of all three risk components, was higher than before the application of Carbo-Iron. On these days, concentrations of ethane, ethene and 1,1-dichloroethene and 1,2-dichloroethene reached their maximum values. Similarly, increased concentrations were observable for all zones investigated in the study. In zone II, the measured concentrations exceeded the relatively low PNEC values for 1,1-dichloroethene and 1,2-dichloroethene. These increased risk ratios represent the main reason for the increased ecotoxicological risk in zone II. The presence of these transformation products and the simultaneous absence of vinyl chloride is typical for PCE degradation by Carbo-Iron and thus indicates proper functioning of the remediation (Mackenzie et al., 2012). Yet, the increased risk is not desirable, especially in the long term. In the present study, effects of Carbo-Iron on the pollutants beyond d 190 were not evaluated and the fate of the transformation products was not examined. However, Vogel et al. (2018) observed in a field study

that 600 days after treatment with Carbo-Iron groundwater microorganisms grew on the active carbon component of Carbo-Iron and that biogenic dehalogenation of the halogenated alkenes occurred. Thus, in the long term and considering the decreasing influence of Carbo-Iron on the physico-chemical risk index, further decreasing values for the environmental risk are expected.

These findings indicate that the use of Carbo-Iron for the treatment of groundwater contaminated with chlorinated alkenes is promising. Still, it should be kept in mind that further remediation methods are available. To choose the most appropriate method for the respective groundwater, the environmental risk of these methods should be assessed and compared to the risk indices obtained in the present study. While a detailed assessment of these methods was not feasible in the present thesis, in the following a brief and tentative evaluation of several techniques available is provided.

Conventional *ex situ* processes, e.g. soil excavation and pump and treat, have been used for the remediation of PCE and TCE in groundwater (see reviews by Lemming et al., 2010; Pant and Pant, 2010). However, remediation of groundwater polluted with chlorinated hydrocarbons with these techniques is usually progressing relatively slow, the costs are high (mainly because of a high energy demand by the equipment), the structure of the aquifer was often physically destroyed by excavation and the treatment was inefficient (Bankston et al., 2013; Majone et al., 2015). The low efficiency of soil excavation is based on the density of PCE and TCE, which is higher than the density of water, leading to an enrichment of the pollutants below the groundwater (Pant and Pant, 2010). Water extraction techniques and subsequent *ex situ* treatment are impeded by the low water solubility and high volatility of the chlorinated alkenes: the pollutants easily adsorb to organic and sand particles (Aggarwal et al., 2006; Lee et al., 2007; Zytner, 1992) and volatilize into porous media in the head space of the groundwater (Marrin and Kerfoot, 1988; Pavlostathis and Mathavan, 1992). Based on their lack of efficiency and intrusion in environmental structures in the aquifer, conventional *ex situ* methods are not suited for the environmentally safe remediation of chlorinated hydrocarbon pollution in groundwater (Lemming et al., 2010b; Majone et al., 2015).

Thus, *in situ* treatment methods have been developed and increasingly used for the treatment of chlorinated hydrocarbons in the last two decades (Lemming et al., 2010a). To operate effectively with minimal maintenance over the time necessary for remediation, the *in situ* concept was further developed to establish permeable reactive barriers, emplaced into the groundwater to intercept the flow path of a contaminant plume (Faisal et al., 2018). With *in situ* methods, chemical oxidation of chlorinated hydrocarbons with permanganate (Watts and Teel, 2006), hydrogen peroxide (Gates

and Siegrist, 1995) and persulfate (Tsitonaki et al., 2010) were investigated. These oxidative treatments are expected to lead to a full mineralization of e.g. PCE to chloride, water and carbon dioxide (Yan and Schwartz, 1999). However, hydrogen peroxide is highly unstable and persulfate is only moderately stable in groundwater (Watts and Teel, 2006), demanding constant control of the remediation process and high amounts of the respective remedial agent. Additionally, transformation products of oxidative degradation often include reactive transformation products, potentially having a high toxicity. Considering the demand for large amounts of the remedial agent and the toxicity arising from reactive transformation products, the environmental risk of oxidative remedial techniques is likely to be higher than for the reductive-acting Carbo-Iron.

Reductive treatment for removal of chlorinated alkenes is an attractive option, based on high dechlorination rates, even at low temperatures, and the theoretical absence of chlorinated end products (Bruin et al., 1992). Compared to oxidative treatment techniques, the stoichiometric efficiency of reductive chlorinated hydrocarbons degradation is clearly higher. Several remediation agents are available and from those, $n\text{Fe}^0$ and composites with $n\text{Fe}^0$ were emerging in the past decade (Patil et al., 2016; Tosco et al., 2014). Though extensively used in the USA (Mueller et al., 2012) ERA for iron-based remedial agents are not available. However, based on results from ecotoxicity tests with several nano-iron particles (Bhuvaneshwari et al., 2017; Hjorth et al., 2017; Nguyen et al., 2018; Patil et al., 2016; Schiwy et al., 2016; Semerád et al., 2018; Xue et al., 2018; Zheng et al., 2008) it seems unlikely that the environmental risk of these remediation agents is higher than that of Carbo-Iron investigated in the present thesis.

Another *in situ* technique for the removal of chlorinated hydrocarbons from groundwater is bioremediation. This involves the extraction of groundwater, but unlike the pump & treat technology, the extracted groundwater is enriched with nutrients (e.g. soybean and lactate (Lemming et al., 2012)) and injected in a recharge well. The nutrients then activate the bacteria present in the groundwater, which results in the degradation of the contamination (Juwarkar et al., 2010). Three metabolic processes are able to degrade chlorinated ethenes: reductive dechlorination in anaerobic conditions, co-metabolism under anaerobic conditions and oxidation in aerobic or anaerobic conditions (Pant and Pant, 2010). Factors such as low temperature, anaerobic conditions, low levels of nutrients and co-substrates, the presence of contaminants in concentrations that can be toxic for the bacteria, and the physiological potential of microorganisms can limit the efficiency of microbial degradation of contaminants (Megharaj et al., 2011). Furthermore, in anaerobic conditions and depending on the presence of other organics acting as

electron donors, the possibility exists that the final or long-term transformation products of this remediation are dichloroethenes or vinyl chloride (Bardos et al., 2018; Russell et al., 1992). Dichloroethenes and vinyl chloride are more mobile than PCE and TCE (Chambon et al., 2010) and vinyl chloride is cancerogenic (see section 3.2). Moreover, the PNEC of 0.025 mg/L and the target value of 0.005 mg/L for vinyl chloride are the lowest of the pollutants investigated in the present thesis [D.1, Table 2 and D.2, Table S10]. Increasing concentrations of vinyl chloride would thus increase the chemical and ecotoxicological risk and the resulting environmental risk. This is, however, strongly depending on the aforementioned conditions in the groundwater.

A further alternative to the treatment of groundwater with Carbo-Iron is a no-action scenario. In this case, concentrations of the pollutants would be diluted by infiltrating ground water (Lemming et al., 2012). While this leads to lower pollutant concentrations, the contamination is spread over a larger area. Depending on the microbial community in the aquifer, natural bioremediation could potentially occur (Hancock et al., 2005). This process would take longer than any of the aforementioned remediation techniques and as mentioned for the induced bioremediation, the degradation of chlorinated alkenes to vinyl chloride is possible. Depending on the transformation products of the biological degradation (e.g. vinyl chloride) and the flow rates of the infiltrating groundwater, the environmental risk in the contaminated area would decrease very slowly: Lemming et al. (2012) estimated a time frame of 800 years necessary until TCE concentrations in the groundwater meet the quality criteria.

In summary, the *in situ* instalment of a reactive barrier with the reductive remediation agent Carbo-Iron is highly suitable for the treatment of chlorinated alkenes. Compared to pure $n\text{Fe}^0$, the composites of activated carbon and $n\text{Fe}^0$ have the benefit of higher remediation efficiency based on the adsorptive enrichment of hydrophobic contaminants (e.g. chlorinated alkenes) on the active carbon component and subsequent reductive reaction with the $n\text{Fe}^0$ component (Mackenzie et al., 2012). Additionally, the increased mobility of Carbo-Iron (Busch et al., 2015, 2014) facilitates the *in situ* installation of a permeable reactive barrier in the aquifer (Georgi et al., 2015).

However, a certain environmental risk of Carbo-Iron exists (i.e. by potentially temporary transformation products and Carbo-Irons impact on physico-chemical parameters in the groundwater, see section 4.4), though it is most likely limited to the area close to injection points in the contaminated site. Considering the comparatively low environmental risk (Lemming et al., 2010b), *in situ* bioremediation may represent a suitable alternative to the groundwater treatment with Carbo-Iron. During bioremediation, the favoured reductive dechlorination pathway of the

pollutants provided by $n\text{Fe}^0$ is possible, too. However, as mentioned above, degradation might not proceed completely to nontoxic products and dichloroethenes and vinyl chloride can accumulate. A thorough assessment of the respective contaminated site and the conditions in the groundwater is thus necessary to determine the suitability of bioremediation. In this context it should be considered that a stimulation of bioremediation was observed after the treatment of groundwater with $n\text{Fe}^0$ (Bardos et al., 2018) and Carbo-Iron (Vogel et al., 2018).

6 Conclusion and outlook

According to the OECD Working Party on Manufactured Nanomaterials, many existing OECD test guidelines are suitable for nanomaterials, while some need to be adapted to address specific methodological aspects. New test guidelines and guidance documents may be required to address endpoints that are more relevant to nanomaterials (see Rasmussen et al. 2016). This was criticized by Hansen et al. (2016), because the test guidelines had not been systematically checked for their suitability for the testing of nanomaterials. Moreover, the usually performed “round robin”-testing of the test methods for this validation had completely been neglected. By using the decision trees [A.1] test methods are subdivided in crucial steps. This could contribute to a harmonised approach for the systematic check of the suitability of existing guidelines as demanded by Hansen et al. (2016). Furthermore, the methods shown here were recently partially integrated in the OECD draft guidance document on aquatic and sediment toxicological testing of nanomaterials (1st commenting round, October 2018). Focusing on the first research question of the present study on appropriate testing strategies, the present results clearly outline how ecotoxicity tests should be designed to generate ecotoxicity data that fulfil the requirements for the ERA.

In the present thesis, standard test methods were modified by the integration of the aforementioned decision tools and effects of Carbo-Iron were determined with several organisms. By including additional endpoints and modified exposure durations, lower effect concentrations were obtained than in tests closely based on the respective test guidelines. The identified route of uptake for Carbo-Iron in the fish *D. rerio* [B.1] and the crustaceans *H. azteca* [C.1] and *D. magna* [D.1] was via ingestion into the gut. In fish, no effects on standard test endpoints were observed at concentrations up to 25 mg/L, but a significant effect of Carbo-Iron on the gut structure was recorded and a NOEC of 2.5 mg/L was determined. It remains to be clarified if and how this effect would influence fish at the population level. However, it should be noted that an exposure of pelagic fish to Carbo-Iron concentrations as described in the present study is highly unlikely. In case of an unintended release of Carbo-Iron into the environment, e.g. spilling, Carbo-Iron would be available in the water phase only briefly. *D. rerio* excreted Carbo-Iron completely after 5 d under control conditions and during that time the number of microvilli recovered to control level, indicating no persisting impairment and, thus, a low risk. Upon the intended release of Carbo-Iron for the remediation of groundwater, fish are not a relevant functional group. The few fish species that live in groundwater require cavernous aquifers as habitat. For such aquifers, a treatment with Carbo-Iron would not be suitable, mainly due to the comparable high flow velocities and the open spaces in this type of groundwater and the resulting problems on establishing a permeable reactive barrier. However, the precipitation of Carbo-Iron to the sediment leads to exposure of sediment-

associated invertebrates. Many crustacean species, among them *H. azteca*, forage on the sediment surface. Additionally, crustacea are abundant in groundwater. Therefore, the ecotoxicity tests with the two organisms of this group, *D. magna* and *H. azteca*, are highly relevant for the risk assessment of Carbo-Iron. In the present study, the retarded excretion of ingested Carbo-Iron observed in *H. azteca* resulted in effects on the energy budget, the offspring of exposed parental *H. azteca* and, ultimately, death. A similar mode of action is assumed for *D. magna* based on the findings in the present thesis. Overall, the most sensitive endpoint was reproduction in the chronic test with *D. magna* (NOEC=1 mg/L). A PNEC of 0.1 mg/L was derived for Carbo-Iron [D.1]. With the ecotoxicity tests performed, effect concentrations for Carbo-Iron were derived, which contribute to answering the second research question of the present thesis.

Using available data from column studies and a field study with Carbo-Iron to remediate a groundwater contaminated with chlorinated alkenes, environmental concentrations of Carbo-Iron were estimated [D.1]. In an area of approx. 10 m around the injection ports of Carbo-Iron, the risk quotients (i.e. the PEC/PNEC ratio) for Carbo-Iron are very high (5 to 6500). However, migration of Carbo-Iron beyond this area was considered unlikely, indicating and no environmental risk due to Carbo-Iron. These findings provide solid evidence to the third research question on the environmental risk of Carbo-Iron.

The injection ports for Carbo-Iron are located in the centre of the zone that is contaminated with chlorinated alkenes. In zone Ic, close to the injection ports, the risk quotients for TCE and PCE were up to 941 and 10, respectively [D.1]. Hence, is very likely that groundwater organisms in this zone were strongly affected by the chlorohydrocarbon pollution. The potentially added environmental risk by the use of Carbo-Iron in this groundwater was considered in the site-specific risk assessment [D.1], addressing the fourth research question, whether the treatment of a contaminated groundwater with Carbo-Iron increased or reduced the local environmental risk.

The results of the present thesis suggest an overall positive effect of Carbo-Iron on the environmental risk in the observed time frame of 190 d after the injection of Carbo-Iron. In the zones heavily contaminated with chlorinated alkenes, Carbo-Iron clearly reduced the environmental risk by reducing the pollutant concentrations. In the zones with lower concentrations of chlorinated alkenes, an increase of the environmental risk due to Carbo-Iron was discernible. However, in comparison to the beneficial effects of Carbo-Iron in the highly contaminated zones, these negative effects are probably temporary and minor.

If remediation of a contaminated site is considered necessary by the responsible authorities, an assessment of different possible treatment techniques should be performed. Among the available remediation agents, Carbo-Iron is highly suitable for the treatment of chlorinated alkenes. Based

on the results of the present thesis and a brief assessment of alternative treatment techniques, bioremediation is another suitable treatment for removal of chlorinated alkenes if the groundwater conditions favour reductive degradation and complete dehalogenation. In all other cases, the use of Carbo-Iron should be considered. Since Carbo-Iron can have positive effects on bioremediation, a combined or sequential use of both treatment methods might be possible.

7 References

- Aggarwal, V., Li, H., Boyd, S.A., Teppen, B.J., 2006. Enhanced sorption of trichloroethene by smectite clay exchanged with Cs⁺. *Environmental Science & Technology* 40, 894–899. DOI: 10.1021/es0500411
- An, D., Xi, B., Ren, J., Wang, Y., Jia, X., He, C., Li, Z., 2017. Sustainability assessment of groundwater remediation technologies based on multi-criteria decision making method. *Resources, Conservation and Recycling, Sustainable development paths for resource-constrained process industries* 119, 36–46. DOI: 10.1016/j.resconrec.2016.08.002
- An, D., Xi, B., Wang, Y., Xu, D., Tang, J., Dong, L., Ren, J., Pang, C., 2016. A sustainability assessment methodology for prioritizing the technologies of groundwater contamination remediation. *Journal of Cleaner Production* 112, 4647–4656. DOI: 10.1016/j.jclepro.2015.08.020
- Aramant, R., Elofsson, R., 1976. Monoaminergic neurons in the nervous system of crustaceans. *Cell Tissue Research* 170, 231–251. DOI: 10.1007/BF00224301
- Arnaud, C.H., 2010. Probing nanotoxicity. *Chemical & Engineering News* 88, 32–34.
- Auffan, M., Achouak, W., Rose, J., Roncato, M.-A., Chanéac, C., Waite, D.T., Masion, A., Woicik, J.C., Wiesner, M.R., Bottero, J.-Y., 2008. Relation between the redox state of iron-based nanoparticles and their cytotoxicity toward *Escherichia coli*. *Environmental Science & Technology* 42, 6730–6735. DOI: 10.1021/es800086f
- Auffan, M., Rose, J., Wiesner, M.R., Bottero, J.-Y., 2009. Chemical stability of metallic nanoparticles: A parameter controlling their potential cellular toxicity *in vitro*. *Environmental Pollution* 157, 1127–1133. DOI: 10.1016/j.envpol.2008.10.002
- Azimi, M., Bahrami, M.R., Hachesu, V.R., Reza, J.Z., Mihanpour, H., Sakhvidi, M.J.Z., Mostaghaci, M., 2017. Primary DNA damage in dry cleaners with perchlorethylene exposure. *International Journal of Occupational and Environmental Health* 8, 1089-224-31. DOI: 10.15171/ijoem.2017.1089
- Bankston, J., Blodgett, E., Karthikeyan, S., Richard, D., 2013. Chlorinated solvent treatment wetland. *Remediation Journal* 23, 59–69. DOI: 10.1002/rem.21366
- Bardos, P., Merly, C., Kvapil, P., Koschitzky, H.-P., 2018. Status of nanoremediation and its potential for future deployment: Risk-benefit and benchmarking appraisals. *Remediation Journal* 28, 43–56. DOI: 10.1002/rem.21559
- Bartsch, H., Montesano, R., 1975. Mutagenic and carcinogenic effects of vinyl chloride. *Mutation Research/Reviews in Genetic Toxicology* 32, 93–113. DOI: 10.1016/0165-1110(75)90001-9
- Bartzas, G., Tinivella, F., Medini, L., Zaharaki, D., Komnitsas, K., 2015. Assessment of groundwater contamination risk in an agricultural area in north Italy. *Information Processing in Agriculture* 2, 109–129. DOI: 10.1016/j.inpa.2015.06.004
- Baun, A., Kløft, L., Bjerg, P.L., Nyholm, N., 1999. Toxicity testing of organic chemicals in groundwater polluted with landfill leachate. *Environmental Toxicology and Chemistry* 18, 2046–2053. DOI: 10.1002/etc.5620180924
- Bhuvaneshwari, M., Kumar, D., Roy, R., Chakraborty, S., Parashar, A., Mukherjee, Anita, Chandrasekaran, N., Mukherjee, Amitava, 2017. Toxicity, accumulation, and trophic transfer of chemically and biologically synthesized nano zero valent iron in a two species freshwater food chain. *Aquatic Toxicology* 183, 63–75. DOI: 10.1016/j.aquatox.2016.12.013
- Bolognesi, C., Bruzzone, M., Ceppi, M., Kirsch-Volders, M., 2017. The lymphocyte cytokinesis block micronucleus test in human populations occupationally exposed to vinyl chloride: A systematic review and meta-analysis. *Mutation Research* 774, 1–11. DOI: 10.1016/j.mrrev.2017.07.003
- Boverhof, D., David, R., 2010. Nanomaterial characterization: considerations and needs for hazard assessment and safety evaluation. *Analytical and Bioanalytical Chemistry* 396, 953–961. DOI: 10.1007/s00216-009-3103-3
- Bruin, W.P. de, Kotterman, M.J., Posthumus, M.A., Schraa, G., Zehnder, A.J., 1992. Complete biological reductive transformation of tetrachloroethene to ethane. *Applied and Environmental Microbiology*. 58, 1996–2000.
- Bundschuh, M., Filser, J., Lüderwald, S., McKee, M.S., Metreveli, G., Schaumann, G.E., Schulz, R., Wagner, S., 2018. Nanoparticles in the environment: where do we come from, where do we go to? *Environmental Sciences Europe* 30, 6. DOI: 10.1186/s12302-018-0132-6

- Bundschuh, M., Zubrod, J.P., Englert, D., Seitz, F., Rosenfeldt, R.R., Schulz, R., 2011a. Effects of nano-TiO₂ in combination with ambient UV-irradiation on a leaf shredding amphipod. *Chemosphere* 85, 1563–1567. DOI: 10.1016/j.chemosphere.2011.07.060
- Bundschuh, M., Zubrod, J.P., Schulz, R., 2011b. The functional and physiological status of *Gammarus fossarum* (Crustacea; Amphipoda) exposed to secondary treated wastewater. *Environmental Pollution* 159, 244–249. DOI: 10.1016/j.envpol.2010.08.030
- Bundschuh, M., Zubrod, J.P., Seitz, F., Stang, C., Schulz, R., 2011c. Ecotoxicological evaluation of three tertiary wastewater treatment techniques via meta-analysis and feeding bioassays using *Gammarus fossarum*. *Journal of Hazardous Materials* 192, 772–778. DOI: 10.1016/j.jhazmat.2011.05.079
- Busch, J., Meißner, T., Potthoff, A., Bleyl, S., Georgi, A., Mackenzie, K., Trabitzzsch, R., Werban, U., Oswald, S.E., 2015. A field investigation on transport of carbon-supported nanoscale zero-valent iron (nZVI) in groundwater. *Journal of Contaminant Hydrology, Fate and Transport of Biocolloids and Nanoparticles in Soil and Groundwater Systems* 181, 59–68. DOI: 10.1016/j.jconhyd.2015.03.009
- Busch, J., Meißner, T., Potthoff, A., Oswald, S.E., 2014. Transport of carbon colloid supported nanoscale zero-valent iron in saturated porous media. *Journal of Contaminant Hydrology* 164, 25–34. DOI: 10.1016/j.jconhyd.2014.05.006
- Chambon, J.C., Broholm, M.M., Binning, P.J., Bjerg, P.L., 2010. Modeling multi-component transport and enhanced anaerobic dechlorination processes in a single fracture-clay matrix system. *Journal of Contaminant Hydrology, Frontiers in Reactive Transport: Microbial Dynamics and Redox Zonation in the Subsurface* 112, 77–90. DOI: 10.1016/j.jconhyd.2009.10.008
- Chen, A., Shang, C., Shao, J., Zhang, J., Huang, H., 2017. The application of iron-based technologies in uranium remediation: A review. *Science of The Total Environment* 575, 1291–1306. DOI: 10.1016/j.scitotenv.2016.09.211
- Clemente, Z., Castro, V.L.S.S., Moura, M.A.M., Jonsson, C.M., Fraceto, L.F., 2014. Toxicity assessment of TiO₂ nanoparticles in zebrafish embryos under different exposure conditions. *Aquatic Toxicology* 147, 129–139. DOI: 10.1016/j.aquatox.2013.12.024
- Coll, C., Notter, D., Gottschalk, F., Sun, T., Som, C., Nowack, B., 2016. Probabilistic environmental risk assessment of five nanomaterials (nano-TiO₂, nano-Ag, nano-ZnO, CNT, and fullerenes). *Nanotoxicology* 10, 436–444. DOI: 10.3109/17435390.2015.1073812
- Compernelle, T., Van Passel, S., Huisman, K., Kort, P., 2014. The option to abandon: Stimulating innovative groundwater remediation technologies characterized by technological uncertainty. *Science of The Total Environment* 496, 63–74. DOI: 10.1016/j.scitotenv.2014.07.019
- Corsi, I., Winther-Nielsen, M., Sethi, R., Punta, C., Della Torre, C., Libralato, G., Lofrano, G., Sabatini, L., Aiello, M., Fiordi, L., Cinuzzi, F., Caneschi, A., Pellegrini, D., Buttino, I., 2018. Ecofriendly nanotechnologies and nanomaterials for environmental applications: Key issue and consensus recommendations for sustainable and ecosafe nanoremediation. *Ecotoxicology and Environmental Safety* 154, 237–244. DOI: 10.1016/j.ecoenv.2018.02.037
- Crane, M., Handy, R.D., Garrod, J., Owen, R., 2008. Ecotoxicity test methods and environmental hazard assessment for engineered nanoparticles. *Ecotoxicology* 17, 421–37.
- Crommentuijn, T., Sijm, D., de Bruijn, J., van Leeuwen, K., van de Plassche, E., 2000. Maximum permissible and negligible concentrations for some organic substances and pesticides. *Journal of Environmental Management* 58, 297–312. DOI: 10.1006/jema.2000.0334
- Cronholm, P., Karlsson, H.L., Hedberg, J., Lowe, T.A., Winnberg, L., Elihn, K., Wallinder, I.O., Möller, L., 2013. Intracellular Uptake and Toxicity of Ag and CuO Nanoparticles: A Comparison Between Nanoparticles and their Corresponding Metal Ions. *Small* 9, 970–982. DOI: 10.1002/smll.201201069
- Cullen, L.G., Tilston, E.L., Mitchell, G.R., Collins, C.D., Shaw, L.J., 2011. Assessing the impact of nano- and micro-scale zerovalent iron particles on soil microbial activities: Particle reactivity interferes with assay conditions and interpretation of genuine microbial effects. *Chemosphere* 82, 1675–1682. DOI: 10.1016/j.chemosphere.2010.11.009
- Cundy, A.B., Hopkinson, L., Whitby, R.L.D., 2008. Use of iron-based technologies in contaminated land and groundwater remediation: A review. *Science of The Total Environment* 400, 42–51. DOI: 10.1016/j.scitotenv.2008.07.002

- Dabrunz, A., Duester, L., Prasse, C., Seitz, F., Rosenfeldt, R., Schilde, C., Schaumann, G.E., Schulz, R., 2011. Biological Surface Coating and Molting Inhibition as Mechanisms of TiO₂ Nanoparticle Toxicity in *Daphnia magna*. *PLoS ONE* 6, e20112. DOI: 10.1371/journal.pone.0020112
- Dagnino, A., Sforzini, S., Dondero, F., Fenoglio, S., Bona, E., Jensen, J., Viarengo, A., 2008. A weight-of-evidence approach for the integration of environmental “Triad” data to assess ecological risk and biological vulnerability. *Integrated Environmental Assessment and Management* 4, 314–326. DOI: 10.1897/IEAM_2007-067.1
- Danielopol, D.L., 1989. Groundwater Fauna Associated with Riverine Aquifers. *Journal of the North American Benthological Society* 8, 18–35.
- Danielopol, D.L., Gibert, J., Griebler, C., Gunatilaka, A., Hahn, D. habil H.J., Messana, G., Notenboom, J., Sket, B., 2004. Comment: Incorporating ecological perspectives in European groundwater management policy. *Environmental Conservation* 31, 185–189.
- Davis, J.M., 2007. How to assess the risks of nanotechnology: learning from past experience. *Journal Nanosciences and Nanotechnologies* 7, 402–409.
- Delmaar, C.J.E., Peijnenburg, W.J.G.M., Oomen, A.G., Chen, J., Jong, W.H. de, Sips, A.J.A.M., Wang, Z., Park, M.V.D.Z., 2015. A practical approach to determine dose metrics for nanomaterials. *Environmental Toxicology and Chemistry* 34, 1015–1022. DOI: 10.1002/etc.2878
- Deni, J., Penninckx, M.J., 1999. Nitrification and autotrophic nitrifying bacteria in a hydrocarbon-polluted soil. *Applied and Environmental Microbiology* 65, 4008–4013.
- Dutra, B.K., Castiglioni, D.S., Santos, R.B., Bond-Buckup, G., Oliveira, G.T., 2007. Seasonal variations of the energy metabolism of two sympatric species of *Hyalella* (Crustacea, Amphipoda, Dogielinotidae) in the southern Brazilian highlands. *Comparative Biochemistry and Physiology Part A: Molecular & Integrative Physiology*, 148, 239–247. DOI: 10.1016/j.cbpa.2007.04.013
- EC, 2006. Directive 2006/118/EC of the European Parliament and of the Council of 12 December 2006 on the protection of groundwater against pollution and deterioration. (No. L 372).
- ECHA, 2017. Guidance on information requirements and chemical safety assessment. Chapter R.7.b: Endpoint specific guidance. European Chemicals Agency.
- ECHA, 2016. Guidance on information requirements and chemical safety assessment - Part E: Risk Characterisation.
- ECHA, 2008. Guidance on information requirements and chemical safety assessment - Chapter R.10: Characterisation of dose [concentration]-response for environment.
- Edgington, A.J., Petersen, E.J., Herzing, A.A., Podila, R., Rao, A., Klaine, S.J., 2014. Microscopic investigation of single-wall carbon nanotube uptake by *Daphnia magna*. *Nanotoxicology* 8, 2–10. DOI: 10.3109/17435390.2013.847504
- EEA. 2018. https://tableau.discomap.eea.europa.eu/t/Wateronline/views/WISE_SOW_gwPollutant/GWB_gwPollutant_Europe_G?:embed=y&:showAppBanner=false&:showShareOptions=true&:display_count=no&:showVizHome=no. Accessed 04. April 2019.
- European Communities, 1998. Council Directive 98/83/EC on the quality of water intended for human consumption.
- Ezzatahmedi, N., Ayoko, G.A., Millar, G.J., Speight, R., Yan, C., Li, J., Li, S., Zhu, J., Xi, Y., 2017. Clay-supported nanoscale zero-valent iron composite materials for the remediation of contaminated aqueous solutions: A review. *Chemical Engineering Journal* 312, 336–350. DOI: 10.1016/j.cej.2016.11.154
- Fairbrother, A., Fairbrother, J.R., 2009. Are environmental regulations keeping up with innovation? A case study of the nanotechnology industry. *Ecotoxicology and environmental safety* 72, 1327–30.
- Faisal, A.A.H., Sulaymon, A.H., Khaliefa, Q.M., 2018. A review of permeable reactive barrier as passive sustainable technology for groundwater remediation. *International Journal of Environmental Science & Technology* 15, 1123–1138. DOI: 10.1007/s13762-017-1466-0
- Fan, D., Gilbert, E.J., Fox, T., 2017. Current state of in situ subsurface remediation by activated carbon-based amendments. *Journal of Environmental Management* 204, 793–803. DOI: 10.1016/j.jenvman.2017.02.014

- Fu, F., Dionysiou, D.D., Liu, H., 2014. The use of zero-valent iron for groundwater remediation and wastewater treatment: A review. *Journal of Hazardous Materials* 267, 194–205. DOI: 10.1016/j.jhazmat.2013.12.062
- Galassi, D.M.P., 2001. Groundwater copepods: diversity patterns over ecological and evolutionary scales. *Hydrobiologia* 453–454, 227–253. DOI: 10.1023/A:1013100924948
- Gates D. D., Siegrist R. L., 1995. *In-situ* chemical oxidation of trichloroethylene using hydrogen peroxide. *Journal of Environmental Engineering* 121, 639–644. DOI: 10.1061/(ASCE)0733-9372(1995)121:9(639)
- Georgi, A., Schierz, A., Mackenzie, K., Kopinke, F.-D., 2015. Colloidal activated carbon for in-situ groundwater remediation — Transport characteristics and adsorption of organic compounds in water-saturated sediment columns. *Journal of Contaminant Hydrology* 179, 76–88. DOI: 10.1016/j.jconhyd.2015.05.002
- Gibert, J., Danielopol, D., Stanford, J.A., 1994. Groundwater ecology. Academic Press, San Diego, USA,
- Gleeson, T., Wada, Y., Bierkens, M.F.P., van Beek, L.P.H., 2012. Water balance of global aquifers revealed by groundwater footprint. *Nature* 488, 197–200. DOI: 10.1038/nature11295
- Gonçalves, J.R., 2016. The soil and groundwater remediation with zero valent iron nanoparticles. *Procedia Engineering, Advances in Transportation Geotechnics III* 143, 1268–1275. DOI: 10.1016/j.proeng.2016.06.122
- Griebler, C., Avramov, M., 2015. Groundwater ecosystem services: a review. *Freshwater Science* 34, 355–367. DOI: 10.1086/679903
- Grieger, K.D., Fjordbøge, A., Hartmann, N.B., Eriksson, E., Bjerg, P.L., Baun, A., 2010. Environmental benefits and risks of zero-valent iron nanoparticles (nZVI) for in situ remediation: Risk mitigation or trade-off? *Journal of Contaminant Hydrology* 118, 165–183. DOI: 10.1016/j.jconhyd.2010.07.011
- Grieger, K.D., Hansen, S.F., Baun, A., 2009. The known unknowns of nanomaterials: Describing and characterizing uncertainty within environmental, health and safety risks. *Nanotoxicology* 3, 222–233. DOI: 10.1080/17435390902944069
- Griffitt, R.J., Luo, J., Gao, J., Bonzongo, J.-C., Barber, D.S., 2008. Effects of particle composition and species on toxicity of metallic nanomaterials in aquatic organisms. *Environmental toxicology and chemistry* 27, 1972–8.
- Hahn, H.J., 2009. A proposal for an extended typology of groundwater habitats. *Hydrogeology Journal* 17, 77–81. DOI: 10.1007/s10040-008-0363-5
- Hahn, H.J., Fuchs, A., 2009. Distribution patterns of groundwater communities across aquifer types in southwestern Germany. *Freshwater Biology* 54, 848–860. DOI: 10.1111/j.1365-2427.2008.02132.x
- Hancock, P.J., Boulton, A.J., Humphreys, W.F., 2005. Aquifers and hyporheic zones: Towards an ecological understanding of groundwater. *Hydrogeology Journal* 13, 98–111. DOI: 10.1007/s10040-004-0421-6
- Handy, Richard D., Brink, N. van den, Chappell, M., Mühlhng, M., Behra, R., Dušinská, M., Simpson, P., Ahtiainen, J., Jha, A.N., Seiter, J., Bednar, A., Kennedy, A., Fernandes, T.F., Riediker, M., 2012. Practical considerations for conducting ecotoxicity test methods with manufactured nanomaterials: what have we learnt so far? *Ecotoxicology* 21, 933–972. DOI: 10.1007/s10646-012-0862-y
- Handy, Richard D, Cornelis, G., Fernandes, T., Tsyusko, O., Decho, A., Sabo-Attwood, T., Metcalfe, C., Steevens, J.A., Klaine, S.J., Koelmans, A.A., Horne, N., 2012. Ecotoxicity test methods for engineered nanomaterials: Practical experiences and recommendations from the bench. *Environmental Toxicology and Chemistry* 31, 15–31. DOI: 10.1002/etc.706
- Handy, R.D., Owen, R., Valsami-Jones, E., 2008. The ecotoxicology of nanoparticles and nanomaterials: current status, knowledge gaps, challenges, and future needs. *Ecotoxicology* 17, 315–25. DOI: 10.1007/s10646-008-0206-0
- Hansen, S.F., Hjorth, R., Skjolding, L.M., Bowman, D.M., Maynard, A., Baun, A., 2016. A critical analysis of the environmental dossiers from the OECD sponsorship programme for the testing of manufactured nanomaterials. *Environmental Science: Nano* 4, 282–291. DOI: 10.1039/C6EN00465B
- Hansen, S.F., Maynard, A., Baun, A., Tickner, J.A., 2008a. Late lessons from early warnings for nanotechnology. *Nature Nanotechnology* 3, 444–447. DOI: 10.1038/nnano.2008.198

- Hansen, S.F., von Krauss, M.K., Tickner, J.A., 2008b. The precautionary principle and risk-risk tradeoffs. *Journal of Risk Research* 11, 423–464. DOI: 10.1080/13669870801967192
- Harzsch, S., 2006. Neurophylogeny: Architecture of the nervous system and a fresh view on arthropod phylogeny. *Integrative and Comparative Biology* 46, 162–194. DOI: 10.1093/icb/icj011
- Heinlaan, M., Kahru, A., Kasemets, K., Arbeille, B., Prensier, G., Dubourguier, H.-C., 2011. Changes in the *Daphnia magna* midgut upon ingestion of copper oxide nanoparticles: a transmission electron microscopy study. *Water Research* 45, 179–190. DOI: 10.1016/j.watres.2010.08.026
- Henry, T.B., Petersen, E.J., Compton, R.N., 2011. Aqueous fullerene aggregates (nC60) generate minimal reactive oxygen species and are of low toxicity in fish: a revision of previous reports. *Current Opinion in Biotechnology* 22, 533–537. DOI: 10.1016/j.copbio.2011.05.511
- Henschler, D., Bonse, G., 1977. Metabolic activation of chlorinated ethylenes: dependence of mutagenic effect on electrophilic reactivity of the metabolically formed epoxides. *Archives of Toxicology* 39, 7–12. DOI: 10.1007/BF00343270
- Hjorth, R., Coutris, C., Nguyen, N.H.A., Sevcu, A., Gallego-Urrea, J.A., Baun, A., Joner, E.J., 2017. Ecotoxicity testing and environmental risk assessment of iron nanomaterials for sub-surface remediation – Recommendations from the FP7 project NanoRem. *Chemosphere* 182, 525–531. DOI: 10.1016/j.chemosphere.2017.05.060
- Hoheisel, S.M., Diamond, S., Mount, D., 2012. Comparison of nanosilver and ionic silver toxicity in *Daphnia magna* and *Pimephales promelas*. *Environmental Toxicology and Chemistry* 31, 2557–2563. DOI: 10.1002/etc.1978
- Höss, S., Fritzsche, A., Meyer, C., Bosch, J., Meckenstock, R.U., Totsche, K.U., 2015. Size- and composition-dependent toxicity of synthetic and soil-derived Fe oxide colloids for the nematode *Caenorhabditis elegans*. *Environmental Science & Technology* 49, 544–552. DOI: 10.1021/es503559n
- Hua, J., Vijver, M.G., Ahmad, F., Richardson, M.K., Peijnenburg, W.J.G.M., 2014. Toxicity of different-sized copper nano- and submicron particles and their shed copper ions to zebrafish embryos. *Environmental Toxicology and Chemistry* 33, 1774–1782. DOI: 10.1002/etc.2615
- Hund-Rinke, K., Simon, M., 2006. Ecotoxic effect of photocatalytic active nanoparticles (TiO₂) on algae and daphnids. *Environmental science and pollution research international* 13, 225–32. DOI: 10.1065/espr2006.06.311
- Icely, J.D., Nott, J.A., 1985. Feeding and digestion in *Corophium volutator* (Crustacea: Amphipoda). *Mar. Biol.* 89, 183–195. DOI: 10.1007/BF00392889
- Jovanović, B., Palić, D., 2012. Immunotoxicology of non-functionalized engineered nanoparticles in aquatic organisms with special emphasis on fish - Review of current knowledge, gap identification, and call for further research. *Aquatic Toxicology* 118–119, 141–151. DOI: 10.1016/j.aquatox.2012.04.005
- Juwarkar, A.A., Singh, S.K., Mudhoo, A., 2010. A comprehensive overview of elements in bioremediation. *Reviews in Environmental Science and Biotechnology* 9, 215–288. DOI: 10.1007/s11157-010-9215-6
- Kargar, M., Nadafi, K., Nabizadeh, R., Nasseri, S., Mesdaghinia, A., Mahvi, A.H., Alimohammadi, M., Nazmara, S., Rastkari, N., 2012. Survey of hazardous organic compounds in the groundwater, air and wastewater effluents near the Tehran automobile industry. *Bulletin of Environmental Contamination and Toxicology* 90, 155–159. DOI: 10.1007/s00128-012-0890-6
- Karlsson, H.L., Gustafsson, J., Cronholm, P., Möller, L., 2009. Size-dependent toxicity of metal oxide particles - a comparison between nano- and micrometer size. *Toxicology Letters* 188, 112–118. DOI: 10.1016/j.toxlet.2009.03.014
- Karn, B., Kuiken, T., Otto, M., 2009. Nanotechnology and in situ remediation: A review of the benefits and potential risks. *Environmental Health Perspectives* DOI: 10.1289/ehp.0900793
- Keller, A.A., Wang, H., Zhou, D., Lenihan, H.S., Cherr, G., Cardinale, B.J., Miller, R., Ji, Z., 2010. Stability and aggregation of metal oxide nanoparticles in natural aqueous matrices. *Environmental Science & Technology* 44, 1962–1967. DOI: 10.1021/es902987d
- Kennedy, A.J., Hull, M.S., Steevens, J. a, Dontsova, K.M., Chappell, M., Gunter, J.C., Weiss, C. 2008. Factors influencing the partitioning and toxicity of nanotubes in the aquatic environment. *Environmental Toxicology and Chemistry* 27, 1932–41. DOI: 10.1897/07-624.1

- Khadam, I.M., Kaluarachchi, J.J., 2003. Multi-criteria decision analysis with probabilistic risk assessment for the management of contaminated ground water. *Environmental Impact Assessment Review* 23, 683–721. DOI: 10.1016/S0195-9255(03)00117-3
- Kløve, B., Ala-aho, P., Bertrand, G., Boukalova, Z., Ertürk, A., Goldscheider, N., Ilmonen, J., Karakaya, N., Kupfersberger, H., Kværner, J., Lundberg, A., Mileusnić, M., Moszczynska, A., Muotka, T., Preda, E., Rossi, P., Siergieiev, D., Šimek, J., Wachniew, P., Angheluta, V., Widerlund, A., 2011. Groundwater dependent ecosystems. Part I: Hydroecological status and trends. *Environmental Science & Policy, Adapting to Climate Change: Reducing Water-related Risks in Europe* 14, 770–781. DOI: 10.1016/j.envsci.2011.04.002
- Kocur, C.M., Chowdhury, A.I., Sakulchaicharoen, N., Boparai, H.K., Weber, K.P., Sharma, P., Krol, M.M., Austrins, L., Peace, C., Sleep, B.E., O’Carroll, D.M., 2014. Characterization of nZVI mobility in a field scale test. *Environmental Science & Technology* DOI: 10.1021/es4044209
- Kristensen, P., Whalley, C., Néry, F., Zal, N., Christiansen, T., 2018. European waters: assessment of status and pressures 2018.
- Kühnel, D., Nickel, C., 2014. The OECD expert meeting on ecotoxicology and environmental fate — Towards the development of improved OECD guidelines for the testing of nanomaterials. *Science of The Total Environment* 472, 347–353. DOI: 10.1016/j.scitotenv.2013.11.055
- Lee Chi-Yuan, Cheng Shung-Zen, Chang Chun-Kai, Lee Fang-Yin, Liao Chiu-Jung, 2007. Simplified approach for rapid estimation of trichloroethylene adsorption onto soils. *Practice Periodical of Hazardous, Toxic, and Radioactive Waste Management* 11, 172–176. DOI: 10.1061/(ASCE)1090-025X(2007)11:3(172)
- Lemming, G., Chambon, J.C., Binning, P.J., Bjerg, P.L., 2012. Is there an environmental benefit from remediation of a contaminated site? Combined assessments of the risk reduction and life cycle impact of remediation. *Journal of Environmental Management*. 112, 392–403. DOI: 10.1016/j.jenvman.2012.08.002
- Lemming, G., Hauschild, M.Z., Bjerg, P.L., 2010a. Life cycle assessment of soil and groundwater remediation technologies: literature review. *International Journal of Life Cycle Assessment* 15, 115. DOI: 10.1007/s11367-009-0129-x
- Lemming, G., Hauschild, M.Z., Chambon, J., Binning, P.J., Bulle, C., Margni, M., Bjerg, P.L., 2010b. Environmental impacts of remediation of a trichloroethene-contaminated site: life cycle assessment of remediation alternatives. *Environmental Science & Technology* 44, 9163–9169. DOI: 10.1021/es102007s
- Li, X., Elliott, D.W., Zhang, W., 2006. Zero-valent iron nanoparticles for abatement of environmental pollutants: materials and engineering aspects. *Critical Reviews in Solid State and Materials Sciences* 31, 111-122. DOI: 10.1080/10408430601057611
- Lin, J., Zhang, H., Chen, Z., Zheng, Y., 2010. Penetration of lipid membranes by gold nanoparticles: insights into cellular uptake, cytotoxicity, and their relationship. *ACS Nano* 4, 5421–5429. DOI: 10.1021/nn1010792
- Lovern, S.B., Owen, H.A., Klaper, R., 2008. Electron microscopy of gold nanoparticle intake in the gut of *Daphnia magna*. *Nanotoxicology* 2, 43–48. DOI: 10.1080/17435390801935960
- Mackenzie, K., Bleyl, S., Georgi, A., Kopinke, F.-D., 2012. Carbo-Iron – An Fe/AC composite – As alternative to nano-iron for groundwater treatment. *Water Research* 46, 3817–3826. DOI: 10.1016/j.watres.2012.04.013
- Mackenzie, K., Bleyl, S., Kopinke, F.-D., Doose, H., Bruns, J., 2016. Carbo-Iron as improvement of the nanoiron technology: From laboratory design to the field test. *Science of The Total Environment*. DOI: 10.1016/j.scitotenv.2015.07.107
- Majone, M., Verdini, R., Aulenta, F., Rossetti, S., Tandoi, V., Kalogerakis, N., Agathos, S., Puig, S., Zanaroli, G., Fava, F., 2015. *In situ* groundwater and sediment bioremediation: barriers and perspectives at European contaminated sites. *New Biotechnology* 32, 133–146. DOI: 10.1016/j.nbt.2014.02.011
- Marrin, D.L., Kerfoot, H.B., 1988. Soil-gas surveying techniques. *Environmental Science & Technology* 22, 740–745. DOI: 10.1021/es00172a001
- Mattsson, K., Adolfsson, K., Ekvall, M.T., Borgström, M.T., Linse, S., Hansson, L.-A., Cedervall, T., Prinz, C.N., 2016. Translocation of 40 nm diameter nanowires through the intestinal epithelium of *Daphnia magna*. *Nanotoxicology* 10, 1160–1167. DOI: 10.1080/17435390.2016.1189615

References

- McShan, D., Ray, P.C., Yu, H., 2014. Molecular toxicity mechanism of nanosilver. *Journal of Food and Drug Analysis, Nanomaterials - Toxicology and Medical Applications* 22, 116–127. DOI: 10.1016/j.jfda.2014.01.010
- Megharaj, M., Ramakrishnan, B., Venkateswarlu, K., Sethunathan, N., Naidu, R., 2011. Bioremediation approaches for organic pollutants: A critical perspective. *Environment International* 37, 1362–1375. DOI: 10.1016/j.envint.2011.06.003
- Moran, M.J., Zogorski, J.S., Squillace, P.J., 2007. Chlorinated solvents in groundwater of the united states. *Environmental Science & Technology* 41, 74–81. DOI: 10.1021/es061553y
- Mueller, N.C., Braun, J., Bruns, J., Černík, M., Rissing, P., Rickerby, D., Nowack, B., 2012. Application of nanoscale zero valent iron (nZVI) for groundwater remediation in Europe. *Environmental Science and Pollution Research* 19, 550–558. DOI: 10.1007/s11356-011-0576-3
- Musolff, A., Leschik, S., Reinstorf, F., Strauch, G., Schirmer, M., 2010. Micropollutant loads in the urban water cycle. *Environmental Science & Technology* 44, 4877–4883. DOI: 10.1021/es903823a
- Nguyen, N.H.A., Von Moos, N.R., Slaveykova, V.I., Mackenzie, K., Meckenstock, R.U., Thümmler, S., Bosch, J., Ševců, A., 2018. Biological effects of four iron-containing nanoremediation materials on the green alga *Chlamydomonas sp.* *Ecotoxicology and Environmental Safety* 154, 36–44. DOI: 10.1016/j.ecoenv.2018.02.027
- Noss, C., Dabrunz, A., Rosenfeldt, R.R., Lorke, A., Schulz, R., 2013. Three-dimensional analysis of the swimming behavior of *Daphnia magna* exposed to nanosized titanium dioxide. *PLoS One* 8. DOI: 10.1371/journal.pone.0080960
- Obiri-Nyarko, F., Grajales-Mesa, S.J., Malina, G., 2014. An overview of permeable reactive barriers for in situ sustainable groundwater remediation. *Chemosphere* 111, 243–259. DOI: 10.1016/j.chemosphere.2014.03.112
- OECD, 2013a. OECD guideline for testing of chemicals. 236. Fish embryo acute toxicity test. Organisation for Economic Co-operation and Development, Paris, France.
- OECD, 2013b. OECD guideline for testing of chemicals. 210. Fish, early life stage toxicity test. Organisation for Economic Co-operation and Development, Paris, France.
- OECD, 2012a. OECD guideline for testing of chemicals. 211. *Daphnia magna* reproduction test. Organisation for Economic Co-operation and Development, Paris, France.
- OECD, 2012b. Guidance on sample preparation and dosimetry for the safety testing of manufactured nanomaterials (No. ENV/JM/MONO(2012)40), Series on the Safety of Manufactured Nanomaterials. Organisation for Economic Co-operation and Development, Paris, France.
- OECD, 2011. OECD guideline for testing of chemicals. 201. Freshwater algae and cyanobacteria, growth inhibition test. Organisation for Economic Co-operation and Development.
- OECD, 2010. Preliminary Guidance Notes on Sample Preparation and Dosimetry for the Safety Testing of Manufactured Nanomaterials (No. ENV/JM/MONO(2010)25). Organisation for Economic Co-operation and Development, Paris, France.
- OECD, 2009. Preliminary review of OECD test guidelines for their applicability to manufactured nanomaterials (No. ENV/JM/MONO(2009)21). Organisation for Economic Co-operation and Development, Paris, France.
- OECD, 2004a. OECD guideline for testing of chemicals. 202. *Daphnia sp.*, acute immobilisation test. Organisation for Economic Co-operation and Development, Paris, France.
- OECD, 2004b. OECD guideline for testing of chemicals. 219. Sediment-water chironomid toxicity test using spiked water. Organisation for Economic Co-operation and Development, Paris, France.
- OECD, 1992a. OECD guideline for testing of chemicals. 203. Fish, acute toxicity test. Organisation for Economic Co-operation and Development, Paris, France.
- Pant, P., Pant, S., 2010. A review: Advances in microbial remediation of trichloroethylene (TCE). *Journal of Environmental Sciences* 22, 116–126. DOI: 10.1016/S1001-0742(09)60082-6
- Patil, S.S., Shedbalkar, U.U., Truskewycz, A., Chopade, B.A., Ball, A.S., 2016. Nanoparticles for environmental clean-up: A review of potential risks and emerging solutions. *Environmental Technology & Innovation* 5, 10–21. DOI: 10.1016/j.eti.2015.11.001

- Pavlostathis, S.G., Mathavan, G.N., 1992. Desorption kinetics of selected volatile organic compounds from field contaminated soils. *Environmental Science & Technology* 26, 532–538. DOI: 10.1021/es00027a014
- Petersen, E.J., Diamond, S.A., Kennedy, A.J., Goss, G.G., Ho, K., Lead, J., Hanna, S.K., Hartmann, N.B., Hund-Rinke, K., Mader, B., Manier, N., Pandard, P., Salinas, E.R., Sayre, P., 2015. Adapting OECD aquatic toxicity tests for use with manufactured nanomaterials: key issues and consensus recommendations. *Environmental Science & Technology* 49, 9532–9547. DOI: 10.1021/acs.est.5b00997
- Petersen, E.J., Zhang, L., Mattison, N.T., O'Carroll, D.M., Whelton, A.J., Uddin, N., Nguyen, T., Huang, Q., Henry, T.B., Holbrook, R.D., Chen, K.L., 2011. Potential release pathways, environmental fate, and ecological risks of carbon nanotubes. *Environmental Science & Technology* 45, 9837–9856. DOI: 10.1021/es201579y
- Phenrat, T., Kim, H.-J., Fagerlund, F., Illangasekare, T., Tilton, R.D., Lowry, G.V., 2009. Particle size distribution, concentration, and magnetic attraction affect transport of polymer-modified Fe⁰ nanoparticles in sand columns. *Environmental Science & Technology* 43, 5079–5085. DOI: 10.1021/es900171v
- Ponder, S.M., Darab, J.G., Mallouk, T.E., 2000. Remediation of Cr(VI) and Pb(II) aqueous solutions using supported, nanoscale zero-valent iron. *Environmental Science & Technology* 34, 2564–2569. DOI: 10.1021/es9911420
- Quaglia, A., Sabelli, B., Villani, L., 1976. Studies on the intestine of Daphnidae (Crustacea, Cladocera) ultrastructure of the midgut of *Daphnia magna* and *Daphnia obtusa*. *Journal of Morphology* 150, 711–725. DOI: 10.1002/jmor.1051500306
- Rail, C.D., 1989. Groundwater contamination: Sources, control, and preventive measures. Lancaster, PA (US); Technomic Publishing Co.
- Rasche, M.E., Hyman, M.R., Arp, D.J., 1990. Biodegradation of halogenated hydrocarbon fumigants by nitrifying bacteria. *Applied and Environmental Microbiology* 56, 2568–2571.
- Rasmussen, K., González, M., Kearns, P., Sintes, J.R., Rossi, F., Sayre, P., 2016. Review of achievements of the OECD working party on manufactured nanomaterials' testing and assessment programme. From exploratory testing to test guidelines. *Regulatory Toxicology and Pharmacology* 74, 147–160. DOI: 10.1016/j.yrtph.2015.11.004
- Ren, L., He, L., Lu, H., Li, J., 2017. Rough-interval-based multicriteria decision analysis for remediation of 1,1-dichloroethane contaminated groundwater. *Chemosphere* 168, 244–253. DOI: 10.1016/j.chemosphere.2016.10.042
- Rist, S., Baun, A., Hartmann, N.B., 2017. Ingestion of micro- and nanoplastics in *Daphnia magna* - Quantification of body burdens and assessment of feeding rates and reproduction. *Environmental Pollution* 228, 398–407. DOI: 10.1016/j.envpol.2017.05.048
- Roy, R., Das, M., Dwivedi, P.D., 2015. Toxicological mode of action of ZnO nanoparticles: Impact on immune cells. *Molecular Immunology* 63, 184–192. DOI: 10.1016/j.molimm.2014.08.001
- Russell, H.H., Matthews, J.E., Sewell, G.W., 1992. Ground water issue: TCE removal from contaminated soil and ground water. US EPA, EPA/540/S-90/002.
- Schäfers, C., Wenzel, A., Lukow, T., Sehr, I., Egert, E., 2001. Ökotoxikologische Prüfung von Pflanzenschutzmitteln hinsichtlich ihres Potentials zur Grundwassergefährdung. UBA Texte 76.
- Schiwy, A., Maes, H.M., Koske, D., Flecken, M., Schmidt, K.R., Schell, H., Tiehm, A., Kamptner, A., Thümmler, S., Stanjek, H., Heggen, M., Dunin-Borkowski, R.E., Braun, J., Schäffer, A., Hollert, H., 2016. The ecotoxic potential of a new zero-valent iron nanomaterial, designed for the elimination of halogenated pollutants, and its effect on reductive dechlorinating microbial communities. *Environmental Pollution*. DOI: 10.1016/j.envpol.2016.05.051
- Seitz, F., Rosenfeldt, R.R., Schneider, S., Schulz, R., Bundschuh, M., 2014. Size-, surface- and crystalline structure composition-related effects of titanium dioxide nanoparticles during their aquatic life cycle. *Science of The Total Environment*. 493, 891–897. DOI: 10.1016/j.scitotenv.2014.06.092
- Semerád, J., Čvančarová, M., Filip, J., Kašík, J., Zlotá, J., Soukupová, J., Cajthaml, T., 2018. Novel assay for the toxicity evaluation of nanoscale zero-valent iron and derived nanomaterials based on lipid peroxidation in bacterial species. *Chemosphere* 213, 568–577. DOI: 10.1016/j.chemosphere.2018.09.029

References

- Sevcikova, M., Modra, H., Slaninova, A., Svobodova, Z., 2011. Metals as a cause of oxidative stress in fish: a review. *Veterinární Medicína* 56, 537–546. DOI: 10.17221/4272-VETMED
- Skjolding, L.M., Sørensen, S.N., Hartmann, N.B., Hjorth, R., Hansen, S.F., Baun, A., 2016. Aquatic ecotoxicity testing of nanoparticles - The quest to disclose nanoparticle effects. *Angewandte Chemie International Edition* 55, 15224–15239. DOI: 10.1002/anie.201604964
- Song, W., Zhang, Jinyang, Guo, J., Zhang, Jinhua, Ding, F., Li, L., Sun, Z., 2010. Role of the dissolved zinc ion and reactive oxygen species in cytotoxicity of ZnO nanoparticles. *Toxicology Letters* 199, 389–397. DOI: 10.1016/j.toxlet.2010.10.003
- Storch, V., 1987. Microscopic anatomy and ultrastructure of the stomach of *Porcellio scaber* (Crustacea, Isopoda). *Zoomorphology* 106, 301–311. DOI: 10.1007/BF00312004
- Stuart, M., Lapworth, D., Crane, E., Hart, A., 2012. Review of risk from potential emerging contaminants in UK groundwater. *Science of The Total Environment* 416, 1–21. DOI: 10.1016/j.scitotenv.2011.11.072
- Swartjes, F.A., 1999. Risk-based assessment of soil and groundwater quality in the Netherlands: Standards and remediation urgency. *Risk Analysis* 19, 1235–1249. DOI: 10.1023/A:1007003332488
- Thwala, M., Klaine, S.J., Musee, N., 2016. Interactions of metal-based engineered nanoparticles with aquatic higher plants: A review of the state of current knowledge. *Environmental Toxicology and Chemistry* 35, 1677–1694. DOI: 10.1002/etc.3364
- Tirelli, V., Mayzaud, P., 2005. Relationship between functional response and gut transit time in the calanoid copepod *Acartia clausi*: role of food quantity and quality. *Journal of Plankton Research* 27, 557–568. DOI: 10.1093/plankt/fbi031
- Tosco, T., Petrangeli Papini, M., Cruz Viggi, C., Sethi, R., 2014. Nanoscale zerovalent iron particles for groundwater remediation: a review. *Journal of Cleaner Production, Emerging Industrial Processes For Water Management* 77, 10–21. DOI: 10.1016/j.jclepro.2013.12.026
- Tsitonaki, A., PETRI, B., CRIMI, M., MOSBÆK, H., SIEGRIST, R.L., BJERG, P.L., 2010. *In situ* chemical oxidation of contaminated soil and groundwater using persulfate: a review. *Critical Reviews in Environmental Science and Technology* 40, 55–91. DOI: 10.1080/10643380802039303
- US EPA, 2000. 600/R-99/064 Methods for measuring the toxicity and bioaccumulation of sediment-associated contaminants with freshwater invertebrates. Washington, D.C., USA.
- Valko, M., Morris, H., Cronin, M.T.D., 2005. Metals, toxicity and oxidative stress. *Current Medicinal Chemistry* 12, 1161–1208.
- Vogel, M., Nijenhuis, I., Lloyd, J., Boothman, C., Pöritz, M., Mackenzie, K., 2018. Combined chemical and microbiological degradation of tetrachloroethene during the application of Carbo-Iron at a contaminated field site. *Science of The Total Environment* 628–629, 1027–1036. DOI: 10.1016/j.scitotenv.2018.01.310
- Wang, F.-I., Kuo, M.-L., Shun, C.-T., Ma, Y.-C., Wang, J.-D., Ueng, T.-H., 2002. Chronic toxicity of a mixture of chlorinated alkanes and alkenes in ICR mice. *Journal of Toxicology and Environmental Health, Part A* 65, 279–291. DOI: 10.1080/15287390252800864
- Watts Richard J., Teel Amy L., 2006. Treatment of contaminated soils and groundwater using ISCO. *Practice Periodical of Hazardous, Toxic, and Radioactive Waste Management* 10, 2–9. DOI: 10.1061/(ASCE)1090-025X(2006)10:1(2)
- Weil, M., Scholz, S., Zimmer, M., Sacher, F., Duis, K., 2009. Gene expression analysis in zebrafish embryos - a potential approach to predict effect concentrations in the fish early life stage test. *Environmental Toxicology & Chemistry* 28, 1970–1978. DOI: 10.1897/08-627.1
- Weiss, N.S., 1995. Cancer in relation to occupational exposure to perchloroethylene. *Cancer Causes Control* 6, 257–266. DOI: 10.1007/BF00051797
- Wild, E., Jones, K.C., 2009. Novel method for the direct visualization of in vivo nanomaterials and chemical interactions in plants. *Environmental Science & Technology* 43, 5290–5294. DOI: 10.1021/es900065h
- Xue, W., Huang, D., Zeng, G., Wan, J., Cheng, M., Zhang, C., Hu, C., Li, J., 2018. Performance and toxicity assessment of nanoscale zero valent iron particles in the remediation of contaminated soil: A review. *Chemosphere* 210, 1145–1156. DOI: 10.1016/j.chemosphere.2018.07.118

- Yan, Y.E., Schwartz, F.W., 1999. Oxidative degradation and kinetics of chlorinated ethylenes by potassium permanganate. *Journal of Contaminant Hydrology* 37, 343–365. DOI: 10.1016/S0169-7722(98)00166-1
- Yang, A.L., Huang, G.H., Qin, X.S., Fan, Y.R., 2012. Evaluation of remedial options for a benzene-contaminated site through a simulation-based fuzzy-MCDA approach. *Journal of Hazardous Materials* 213–214, 421–433. DOI: 10.1016/j.jhazmat.2012.02.027
- Zhang, B., Cho, M., Fortner, J.D., Lee, J., Huang, C.-H., Hughes, J.B., Kim, J.-H., 2009. Delineating oxidative processes of aqueous C60 preparations: role of THF peroxide. *Environmental Science & Technology* 43, 108–113. DOI: 10.1021/es8019066
- Zheng, T., Zhan, J., He, J., Day, C., Lu, Y., McPherson, G.L., Piringer, G., John, V.T., 2008. Reactivity characteristics of nanoscale zerovalent iron–silica composites for trichloroethylene remediation. *Environmental Science & Technology* 42, 4494–4499. DOI: 10.1021/es702214x
- Zytner, R.G., 1992. Adsorption-desorption of trichloroethylene in granular media. *Water Air Soil Pollution* 65, 245–255. DOI: 10.1007/BF00479890

Appendices

[A.1]: Towards sensible toxicity testing for nanomaterials: Proposal for the specification of test design	53
[B.1]: The oxidized state of the nanocomposite Carbo-Iron® causes no adverse effects on growth, survival and differential gene expression in zebrafish	77
[B.2]: Supplemental information to: The oxidized state of the nanocomposite Carbo-Iron® causes no adverse effects on growth, survival and differential gene expression in zebrafish.....	109
[C.1]: Oxidized Carbo-Iron causes reduced reproduction and lower tolerance of juveniles in the amphipod <i>Hyalella azteca</i>	117
[C.2]: Supplemental information to: Oxidized Carbo-Iron causes reduced reproduction and lower tolerance of juveniles in the amphipod <i>Hyalella azteca</i>	141
[D.1]: Environmental risk or benefit? Comprehensive risk assessment of groundwater treated with nano Fe ⁰ -based Carbo-Iron®	161
[D.2]: Supplemental information to: Environmental risk or benefit? Comprehensive risk assessment of groundwater treated with nano Fe ⁰ -based Carbo-Iron®	189
[E.1]: Curriculum vitae.....	235

Appendix A.1

Towards sensible toxicity testing for nanomaterials: Proposal for the specification of test design

Annegret Potthoff, Mirco Weil, Tobias Meißner, Dana Kühnel

**Published in: Science and Technology of Advanced Materials (2015),
Vol.: 16, 065006.**

Keywords

harmonization, toxicity test design, hazard assessment, engineered nanomaterials, decision support, physical-chemical characterisation

Abstract

During the last decade, nanomaterials were extensively tested for potential harmful effects towards humans and environmental organisms. However, a sound hazard assessment was so far hampered by many uncertainties and a low comparability of test results. The reason for the low comparability is a high variation (1) in the type of NM tested with regard to raw material, size and shape and (2) during all steps of the testing procedures before and during the toxicity testing. This calls for tailored, nanomaterial-specific protocols. Here, decision trees can be a versatile tool for structuring the test procedures involved, leading to test protocols not only tailored for a specific type of nanomaterial, but also for the respective test system intended to be used for toxicity testing. There are existing standards on single procedures involving nanomaterials, however, not all relevant procedures are covered by standards. Hence, our approach offers a more detailed way of weighting several plausible alternatives for e.g. sample preparation, in order to decide on the procedure most meaningful for a specific nanomaterial and toxicity test.

Decision trees are flexible both in starting point and extend, which makes them universal in use and adoptable to specific research questions. Hence, a framework of several decision trees and flow charts to support testing of NM is proposed here as a basis for further refinement and in-depth elaboration. Decision trees and flow charts were drafted for (1) General procedure – Physical-chemical characterisation, (2) Choice of test media, (3) Decision on test scenario and application of NM to liquid media, (4) Application of NM to the gas phase, (5) Application of NM to soil and sediments, (6) Dose metrics, (S1) Definition of a nanomaterial, and (S2) Dissolution.

The applicability of the proposed approach was surveyed by using experimental data retrieved from studies on nanoscale CuO. This survey demonstrated the decision trees and flow charts to be a convenient tool to systematically decide upon test procedures and processes, and hence pose an important step towards harmonization of NM testing.

1. Introduction

During the last decade, enormous effort has been put into the assessment of potential adverse effects of ENMs for both humans and the environment. However, up to now a sound hazard assessment is often hampered by results that are difficult to compare and may be contradictory (Warheit and Donner, 2015). This is often due to (1) missing information about the nanomaterial identity and characteristics, (2) interaction of NM with the particular test media and the dispersion procedure applied, (3) unpredictable behaviour of NM during the test and (4) difficulties in dose metrics and data interpretation.

So far there is no generally applicable model for identification of hazards of nanomaterials and scientists as well as regulatory committees recommend a case by case approach for hazard assessment (SCENIHR, 2009, Oomen et al., 2014). The high variability of different nanomaterials with regard to raw material, size and shape (among others) calls for tailored, nanomaterial-specific protocols.

At present, several studies suggest that the REACH approach is suitable for hazard assessment and risk characterisation nanomaterials (EC, 2012). Concerning the performance of toxicological tests the OECD test guidelines comprise internationally agreed testing methods. Tests performed according to these guidelines are useful for both risk assessment and classification purposes (ECHA, 2012). But the specific properties of nanomaterials are not considered in test guidelines developed for usual chemicals, and disregarding them was shown to lead to undesired interferences between nanomaterials and abiotic and biotic factors in the test (e.g. Schwab et al., 2011, Tournebize et al., 2013, Worle-Knirsch et al., 2006, Handy et al., 2012b). Hence, though generally appropriate for testing of nanomaterials, methodological modifications of these guidelines may be necessary (Grieger et al., 2010). The inadequacies for testing of nanomaterials are mostly related to material characterisation, properties and metrology (OECD, 2009, Kühnel and Nickel, 2014). These findings suggest that extensive modification of OECD test guidelines are unnecessary and nanomaterial-specific issues might be addressed in guidance documents on how existing test guidelines could be used in testing of nanomaterials.

Accordingly, as a first resource to reach this goal, a structured approach employing decision trees and flow charts is proposed here to guide through the process of choosing appropriate testing schemes for a specific type of NM. The suite of decisions trees and flow charts developed summarize the main considerations for setting up a well-designed toxicity test for nanomaterials. They are flexible in starting point and extent, and have been suggested by several scientists to be a valuable tool in nanotoxicology (Stone et al., 2010, Kühnel and Nickel, 2014, Handy et al., 2012a).

As the resulting decisions are material- and toxicity test dependent, the trees illustrate the hierarchical, consecutive decisions, without weighting alternative approaches. The final decision on which way to choose is left to expert knowledge depending on the intended testing goal. Recently, a decision tree-like approach has been used to assign the hazard potential to specific NM in relation to the intended use (Hansen et al., 2013).

The applicability domain of the structured approach developed here comprises all nanomaterials irrespective of their raw materials, under the precondition that they are both toxicological relevant and dispersible to a degree acceptable for toxicological assays, for example with regard to aggregate size and wettability. Two test scenarios are considered, referred to as worst-case (optimized for stable NM dispersions) and realistic scenario (testing under relevant conditions, accepting agglomeration of NM). To minimize the main causes of variations during testing as described above, the following decision trees and flow charts were drafted: (1) General procedure – Physical-chemical characterisation, (2) Choice of test media, (3) Decision on test scenario and application of NM to liquid media, (4) Application of NM to the gas phase, (5) Application of NM to soil and sediments, (6) Dose metrics, (S1) Definition of a nanomaterial, and (S2) Dissolution. They were developed in accordance with current regulations and definitions for NM.

The major aims of this work were to (1) provide a specific, yet variable frame for NM type specific testing, (2) provide a stepwise approach to design NM toxicity tests and in consequence (3) provide guidance and foster harmonization in testing. Not only results from current analysis will be more reliable, reproducible and comparable, but also the retrospective analysis of existing data with regard to their reliability is conceivable.

In order to assess the applicability of the proposed approach, the procedure was tested using experimental data retrieved from studies on nanoscale CuO. The decision trees were then used to define the testing schemes leading to most reliable results while considering the intended test scenario. They were shown to be a convenient tool to systematically structure test procedures and processes, and hence to be suitable to define a reliable test design. Thus, the decision trees and flow charts presented here provide a basal, superordinate procedure to structure the workflow and measures to be taken based on ENM specific, toxicity test specific, but also research question specific considerations. Accordingly, they may also provide a structured approach to develop SOPs for the testing of NM. They can hence be seen as a backbone for testing and may be extended and further specified in the future.

2. Approach and methods

2.1 Drafting of decision trees and flow charts

A decision tree is a tool using a tree-like graph or model of decisions and their possible consequences to help identify a strategy most likely to reach a specified goal. A flow chart is a representation of the sequence single steps are performed in order to reach a specific goal or solve a problem.

The decision trees and flow charts apply to all engineered nanomaterials (ENMs) irrespective of their raw material given that they are both toxicological relevant and dispersible to a degree acceptable for toxicological assays, for example with regard to aggregate size and wettability. Decision trees and flow charts were drafted in an iterative process taking practical experience from earlier experimental procedures and existing standards into account (ISO, 2010, ISO, 2012). Furthermore, the decision trees were developed to be applicable for several toxicological test systems.

2.2 Example study involving experimental data on nanoscale CuO

The approach was tested for applicability, suitability and comprehensiveness by choosing one type of engineered nanomaterial. CuO (NNV-011, delivered by Nanologica AB) represents a nanoscaled powder, which is dispersible into submicronscaled aggregates. The main NM properties and characteristics of the powder are summarized in Table 1, a SEM image is shown in Figure 1.

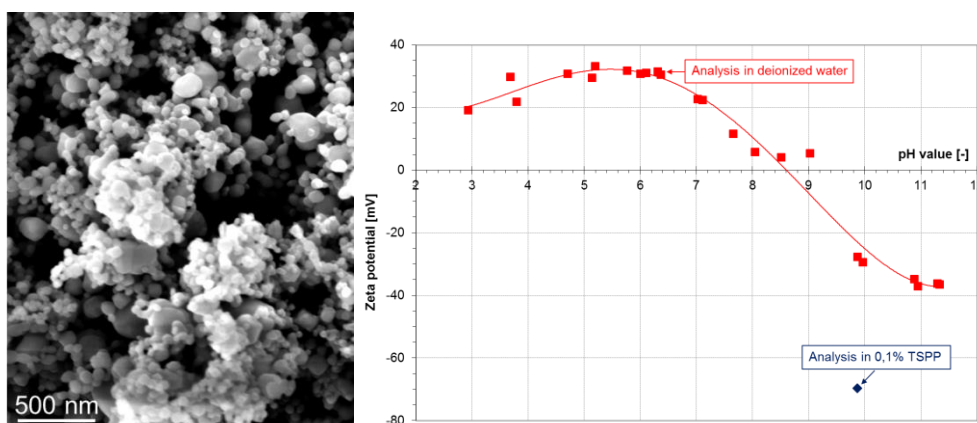


Figure 1: SEM image of CuO (NNV-011). Zeta potential in dependence on pH value (red squares), as well as in presence of 0.1 % TSPP (blue diamond).

The purpose was to cover different initial states of NM such as powders and suspensions, and different testing scenarios (see Figure 2). For example, different states of agglomeration may be used in an experiment, which defines how much effort is put into the dispersion and stabilization of a NM. Since the properties of nanomaterials strongly depend on their surroundings the following two test scenarios were compared:

2.2.1 *Daphnia magna* immobilization test according to OECD guideline 202

The test guideline is well-established for the testing of chemicals; however, adaptations are required specific to NM testing. Sample preparation, in particular the dispersion of powder in liquid may determine the test results. Two different approaches will be considered: (a) use of dispersant aids to improve the colloid chemical stability of the suspension, such as polyphosphates (e.g. Nickel et al., 2014, Meißner et al., 2010, Li et al., 2014); (b) the same particle concentration, energy input etc. as in (a) are chosen, but the test will be conducted without dispersants. A modified ADaM medium was used for organisms exposure (after Klüttgen et al., 1994). Approach (a) will involve stabilized nanomaterials, assuming that organisms are exposed to smaller sized particles compared to approach (b). Accordingly, approach (a) was termed 'worst-case'-scenario, whereas approach (b) was termed 'realistic' scenario, as organisms will more likely contact the agglomerates.

Table 1: Relevant characteristics of nanoscaled CuO employed in the example studies.

Properties / Characteristics	CuO NNV-011	CuO NNV-011 + 0.1 % TSPP
CAS number	1317-38-0	
Chemical composition	CuO	
Crystallinity	CuO, contains small amounts of Cu ₂ O	
Specific surface area (BET)	27 m ² /g	
primary particle size x_{BET}	35 nm	
Particle size in stock suspension after dispersion (at t=0; smallest dispersable unit) x_{DLS}	144 ± 5 nm	136 ± 5 nm
Zeta potential in stock suspension	+ 31 mV	- 69 mV

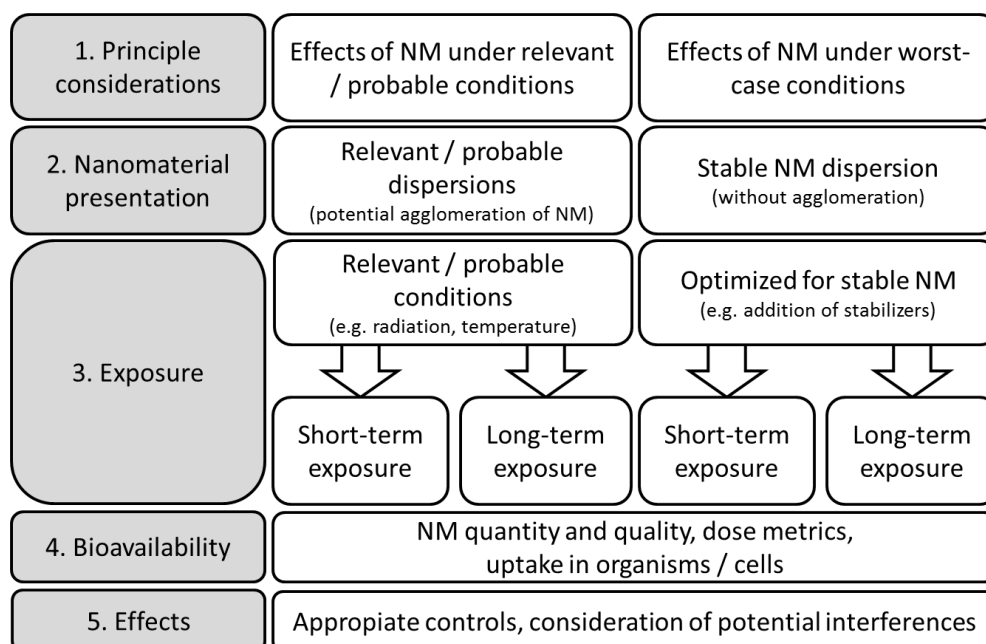


Figure 2: Principle consideration for the testing of nanomaterials (modified after Kroll et al., 2013).

2.2.2 *Daphnia magna* immobilization test conducted in real waters

Scenario (1) represents a well-defined test involving artificial test media. To cover further testing approaches, the same test protocol was followed but exposure was conducted in real waters from two surface water sources of different composition. The waters (named water 1 and water 2) differed in relevant parameters such as dissolved matter and chloride content as well as conductivity. Especially the latter one determines the behaviour of CuO particles in media and is connected with ionic strength. ADaM shows the highest amount of soluble salts and hence, it improves the tendency for particle agglomeration.

The properties of the applied test media for these tests are summarized in Table 2.

Table 2: Relevant characteristics of test media and natural waters used in the example studies.

	Test according to OECD guideline	Lake water I	Lake water II
DOC (mg C/l)	---	3.4	1.1
pH	7.4	8.2	8.3
Ca ²⁺ (mg/l)	73.7	48.6	37.4
Cl ⁻ (mg/l)	267.2	23.7	1.6
Conductivity (µS/cm)	997	390	200

3. Results

3.1 Decision trees and flow charts

In total, six decision trees (DT) and two flow charts supporting the toxicity testing of NM were developed: (Flow chart 1) General procedure – Physical-chemical characterisation, (Flow chart 2) Choice of test media, (DT 3) Decision on test scenario and application of NM to liquid media, (DT 4) Application of NM to the gas phase, (DT 5) Application of NM to soil and sediments, (DT 6) Dose metrics (see figures 3-8), (DT S1) Definition of a nanomaterial, and (DT S2) Dissolution (see supporting information). They were developed in concordance with current regulations and definitions for NM (ISO, 2008, ISO, 2010). The area of applicability of the decision trees is depicted in detail in tree S1 NM definition (supplement S1).

The general procedures are summarized in Figure 3 and 4. Depending on the type of NM and the specific tests under consideration, the trees are linked with each other as indicated in the figures. For each specific decision tree and flow chart, data and pre-assessments are required in order to reach the final decision. The required data can either be deduced from manufactures information, or have to be assessed by the researcher choosing among various methods in order to proceed and make relevant decisions for the test system. Some data are difficult to obtain for NM, e.g. behaviour in soil and sediment; hence, data gaps and methodological limitations are likewise identified and reported. Finally, the major outputs and the way to proceed with other trees are explained.

3.2 DT (1) General procedure - Physical-chemical characterisation of the original NM

An unknown powder or a suspension is to be tested. As the following procedure mainly covers testing of nanoscaled materials, the first step (S1) is to determine whether the material is a nanomaterial. If this is verified, the testing proceeds with the physical-chemical characterisation as shown in Figure 3.

This flow chart describes the initial characterisation of a pristine / as-delivered nanomaterial according to ISO/TR 13014:2012. It involves the assessment of powder or suspension characteristics such as particle size.

Special attention has to be paid to changes of nanomaterials properties under storage and test conditions. In general, due to the influence of parameters such as temperature, light, pH or due to interactions with vessels for storage, nanomaterials may change their over time. Therefore, especially for nanodispersions it is necessary to repeat characterisation procedures before further (toxicological) testing, in case a longer time period has passed between these two steps. This improves the interpretation of toxicological effects from different studies and improves the comparability of test results (e.g. Jemec et al., submitted).

Additional important aspects to consider are effects from variations occurring during the production process of the NM. Various batches of the same material may differ in chemical properties (as content of impurities or thickness of coating) or in physical properties (as strength of agglomerates or aggregates) (Yin et al., 2015, Motzkus et al., 2014). As a result, different batches of the same material may need to be investigated separately. Hence, the knowledge of initial NM characteristics is considered as indispensable. However, more research is needed to determine the crucial parameters and time-dependency for aging of specific nanomaterials. This is marked in Fig. 3 as 'area of research'.

Dispersion is defined as the homogenous introduction of solid particles into gas, liquids or solids, by applying one or more of various mixing methods. During the mixing procedure, the initial ENM may be separated into smaller units, depending on ENM and media characteristics, energy input and research question. The latter also defines the choice of dispersion protocol, i.e. whether realistic (acceptance of larger agglomerates) or worst-case conditions (dispersion until the 'smallest dispersible unit' is obtained) are applied (see also Figure 2 and 5). Furthermore, it is suggested to assess the stability of a NM suspension over the anticipated duration of a toxicity test (see Figure 8).

Dissolution testing is only necessary in case release of ions from the NM is expected or when there are concerns regarding the toxicity of the released material.

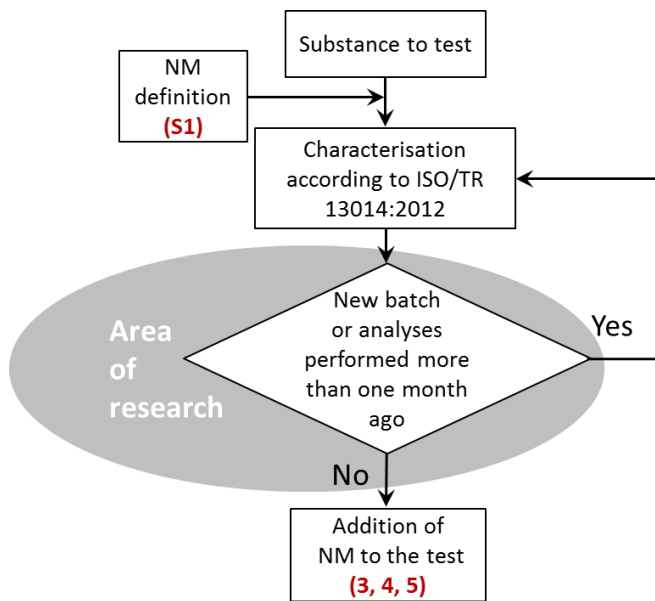


Figure 3: Flow chart 1: General procedure - Physical-chemical characterisation of the nanomaterial. Numbers given in parenthesis relate to the detailed decision trees shown in Figures S1, 5, 6, and 7. More specification of the phenomena underlying the aging process is needed, hence this is marked as area of research.

3.2.1 Representative study Flow chart 1

In the present study, a Copper Oxide (CuO) powder (NNV-011) has been chosen for testing the applicability of the structured approach. According to specific surface area and SEM images the powder suits the requirements of a nanomaterial as defined in S1 (Suppl. Figure 1): With a specific surface area of 27 m²/g and a theoretical density of 6,31 m²/g a primary particle size x_{BET} of 35 nm is calculated (Table 1). This is in good accordance with the SEM image, which shows primary particle sizes between 20 and 100 nm (Fig. 1). Hence, all relevant parameters according to ISO/TR13014:2013 were assessed for nCuO powder.

3.3 Flow chart (2) Choice of test media

The choice of test media depends on the type of ENM, the research question, the choice of a test system (e.g. a cell line, an aquatic organism) and with regard to risk assessment on the use of the respective ENM. As NM and test system will interact with each other, this will affect all subsequent decisions and implies the need for tailored approaches. In principle, ENMs are added to the gas phase (e.g. air), the solid phase (e.g. feed in feeding studies, soil) or liquid phase (e.g. cell culture media, different aqueous media used in ecotoxicology). For the first two application methods,

direct or indirect dosing is possible. The indirect dosing is achieved by an intermediate dispersal in liquid media before addition to either the gas or the solid phase solid phase. (Figure 4)

With regard to ecotoxicity testing, pre-assessment of environmental fate may guide the choice of tests by determining the partitioning behaviour of the NM, i.e. into which environmental compartment or compartments the nanomaterial will partition, and consequently which series of ecological tests are most relevant for priority testing. For example, if it is expected that a NM partitions exclusively into the water compartment, then tests with pelagic test organisms would need to be conducted. However, if strong adsorption is expected, or the nanomaterial has a very high sedimentation tendency, then it may be expected to partition into soil or sediment compartments and therefore ecotoxicity testing would be needed for those compartments (OECD, 2010).

In any case, the variability in the composition of different media used in testing procedures is very high, and both the dispersal procedure (e.g. use of dispersant aids) and the characterization techniques have to be adapted on a case-by-case basis.

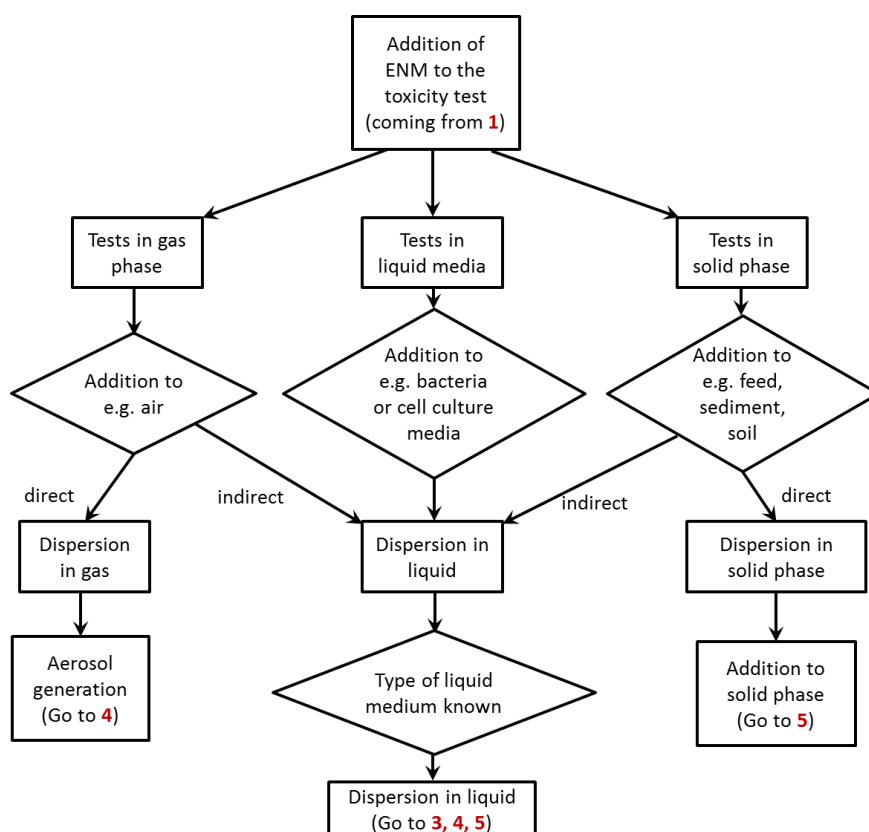


Figure 4: Flow chart on the choice of test media and considerations on dosing. Numbers given in parenthesis relate to the detailed decision trees shown in Figures 5-7.

3.3.1 Representative study Flow chart 2

The subsequent toxicity tests are performed in liquid media, as toxicity to aquatic organisms shall be assessed. Two different types of media were chosen, namely ADaM, an artificial medium of known composition, and natural waters, where the most crucial parameters such as pH and DOC content were assessed. Hence, the media applied show a high variability in composition (Table 2).

3.4 DT (3) Choice of test scenario and application of NM to liquid media

The addition to the liquid phase is frequently used for *in-vitro* studies and aquatic ecotoxicological tests. An ENM powder may either be directly added to the respective liquid, or a predispersion (stock solution) in water is prepared. As specified in Figure 2 and 5, toxicity testing of ENMs can be conducted under different preconditions: (1) Avoidance of NM agglomeration ('worst-case') or (2) acceptance of agglomeration ('realistic conditions'). These two scenarios result in different preliminary demands and considerations regarding toxicity testing. Depending on the scenario chosen, the use of dispersing agents in order to keep particles separated from each other is an option. The characteristics of a given NM may differ due to the medium composition, with factors like pH, salt content, use of dispersant aids, presence of chelators influencing NM behaviour, making it inevitable to assess the characteristics of individual NM-medium combinations. In order to demonstrate the implications in detail, both scenarios are covered by the CuO representative study.

In some cases, the dispersion of a nanomaterial in liquid media is impossible, e.g. for powders with a poor wettability. Without dispersant aids no further testing in liquid media is possible, however this does not affect NM powders to be tested in aerosols and soils and sediments (Figure 5).

without the dispersing agent TSPP. While the impact of stabilization on x_{DLS} was not significant (see Table 1), the absolute value of the zeta potential rose from around +30 mV for the unstabilized nCuO to around -65 mV for the stabilized stock suspension, implying a substantial increase in stability (Figure 1). The use of stabilizer also had an impact on long-term stability of the stock suspension, as in the presence of TSPP, repeated preparation of identical nCuO suspensions in ADaM was achieved up to a stock suspension age of 96 h, leading to an increase in reproducibility (data not shown). Neither without TSPP, nor by mixing nCuO, ADaM and TSPP upon start of the toxicity test, a stable nCuO suspension was achieved. When dispersing unstabilized stock suspension in ADaM or lake water, nCuO starts to agglomerate immediately, making the determination of the zeta potential impossible (Table 3).

Table 3: Characteristics of nanoscaled CuO in the ADaM test media under realistic and worst-case conditions.

Properties / Characteristics	CuO NNV-011	CuO NNV-011 + 0.1 % TSPP
Particle size in ADaM after dispersion (at $t=0$; smallest dispersible unit) xDLS	Not measurable	132 ± 5 nm
Zeta potential in ADaM	Not measurable	- 64 mV

3.5 DT (4) Addition of ENM to the gas phase

The addition of ENMs to the gas phase, e.g. for inhalation studies requires the generation of an aerosol containing the ENM. This can be achieved by either using an ENM powder (direct dosing) or an ENM suspension (indirect dosing). In any case, the respective dispersion procedure needs to be specifically adapted to the shape of the nanomaterial under study, as particles, fibres and plates will disperse and behave differently in the gas phase (Figure 6). In addition, changes in NM properties upon contact with biological fluids, such as lung surfactant, need to be taken into account (e.g. Kasper et al., 2015). In the example of nanoscale CuO employed in aquatic toxicity tests, this tree is not relevant.

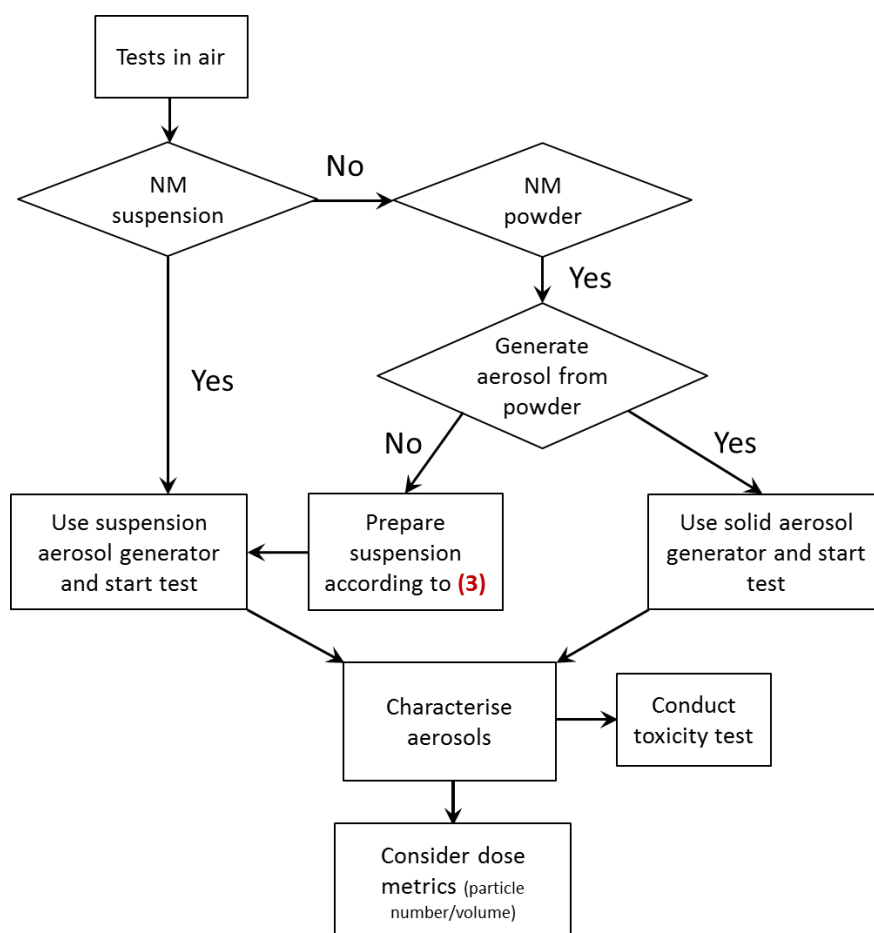


Figure 6: Decision tree 4: Application of nanomaterials to the gas phase. Number given in parenthesis relate to the decision trees shown in Figure 5.

3.6 DT (5) Addition of ENM to the solid phase

If tests are conducted in soils and sediment, basic data on NM physical-chemical properties is often the sole information on ENM characteristics because there is a lack of techniques to characterize NM in these compartments.

ENM addition to the solid phase is required e.g. in feeding studies or for soil and sediment testing. Direct (dry-spiking, powder) and indirect (wet-spiking, suspension) methods can be used. The latter method requires the preparation of a NM suspension from a powder, which is then added to the solid (Figure 7). In this case, it is possible to assess NM characteristics in liquid before mixing with the solid matrix. The aging / pre-treatment step after the addition of NM is suggested according to McShane et al. (2014).

The analytical techniques to determine ENM characteristics in solid test media are still inadequate, resulting in a lack of information on behaviour and interactions of ENMs and the solid matrix (e.g. Kühnel & Nickel, 2014). This is marked as 'area of research' in Fig. 7, as future method development

may allow a specification of the procedure. In the example of nanoscale CuO employed in aquatic toxicity tests, this tree is not relevant.

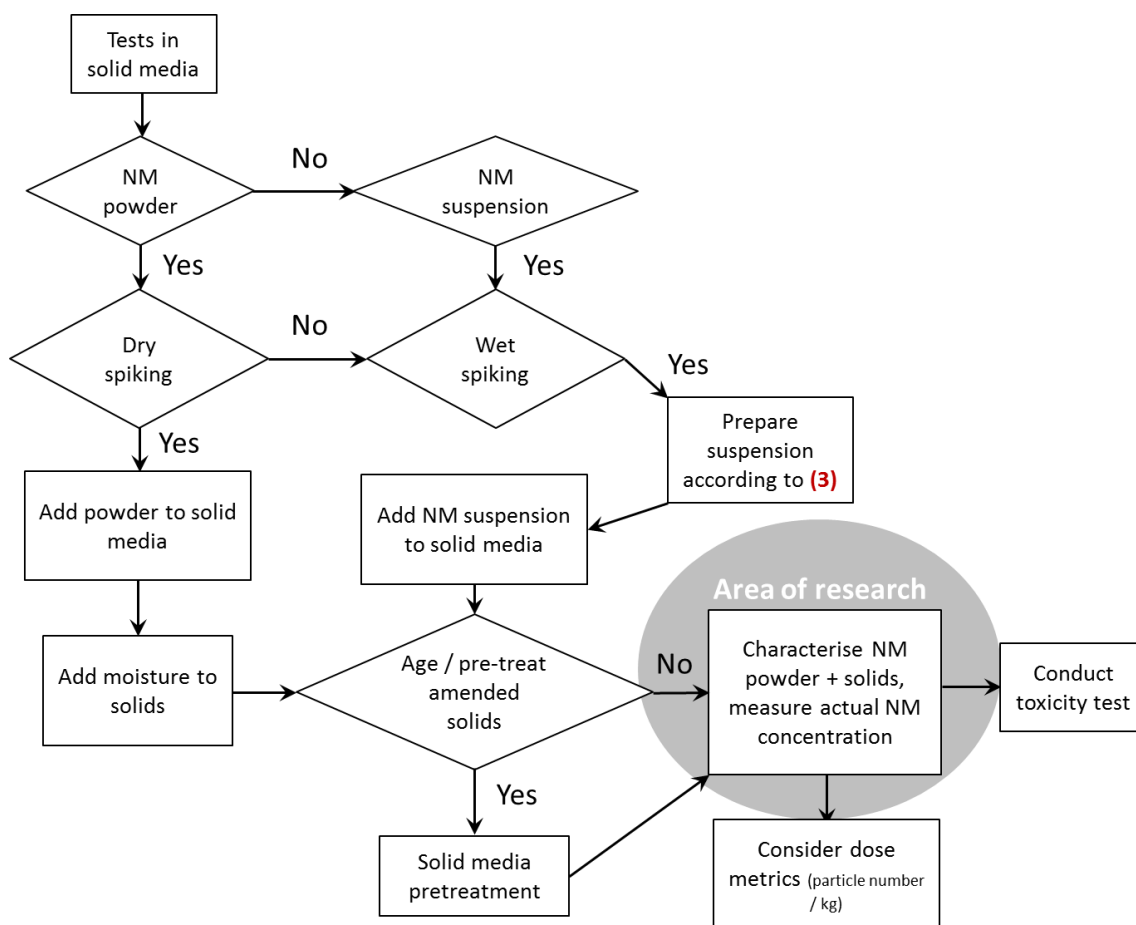


Figure 7: Decision tree 5: Application of nanomaterials to solid test media. Number given in parenthesis relate to the decision tree shown in Figure 5.

3.7 DT (6) Dose metrics in liquid media

The determination of ENM dose in liquid media is important to interpret toxicological results and on a regulatory basis has a high significance to determine toxic concentrations and e.g. exposure limits. The suitability of mass-based dose metrics is a scientific matter of debate and number- or surface-based dose metrics have been suggested (Delmaar et al., 2015, Kühnel and Nickel, 2014). In any case, knowledge on initial ENM properties and characteristics need to be as extensive as possible. In addition, ENM behaviour in a given test, specifically parameters such as agglomeration, dissolution, sedimentation, have to be taken into account.

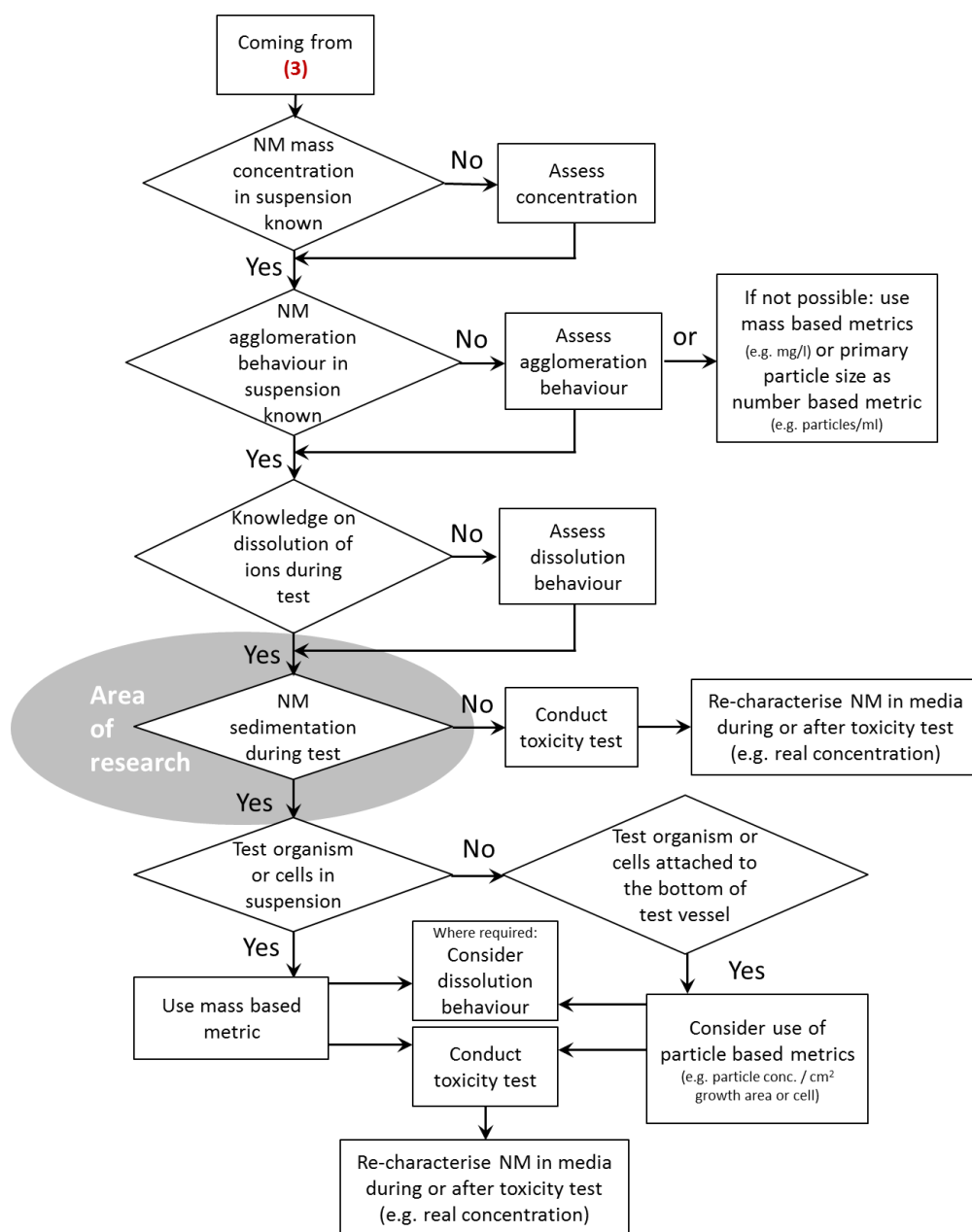


Figure 8: Decision tree 6: Dose metrics in liquid media. The decision node on sedimentation is marked as 'area of research', as currently no protocols for a reliable quantification of the amount of nanomaterials settled out during the tests are available. Numbers given in parenthesis relate to the decision tree on liquid media shown in Figure 5.

3.7.1 Representative study Decision tree 6

The nCuO suspensions were prepared according to mass concentration, and depending on exposure scenario chosen and the type of test medium used, the particles underwent agglomeration resulting in sedimentation of particles (Table 4).

Daphnia magna is a free-swimming filter feeder and hence contacts nCuO suspended in the water phase as well as larger particles deposited on the bottom of the test vessels. Dissolution plays a role for CuO particles, but was low for the nanomaterial under study (Table 4). Hence, for the effect values determined in the different toxicity tests, mass-based dose metrics were chosen. The effect values (EC₅₀) for the different media and test scenarios are presented in Table 5, in the case of nCuO the unstabilized form (representing the 'realistic' scenario) was the most toxic, whereas the test under stabilized conditions (representing the 'worst-case' scenario) showed the lowest toxicity.

Table 4: Agglomeration and dissolution behaviour of nCuO in ADaM with 0.1 % TSPP over 48 h. After 48 h agglomeration and sedimentation of nCuO occurred making the determination of zeta potential was impossible.

t (in h)	xDLS (in nm)	Zeta potential (in mV)	Dissolved Cu (in mg/l)
0	132	-64.3	3.5
6	132	-41.3	4.63
24	146	-38.3	5.41
48	230	Not measurable	6.1

Table 5: Effect values (EC₅₀ in mg/l) in *Daphnia magna* after 48 h exposure to nanoscale CuO in the different media.

CuO + 0.1 % TSPP (in ADaM)	CuO (unstabilized) (in ADaM)	Lake water I	Lake water II
11.23	0.44	5.64	6.84

4. Discussion

When choosing a test design for assessing NMs hazard towards organisms, various considerations on all steps of the testing procedure have to be taken into account, namely before (e.g. preparation of suspensions), during (behaviour of ENMs in the test media over time) and after conducting a test (NM re-characterisation, data interpretation). Here, the suitability of decision trees and flow charts as a tool to support a consistent and structured testing of ENM was explored. They provide a stepwise approach, dividing a method or process into crucial steps. Further, they allow identifying the most favorable option for a specific research question out of two or more alternatives. The whole approach is intended to be used for testing with both scientific as well as regulatory background.

The need for test procedures specific to ENMs arises from their unique properties and behaviour, which in many aspects differs substantially from that of conventional chemicals. The experience from numerous studies have shown that the translation of test protocols developed for chemicals is not recommendable. Rather, the test design for ENMs has to be reconsidered and amendments need to be implemented (Nickel et al., 2015, Kühnel and Nickel, 2014). Additionally, the huge variety of NM tested implies that testing schemes need adaptations considering the specific peculiarities of a given nanomaterial. For example, the preparation of suspensions requires material specific procedures, mostly involving energy input of varying intensity and therefore different side effects like radical formation or wear debris from the probe tip can occur (Taurozzi et al., 2011, Meißner et al., 2014). In consequence, a structured approach to take controlled decisions on all necessary steps, such as characterisation procedures, dispersal and the actual toxicity testing to assess the hazard of a NM, is proposed here involving a series of decision trees and a flow chart.

In order to prove the applicability and correctness of the logical sequence in which decisions are taken, an example study employing a CuO powder was conducted, and different preconditions for testing were assumed. From the different testing scenarios, the need to disperse the CuO NM in test media showing a high variance in compositions arose, either with or without stabilizers. The decision trees and flow charts were developed to cover these broad demands and were found to perform well. For the test scenario avoiding the use of stabilizers, agglomeration and sedimentation processes hinder the proper assessment of NM behaviour in media, as with the techniques applied neither the zeta potential nor particle size were measurable (Table 3). As demonstrated in Table 5, the different test conditions had a clear influence on the effect values observed in the toxicity tests, with EC₅₀ values for nCuO ranging from 0.44 – 11.23 mg/l. Hence, the decision trees were found to be helpful in defining a test scenario, in developing a test protocol (SOP) as well as in interpreting

final test results due to detailed knowledge on NM characteristics under the respective test condition. For SOP development, following the logical sequence specified by the decision trees prevents inconsistencies and errors in the experimental design. Likewise, the decision trees and flow charts may be used to assess the reliability of existing data on NM. In that sense, the whole approach is also supporting the specification of established test guidelines with regard to the testing of nanomaterials, fostering harmonization of NM testing in the future (Jaworska and Hoffmann, 2010). Beyond the example of CuO, decision trees help in making material specific decisions whenever needed e.g. when aging processes become relevant. Hence, the decision trees and flow charts are applicable to various NM with different prerequisites regarding composition and state (powder / suspension).

In case of information gaps, passing through a tree may become impossible and hence the information has to be retrieved before conducting any test. This also fosters the assessment of minimal NM properties and characteristics before actually testing an NM, and a growing database on NM physical-chemical properties will allow to better link NM properties to observed toxicological effects. With regard to intelligent testing strategies for nanomaterials, the linkage between NM properties and toxicological outcome is valuable for the development of grouping strategies for nanomaterials (Oomen et al., 2014, Stone et al., 2014).

5. Conclusion & Outlook

A proposal for defined procedures in toxicity testing of NM was presented by structuring all relevant considerations in the frame of decision trees and flow charts. They were found to be a versatile tool applicable to different testing preconditions and scenarios. Likewise, decision trees are adaptable and flexible, hence being suitable for different types of NM and allowing the integration of new knowledge.

The approach presented here provide a basic framework and both the degree of detail and the extent can be further elaborated, or integrated into additional decision trees. Future issues to be integrated into the decision trees include those marked as 'areas of research' in the proposed decision trees, for example aging and sedimentation processes, and issues not yet considered such as transformation and degradation processes (e.g. coating), and the selection of proper controls for toxicity testing.

Acknowledgement

We appreciate the valuable contributions of Heather McShane and Will Hendershot (McGill University, Canada) and Pilar Lobera Gonzales (University of Zaragoza, Spain) to the decision trees

on toxicity testing in soil and aerosols. We thank Laura Sigg from EAWAG (Dübendorf, Switzerland) for providing the characteristics of the natural waters.

The work presented here received funding from the European Community's Seventh Framework Programme (FP7/2007-2013) under grant agreement n° 263147 (NanoValid - Development of reference methods for hazard identification, risk assessment and LCA of engineered nanomaterials) and the project Fe-NANOSIT (FKZ 03X0082 A-F) funded by the German Ministry for Education and Research (BMBF).

References

- Delmaar, C. J. E., Peijnenburg, W. J. G. M., Oomen, A. G., Chen, J., de Jong, W. H., Sips, A. J. A. M., Wang, Z. & Park, M. V. D. Z. 2015. A practical approach to determine dose metrics for nanomaterials. *Environmental Toxicology and Chemistry*, 34, 1015-1022.
- EC 2012. Communication from the Commission to the European Parliament, the Council and the European Economic and Social Committee *Second regulatory review on nanomaterials.*, European Commission, Belgium.
- ECHA 2012. Guidance on information requirements and chemical safety assessment. *European Chemicals Agency*, Endpoint specific guidance.
- Grieger, K D., Baun, A. & Owen, R. 2010. Redefining risk research priorities for nanomaterials. *Journal of Nanoparticle Research*, 12, 383-392.
- Handy, R. D., Cornelis, G., Fernandes, T., Tsyusko, O., Decho, A., Sabo-Attwood, T., Metcalfe, C., Steevens, J. a., klaiNE, S. J., Koelmans, A. A. & Horne, N. 2012a. Ecotoxicity test methods for engineered nanomaterials: practical experiences and recommendations from the bench. *Environ Toxicol Chem*, 31, 15-31.
- Handy, R. D., Van den Brink, N., Chappell, M., Muhling, M., Behra, R., Dusinska, M., Simpson, P., Ahtiainen, J., Jha, A. N., Seiter, J., Bednar, A., Kennedy, A., Fernandes, T. F. & Riediker, M. 2012b. Practical considerations for conducting ecotoxicity test methods with manufactured nanomaterials: what have we learnt so far? *Ecotoxicology*, 21, 933-972.
- Hansen, S., Jensen, K. & Baun, A. 2013. NanoRiskCat: a conceptual tool for categorization and communication of exposure potentials and hazards of nanomaterials in consumer products. *Journal of Nanoparticle Research*, 16, 1-25.
- ISO 2010. ISO/TS 80004-1:2010 Nanotechnologies -- Vocabulary -- Part 1: Core terms. *International Organisation for Standardisation*.
- ISO 2012. ISO/TR 13014:2012 Nanotechnologies -- Guidance on physico-chemical characterization of engineered nanoscale materials for toxicologic assessment. *International Organisation for Standardisation*.
- Jaworska, J. & Hoffmann, H. 2010. Integrated Testing Strategy (ITS) – Opportunities to better use existing data and guide future testing in toxicology. *ALTEX*, 4/10, 231-242.
- Jemec, A., Kahru, A., Potthoff, A., Drobne, D., Heinlaan, M., Böhme, S., Geppert, M., Novak, S., Schirmer, K., Rohit, R., Singh, S., Aruoja, V., Sihtmäe, M., Juganson, K., Käkinen, A. & Kühnel, D. 2016. An interlaboratory comparison of silver nanoparticle characterisation and hazard data demonstrates the importance of harmonizing techniques. *Environment International*, 87, 20-32.
- Kasper, J. Y., Feiden, L., Hermanns, M. I., Bantz, C., Maskos, M., Unger, R. E. & Kirkpatrick, C. J. 2015. Pulmonary surfactant augments cytotoxicity of silica nanoparticles: Studies on an in vitro air–blood barrier model. *Beilstein Journal of Nanotechnology*, 6, 517-528.

-
- Klüttgen, B., Dülmer, U., Engels, M. & Ratte, H. T. 1994. ADaM, an artificial freshwater for the culture of zooplankton. *Water Research*, 28, 743-746.
- Kroll, A., Kühnel, D. & Schirmer, K. 2013. Testing nanomaterial toxicity in unicellular eukaryotic algae and fish cell lines. *Oxidative Stress and Nanotechnology: Methods and Protocols*, In: Armstrong, D., Bharali, D.J., (eds.), *Methods in Molecular Biology* 1028, Humana Press, Totowa, NJ, 165 - 195.
- Kühnel, D. & Nickel, C. 2014. The OECD expert meeting on ecotoxicology and environmental fate — Towards the development of improved OECD guidelines for the testing of nanomaterials. *Science of The Total Environment*, 472, 347-353.
- Li, N., Meng, Q. & Zhang, N. 2014. Dispersion stabilization of antimony-doped tin oxide (ATO) nanoparticles used for energy-efficient glass coating. *Particuology*, 17, 49-53.
- McShane, H. V. A., Sunahara, G. I., Whalen, J. K. & Hendershot, W. H. 2014. Differences in soil solution chemistry between soils amended with nanosized CuO or Cu Reference materials: implications for nanotoxicity tests. *Environmental Science & Technology*, 48, 8135-8142.
- Meißner, T., Kühnel, D., Busch, W., Oswald, S., Richter, V., Michaelis, A., Schirmer, K. & Potthoff, A. 2010. Physical-chemical characterization of tungsten carbide nanoparticles as a basis for toxicological investigations. *Nanotoxicology*, 4, 196-206.
- Meißner, T., Oelschlagel, K. & Potthoff, A. 2014. Dispersion of nanomaterials used in toxicological studies: a comparison of sonication approaches demonstrated on TiO₂ P25. *Journal of Nanoparticle Research*, 16.
- Motzkus, C., Gaie-Levrel, F., Ausset, P., Maille, M., Baccile, N., Vaslin-Reimann, S., Idrac, J., Oster, D., FISCHER, N. & MACE, T. 2014. Impact of batch variability on physicochemical properties of manufactured TiO₂ and SiO₂ nanopowders. *Powder Technology*, 267, 39-53.
- Nickel, C., Angelstorf, J., Bienert, R., Burkart, C., Gabsch, S., Giebner, S., Haase, A., Hellack, B., Hollert, H., Hund-Rinke, K., Jungmann, D., Kaminski, H., Luch, A., Maes, H., Nogowski, A., Oetken, M., Schaeffer, A., Schiwy, A., Schlich, K., Stintz, M., von der Kammer, F. & Kuhlbusch, T. J. 2014. Dynamic light-scattering measurement comparability of nanomaterial suspensions. *Journal of Nanoparticle Research*, 16, 1-12.
- Nickel, C., Gabsch, S., Hellack, B., Nogowski, A., Babick, F., Stintz, M. & Kuhlbusch, T. A. J. 2015. Mobility of coated and uncoated TiO₂ nanomaterials in soil columns – Applicability of the tests methods of OECD TG 312 and 106 for nanomaterials. *Journal of Environmental Management*, 157, 230-237.
- OECD 2009. Preliminary review of OECD test guidelines for their applicability to manufactured nanomaterials. *Series on the Safety of Manufactured Nanomaterials*, No. 15, OECD, Paris.
- OECD 2010. Guidance Manual for the Testing of Manufactured Nanomaterials: OECD Sponsorship Programme: First Revision. *Series on the Safety of Manufactured Nanomaterials No. 25*, ENV/JM/MONO(2009)20/REV.
- Oomen, A. G., Bos, P. M. J., Fernandes, T. F., Hund-Rinke, K., Boraschi, D., Byrne, H. J., Aschberger, K., Gottardo, S., von der kammer, F., Kühnel, D., Hristozov, D., Marcomini, A., Migliore, L., Scott-
-

- Fordsmand, J., Wick, P. & Landsiedel, R. 2014. Concern-driven integrated approaches to nanomaterial testing and assessment - report of the NanoSafety Cluster Working Group 10. *Nanotoxicology*, 8, 334-348.
- SCENIHR 2009. Risk assessment of products of nanotechnologies. *European Commission, Scientific Committee on Emerging and Newly Identified Health Risks*.
- Schwab, F., Bucheli, T. D., Lukhele, L. P., Magrez, A., Nowack, B., Sigg, L. & Knauer, K. 2011. Are Carbon Nanotube Effects on Green Algae Caused by Shading and Agglomeration? *Environmental Science & Technology*, 45, 6136-6144.
- Stone, V., Nowack, B., Baun, A., van den Brink, N., von der Kammer, F., Dusinska, M., Handy, R., Hankin, S., Hasselov, M., Joner, E. & Fernandes, T. F. 2010. Nanomaterials for environmental studies: Classification, reference material issues, and strategies for physico-chemical characterisation. *Science of The Total Environment*, 408, 1745-1754.
- Stone, V., Pozzi-Mucelli, S., Tran, L., Aschberger, K., Sabella, S., Vogel, U., Poland, C., Balharry, D., Fernandes, T., Gottardo, S., Hankin, S., Hartl, M., Hartmann, N., Hristozov, D., Hund-Rinke, K., Johnston, H., Marcomini, A., Panzer, O., Roncato, D., Saber, A., Wallin, H. & Scott-Fordsmand, J. 2014. ITS-NANO - Prioritising nanosafety research to develop a stakeholder driven intelligent testing strategy. *Particle and Fibre Toxicology*, 11, 9.
- Taurozzi, J. S., Hackley, V. A. & Wiesner, M. R. 2011. Ultrasonic dispersion of nanoparticles for environmental, health and safety assessment - issues and recommendations. *Nanotoxicology* 5, 711-729.
- Tournebize, J., Sapin-Minet, A., Bartosz, G., Leroy, P. & Boudier, A. 2013. Pitfalls of assays devoted to evaluation of oxidative stress induced by inorganic nanoparticles. *Talanta*, 116, 753-763.
- Warheit, D. B. & Donner, E. M. 2015. How meaningful are risk determinations in the absence of a complete dataset? Making the case for publishing standardized test guideline and 'no effect' studies for evaluating the safety of nanoparticulates versus spurious 'high effect' results from single investigative studies. *Science and Technology of Advanced Materials*, 16, 034603.
- Worle-Knirsch, J. M., Pulskamp, K. & Krug, H. F. 2006. Oops they did it again! Carbon nanotubes hoax scientists in viability assays. *Nano Letters.*, 6, 1261-1268.
- Yin, H., Coleman, V. A., Casey, P. S., Angel, B., Catchpoole, H. J., Waddington, L. & McCall, M. J. 2015. A comparative study of the physical and chemical properties of nano-sized ZnO particles from multiple batches of three commercial products. *Journal of Nanoparticle Research*, 17.

Appendix B.1

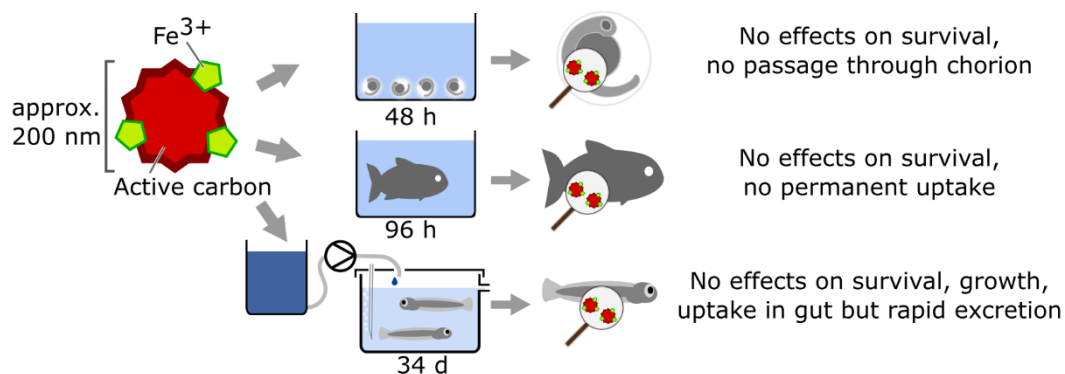
The oxidized state of the nanocomposite Carbo-Iron® causes no adverse effects on growth, survival and differential gene expression in zebrafish

Mirco Weil, Tobias Meißner, Wibke Busch, Armin Springer, Dana Kühnel,
Ralf Schulz, Karen Duis

Published in: Science of the Total Environment (2015),

Vol.: 530–531, Pages198–208.

Graphical abstract



Keywords

iron-based nanocomposite, groundwater remediation, fish toxicity, uptake, excretion

Highlights

- The nanomaterial Carbo-Iron is developed for remediation of contaminated aquifers
- No effects on survival and growth of different life stages of zebrafish occurred
- Particles were incorporated into the gut but excreted under control conditions
- A method for particle concentration measurement in test suspensions was refined

Abstract

For degradation of halogenated chemicals in groundwater Carbo-Iron[®], a composite of activated carbon and nano-sized Fe⁰, was developed (Mackenzie et al., 2012). Potential effects of this nanocomposite on fish were assessed. Beyond the contaminated zone Fe⁰ can be expected to have oxidized and Carbo-Iron was used in its oxidized form in ecotoxicological tests.

Potential effects of Carbo Iron in zebrafish (*Danio rerio*) were investigated using a 48 h embryo toxicity test under static conditions, a 96 h acute test with adult fish under semi-static conditions and a 34 d fish early life stage test (FELST) in a flow-through system. Particle diameters in test suspensions were determined via dynamic light scattering (DLS) and ranged from 266 to 497 nm. Particle concentrations were measured weekly in samples from the FELST using a method based on the count rate in DLS. Additionally, uptake of particles into test organisms was investigated using microscopic methods. Furthermore, effects of Carbo-Iron on gene expression were investigated by microarray analysis in zebrafish embryos.

In all tests performed, no significant lethal effects were observed. Furthermore, Carbo-Iron had no significant influence on weight and length of fish as determined in the FELST. In the embryo test and the early life stage test, growth of fungi on the chorion was observed at Carbo-Iron concentrations between 6.3 and 25 mg/L. Fungal growth did not affect survival, hatching success and growth. In the embryo test, no passage of Carbo-Iron particles into the perivitelline space or the embryo was observed. In juvenile and adult fish, Carbo-Iron was detected in the gut at the end of exposure. In juvenile fish exposed to Carbo-Iron for 29 d and subsequently kept for 5 d in control water, Carbo-Iron was no longer detectable in the gut. Global gene expression in zebrafish embryos was not significantly influenced by Carbo-Iron.

1. Introduction

The use of zerovalent iron nanoparticles (nZVI) for remediation of contaminated groundwater has increased during the last years (Grieger et al., 2010). The efficiency of nZVI for removal of a broad range of contaminants, especially halogenated organics such as perchloroethylene, was demonstrated in several studies (e.g. Cundy et al., 2008; Xiong et al., 2007; Zhang, 2003). Nevertheless, some properties of nZVI, such as strong agglomeration and limited mobility in the aquifer, are not ideal for *in situ* treatment (Jiemvarangkul et al., 2011; Kharisov et al., 2012; Lin et al., 2010). Carbo-Iron, a composite of nZVI and granulated activated carbon, combines the reactivity of nZVI with the adsorbent properties and the mobility of active carbon (Bleyl et al., 2012; Mackenzie et al., 2012). Carbo-Iron is a nanostructured material and can be described as a nanocomposite according to ISO (2011). For remediation of aquifers, Carbo-Iron concentrations of up to 10 g/L (K. Mackenzie, pers. comm.) are injected at the contaminated site. The mean proportion of nZVI in Carbo-Iron is approximately 21% (w/w, K. Mackenzie, pers. comm.). In aqueous media with circumneutral pH and environmentally relevant oxygen concentrations, the nZVI in Carbo-Iron rapidly oxidizes to Fe^{2+} and, subsequently, Fe^{3+} (Mackenzie et al., 2012). Therefore, the present study focuses exclusively on ecotoxicological tests with aged, i.e. oxidized, Carbo-Iron.

Toxicity of nanomaterials to aquatic organisms can be caused by physical or mechanical effects, e.g. by clogging of the filter apparatus or intestinal tract in *Daphnia magna* (e.g. Li and Huang, 2011; Zhu et al., 2010). Toxicity of metal-based nanomaterials is often also related to dissolution of ions into the aqueous phase and subsequent intoxication (Auffan et al., 2009). For reactive ions such as Fe^{2+} toxicity can be caused by reactive oxygen species (ROS). Fe^{2+} reacts with hydrogen peroxide to form Fe^{3+} , hydroxide and ROS. At contaminated sites, ROS can oxidize chemical structures such as halogenated organics, whereas in organisms ROS can lead to oxidative stress mediated cellular damage or disturbance of electron or ion transport cascades at cell membranes (Auffan et al., 2008). Nanomaterials could also act by a Trojan horse mechanism, entering cells and once inside the cell releasing either metallic ions (Park et al., 2010) or previously absorbed substances (e.g. Fan et al., 2012).

Effects of iron-based nanostructured particles on aquatic organisms were detected in the mg/L range. Colloidal iron influenced reproduction of the nematode *Caenorhabditis elegans* and EC_{50} -values between 4 and 29 mg Fe/L were calculated (Höss et al., 2015). García et al. (2011) determined an EC_{50} of 2.3 mg/L for Fe_3O_4 nanoparticles with a primary particle size of 6 nm in a *Daphnia magna* acute toxicity test and an EC_{50} of 240 mg/L in a bioluminescence test with *Vibrio*

fischeri. Zhu et al. (2012) investigated Fe₂O₃ nanoparticles with a primary particle size of 30 nm and a mean measured particle size of 1025 nm in test suspensions. Nominal Fe₂O₃ concentrations of 50 and 100 mg/L caused malformations and led to 45% and 75% mortality, respectively, in the exposed zebrafish larvae 168 h after fertilization, while concentrations between 0.1 and 10 mg/L elicited no effects.

So far, information on the potential toxicity of Carbo-Iron to aquatic invertebrates and fish has not been available. In the present study, a dispersion method for reproducible preparation of test suspensions was developed and the stability of aged Carbo-Iron in these suspensions was investigated. Effects of Carbo-Iron on different life stages of zebrafish were investigated in acute tests with embryos and adult fish and in a chronic test with early life stages. During the exposures test suspensions were characterized. In particular, a method for *in situ* particle concentration measurement based on the scattered light intensity was developed to determine actual exposure concentrations. Potential uptake of Carbo-Iron into the test organisms was evaluated by microscopic analysis. Since gene expression analysis is a sensitive method for detecting sublethal stress responses in fish and was used successfully to observe effects of different nanoparticles (Chae et al., 2009; Chen et al., 2011; Choi et al., 2010; Park and Yeo, 2013), differential gene expression in zebrafish embryos was analyzed with microarrays.

2. Material and methods

2.1 Preparation of test suspensions

A two-step approach (Meißner et al., 2010) was applied by first preparing a stable stock suspension in a dispersant solution and subsequently preparing test suspensions by diluting the stock suspension. Carboxymethyl cellulose (CMC; Antisol® FL 30, Sigma-Aldrich Chemie GmbH, Munich, Germany) was chosen as dispersant in the toxicity tests, since it is also used to stabilize Carbo-Iron during application for remediation of aquifers. For the dispersant solution, 2 g of CMC and 0.1 mL of NaOH (1 M, Sigma-Aldrich Chemie GmbH, Munich, Germany) were added to 1 L of deionized water and stirred overnight at room temperature. Subsequently, CMC solution was filtered with a 0.4 µm filter (MN GF-5, Macherey-Nagel GmbH & Co. KG, Dueren, Germany) and stored for a maximum of 7 d at 4°C. Before use, the dispersant solution was diluted with deionized water to 200 mg CMC/L.

Carbo-Iron was obtained from K. Mackenzie (Helmholtz Centre for Environmental Research – UFZ, Leipzig, Germany) and stock suspensions (1 g/L) with 200 mg/L of CMC, i.e. 20% (w/w) relative to Carbo-Iron, were prepared by adding 100 mg Carbo-Iron to 100 mL CMC solution. The suspensions were placed on ice and treated with an ultrasonic probe (Hielscher UP200S, 14 mm probe diameter)

at approx. 80 W for 7 min. Calorimetric measurements and calculations were performed according to Taurozzi et al. (2010) and the specific energy in the dispersion process was $1.7 \cdot 10^5$ kJ/m³. If volumes > 100 mL were needed, this procedure was repeated and the obtained suspensions were pooled until sufficient volume was prepared. The Carbo-Iron stock suspensions were used within 2 h after preparation.

Fish culture water was prepared according to OECD test guideline 203 (1992; CaCl₂ · 2 H₂O: 294 mg/L, MgSO₄ · 7 H₂O: 123.2 mg/L, NaHCO₃: 64.8 mg/L, KCl: 5.8 mg/L; purity of all substances ≥ 99.5%). With exception of tests conducted for microarray analysis, the fish culture water was diluted with an equal part of deionized water and supplemented with 1% (v/v) reconstituted sea water (28 g/L Tropic marin®, Dr. Biener GmbH, Wartenberg, Germany) before use.

Test suspensions were then prepared by adding the required volumes of Carbo-Iron stock suspension and CMC solution to culture water. Additionally to the control (fish culture water), a dispersant control was included in all tests. In the fish embryo test, the acute fish test and the fish early life stage test, CMC concentration was 20 mg/L in all treatments and the CMC control. In fish embryo tests conducted for microarray analysis, a CMC concentration of 2 mg/L CMC was used to stabilize the Carbo-Iron (only one concentration of 10 mg/L was tested).

2.2 Determination of particle characteristics

2.2.1 Sampling of test suspensions for particle measurements

Particle diameters were measured in the lowest, medium and highest test concentration from the fish acute toxicity test and the early life stage test, and all test concentrations were analyzed in the embryo toxicity test. Additionally, samples from controls with and without CMC and from Carbo-Iron stock suspensions were analyzed. With a glass pipette 20 mL test suspension were taken from the vertical center of the water column in the test vessel, and stored in polypropylene vials. On the same day, the samples were sent by overnight express to the analysis laboratory and analyzed upon arrival, i.e. within 24 h after sampling. Any influence of transport on agglomeration of Carbo-Iron was investigated during the acute fish test and the embryo toxicity test by comparing analysis results obtained on-site, i.e. immediately after sampling, and after transport via overnight express to the analysis laboratory.

2.2.2 Specific surface and hydrodynamic diameter

The specific surface area of Carbo-Iron powder was determined with the Brunauer-Emmett-Teller method (Brunauer et al., 1938) using an ASAP 2020 accelerated surface area and porosimetry

analyzer (Micromeritics GmbH, Moenchengladbach, Germany). Scanning electron micrographs of the powder were taken with a Zeiss Ultra 55 (Carl Zeiss SMT, Germany).

Upon arrival at the analysis laboratory, water samples were divided in 2 subsamples and each subsample was measured 3 times with dynamic light scattering (DLS). For determination of the size of suspended Carbo-Iron particles, stock suspensions (1 g/L Carbo-Iron with 200 mg/L CMC) were diluted to 50 mg/L, while the samples from test suspensions (see below) were analyzed without dilution. Particle size was measured by DLS in 10 mm disposable optical polystyrene cuvettes using a Zetasizer Nano ZS (Malvern Instruments GmbH, Herrenberg, Germany). As recommended in ISO test guideline 22412 (2008), the cumulant method was used to determine the mean hydrodynamic particle diameter and the polydispersity index (PI).

2.2.3 Measurement of particle concentrations

For measuring Carbo-Iron concentrations in the test suspensions from the fish early life stage test, a method based on dynamic light scattering (Zetasizer Nano ZS) was used. The main principle is described by Smeraldi et al. (2012). The method was adopted to the requirements of Carbo-Iron and the concentrations used in the test suspensions. The count rate of the scattered light relative to the nominal concentration of Carbo-Iron was determined. Such a correlation was possible because Carbo-Iron suspensions were stable and particle agglomeration was inhibited by the presence of CMC in the test suspensions. Before measuring samples, individual calibration curves were generated with freshly prepared suspensions and linear regressions were obtained for concentrations up to 25 mg/L. As described above, samples were divided in 2 subsamples and each subsample was measured 3 times.

2.2.4 Release of Fe ions from Carbo-Iron

Leaching of iron ions from Carbo-Iron into the test suspensions was measured with a photometric test (LCW 021, Hach Lange GmbH, Düsseldorf, Germany) for analysis of Fe²⁺ according to the manufacturer's protocol. Samples were taken from all test concentrations and from controls with and without CMC. Subsequently, 5 mL of sample were filtered twice with 0.45 µm syringe filters (Roth, Karlsruhe, Germany) and acidified with hydrochloric acid (1 M) to pH 4. Ascorbic acid was used to reduce any Fe³⁺ to Fe²⁺ immediately before photometric measurement (XION 500, Dr. Lange, Düsseldorf, Germany) at 564 nm.

2.3 Test organisms

Zebrafish (*Danio rerio*) were purchased from a local retailer and have been held and bred at ECT since 2010. They were kept in aquaria with internal ceramic filters in fish culture water and fed daily

with newly hatched nauplii of *Artemia* spp. (Sanders, Ogden, Utah, USA) and flake food (TetraMin®, Melle, Germany). All fish were held at $26 \pm 2^\circ\text{C}$ with a 12:12 h light:dark photoperiod. Zebrafish were held in a sex ratio ranging from approx. 1.4 to 2 males to 1 female. Eggs for the embryo test and the early life stage test were collected by placing glass trays covered with stainless steel mesh (mesh size 3 mm) in the aquaria. On each tray, plants (*Microsorium pteropus*) were placed as spawning substrate. Spawning was stimulated by the onset of light and trays were removed 30 min after initiation of the light cycle. Eggs were rinsed with fish culture water and collected in a glass crystallization dish. Immediately after selection of a sufficient number of fertilized eggs (fertilization rate > 70%) using a dissection microscope, groups of 5 eggs were transferred into each test vessel for all controls and treatments. This procedure was repeated until the desired number of eggs per test vessel was achieved. At the start of exposure, embryos were in late cleavage period (less than 2 h post fertilization).

Zebrafish eggs used for microarray analysis were obtained from fish purchased in 2007 from a local retailer and cultured at the UFZ for several generations. Fish were held in dechlorinated tap water at 26°C and a light:dark cycle of 14:10 h. Eggs were obtained from spawning groups as described above. At the onset of exposure, embryos were in the 2-cell stage.

2.4 Fish embryo toxicity test

The zebrafish embryo toxicity test was conducted similarly as described in the OECD draft guideline (OECD, 2006). Crystallization dishes (borosilicate glass, 80 mm diameter, 45 mm height) filled with 100 mL of the respective test water were used as test vessels. Exposure was performed for 48 h under static conditions. Carbo-Iron concentrations ranging from 1.6 to 100 mg/L with a spacing factor of 2 were tested. For each test concentration and control, 4 biological replicates (each with 10 embryos) were used, and two additional vessels were prepared that also contained test organisms but were only used to measure particle diameters.

After 3, 8, 24, 32, and 48 h, lethal and sublethal effects (edemas, deformations, lack of spontaneous movement) were evaluated as described in Weil et al. (2009) and dead embryos were removed. Oxygen content, pH and temperature were measured in all test vessels at the beginning (0 h) and end of the exposure (48 h). Measured oxygen concentrations were between 8.1 and 9.0 mg/L, pH was between 7.3 and 7.4 and temperature was between 25.9 and 26.0°C . Temperature measured continuously in an additional vessel was between 25.9 and 26.1°C .

Particle diameters were measured at 0, 24 and 48 h, concentration of Fe ions after 48 h. At the end of the test, 5 embryos from each treatment were sampled for analysis of particle uptake as described in section 2.7.

2.5 Acute fish toxicity test

Acute toxicity of aged Carbo-Iron to adult zebrafish was assessed according to OECD test guideline 203 (OECD, 1992). For each treatment, 7 fish were exposed to 3 L aerated test water in 8 L all-glass aquaria for 96 h under semi-static conditions. The nominal Carbo-Iron concentrations were 4.3, 9.4, 20.7, 45.5 and 100 mg/L. Fish were transferred into fresh test water after 48 h of exposure. Fish with a standard length of 27 ± 2 mm and a weight of 184 ± 40 mg (mean \pm sd, n=13) were used. From one day before test start until test end, fish were not fed. Test suspensions with 20.7, 45.5 mg/L and 100 mg/L Carbo-Iron exhibited an increasing turbidity. In these suspensions, daily observations were performed by using a pocket torch on the rear side of the respective test vessels, and were limited to assessing the number of moving (i.e. surviving) fish. Oxygen content, pH and temperature were measured in all test vessels at the beginning of the test and daily during exposure. Measured oxygen concentrations were between 7.8 and 8.2 mg/L, pH ranged from 7.2 to 7.4 and temperature was between 23.7 and 24.6°C.

Samples for particle diameter measurement and analysis of Fe ions were taken at 0, 24 and 48 h. At test end, all fish were killed with MS-222 (600 mg/L, buffered with 300 mg/L NaHCO₃; Sigma-Aldrich Chemie GmbH, Munich, Germany) and stored for microscopic analysis as described in section 2.7. For a detailed investigation of potential uptake of Carbo-Iron into the fish, SEM analysis was performed on gill and gut tissue.

2.6 Fish early life stage test

For the fish early life stage test (OECD test guideline 210, OECD, 2013b), crystallization dishes (borosilicate glass, 140 mm diameter, 80 mm height) were used in a flow-through system with four replicates per treatment and 20 eggs per replicate. At any time during the test, fish were exposed to approximately 600 mL of the respective test water. Each day, 5 L of each test suspension (0.25, 0.79, 2.5, 7.9 and 25 mg Carbo-Iron/L) were prepared by dilution of a newly prepared stock suspension, and stored in polyethylene reservoirs. The test suspensions in the reservoirs were aerated vigorously to ensure thorough mixing. Through an outlet at the bottom of each reservoir, test suspensions as well as control and CMC control water were delivered to the test vessels with two peristaltic pumps (BVP 24-channel, IDEX Health & Science GmbH, Wertheim, Germany). With this setup, each test vessel received 1.25 ± 0.1 L test water per day (exchange rate: 2.1 vessel volumes/day).

Fertilized zebrafish eggs were selected and transferred into the test vessels as described in section 2.3. Eggs were placed in sieves (0.2 mm mesh size) held approximately 10 mm above the bottom of the test vessels to prevent them from being covered by precipitated Carbo-Iron agglomerates. Each

sieve was set in a circular polyethylene frame (120 mm diameter, 80 mm height) that was fixed with stainless steel sticks on the rim of the test vessel. Starting on the day of first hatch until one day before test end, fish were fed at least three times per day *ad libitum* with a combined diet of dry food (NovoBaby®, JBL GmbH & Co. KG, Neuhofen, Germany), *Paramecium caudatum*, and *Artemia* spp. nauplii. Each day, any debris on the bottom and sides of the test vessels was thoroughly removed with a siphoning tube.

Hatching success, time to hatch and survival of the fish were assessed daily. Since test suspensions were increasingly opaque at concentrations ≥ 2.5 mg/L, the respective test vessels were inspected on a light table. Five days after the start of exposure, when all fish were free swimming, the sieves were carefully removed from the vessels. The test was terminated 30 d after 80% of embryos have hatched, i.e. 34 d after test start. Four days before test end, 12 fish from each treatment and control were chosen randomly and transferred to vessels with control water to evaluate Carbo-Iron depuration from the gut. At the end of the test, fish were killed with MS-222 (600 mg/L, buffered with 300 mg/L NaHCO₃) and dried with a tissue paper before measuring total length of each fish and weight. The weight of all (pooled) fish in each test vessel was measured, and the weight of individual fish at test end was obtained by dividing by the number of surviving fish. From each treatment and control, 7 fish were sampled for microscopic analysis (section 2.7).

Oxygen content, pH, total ammonia and temperature were measured in all test vessels 3 times per week; additionally temperature was continuously recorded in a supplemental test vessel. Oxygen concentrations were 6.4 to 7.4 mg/L, pH was 7.3 to 7.5. The continuously measured temperature over the whole test period was between 25.9 and 26.9°C; temperature difference between test vessels at any time point did not exceed 0.4°C. The maximum concentration of total ammonia was 1.0 mg/L in one replicate of the CMC control and the test concentrations 2.5 and 7.9 mg/L Carbo-Iron, respectively, on one day of measurement during the experiment. However, all other times (at 12 out of 13 measurements per control or treatment) ammonia concentrations were ≤ 0.4 mg/L. Samples for analysis of particle diameters, particle concentrations and concentrations of iron ions were taken on d 0, 7, 14, 21, 28 and 34.

2.7 Investigation of particle uptake

Fish and fish embryos were sampled at the end of the respective tests for microscopic analysis of Carbo-Iron distribution in the body. Fish samples were preserved in a mixture of 2.5% glutaraldehyde and 3.7% formaldehyde in phosphate buffered saline (PBS) buffer at 4°C until analysis.

2.7.1 Scanning electron microscopy (SEM)

Samples for conventional scanning electron microscopy (SEM) were washed with PBS, dehydrated in a graduated series of acetone and critical point-dried (CPD 030, BAL-TEC GmbH, Schalksmühle, Germany). Samples were mounted on SEM steps and carbon coated under vacuum. Analysis was performed using a Philips FEG-ESEM XL 30 (FEI Eindhoven, The Netherlands) with a secondary electron detector. Individual detection parameters are shown in the corresponding figures in section 3.

For scanning electron microscopy of the block surface, fixed samples were washed with PBS, post-fixed with 2% osmium tetroxyde, dehydrated in a graduated series of acetone (including a contrast enhancing step with 1% uranyl acetate in 50% acetone) and infiltrated with pure epoxy resin (Spurr, 1969) at room temperature. After polymerisation at 60°C for 72 h samples were milled to appropriate shape (Leica EM Trimm, Leica Microsystems, Wetzlar, Germany) equipped with a diamond mill (Diatome AG, Biel, Switzerland). A Leica EM UCT 6 ultramicrotome equipped with a Diatome diamond knife was used to prepare a flat surface of the block face of the samples. Samples were mounted on SEM steps and carbon coated under vacuum. Finally, the samples were analyzed using a Philips FEG-ESEM XL 30 with a backscatter electron detector. Individual detection parameters are shown in the data bars of the respective figures in section 3.

2.7.2 Transmission electron microscopy (TEM)

Samples were washed with PBS at room temperature, post-fixed with 1% osmium tetroxyde, dehydrated in a graduated series of acetone (including a staining step with 1% uranyl acetate) and embedded in epoxy resin according to Spurr (1969). Ultra-thin sections (50–70 nm) of samples were prepared on a Leica EM UCT 6 ultramicrotome, mounted on pioloform coated copper grids, post-stained with uranyl acetate and lead citrate (Reynolds, 1963) and analyzed with a Zeiss CTEM 902 (Zeiss, Oberkochen, Germany; EM-facility of the Department Cell Biology of the University of Bayreuth) at 80 kV accelerating voltage.

As a measure for effects of Carbo-Iron on the intestine, the ultrastructure of the gut lumen was analyzed. The density of microvilli per μm gut length was counted on TEM pictures (one-dimensional measurement) in control fish and fish exposed to 7.9 and 25 mg/L aged Carbo-Iron ($n=11-12$). Additionally, fish were analyzed, which had been exposed for 30 d to 7.9 and 25 mg/L aged Carbo-Iron and subsequently held for 4 d in control water ($n=11-12$).

2.7.3 Energy dispersive x-ray microanalysis (EDX)

Samples prepared for conventional scanning electron microscopy and electron microscopy of the block face were analyzed with regard to chemical elements by energy dispersive X-ray microanalysis

(EDX). EDX-analysis and element mapping was performed with a Philips FEG-ESEM XL 30 equipped with an EDAX detecting unit and EDAX software (EDAX Inc., Mahwah, U.S.A.). Iron was detectable in fractions above approximately $\geq 0.1\%$ (m/m).

2.8 Differential gene expression in zebrafish embryos

The effect of Carbo-Iron on gene expression in zebrafish embryos was investigated in an accompanying study, which investigated the toxicity of perchloroethylene (PCE) with and without combined exposure to aged Carbo-Iron. The concentration of aged Carbo-Iron in this study was 10 mg/L. This design of the study allowed a statistical comparison between all treatments containing Carbo-Iron (CI) and all treatments not containing Carbo-Iron (nCI). The results of the effects of PCE on gene expression are considered here but will be published separately (König et al. in prep.).

Test suspensions were prepared by adding 10 mg/L aged Carbo-Iron with 2 mg/L CMC to undiluted fish culture water (see section 2.1). Subsequently PCE was added via an appropriate amount of an aqueous stock solution (0.36 mg/L). Zebrafish embryos were collected as described in section 2.3 and exposed for 12 (36-48 hpf) and 24 h (24-48 hpf) to 10 mg/L aged Carbo-Iron with 2 mg/L CMC, a series of different concentrations of PCE, and a series of different concentrations of PCE, each combined with 10 mg/L aged Carbo-Iron. For each treatment, 3 test vessels with 18 embryos per vessel (40 mL glass vials with gas tight valve lids filled with 36 mL of test water) were used. Six test vessels with 18 embryos per vessel were used for the control (fish culture water). RNA was isolated using Trizol (Invitrogen, Karlsruhe, Germany) according to the manufacturer's instruction. RNA was further purified using the Qiagen RNeasy Kit (Qiagen, Hilden, Germany). RNA concentration and RNA integrity were evaluated with the automated electrophoresis system Bioanalyzer (Agilent Technologies, Waldbronn, Germany). RNA from embryos of 3 test vessels of each treatment and control was pooled and used for synthesis of fluorescent Cy3-labeled cRNA. The labeling reactions and hybridization to a custom zebrafish 8x60 k array (Agilent Technologies, Weilbronn, Germany) were performed using the one-color Quick Amp labeling kit (Agilent Technologies) according to the manufacturer's instructions. The design of the used oligonucleotide array was based on a commercially available Agilent 4x44 k zebrafish array (<https://earray.chem.agilent.com>, design ID AMADID#031241) but was modified to fit to an 8x60 k format. Hybridized microarray slides were scanned with an Agilent DNA-microarray scanner.

2.9 Data analysis

Statistical analyses of the results of the fish embryo test, the acute fish toxicity test and the fish early life stage test were carried out using R V2.15 (R Development Core Team, 2011) and extension packages ,car', 'multcomp', 'nparcomp' and 'plotrix' (Fox and Weisberg, 2011; Hothorn et al., 2008; Konietzschke, 2012; Lemon, 2006). Statistical analysis was based on replicate means; proportional data were arcsine-transformed before analysis. For comparing data from control and CMC control the two-sided Welch two-sample t-test was used. All other treatments were compared to the CMC control (OECD, 2006). Data were checked for homogeneity of variances (Bartlett's test) and normal distribution (visual examination of residual distribution and Shapiro-Wilk test). If requirements for parametric testing were fulfilled, ANOVA and Dunnett's two-sided post-hoc test were performed. If requirements were not met, a Kruskal-Wallis test and, subsequently, two-sided non-parametric multiple comparisons for relative contrast effects based on Dunnett contrasts were applied. To evaluate differences between numbers of microvilli in fish from the early life stage test ANOVA and subsequent multiple comparison of means with the Tukey test for unequal sample sizes was performed. For all tests, a significance level of $p \leq 0.05$ was used (OECD, 2006).

Microarray data were analyzed with R V2.15 and the limma extension package V3.16.5 (Smyth, 2005). Data preprocessing comprised feature extraction (Agilent feature extraction software V11.5.1.1), quantile normalization between arrays, calculating averages of control replicate probe intensities, and correction of batch effects by subtraction of the mean log intensities per day of egg collection from the fish tanks and per gene. Statistical comparisons between groups (e.g. Carbo-Iron-treated vs. non-treated) were performed using the empirical Bayesian statistics of the limma package.

3. Results

3.1 Determination of particle characteristics

The specific surface area of aged Carbo-Iron powder as measured with the Brunauer-Emmett-Teller method was 682 m²/g. Scanning electron micrographs of Carbo-Iron showed a highly porous nanocomposite with a structure typical for activated carbon, the main component of Carbo-Iron (Fig. S1). In the stock suspensions used in the embryo toxicity test and the acute toxicity test, the mean hydrodynamic diameters of Carbo-Iron were 274 and 337 nm, respectively (Fig. 1). The polydispersity indices (PI) were 0.24 and 0.28, respectively, indicating a relatively broad particle size distribution.

In the samples from test suspensions measured immediately after sampling, mean particle diameters ranged from 329 to 332 nm for the embryo toxicity test (static exposure) and from 332 to 355 nm for the acute toxicity test with adult fish (semi-static exposure) (Fig. 1). No clear influence of the nominal concentrations on measured particle size was observed (Tab. S1 and S2; this also applies to the fish early life stage test, see Tab. 1). PI values in the embryo toxicity test and the acute toxicity test were between 0.17 and 0.57 with highest PIs at low particle concentrations.

Comparison of hydrodynamic diameters measured before and after shipment of samples from test and stock suspensions from these two tests showed only minor differences ($\leq 10\%$; Tab. S1 and S2). Hence, the shipping procedure was considered to have little impact on particle size measurements and was employed during the fish early life stage test.

Under flow-through conditions in the fish early life stage test particle diameters were higher than in the two abovementioned tests. The hydrodynamic diameters in stock suspensions were between 380 and 395 nm, those in test suspensions between 439 and 486 nm (Fig. 1 and Tab. S3). The PI ranged from 0.39 to 0.54 in stock and test suspensions.

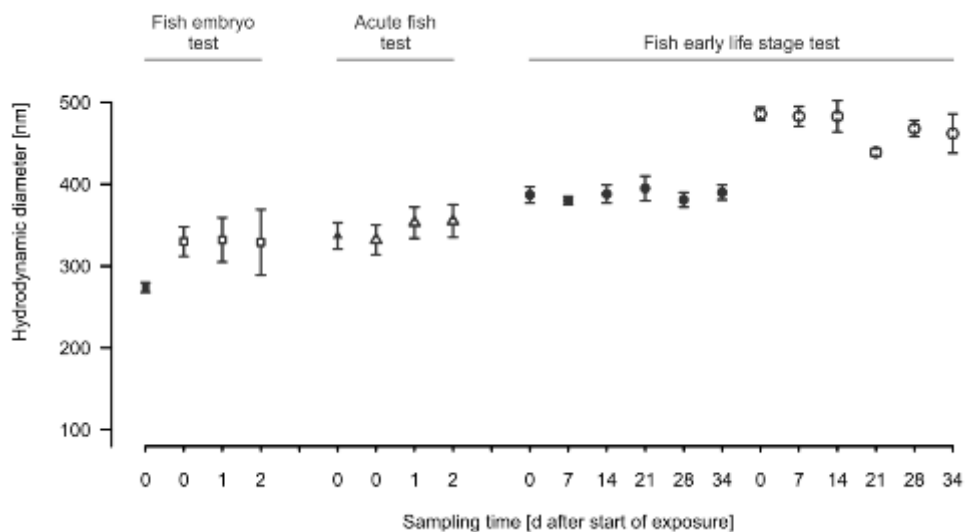


Fig 1: Mean (\pm sd) hydrodynamic diameters of aged Carbo-Iron in stock suspensions (solid symbols) and test suspensions (open symbols) during the fish embryo toxicity test, acute fish toxicity test and early life stage test. Error bars represent the standard deviation of technical replicates of DLS measurements of one sample, i.e. samples were divided in 2 subsamples and each subsample was measured 3 times with dynamic light scattering.

The concentrations of Carbo-Iron in the test suspensions of the fish early life stage test were determined based on the count rate in the DLS measurement. Prior to measuring samples from the

test, individual calibration curves were generated with freshly prepared Carbo-Iron suspensions. Linear regressions were obtained for concentrations up to 25 mg/L (Tab. S4 and Fig. S2). Measured concentrations deviated less than 20% from nominal concentrations (Tab. 1).

Tab. 1: Mean particle concentrations \pm sd (samples were divided in 2 subsamples and each subsample was measured 3 times with dynamic light scattering) in test suspensions in the fish early life stage test, calculated on basis of the calibration curve generated for each sampling date. Test suspensions were prepared daily and stored in a tank, from which suspensions constantly flowed into the test vessels. Before measurement, samples from stock suspensions were diluted by factor 20. All samples were transferred to the analysis laboratory and measured upon arrival (18 - 24 h after sampling).

Nominal conc. [mg/L]	Measured concentration [mg/L] (% of nominal concentration)					
	d 0	d 7	d 14	d 21	d 28	d 34
2.5	2.7 \pm 0.1 (108)	2.5 \pm 0.1 (100)	2.9 \pm 0.1 (116)	2.7 \pm 0.1 (108)	2.7 \pm 0.1 (108)	2.4 \pm 0.1 (96)
7.9	8.1 \pm 0.1 (103)	8.7 \pm 0.3 (110)	8.0 \pm 0.3 (101)	8.5 \pm 0.2 (108)	8.3 \pm 0.3 (105)	7.5 \pm 0.1 (95)
25.0	21.0 \pm 0.5 (84)	24.6 \pm 0.8 (98)	22.5 \pm 0.2 (90)	23.4 \pm 0.8 (94)	22.1 \pm 0.3 (88)	22.8 \pm 0.8 (91)

In all test suspensions, the measured concentrations of dissolved iron increased with increasing Carbo-Iron concentrations. They were between 5 and 29 μ g/L in the controls of the three toxicity tests, between 38 and 68 μ g/L at 25 mg/L Carbo-Iron in the embryo toxicity and the early life stage test, and 49 and 53 μ g/L at 100 mg/L Carbo-Iron in the fish embryo and fish acute test (Tab. S5, S6 and S7).

3.2 Fish embryo toxicity test

At the test end, embryos exposed to Carbo-Iron concentrations \geq 12.5mg/L were covered with a clearly visible amount of precipitated nanocomposite. Therefore, embryos exposed to 50 and 100 mg/L aged Carbo-Iron had to be rinsed with culture water before microscopic evaluation of lethal and sublethal effects. Carbo-Iron did not significantly affect survival of zebrafish embryos in any of the test concentrations (mortality < 10%, Tab. 2). An increasing number of embryos with fungal growth on the chorion were observed at concentrations \geq 12.5 mg/L (Fig S3). This effect was significant at 25 and 50 mg/L (Fig. 2). No other sublethal effects, such as edemas or malformations, were observed.

SEM analysis of zebrafish embryos showed adherence of particles with Carbo-Iron-like morphology to the chorion (Fig. 3a). These particles were identified as Carbo-Iron by the presence of iron in the particle via EDX. Investigations with TEM showed that Carbo-Iron particles were found only on the outer surface of the chorion but not in the perivitelline space or in the embryo (Fig. 3b).

Tab 2: Lethal and sublethal effects in zebrafish embryos (% of number of eggs at the beginning of exposure (means \pm sd; n=4) after 48 h of exposure to Carbo-Iron. No significant differences compared to the control were detected (Kruskal-Wallis test).

Carbo-Iron [mg/L]	Lethal effects	Sublethal effects
Control	10 \pm 12	0
CMC control	3 \pm 5	0
1.6	3 \pm 5	0
3.2	3 \pm 5	0
6.3	0	0
12.5	3 \pm 5	0
25	8 \pm 10	0
50	8 \pm 10	0
100	0	0

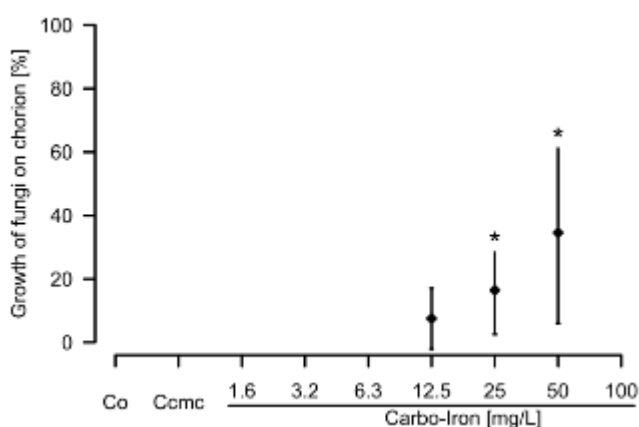


Fig. 2: Embryos with growth of fungi on the chorion (% of surviving embryos, means \pm sd, n=4); Co: control, Ccmc: control with the dispersant carboxymethyl cellulose (CMC; 20 mg/L). Asterisks indicate significant difference compared to Ccmc (Kruskal-Wallis test, non-parametric multiple comparisons for relative contrast effects based on Tukey contrasts, $p < 0.05$).

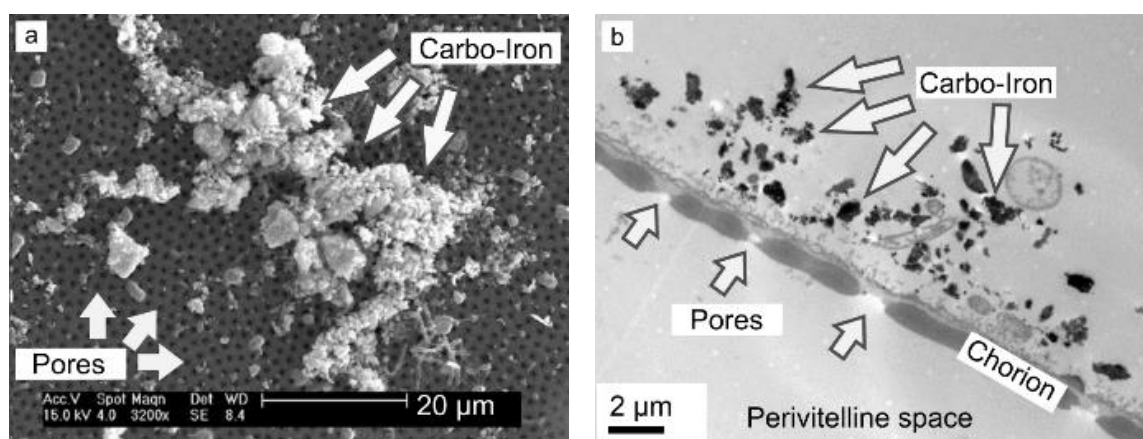


Fig. 3: (a) Scanning electron micrographs of a zebrafish egg after exposure to aged Carbo-Iron (25 mg/L) shows adherence of agglomerated particles (white) with Carbo-Iron like morphology to the chorion. Detection parameters: beam accelerating voltage (Acc. V.) = 15 kV, spot size (spot) = 4 nm, magnification (Magn.) = 3200x, detector = secondary electron detector, working distance (WD) = 8.4 mm. **(b)** Lateral cut (ultrathin section, TEM) through the zebrafish egg shows Carbo-Iron on the outside of the egg (dark particles). The lack of Carbo-Iron particles in the chorion pores and the perivitelline space indicates that the chorion acts as barrier for the uptake of Carbo-Iron.

3.3 Acute fish toxicity test

In the acute fish test, no mortalities were recorded in the controls and in any of the tested Carbo-Iron concentrations (4.3-100 mg/L). At test end, fish from the highest test concentration were visibly darker than fish from the control, indicating Carbo-Iron adhering to the skin. Upon transfer of the fish to the solution with MS-222 the particles were quickly removed. Subsequent observations with a dissection microscope did not reveal any particles adhering to the body or to the surface of the gills.

In fish exposed to concentrations ≥ 20.7 mg/L, particles were detected in the gut (Fig. 4a) and identified as Carbo-Iron using EDX (Fig. 4b). No Carbo-Iron was detected by SEM in the tissues surrounding the gut of fish exposed to Carbo-Iron. This provides evidence that Carbo-Iron did not pass the intestinal wall during the 96 h of exposure. SEM analyses of gills surfaces confirmed microscopic observations, i.e. no Carbo-Iron was detected on the surface of the zebrafish gills.

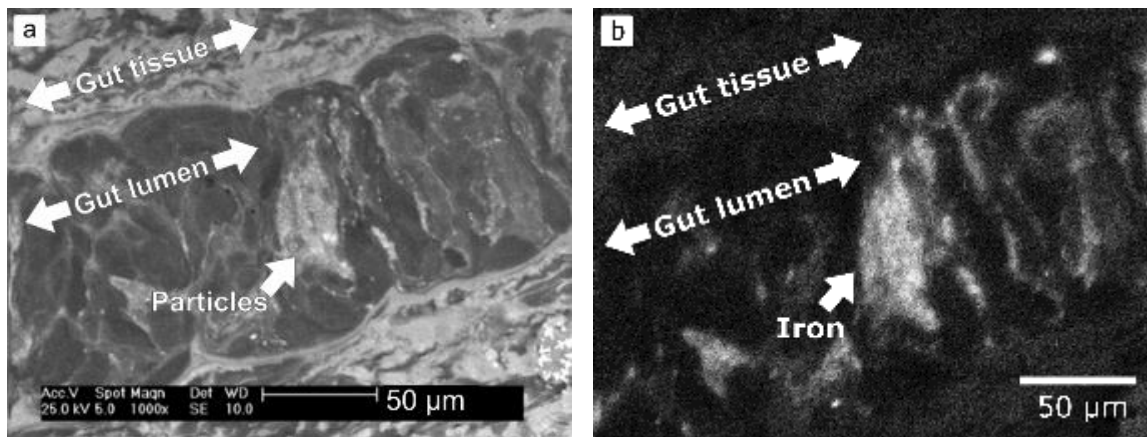


Fig. 4: (a) Scanning electron micrograph of the gut of an adult zebrafish (lateral cut) after 96 h of exposure to 100 mg/L of aged Carbo-Iron. The white areas in the lumen of the gut represent particles with Carbo-Iron-like morphology. Detection parameters: beam accelerating voltage (Acc. V.) = 25 kV, spot size (spot) = 5 nm, magnification (Magn.) = 1000x, detector = secondary electron detector, working distance (WD) = 10 mm. (b) EDX mapping of the same area detected presence of iron in the particles and confirmed that they represent Carbo-Iron. The respective areas are highlighted as white clusters in the gut lumen.

3.4 Fish early life stage test

In the fish early life stage test, growth of fungi on the chorion of embryos exposed to Carbo-Iron concentrations ≥ 7.9 mg/L occurred 2 to 3 d after the start of exposure, i.e. similarly as observed in the fish embryo test. However, all embryos hatched between 2 and 5 days post fertilization and no effects related to the presence of fungi on hatching or any other evaluated endpoint could be observed. Mean post-hatch survival of fish exposed to aged Carbo-Iron on d 34 was between $88 \pm 4\%$ (25 mg/L) and $98 \pm 1\%$ (0.79 mg/L) and was not significantly different from survival in the CMC control ($89 \pm 1\%$; Fig. 5a). However, in one of the replicates exposed to the highest Carbo-Iron concentration (25 mg/L), only 60% of the fish survived until the end of the test. Due to the reduced number of fish the remaining fish in this test vessel grew considerably more as indicated by the increased weight and length of the fish. For statistical analysis of the endpoints weight and length, data were tested with and without inclusion of this replicate. Length of fish at test end (Fig. 5b) was significantly different between control (11 ± 1 mm) and dispersant control (12 ± 1 mm) (two-sided Welch two sample t-test), but no significant effects between the treatments and the CMC control were detected. Individual fresh weight of fish at test end was 12 ± 1 μ g in the control and 14 ± 2 μ g in the CMC control, but this difference was not significant. The fresh weight increased with increasing Carbo-Iron concentrations from 14 ± 2 μ g at 0.25 mg/L to 17 ± 1 μ g (excluding the abovementioned replicate with a reduced survival rate) and 20 ± 6 μ g (including all replicates) at

25 mg/L. Fresh weight of fish exposed to 7.9 mg/L Carbo-Iron ($19 \pm 1 \mu\text{g}$) was significantly higher than in the CMC control (Fig. 5c).

Since in the acute toxicity test Carbo-Iron had been detected in the gut of adult zebrafish but not in the gills, uptake of Carbo-Iron via the intestines was further investigated in the fish early life stage test. SEM and EDX showed uptake of Carbo-Iron into the gut of exposed fish (Fig. 6a and b). No Carbo-Iron was detected in the guts of fish transferred to vessels with fish culture water 4 d before test end (Fig. 6c and d). Analysis of the gut structure revealed a significantly lower density of microvilli in fish exposed to 7.9 and 25 mg/L of aged Carbo-Iron for 34 d compared the CMC control (Fig. 7). The density of microvilli in the guts of fish exposed to 7.9 and 25 mg/L Carbo-Iron for 30 d and subsequently held in control water for 4 d were similar to controls.

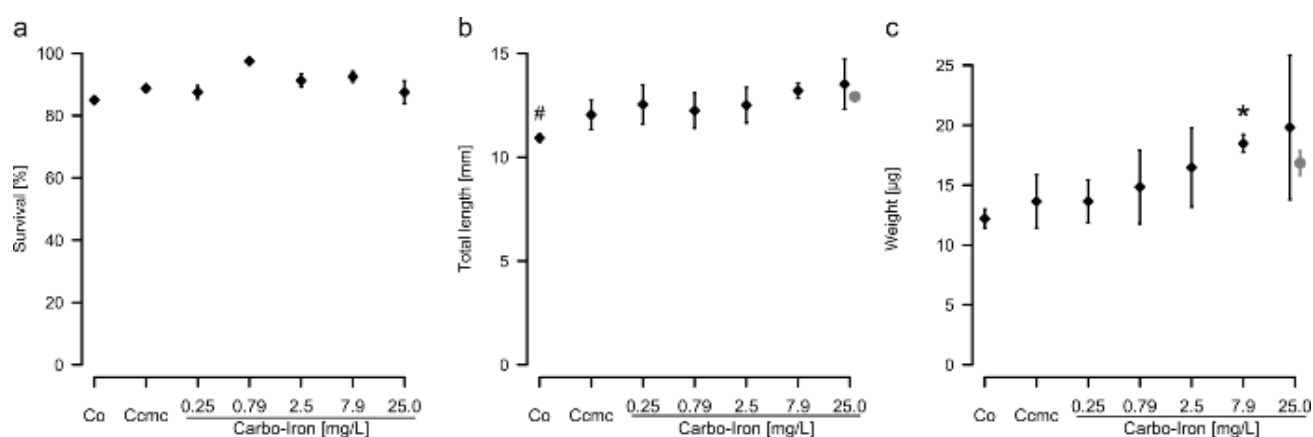


Fig. 5: (a) Overall survival (% of number of eggs at the start of exposure), (b) total length, and (c) individual fresh weight of zebrafish at the end of the fish early life stage test (34 days post fertilization). All embryos hatched successfully. Data represent means \pm sd ($n=4$) except for length and weight in the highest test concentration, where data are also presented excluding one replicate with a lower survival rate, which led to a faster growth (gray circles, $n=3$). Co: control, Ccmc: control with the dispersant carboxymethyl cellulose (CMC, 20 mg/L); # indicates a significant difference to Co (two-sided Welch t-test, $p < 0.05$), the asterisk indicates a significant difference to Ccmc (ANOVA; two sided Dunnett test, $p < 0.05$).

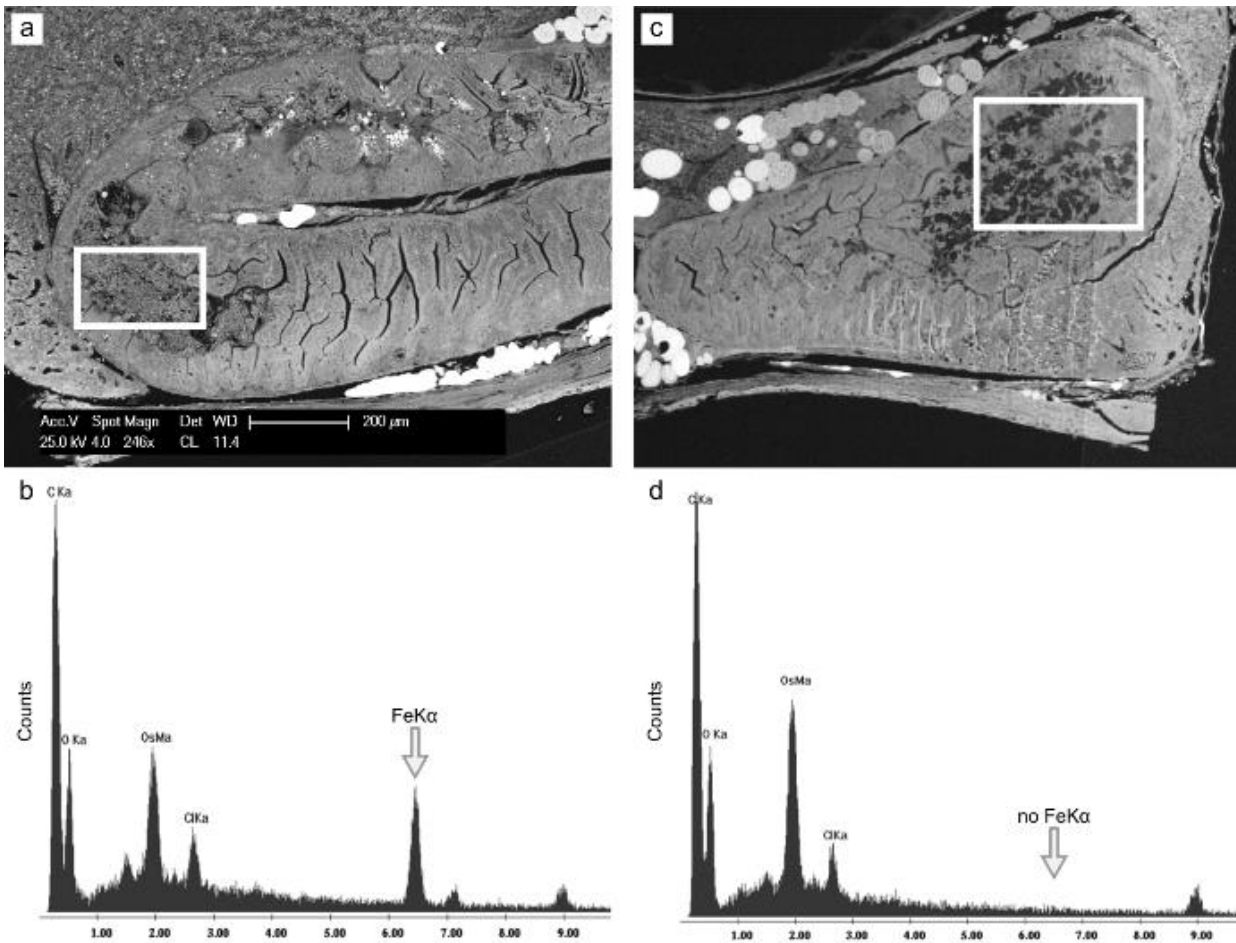


Fig. 6: (a) Scanning electron micrographs of the gut of zebrafish exposed to 25 mg/L of aged Carbo-Iron for 34 d. In the area highlighted by the white rectangle, energy-dispersive X-ray (EDX) spectroscopy was performed. (b) The EDX spectrum for this area shows a peak for the characteristic $K\alpha$ -wavelength of iron (caused by electrons transitioning from atomic shell L to K) as indicated by the arrow. The high iron content in the zebrafish gut indicates the presence of aged Carbo-Iron. (c) SEM micrograph of the gut of zebrafish exposed to 25 mg/L of aged Carbo-Iron for 30 d and subsequently held in control water for 4 d, EDX spectroscopy was performed in the area highlighted by the white rectangle. (d) The corresponding EDX analysis shows no elevated iron concentrations. Detection parameters for (a) and (b): beam accelerating voltage (Acc. V.) = 25 kV, spot size (spot) = 4 nm, magnification (Magn.) = 246x, detector = cathodoluminescence detector, working distance (WD) = 11.4 mm.

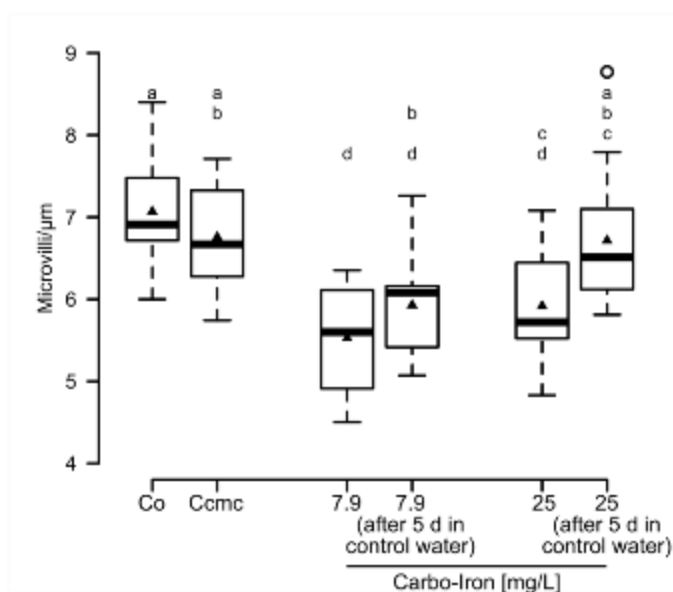


Fig. 7: Density (number/ μm) of microvilli in the gut of zebrafish at the end of the early life stage test. Boxes represent the upper and lower quartile and the medians (dash in each box), vertical lines represent the data range without outliers. Triangles indicate mean values; the circle represents a value outside the 1.5x range of the quartiles. Analysis was performed after 34 d of exposure to control (Co), dispersant control (Ccmc), 7.9 and 25 mg/L aged Carbo-Iron. Additionally, fish exposed to 7.9 and 25 mg/L aged Carbo-Iron for 30 d and subsequently held for 4 d under control conditions were analyzed (n=11-12). Treatments sharing the same letter are not significantly different from each other (ANOVA, Tukey-Test for unequal sample sizes; $p > 0.05$).

3.5 Differential gene expression

In the microarray experiment with aged Carbo-Iron and perchloroethylene (PCE), a clear concentration-dependent increase of genes, which changed significantly in their expression as compared to the control, was observed in embryos exposed to PCE (König et al., in preparation). However, aged Carbo-Iron did not cause any differential gene expression in the exposed zebrafish embryos (Fig. S4).

4. Discussion

The stability of nanomaterial suspensions in biological test systems is an important issue with respect to the reproducibility of experimental data and the standardization of test methods. The dispersant CMC proved to be suitable for stabilizing stock suspensions in deionized water. During the static test with zebrafish embryos and the semi-static test with adult zebrafish, no clear changes in the mean hydrodynamic diameter of Carbo-Iron and the polydispersity index were found within the first 48 h after preparation of the test suspensions.

To maintain constant concentrations of aged Carbo-Iron in test suspensions for ≥ 48 h, a flow-through system was developed and used in the 34 d test with early life stages of zebrafish. By adjusting the system to an exchange rate of two vessel volumes per day and by daily removal of precipitates constant exposure concentrations of Carbo-Iron in the aqueous phase were achieved. The measured hydrodynamic diameter of Carbo-Iron in the stock suspension prepared for the fish embryo test (274 ± 6 nm) was considerably smaller than in the stock suspensions for the acute toxicity test (337 ± 16 nm) and in those for the fish early life stage test (380 ± 5 nm to 390 ± 9 nm). As described in section 2.1, the volumes prepared during each ultrasonic treatment were limited to 100 mL in order to achieve a constant specific energy input during dispersion of Carbo-Iron powder. To gain sufficient volumes for the fish acute toxicity test (600 mL prepared) and the fish early life stage test (700 mL prepared), consecutive preparation of 100 mL aliquots of stock solutions and pooling were necessary. Apparently, measured Carbo-Iron diameters increased with the volume of the prepared stock suspension. A possible explanation is that the sonication probe became very hot during preparation of the first 100 mL aliquot and did not cool down before starting to prepare the next aliquot, although the stock suspensions were placed on ice during sonication. Additionally, mixing of the various aliquots by itself could have influenced particle size due to the input of mechanical energy.

Irrespective of the different hydrodynamic diameters of Carbo-Iron in the stock suspensions for the static fish embryo test and the semi-static acute fish test, the mean diameters of the particles in the test suspensions were in a very similar range in both tests (329 - 332 nm in the embryo toxicity test, 332 - 355 nm in the acute toxicity test; Fig. 1). However, in the test suspensions from the fish early life stage test, mean measured diameters (462 - 486 nm, Fig. 1) were considerably larger. This may have been caused by the peristaltic pumps used for delivery of the test water from the storage tank to the test vessels, which elicited pressure on the tubing and, thus, the particles in the test suspensions. Although the measured hydrodynamic diameters in the test suspensions differed

between the three tests, variation of Carbo-Iron size in each of the tests was low indicating that exposure conditions were constant and reproducible.

To verify nominal nanoparticle concentrations as required e.g. by ECHA (2012) and OECD (2010), chemical analysis of one constituent of the particle is often used (e.g. Ramsden et al., 2013; Seitz et al., 2013), occasionally with preceding digestion of the particles (Filser et al., 2013; Schlich et al., 2013). In preliminary experiments for the present study, such methods did not yield satisfactory results, mainly because of the background concentrations of iron and carbon, the two constituents of Carbo-Iron, in samples from test vessels. Thus, an alternative method based on DLS was developed and shown to deliver reliable particle concentrations. The advantage of this DLS-based method is its direct information on the concentration of particles without the need to digest the samples and to subsequently analyze the constituents. Using this method a good agreement of measured and nominal concentrations was found in the stock and test suspensions from the fish early life stage test.

In the tests with zebrafish, aged Carbo-Iron exhibited no toxicity in the investigated concentration ranges up to 100 mg/L. The growth of fungi on the chorion observed in the 48 h test with embryos and the 34 d test with early life stages of zebrafish had no impact on hatching and survival of the fish. The slight difference in weight and length between fish from the control and the CMC control in the fish early life stage test is most likely due to the fact that CMC is a polysaccharide, i.e. a potential source of nutrition for microorganisms. It can be assumed that a higher abundance of microorganisms in the CMC control and the Carbo-Iron treatments served as an additional food source for the fish early life stages. However, this does not explain the increase in body weight with increasing Carbo-Iron concentration observed in the test, as the concentration of CMC was constant (20 mg/L) in all treatments. Since no increase in length was observed, Carbo-Iron agglomerates present in the gut of the fish might have contributed to the increase of weight of the exposed fish as Carbo-Iron has a higher specific weight than water (determined by its tendency to sediment in aqueous media). Nevertheless, this only partly explains the weight differences observed.

The dissolution of ions into the aqueous phase is one of the most important factors resulting in toxicity of nanomaterials to aquatic organisms, as it can lead to subsequent metal intoxication (Auffan et al., 2009; Hoheisel et al., 2012). In the present study, the highest measured concentration of iron ions in test suspensions was 68 µg/L (compared to ≤ 29 µg/L in control water). Dave (1985) reported that Fe³⁺ concentrations up to 32 mg/L caused no adverse effects in zebrafish during 16 d after fertilization. Brenner & Cooper (1978) detected no effects of 3 mg/L Fe(OH)₃ (1.6 mg/L of Fe) on the development of early life stages of Coho salmon (*Oncorhynchus kisutch*). The amounts of

ionic iron released in the present experiments from aged Carbo-Iron were, thus, much lower than iron concentrations that have been found to be toxic to fish early life stages.

Direct contact with the organism and/or incorporation of particles by the organism can be crucial for the toxicity of nanomaterials even in case that toxicity is mediated by leaching metal ions (Wang, 2011). In zebrafish eggs, pore channels in the three-layered chorion could represent an efficient barrier for uptake of particles into the perivitelline space and subsequently the embryo. Lee et al. (2007) measured diameters between 500 and 700 nm for the outer opening of the pores. In the present study, Carbo-Iron agglomerates in fish culture water were ≥ 300 nm in diameter and hence of similar size as the pores. The smallest Carbo-Iron particles visible in the TEM image (Fig. 3b) were smaller than the pores. However, the inner surface of the pore channels is lined with microvilli (Hart and Donovan, 1983). These microvilli may hinder the passage of large particles and reduce the effective pore diameter. Applying TEM and SEM coupled with EDX, Carbo-Iron was not detected in the embryo or in the perivitelline space in the present study. Lee et al. (2007) observed passive diffusion of 12 nm silver particles into the perivitelline space of *D. rerio* eggs, and Asharani et al. (2008, 2011) reported the presence of nano-silver, nano-gold, and nano-platinum particles with diameters ≤ 35 nm in *D. rerio* embryos. Yet, silica nanoparticles of 60 nm and 200 nm diameter did not pass through the chorion of *D. rerio* (Fent et al., 2010). Thus, a size cut off seems to exist for the passage of particles through the chorion of zebrafish embryos. Particle characteristics such as surface charge or shape, which influence uptake in various organisms (Handy et al., 2008; Shaw and Handy, 2011; Treuel et al., 2013; van Hoecke et al., 2008), are likely to be relevant for the passage through the chorion, too. In case of aged Carbo-Iron, the chorion seems to represent an effective barrier.

Further evidence for the lack of toxicity of Carbo-Iron to zebrafish embryos was provided by the results from the microarray experiments. Differential gene expression in zebrafish embryos has been shown to be a sensitive endpoint in studies with metal-based nanoparticles (Choi et al., 2010; Griffitt et al., 2013; Park and Yeo, 2013; Yeo and Park, 2012). However, no effect of Carbo-Iron on gene expression levels was detected in the present study. This finding is in good agreement with the abovementioned observation in the present study, considering that Carbo-Iron was not able to cross the chorion and that concentrations of dissolved iron were clearly below toxic levels.

The primary routes of uptake of nanomaterials into juvenile and adult fish are via the intestine and via the gills. Particles or dissolved ions could then be distributed to other tissues (Baker et al., 2014; Jovanović and Palić, 2012; Scown et al., 2010; Shaw et al., 2012). In the present study, no uptake via the gills was detected, but uptake of aged Carbo-Iron into the gut of zebrafish was observed in

adult fish after 96 h of exposure as well as in early life stages after 34 d of exposure. Yet, no passage of particles from the gut into the surrounding tissues was detected. The large particle size and the positive charge of Carbo-Iron may have restricted transport through the intestinal mucous layer (Hussain et al. 2001). In the fish early life stage test with Carbo-Iron, a reduced density of microvilli was observed in the zebrafish gut at the end of the exposure. This might be a consequence of a mechanical effect of the particles. However, Carbo-Iron was excreted from the intestine after juvenile fish had been held in culture water for 4 d and density of the microvilli recovered to values close to control values. In ecotoxicity tests with the sediment-dwelling oligochaete *Lumbriculus variegatus*, Pakarinen et al. (2011) observed damaged cuticle fibers after exposure to 50 mg fullerenes / kg sediment. Waissi-Leinonen et al. (2012) performed sediment tests with larvae of the midge *Chironomus riparius* and fullerenes and detected morphological changes in the gut and microvilli similar to the effects determined in the present study. Furthermore, both studies did not find uptake of particles into other tissue or cells in the organisms.

To summarize, no uptake of Carbo-Iron through the chorion, through the gills and from the intestine to the surrounding tissue of zebrafish was observed. Accordingly, aged Carbo-Iron concentrations of up to 100 mg/L did not exhibit any acute toxicity to adult fish and fish embryos. Gene expression in fish embryos was not affected by ≤ 10 mg/L of Carbo-Iron, and concentrations ≤ 25 mg/L had not adverse effects in the fish early life stage test.

Acknowledgements

The present work was funded by the German Ministry of Education and Research (project numbers 03X0082 A, B, C and F). The sole responsibility for the content of this publication lies with the authors. The authors thank Dr. Stefan Scholz for extensive review and helpful advice on the present manuscript.

References

- Asharani PV, Lian Wu Y, Gong Z, Valiyaveettil S, 2008. Toxicity of silver nanoparticles in zebrafish models. *Nanotechnology* 19, 1-8. DOI: 10.1088/0957-4484/19/25/255102
- Asharani PV, Lian Wu Y, Gong Z, Valiyaveettil S, 2011. Comparison of the toxicity of silver, gold and platinum nanoparticles in developing zebrafish embryos. *Nanotoxicology* 5, 43–54. DOI: 10.3109/17435390.2010.489207
- Auffan M, Achouak W, Rose J, Roncato M-A, Chanéac C, Waite DT, Masion A, Woicik JC, Wiesner MR, Bottero JY, 2008. Relation between the redox state of iron-based nanoparticles and their cytotoxicity toward *Escherichia coli*. *Environmental Science & Technology* 42, 6730–6735. DOI: 10.1021/es800086f
- Auffan M, Rose J, Wiesner MR, Bottero JY, 2009. Chemical stability of metallic nanoparticles: a parameter controlling their potential cellular toxicity *in vitro*. *Environmental Pollution* 157, 1127–1133. DOI: 10.1016/j.envpol.2008.10.002
- Baker TJ, Tyler CR, Galloway TS, 2014. Impacts of metal and metal oxide nanoparticles on marine organisms. *Environmental Pollution* DOI: 10.1016/j.envpol.2013.11.014
- Bleyl S, Kopinke FD, Mackenzie K, 2012. Carbo-Iron® — synthesis and stabilization of Fe(0)-doped colloidal activated carbon for *in situ* groundwater treatment. *Chemical Engineering Journal* 191, 588–595. DOI: 10.1016/j.cej.2012.03.021
- Boyle D, Al-Bairuty GA, Henry TB, Handy RD, 2013. Critical comparison of intravenous injection of TiO₂ nanoparticles with waterborne and dietary exposures concludes minimal environmentally-relevant toxicity in juvenile rainbow trout *Oncorhynchus mykiss*. *Environmental Pollution* 182, 70–79. DOI: 10.1016/j.envpol.2013.07.001
- Brenner FJ, Cooper WL, 1978. Effect of suspended iron hydroxide on the hatchability and embryonic development of the coho salmon. *Ohio Journal of Science*. 78, 34-38.
- Brunauer S, Emmett PH, Teller E, 1938. Adsorption of gases in multimolecular layers. *Journal of the American Chemical Society* 60, 309–319. DOI: 10.1021/ja01269a023
- Bystrzejewska-Piotrowska G, Golimowski J, Urban PL, 2009. Nanoparticles: their potential toxicity, waste and environmental management. *Waste Management* 29, 2587–2595. DOI: 10.1016/j.wasman.2009.04.001
- Chae YJ, Pham CH, Lee J, Bae E, Yi J, Gu MB, 2009. Evaluation of the toxic impact of silver nanoparticles on Japanese medaka (*Oryzias latipes*). *Aquatic Toxicology* 94, 320–327. DOI: 10.1016/j.aquatox.2009.07.019
- Chen D, Zhang D, Yu JC, Chan KM, 2011. Effects of Cu₂O nanoparticle and CuCl₂ on zebrafish larvae and a liver cell-line. *Aquatic Toxicology* 105, 344–354. DOI: 10.1016/j.aquatox.2011.07.005
-

-
- Chen PJ, Tan SW, Wu WL, 2012. Stabilization or oxidation of nanoscale zerovalent iron at environmentally relevant exposure changes bioavailability and toxicity in medaka fish. *Environmental Science & Technology* 46, 8431–8439. DOI: 10.1021/es3006783
- Choi JE, Kim S, Ahn JH, Youn P, Kang JS, Park K, Yi J, Ryu DY, 2010. Induction of oxidative stress and apoptosis by silver nanoparticles in the liver of adult zebrafish. *Aquatic Toxicology* 100, 151–159. DOI: 10.1016/j.aquatox.2009.12.012
- Cundy AB, Hopkinson L, Whitby RLD, 2008. Use of iron-based technologies in contaminated land and groundwater remediation: A review. *Science of the Total Environment* 400, 42–51. DOI: 10.1016/j.scitotenv.2008.07.002
- Dalai S, Pakrashi S, Chandrasekaran N, Mukherjee A, 2013. Acute toxicity of TiO₂ nanoparticles to *Ceriodaphnia dubia* under visible light and dark conditions in a freshwater system. *PLoS ONE* 8, e62970. DOI: 10.1371/journal.pone.0062970
- Dave, G, 1985. The influence of pH on the toxicity of aluminum, cadmium, and iron to eggs and larvae of the zebrafish, *Brachydanio rerio*. *Ecotoxicology and Environmental Safety* 10, 253–267.
- ECHA, 2012. Guidance on information requirements and chemical safety assessment. Appendix R7-1 Recommendations for nanomaterials applicable to Chapter R7a Endpoint specific guidance. ECHA-12-G-03-EN. European Chemicals Agency, Helsinki, Finland.
- Fan Y, Li C, Cao H, Li F, Chen D, 2012. The intranuclear release of a potential anticancer drug from small nanoparticles that are derived from intracellular dissociation of large nanoparticles. *Biomaterials* 33, 4220–4228. DOI: 10.1016/j.biomaterials.2012.02.038
- Fent K, Weisbrod CJ, Wirth-Heller A, Pielers U, 2010. Assessment of uptake and toxicity of fluorescent silica nanoparticles in zebrafish (*Danio rerio*) early life stages. *Aquatic Toxicology* 100, 218–228. DOI: 10.1016/j.aquatox.2010.02.019
- Filser J, Arndt D, Baumann J, Geppert M, Hackmann S, Luther EM, Pade C, Prenzel K, Wigger H, Arning J, Hohnholt MC, Köser J, Kück A, Lesnikov E, Neumann J, Schütrumpf S, Warrelmann J, Bäumer M, Dringen R, von Gleich A, Swiderek P, Thöming J, 2013. Intrinsically green iron oxide nanoparticles? From synthesis via (eco-)toxicology to scenario modelling. *Nanoscale* 5, 1034. DOI: 10.1039/c2nr31652h
- Fox J, Weisberg S, 2011. An R companion to applied regression, Second. ed. Sage, Thousand Oaks, CA, USA.
- García A, Espinosa R, Delgado L, Casals E, González E, Puentes V, Barata C, Font X, Sánchez A, 2011. Acute toxicity of cerium oxide, titanium oxide and iron oxide nanoparticles using standardized tests. *Desalination* 269, 136–141. DOI: 10.1016/j.desal.2010.10.052
-

- Grieger KD, Fjordbøge A, Hartmann NB, Eriksson E, Bjerg PL, Baun A, 2010. Environmental benefits and risks of zero-valent iron nanoparticles (nZVI) for in situ remediation: Risk mitigation or trade-off? *Journal of Contaminant Hydrology* 118, 165–183. DOI: 10.1016/j.jconhyd.2010.07.011
- Griffitt RJ, Lavelle CM, Kane AS, Denslow ND, Barber DS, 2013. Chronic nanoparticulate silver exposure results in tissue accumulation and transcriptomic changes in zebrafish. *Aquatic Toxicology* 130/131, 192–200. DOI: 10.1016/j.aquatox.2013.01.010
- Handy RD, Henry TB, Scown TM, Johnston BD, Tyler CR, 2008. Manufactured nanoparticles: their uptake and effects on fish – a mechanistic analysis. *Ecotoxicology* 17, 396–409. DOI: 10.1007/s10646-008-0205-1
- Hart NH, Donovan M, 1983. Fine structure of the chorion and site of sperm entry in the egg of *Brachydanio*. *J. Exp. Zool.* 227, 277–296. DOI: 10.1002/jez.1402270212
- Hoheisel SM, Diamond S, Mount D, 2012. Comparison of nanosilver and ionic silver toxicity in *Daphnia magna* and *Pimephales promelas*. *Environmental Toxicology and Chemistry* 31, 2557–2563. DOI: 10.1002/etc.1978
- Höss S, Fritzsche A, Meyer C, Bosch J, Meckenstock RU, Totsche KU, 2015. Size- and composition-dependent toxicity of synthetic and soil-derived Fe oxide colloids for the nematode *Caenorhabditis elegans*. *Environmental Science & Technology* 49, 544–552. DOI: 10.1021/es503559n
- Hothorn T, Bretz F, Westfall P, 2008. Simultaneous inference in general parametric models. *Biometrical Journal* 50, 346–363. DOI: 10.1002/bimj.200810425
- Hussain N, Jaitley V, Florence AT. 2001. Recent advances in the understanding of uptake of microparticulates across the gastrointestinal lymphatics. *Advanced drug delivery reviews* 50(1): 107–142.
- ISO, 2008. ISO 22412:2008. Particle size analysis - Dynamic light scattering (DLS). International Organization for Standardization, Geneva, Switzerland.
- ISO , 2011. SO/TS 80004-4:2011. Nanotechnologies - Vocabulary - Part 4: Nanostructured materials. International Organization for Standardization, Geneva, Switzerland.
- Jiemvarangkul P, Zhang W, Lien HL, 2011. Enhanced transport of polyelectrolyte stabilized nanoscale zero-valent iron (nZVI) in porous media. *Chemical Engineering Journal* 170, 482–491. DOI: 10.1016/j.cej.2011.02.065
- Jovanović B, Palić D, 2012. Immunotoxicology of non-functionalized engineered nanoparticles in aquatic organisms with special emphasis on fish — Review of current knowledge, gap identification, and call for further research. *Aquatic Toxicology* 118–119, 141–151. DOI: 10.1016/j.aquatox.2012.04.005
- Ju-Nam Y, Lead JR, 2008. Manufactured nanoparticles: An overview of their chemistry, interactions and potential environmental implications. *Science of the Total Environment* 400, 396–414. DOI: 10.1016/j.scitotenv.2008.06.042
-

-
- Kadar E, Dyson O, Handy RD, Al-Subiai SN, 2013. Are reproduction impairments of free spawning marine invertebrates exposed to zero-valent nano-iron associated with dissolution of nanoparticles? *Nanotoxicology* 7, 135–143. DOI: 10.3109/17435390.2011.647927
- Kharisov BI, Rasika Dias HV, Kharissova OV, Jiménez-Pérez VM, Olvera Pérez B, Muñoz Flores B, 2012. Iron-containing nanomaterials: synthesis, properties, and environmental applications. *RSC Adv.* 2, 9325. DOI: 10.1039/c2ra20812a
- Klaine SJ, Alvarez PJJ, Batley GE, Fernandes TF, Handy RD, Lyon DY, Mahendra S, McLaughlin MJ, Lead JR, 2008. Nanomaterials in the environment: behavior, fate, bioavailability, and effects. *Environmental Toxicology and Chemistry* 27, 1825–1851.
- Klaine SJ, Koelmans AA, Horne N, Carley S, Handy RD, Kapustka L, Nowack B, von der Kammer F, 2012. Paradigms to assess the environmental impact of manufactured nanomaterials. *Environmental Toxicology and Chemistry* 31, 3–14. DOI: 10.1002/etc.733
- Konietschke F, 2012. nparcomp: Perform multiple comparisons and compute simultaneous confidence intervals for the nonparametric relative contrast effects. <http://cran.r-project.org/web/packages/nparcomp/index.html> (retrieved 12. February 2014).
- Lee KJ, Nallathamby PD, Browning LM, Osgood CJ, Xu XHN, 2007. *In vivo* imaging of transport and biocompatibility of single silver nanoparticles in early development of zebrafish embryos. *ACS Nano* 1, 133–143. DOI: 10.1021/nn700048y
- Lemon J, 2006. Plotrix: a package in the red light district of R. *R-News* 6, 8–12.
- Li M, Huang CP, 2011. The responses of *Ceriodaphnia dubia* toward multi-walled carbon nanotubes: effect of physical–chemical treatment. *Carbon* 49, 1672–1679. DOI: 10.1016/j.carbon.2010.12.052
- Lin J, Zhang H, Chen Z, Zheng Y, 2010. Penetration of lipid membranes by gold nanoparticles: insights into cellular uptake, cytotoxicity, and their relationship. *ACS Nano* 4, 5421–5429. DOI: 10.1021/nn1010792
- Lin YH, Tseng HH, Wey MY, Lin MD, 2010. Characteristics of two types of stabilized nano zero-valent iron and transport in porous media. *Science of the Total Environment* 408, 2260–2267. DOI: 10.1016/j.scitotenv.2010.01.039
- Mackenzie K, Schierz A, Georgi A, Kopinke F-D. 2008. “Colloidal activated Carbon and Carbo-Iron - novel materials for in-situ groundwater treatment.” *Global NEST Journal* 10 (1), 54–61.
- Mackenzie K, Bleyl S, Georgi A, Kopinke FD, 2012. Carbo-Iron – an Fe/AC composite – as alternative to nano-iron for groundwater treatment. *Water Res.* 46, 3817–3826. DOI: 10.1016/j.watres.2012.04.013
- Meißner T, Kühnel D, Busch W, Oswald S, Richter V, Michaelis A, Schirmer K, Potthoff A, 2010. Physical-chemical characterization of tungsten carbide nanoparticles as a basis for toxicological investigations. *Nanotoxicology* 4, 196–206. DOI: 10.3109/17435391003605455
-

- OECD, 1992. OECD guideline for testing of chemicals. No. 203. Fish, acute toxicity test. Organisation for Economic Co-operation and Development, Paris, France.
- OECD, 2006. OECD series on testing and assessment. No. 54. Current approaches in the statistical analysis of ecotoxicity data: a guidance to application. Organisation for Economic Co-operation and Development, Paris, France.
- OECD, 2010. Guidance manual for the testing of manufactured nanomaterials: OECD's sponsorship programme.; First revision. Organisation for Economic Co-operation and Development, Paris, France.
- OECD, 2013a. OECD guideline for testing of chemicals. No. 236. Fish embryo acute toxicity test. Organisation for Economic Co-operation and Development, Paris, France.
- OECD, 2013b. OECD guideline for testing of chemicals. No. 210. Fish, early life stage toxicity test. Organisation for Economic Co-operation and Development, Paris, France.
- OECD draft, 2006. Fish embryo toxicity (FET) test. Draft proposal for a new guideline. 1st version. Organisation for Economic Co-operation and Development, Paris, France.
- Pakrashi S, Dalai S, Humayun A, Chakravarty S, Chandrasekaran N, Mukherjee A, 2013. *Ceriodaphnia dubia* as a potential bio-indicator for assessing acute aluminum oxide nanoparticle toxicity in fresh water environment. *PLoS ONE* 8, 1–13. DOI: 10.1371/journal.pone.0074003
- Park EJ, Yi J, Kim Y, Choi K, Park K, 2010. Silver nanoparticles induce cytotoxicity by a Trojan-horse type mechanism. *Toxicol. in vitro* 24, 872–878. DOI: 10.1016/j.tiv.2009.12.001
- Park HG, Yeo MK, 2013. Comparison of gene expression changes induced by exposure to Ag, Cu-TiO₂, and TiO₂ nanoparticles in zebrafish embryos. *Molecular & Cellular Toxicology* 9, 129–139. DOI: 10.1007/s13273-013-0017-0
- R Development Core Team, 2011. R: A Language and Environment for Statistical Computing. Vienna, Austria.
- Ramsden CS, Henry TB, Handy RD, 2013. Sub-lethal effects of titanium dioxide nanoparticles on the physiology and reproduction of zebrafish. *Aquatic Toxicology* 126, 404–413. DOI: 10.1016/j.aquatox.2012.08.021
- Reynolds ES, 1963. The use of lead citrate at high pH as an electron-opaque stain in electron microscopy. *J. Cell Biol.* 17, 208–212.
- Schlich K, Klawonn T, Terytze K, Hund-Rinke K, 2013. Effects of silver nanoparticles and silver nitrate in the earthworm reproduction test. *Environmental Toxicology and Chemistry* 32, 181–188. DOI: 10.1002/etc.2030
- Scown TM, van Aerle R, Tyler CR, 2010. Review: Do engineered nanoparticles pose a significant threat to the aquatic environment? *Critical Reviews in Ecotoxicology* 40, 653–670. DOI: 10.3109/10408444.2010.494174
-

-
- Seitz F, Bundschuh M, Rosenfeldt RR, Schulz R, 2013. Nanoparticle toxicity in *Daphnia magna* reproduction studies: The importance of test design. *Aquatic Toxicology* 126, 163–168. DOI: 10.1016/j.aquatox.2012.10.015
- Shaw BJ, Al-Bairuty G, Handy RD, 2012. Effects of waterborne copper nanoparticles and copper sulphate on rainbow trout (*Oncorhynchus mykiss*): physiology and accumulation. *Aquatic Toxicology* 116/117, 90–101. DOI: 10.1016/j.aquatox.2012.02.032
- Shaw BJ, Handy RD, 2011. Physiological effects of nanoparticles on fish: a comparison of nanometals versus metal ions. *Environment International* 37, 1083–1097. DOI: 10.1016/j.envint.2011.03.009
- Smyth GK, 2005. limma: Linear Models for Microarray Data, in: Gentleman R, Carey VJ, Huber W, Irizarry RA, Dudoit S (Eds.), *Bioinformatics and computational biology solutions using r and bioconductor, statistics for biology and health*. Springer, New York, pp. 397–420.
- Spurr AR, 1969. A low-viscosity epoxy resin embedding medium for electron microscopy. *Journal of Ultrastructure Research* 26, 31–43. DOI: 10.1016/S0022-5320(69)90033-1
- Taurozzi JS., Hackley VA, Wiesner MR, 2011. Ultrasonic dispersion of nanoparticles for environmental, health and safety assessment--issues and recommendations. *Nanotoxicology* 5, 711–729. DOI: 10.3109/17435390.2010.528846
- Treuel L, Jiang X, Nienhaus GU, 2013. New views on cellular uptake and trafficking of manufactured nanoparticles. *J. R. Soc. Interface* 10. DOI: 10.1098/rsif.2012.0939
- Van Hoecke K, De Schamphelaere KC, Van der Meeren P, Lucas S, Janssen CR, 2008. Ecotoxicity of silica nanoparticles to the green alga *Pseudokirchneriella subcapitata*: importance of surface area. *Environmental Toxicology and Chemistry* 27, 1948–1957.
- Wang WX, 2011. Incorporating exposure into aquatic toxicological studies: an imperative. *Aquatic Toxicology* 105, 9–15. DOI: 10.1016/j.aquatox.2011.05.016
- Weil M, Scholz S, Zimmer M, Sacher F, Duis K, 2009. Gene expression analysis in zebrafish embryos – a potential approach to predict effect concentrations in the fish early life stage test. *Environmental Toxicology and Chemistry* 28, 1970–1978. DOI: 10.1897/08-627.1
- Xiong Z, Zhao D, Pan G, 2007. Rapid and complete destruction of perchlorate in water and ion-exchange brine using stabilized zero-valent iron nanoparticles. *Water Research* 41, 3497–3505. DOI: 10.1016/j.watres.2007.05.049
- Yeo MK, Park HG, 2012. Gene expression in zebrafish embryos following exposure to Cu-doped TiO₂ and pure TiO₂ nanometer-sized photocatalysts. *Molecular & Cellular Toxicology* 8, 127–137. DOI: 10.1007/s13273-012-0016-6
-

Zhang W, 2003. Nanoscale iron particles for environmental remediation: an overview. *Journal of Nanoparticle Research* 5, 323–332. DOI: 10.1023/A:1025520116015

Zhu X, Chang Y, Chen Y, 2010. Toxicity and bioaccumulation of TiO₂ nanoparticle aggregates in *Daphnia magna*. *Chemosphere* 78, 209–215. DOI: 10.1016/j.chemosphere.2009.11.013

Zhu X, Tian S, Cai Z, 2012. Toxicity assessment of iron oxide nanoparticles in zebrafish (*Danio rerio*) early life stages. *PLoS ONE* 7, e46286. DOI: 10.1371/journal.pone.0046286

Appendix B.2:

Supplemental information to:

The oxidized state of the nanocomposite Carbo-Iron® causes no adverse effects on growth, survival and differential gene expression in zebrafish

Mirco Weil ^a, Tobias Meißner ^b, Wibke Busch ^c, Armin Springer ^d, Dana Kühnel ^c,
Ralf Schulz ^d, Karen Duis ^a

^a ECT Oekotoxikologie GmbH, Böttgerstrasse 2-14, 65439 Flörsheim, Germany
m.weil@ect.de; lydia.huebler@gmail.com; k-duis@ect.de

^b Fraunhofer Institute for Ceramic Technologies and Systems, Winterbergstrasse 28, 01277
Dresden, Germany
tmeiss@gmx.net

^c Helmholtz Centre for Environmental Research – UFZ, Dept. Bioanalytical Ecotoxicology,
Permoser Strasse 15, 04318 Leipzig, Germany
wibke.busch@ufz.de, dana.kuehnel@ufz.de

^d Centre for Translational Bone, Joint and Soft Tissue Research, Technical University Dresden,
Fetscherstrasse 74, 01307, Dresden, Germany
armin.springer@tu-dresden.de

^e Institute for Environmental Sciences, University of Koblenz-Landau, Fortstrasse 7, 76829 Landau,
Germany
schulz@uni-landau.de

Corresponding author: Mirco Weil, ECT Oekotoxikologie GmbH, Böttgerstrasse 2-14, 65439
Flörsheim, Germany, m.weil@ect.de, +49 6145 956466

Tab. S1: Mean hydrodynamic particle diameters (x_{DLS}) \pm sd (samples were divided in 2 subsamples and each subsample was measured 3 times with dynamic light scattering) in stock and test suspensions during 48 h of exposure in the embryo toxicity test. Before measurement, the sample from the stock suspension was diluted by factor 20. All suspensions were measured immediately after sampling on site, i.e. in the laboratory where the tests were performed. Additionally, samples taken from the respective suspensions at test start (0 h) and 24 h later were transported to the analysis laboratory. These samples were analyzed upon arrival, i.e. 18-24 h later. PI: polydispersity indices.

Day of sampling [h after start of exposure]	Nominal Carbo- Iron concentration [mg/L]	Measured directly (immediately after sampling)		Measured after shipment (18-24 h after sampling)		Increase of particle size after shipping [%]
		x_{DLS} [nm]	PI	x_{DLS} [nm]	PI	
0	Stock suspension (1000 mg/L)	274 \pm 6	0.24	296 \pm 2	0.25	8
0	1.6	346 \pm 25	0.57	372 \pm 13	0.45	7
0	3.1	338 \pm 19	0.45	358 \pm 17	0.39	6
0	6.3	333 \pm 14	0.38	366 \pm 13	0.37	10
0	12.5	334 \pm 6	0.36	359 \pm 6	0.33	7
0	25	339 \pm 8	0.32	357 \pm 5	0.31	5
0	50	325 \pm 18	0.24	346 \pm 6	0.30	6
0	100	292 \pm 16	0.20	306 \pm 5	0.25	5
24	1.6	345 \pm 19	0.47	358 \pm 29	0.44	4
24	3.1	354 \pm 10	0.43	366 \pm 8	0.41	3
24	6.3	347 \pm 13	0.37	359 \pm 10	0.38	4
24	12.5	347 \pm 5	0.36	356 \pm 5	0.35	2
24	25	335 \pm 8	0.33	345 \pm 4	0.32	3
24	50	321 \pm 5	0.29	326 \pm 6	0.28	2
24	100	275 \pm 2	0.22	283 \pm 4	0.21	3
48	1.6	383 \pm 18	0.45	-	-	-
48	3.1	365 \pm 5	0.38	-	-	-
48	6.3	342 \pm 6	0.37	-	-	-
48	12.5	328 \pm 8	0.32	-	-	-
48	25	324 \pm 5	0.31	-	-	-
48	50	296 \pm 2	0.27	-	-	-
48	100	266 \pm 1	0.17	-	-	-

Tab. S2: Mean hydrodynamic particle diameters (x_{DLS}) \pm sd (samples were divided in 2 subsamples and each subsample was measured 3 times with dynamic light scattering) in stock and test suspensions in the acute fish toxicity test. Test suspensions in the test vessels were exchanged after 48 h of exposure, particle size measurement was performed at test start, 24 and 48 h later. Before measurement, the sample from the stock suspension was diluted by factor 20. All suspensions were measured immediately after sampling on site, i.e. in the laboratory where the tests were performed. Additionally, samples taken from the respective suspensions on test start (0 h) and 24 h later were transferred to the analysis laboratory. These samples were analyzed upon arrival, i.e. 18-24 h later. PI: polydispersity indices.

Day of sampling [h after start of exposure]	Nominal Carbo-Iron concentration [mg/L]	Measured directly (immediately after sampling)		Measured after shipment (18- 24 h after sampling)		Increase of particle size after shipping [%]
		x_{DLS} [nm]	PI	x_{DLS} [nm]	PI	
0	Stock suspension (1000 mg/L)	337 \pm 16	0.28	355 \pm 4	0.29	5
0	6.3	336 \pm 17	0.42	343 \pm 9	0.43	2
0	12.5	346 \pm 9	0.38	356 \pm 9	0.40	3
0	25	347 \pm 17	0.35	362 \pm 11	0.35	4
0	50	329 \pm 12	0.33	349 \pm 8	0.34	6
0	100	304 \pm 14	0.24	318 \pm 6	0.24	5
24	6.3	353 \pm 14	0.42	376 \pm 16	0.43	6
24	12.5	349 \pm 5	0.34	353 \pm 16	0.32	1
24	25	362 \pm 7	0.33	365 \pm 6	0.32	1
24	50	377 \pm 11	0.30	376 \pm 4	0.34	0.4
24	100	326 \pm 9	0.23	327 \pm 7	0.23	0.5
48	6.3	361 \pm 5	0.37	-	-	-
48	12.5	355 \pm 15	0.35	-	-	-
48	25	371 \pm 9	0.32	-	-	-
48	50	366 \pm 4	0.30	-	-	-
48	100	321 \pm 7	0.23	-	-	-

Tab. S3: Mean hydrodynamic particle diameters (x_{DLS}) \pm sd (samples were divided in 2 subsamples and each subsample was measured 3 times with dynamic light scattering) in stock and test suspensions in the fish early life stage test. Test suspensions were prepared daily and stored in a tank, from which suspensions constantly flowed into the test vessels. Before measurement, samples from stock suspensions were diluted by factor 20. All samples were transferred to the analysis laboratory and measured upon arrival (18 – 24 h after sampling). PI: polydispersity indices.

Nominal conc. [mg/L]	x_{DLS} [nm] (Polydispersity index)					
	d 0	d 7	d 14	d 21	d 28	d 34
2.5	493 \pm 34 (0.54)	481 \pm 35 (0.50)	462 \pm 17 (0.50)	464 \pm 39 (0.51)	460 \pm 36 (0.50)	450 \pm 27 (0.53)
7.9	478 \pm 32 (0.48)	472 \pm 25 (0.44)	491 \pm 33 (0.44)	468 \pm 12 (0.52)	465 \pm 26 (0.40)	447 \pm 10 (0.41)
25.0	487 \pm 12 (0.44)	496 \pm 23 (0.43)	497 \pm 12 (0.41)	474 \pm 18 (0.41)	479 \pm 15 (0.39)	490 \pm 25 (0.44)

Tab. S4: Data measured with dynamic light scattering for generating a calibration curve used to evaluate concentrations of aged Carbo-Iron in the test suspensions on the first sampling date of the fish early life stage test (d 0).

Nominal Carbo-Iron concentration [mg/L]	Count rate [kcps]	SD count rate [kcps]	S.E. mean [kcps]	S.E. mean [%]
2.5	6186	132.1	53.9	0.9
10	24873	644.0	262.9	1.1
20	48166	295.3	120.6	0.3
25	59117	2026.9	827.5	1.4

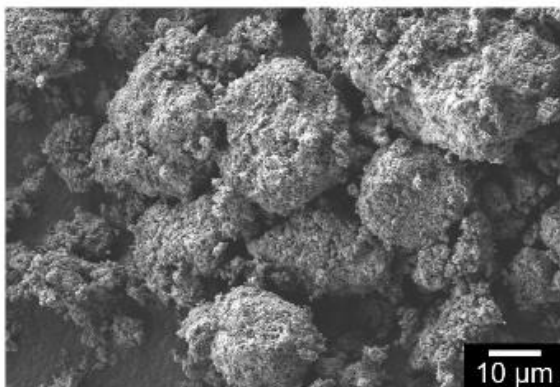


Fig. S1: Scanning electron micrograph of aged Carbo-Iron. The nanocomposite is highly porous with a structure that is typical for activated carbon, the main component of Carbo-Iron. Detection parameters: beam accelerating voltage 3 kV, magnification 1000x, secondary electron detector, working distance 4.3 mm.

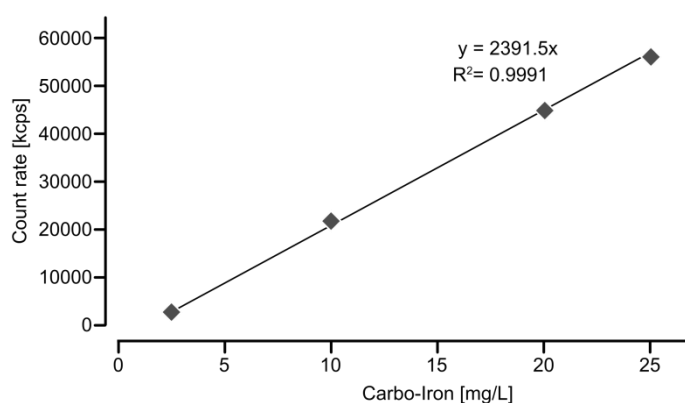


Fig. S2: Calibration curve of particle count data obtained with the data shown in Tab. S4 with dynamic light scattering. The corresponding error indicators for the data shown can be retrieved from Tab. S4. For test concentrations up to 25 mg/L a linear curve could be fitted, for higher concentrations the curve was asymptotically. With each stock suspension used in the test, a calibration curve was generated. Concentrations of Carbo-Iron in the test suspensions were derived based on the count rate determined in the respective test suspension and the calibration equation.

Tab. S5: Concentration of iron ions measured at test end (48 h after begin of exposure) in the fish embryo toxicity test (single measurements). Prior to photometric measurement in a cuvette test at 564 nm, samples were filtered twice with a 0.45 μm syringe filter and acidified with hydrochloric acid (1 M) to pH 4.

Nominal Carbo-Iron concentration [mg/L]	Iron concentration [$\mu\text{g/L}$]
Control	9
CMC control	9
1.6	11
3.2	10
6.3	14
12.5	23
25	39
50	44
100	49

Tab. S6: Concentration of iron ions measured at test end (96 h after the start of exposure) in the acute fish toxicity test (single measurements). Prior to photometric measurement in a cuvette test at 564 nm, samples were filtered twice with a 0.45 µm syringe filter and acidified with hydrochloric acid (1 M) to pH 4.

Nominal Carbo-Iron concentration [mg/L]	Iron concentration [µg/L]
Control	7
CMC control	9
4.3	12
9.4	21
20.7	46
45.5	55
100.0	53

Tab. S7: Concentration of iron ions measured during the fish early life stage test (single measurements). Prior to photometric measurement in a cuvette test at 564 nm, samples were filtered twice with a 0.45 μm syringe filter and acidified with hydrochloric acid (1 M) to pH 4.

Nominal Carbo- Iron concentration [mg/L]	Measured iron concentration [$\mu\text{g/L}$]						
	d 0	d 3	d 7	d 14	d 21	d 28	d 34
Control	8	16	29	21	15	4	10
CMC control	7	9	15	15	24	10	17
0.25	10	12	15	10	11	19	19
0.79	8	35	15	10	7	11	23
2.5	18	11	10	16	10	30	18
7.9	21	26	27	23	22	40	35
25.0	38	58	39	65	45	51	68

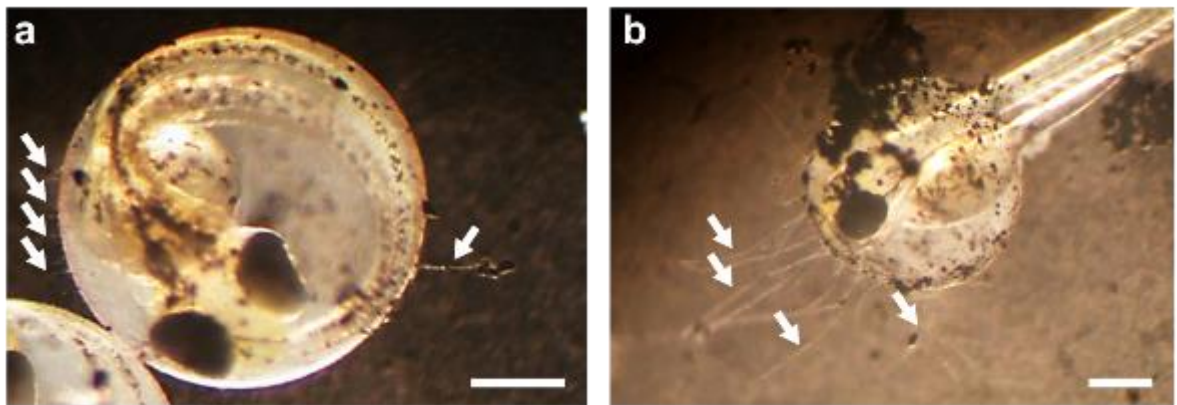


Fig. S3: Zebrafish embryos after 48 h of exposure to 12.5 mg/L (a) and 25 mg/L (b) of aged Carbo-Iron. White arrows indicate fungi growing on the chorion and protruding into the surrounding medium. Scale bars = 250 μm .

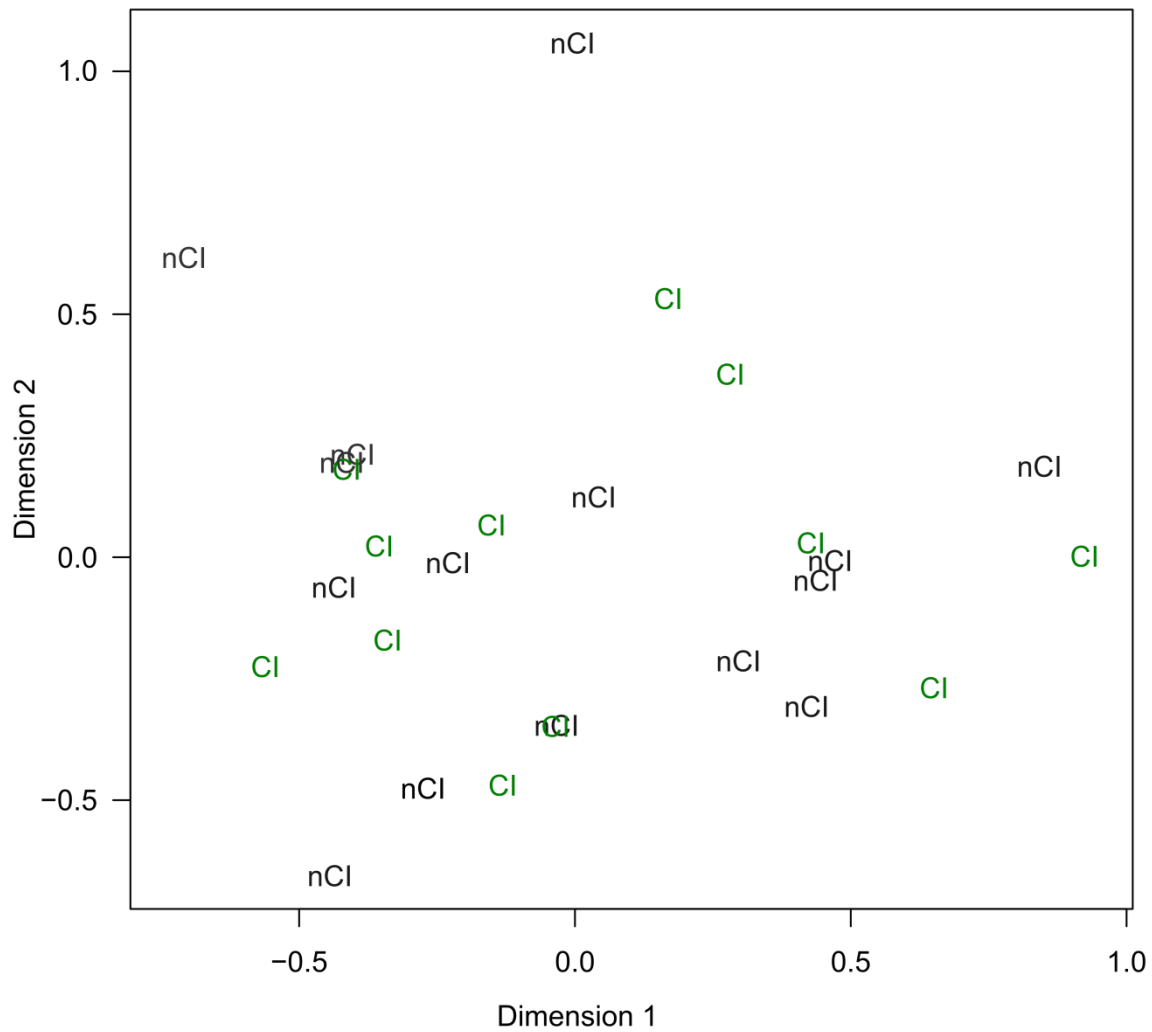


Fig. S4: Multidimensional scaling plot of microarray data. Data analysis was performed with the limma package in R in order to investigate, which genes were potentially affected by aged Carbo-Iron. First, controls were compared to Carbo-Iron treatments only considering samples that were not treated with PCE. Second, all treatments (including PCE treated samples) without Carbo-Iron were compared with all treatments containing Carbo-Iron (including PCE treated samples). This was performed both separately for each time point and for all time points combined. In contrast to PCE, which led to a large number of differentially expressed genes, Carbo-Iron did not show any effect at the gene expression level. No clusters could be identified for samples with (Cl) or without aged Carbo-Iron (nCl). For Carbo-Iron treatments, no genes with significantly altered expression as compared to the corresponding control were found (false discovery rate ≤ 0.05).

Appendix C.1

Oxidized Carbo-Iron causes reduced reproduction and lower tolerance of juveniles in the amphipod *Hyalella azteca*

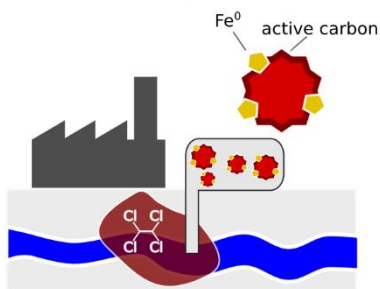
Mirco Weil, Tobias Meißner, Armin Springer, Mirco Bundschuh, Lydia Hübler,
Ralf Schulz, Karen Duis

Published in: *Aquatic Toxicology* (2016),

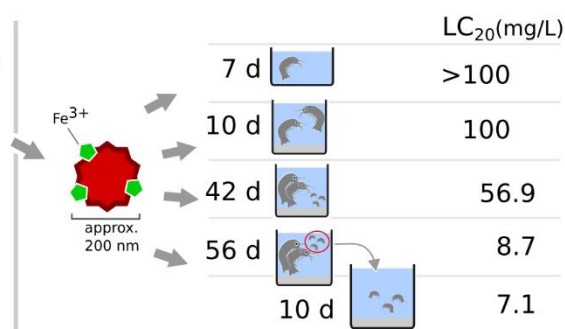
Vol.: 181, Pages94–103.

Graphical abstract

Carbo-Iron developed for
remediation of groundwater



Toxicity of aged Carbo-Iron to *Hyalella azteca*



Keywords

iron-based nanomaterial; nanocomposite; groundwater remediation; environmental risk

Highlights

- Effects on growth, reproduction and survival at ≥ 12.5 mg oxidized Carbo-Iron /L
- Carbo-Iron significantly increases sensitivity of offspring from exposed amphipods
- Toxicity is most likely mediated by an impaired uptake of nutrients and energy

Abbreviations:

CMC: Carboxymethyl cellulose

EC_x: Concentration leading to an effect in x% of organisms (e.g. EC₅₀)

EDX : Energy dispersive X-ray microanalysis

LC_x: Concentration leading to mortality of x% of organisms (e.g. EC₅₀)

nFe⁰: Nanoscaled zerovalent iron

PBS: Phosphate buffered saline

sd: Standard deviation of the group of data values used to calculate e.g. a mean

SEM: Scanning electron microscopy

Funding sources

The present work was funded by the German Ministry of Education and Research (project numbers 03X0082 A, B, C and F). The sole responsibility for the content of this publication lies with the authors.

Ethical statement

The present manuscript is not under consideration by any other journal. All authors have approved the current version of the manuscript. The study did not involve human subjects or vertebrate animals.

Abstract

For in situ remediation of groundwater contaminated by halogenated hydrocarbons Carbo-Iron[®], a composite of microscale activated carbon and nano Fe⁰, was developed. Against the background of intended release of Carbo-Iron into the environment in concentrations in the g/L-range, potential ecotoxicological consequences were evaluated in the present study. The nano Fe⁰ in Carbo-Iron acts as reducing agent and is oxidized in aqueous systems by chlorinated solvents, groundwater constituents (e.g. dissolved oxygen) and anaerobic corrosion. As Carbo-Iron is generally oxidized rapidly after application into the environment, the oxidized state is environmentally most relevant, and Carbo-Iron was used in its oxidized form in the ecotoxicological tests. The amphipod *Hyaella azteca* was selected as a surrogate test species for functionally important groundwater crustaceans. Effects of Carbo-Iron on *H. azteca* were determined in a 10-d acute test, a 7-d feeding activity test and a 42-d chronic test. Additionally, a 56-d life cycle test was performed with a modified design to further evaluate effects of Carbo-Iron on adult *H. azteca* and their offspring. The size of Carbo-Iron particles in stock and test suspensions was determined via dynamic light scattering. Potential uptake of particles into test organisms was investigated using transmission and scanning electron microscopy. At the termination of the feeding and acute toxicity test (i.e. after 7 and 10 d of exposure, respectively), Carbo-Iron had a significant effect on the weight, length and feeding rate of *H. azteca* at the highest test concentration of 100 mg/L. While an uptake of Carbo-Iron into the gut was observed, no passage into the surrounding tissue was detected. In both chronic tests, the number of offspring was the most sensitive endpoint and significant effects were recorded at concentrations ≥ 50 mg/L (42-d experiment) and ≥ 12.5 mg/L (56-d experiment). Parental exposure to oxidized Carbo-Iron significantly exacerbated the acute effects of the nanocomposite on the subsequent generation of *H. azteca* by a factor >10 . The present study indicates risks for groundwater species at concentrations in the mg/L range. Carbo-Iron may exceed these effect concentrations in treated aquifers, but the presence of the pollutant has most likely impaired the quality of this habitat already. The benefit of remediation has to be regarded against the risk of ecological consequences with special consideration of the observed increasing sensitivity of juvenile *H. azteca*.

1. Introduction

Groundwater pollution is among the most severe environmental challenges (Dimitriou et al., 2008; Fatta et al., 2002). Contamination may arise from a multitude of anthropogenic activities, which include landfills, industrial effluents or accidental spillage (Rail, 1989). Groundwater aquifers can provide a habitat for a high diversity of micro- and macroorganisms (among them various crustaceans) including many endemic species (Danielopol and Griebler, 2008; Hahn and Fuchs, 2009). Thus, the protection and remediation of groundwater bodies is of high importance, but also represents a scientific challenge considering the variety of contaminants. In this context, the use of nanoscaled zerovalent iron (nFe^0) for remediation of contaminated groundwater is a promising technique (Xu et al., 2012). For efficient groundwater treatment with nFe^0 , particles should have a certain mobility to build a broad reactive barrier in the aquifer. Yet, mobility of nFe^0 in the receiving medium is impeded by quick agglomeration and sedimentation (Johnson et al., 2013; Yin et al., 2012). To improve mobility and maintain reactivity, a nanocomposite of zerovalent iron nanoparticles and activated carbon was developed (Bleyle et al., 2012; Mackenzie et al., 2012), which is a promising alternative to nFe^0 . For in situ groundwater remediation, several thousand L of a suspension with a Carbo-Iron concentration in the g/L range have to be applied into the aquifer (Mackenzie et al., 2016).

As so far very few ecotoxicity data are available for Carbo-Iron (Weil et al., 2015), potential risks for aquatic ecosystems deserve further investigation. In ecotoxicity testing, semi-static or flow-through test systems are often employed to overcome sedimentation behavior of particles in suspension and increase the probability of the relevant species to interact with the particles, recently especially focused on experiments with nanoparticles (Bundschuh et al., 2012; Seitz et al., 2013). These experimental designs simulate the continuous release of particles via point sources such as wastewater treatment plant effluents. However, sediments represent a sink for particles in suspension (Baun et al., 2008; Poynton et al., 2013). Therefore, ecotoxicity tests with sediment-dwelling organisms are of high relevance for an estimation of environmental risk of Carbo-Iron. Additionally, to minimize the risk that a remediation of an aquifer with Carbo-Iron deteriorates the conditions for groundwater organisms, information on potential effects on such organisms is necessary. For these reasons, the benthic amphipod *Hyalella azteca* was chosen as test organism in the present study as a surrogate species for amphipods inhabiting groundwater. In a study on risk assessment of chemical stressors in groundwater, Schäfers et al. (2001) recommended to place special emphasis on tests with higher crustaceans (e.g. amphipods). Surface water-inhabiting higher crustaceans show comparable sensitivity as related groundwater species (Schäfers et al.,

2001). *H. azteca* are living on the surface of and in the upper few mm of the sediment (Doig and Liber, 2010).

Since ingestion of Carbo-Iron was supposed to be the major route of uptake, the presence of Carbo-Iron particles on and in *H. azteca* was evaluated in a 10-d acute toxicity test in addition to the standard test endpoints survival and growth (US EPA, 2000). The impact of Carbo-Iron on ingestion rates of leaves was investigated during a 7-d exposure. Potential chronic toxicity of Carbo-Iron was studied in a 42-d exposure including reproduction of *H. azteca* as an endpoint (US EPA, 2000). Assuming a higher sensitivity of juveniles released from adults exposed to higher Carbo-Iron concentrations, as has been shown for nano TiO₂ (Bundschuh et al., 2012), the potential impact of Carbo-Iron on amphipod offspring was investigated in an additional chronic experiment.

2. Material and methods

2.1 Culture of *Hyaella azteca*

H. azteca were obtained in 2002 from Dresden University of Technology. They were kept at 20-25°C and 16:8 h light:dark in glass tanks with quartz sand and approximately 5 L culture medium according to Borgmann (1996) with CaCl₂ (110.98 mg/L), MgSO₄ (30.09 mg/L), NaHCO₃ (84.01 mg/L), KCl (3.72 mg/L) and NaBr (1.03 mg/L). The amphipods were fed twice per week with TetraMin® flakes *ad libitum*, the culture medium was exchanged every other week.

Prior to each experiment, a synchronized culture was initiated. Organisms from the culture were siphoned through sieves. *H. azteca* passing through sieves with 500 µm but being retained by 355 µm were considered to be approximately 6 d old (US EPA, 2000). They were transferred to a new culture vessel and kept under the same conditions as the original culture until test start. Before each experiment, a group of 20 animals was removed from the synchronized culture, and length and weight were measured to allow for the quantification of growth during the tests.

2.2 Preparation of test suspensions and artificial sediment

The toxicity tests with *H. azteca* were performed with aged Carbo-Iron, which means that the originally zero-valent iron oxidized to Fe²⁺ and Fe³⁺. Aged Carbo-Iron was provided by the producers Mackenzie and colleagues (see Bleyl et al., 2012; Mackenzie et al., 2012 and Mackenzie et al., 2016 for more details on composition and other particle characteristics); the iron content was approx. 22% (w/w). Stock suspensions were prepared as described by Weil et al. (2015). As stabilizing additive, 2 g carboxymethyl cellulose (CMC; Antisol® FL 30, Sigma-Aldrich, Germany) were added to 1 L of deionized water supplemented with 0.1 mL NaOH (1 M, Sigma-Aldrich, Germany). CMC is

also used for stabilization of Carbo-Iron in suspensions used for application into the groundwater. The CMC solution was stirred overnight at room temperature, subsequently filtered through a 0.4 µm filter (MN GF-5, Macherey-Nagel, Germany) and stored for a maximum of 7 d at 4°C. Before use, the CMC solution was diluted with deionized water to 200 mg CMC/L. Carbo-Iron stock suspensions (1 g/L) with 200 mg/L CMC (i.e. 20% w/w relative to Carbo-Iron) were prepared by adding 100 mg Carbo-Iron to 100 mL CMC solution. The suspensions were placed on ice and treated with an ultrasonic probe (Hielscher UP200S, Germany, 14 mm probe diameter) at approx. 80 W for 7 min. If volumes > 100 mL were needed, this procedure was repeated and the obtained suspensions were pooled until sufficient volume was prepared. The Carbo-Iron stock suspensions were used within 2 h after preparation.

Test suspensions were prepared immediately before starting the ecotoxicity tests by diluting the stock suspension with test medium. Final CMC concentration was 20 mg/L in all test suspensions irrespective of the Carbo-Iron concentration. All tests included controls (culture medium) and dispersant controls (20 mg/L CMC in culture medium).

For the water-sediment test systems, artificial sediment according to OECD (2004a) with 75% quartz sand (Quarzwirke Frechen, Germany), 20% kaolin (Chinafill 100, Ziegler, Germany) and 5% peat (Thomaflor, Germany) was prepared approx. one week before use, and preconditioned at $23 \pm 2^\circ\text{C}$ with aeration. Two days prior to the start of the exposure, glass beakers with screw caps and a total volume of 500 mL were filled with 80 ± 1 g (fresh weight) sediment. Subsequently, 180 mL culture medium were added to each vessel. Test vessels were then incubated at $23 \pm 2^\circ\text{C}$ with slight aeration until test start. Immediately before introduction of *H. azteca*, Carbo-Iron stock suspension (1 g/L Carbo-Iron and 200 mg/L CMC) and CMC solution (200 mg/L) were mixed in the necessary ratios to achieve 10-fold nominal test concentrations in a final volume of 20 mL. This mixture was then added to the respective test vessels.

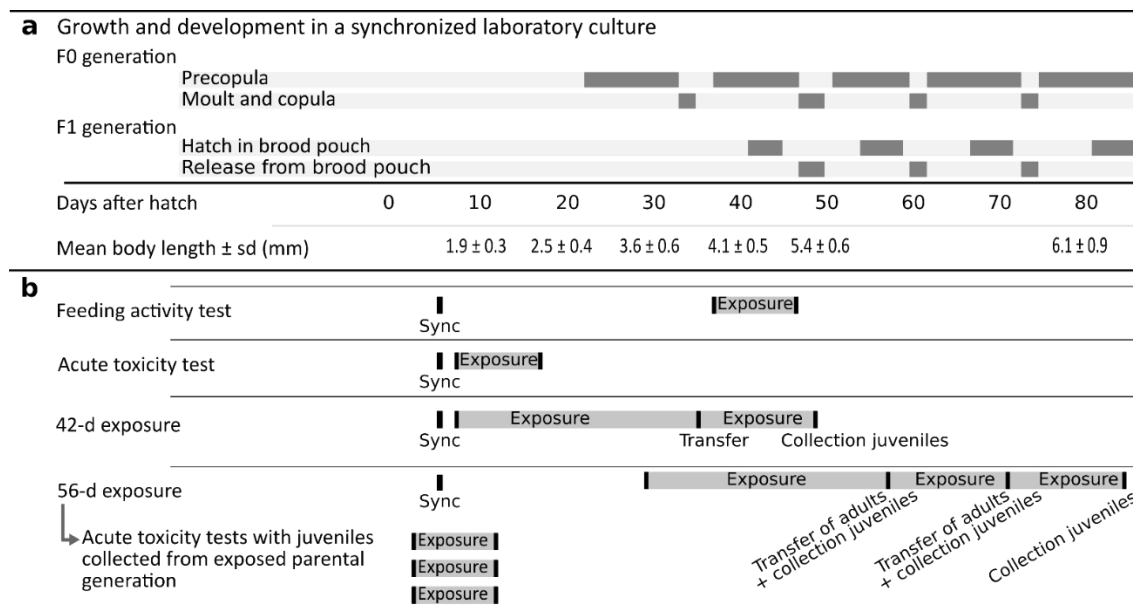


Fig. 1: Overview of the acute and chronic toxicity tests with *H. azteca* (b) in relation to growth and development (a) as observed in a synchronized laboratory culture with approx. 250 animals kept under test conditions ($23 \pm 2^\circ\text{C}$, 16:8 h light:dark photoperiod, aerated medium according to Borgmann (1996), feeding with TetraMin® flakes *ad libitum*). Experimental details for these observations are described in section 1.1 in the supplemental information. Descriptions of the ecotoxicity tests are starting with the synchronization (Sync) of the organisms before the respective test. During the 42 d and 56 d exposures, adults were transferred to freshly prepared test suspensions and juveniles were collected (for a detailed descriptions see 2.3.4 and 2.3.5).

2.3 Ecotoxicity tests

To choose suitable developmental stages of *H. azteca* for the respective tests, development of the laboratory culture was observed over a period of 80 d and results are shown in Fig. 1 (details are available in section 1 in the SI). In the water-sediment test systems, the test vessels were incubated at $23 \pm 2^\circ\text{C}$ with a 16:8 h light:dark photoperiod. The test vessels were aerated with approx. 1-2 bubbles per second starting at d 2 after the onset of exposure. For measurement of physico-chemical parameters (temperature, pH, oxygen and ammonium concentration, hardness and conductivity) during the test and for particle size measurements, one (for the acute toxicity test) and two (for the 42 and 56 d exposures) supplemental replicates were prepared in addition to the biological replicates. These vessels were also used for measuring concentrations of Fe^{2+} and Fe^{3+} in the test media as described in Weil et al. (2015) at test start, each water renewal and test end. Physico-chemical parameters were generally in good agreement with the desired values and are reported in the respective sections 4 to 7 in the SI. Measured iron concentrations were between 0.03 and 0.05 mg/L at test start and 0.17 and 0.28 mg/L after 42 d and no differences between

control and treatments were found. At the end of each test, *H. azteca* were counted and body length was determined as required by the EPA (2000) test protocol. Subsequently, all specimens were dried at 60°C for ≥ 18 h and weighed with an accuracy of 0.01 mg.

2.3.1 Acute toxicity test with previously unexposed organisms

A 10-d test in a water-sediment system with previously unexposed *H. azteca* was performed based on method 100.1 (US EPA, 2000) with four replicates per treatment and control. Final Carbo-Iron concentrations were 6.3, 12.5, 25, 50 and 100 mg/L. Immediately after preparation of test suspensions, 10 organisms from the synchronized culture were added to each replicate. Amphipods were randomly introduced into the test vessels to prevent bias in selection of test organisms. At test start, *H. azteca* were approximately 8 d old with a length of 1.9 ± 0.3 mm (mean \pm sd, n=20) and a mean individual fresh weight of 18 μ g. During the exposure, each test vessel received 50 μ L TetraMin® suspension (50 g/L) three times per week.

2.3.2 Feeding activity test

The feeding test was performed without sediment. Discs of black alder (*Alnus glutinosa*) leaves were prepared as described in Bundschuh et al. (2010). Leaves were collected in the field and stored at -20°C. After thawing, discs with a diameter of 1 cm were cut with a cork borer and incubated in a nutrient medium for 10 d to allow for a microbial colonization. Then, leaves were dried at 60°C for 24 h and weighted (± 0.01 mg). Before use in the test, leaves were soaked in test medium for 24 h to improve bioavailability. The nominal Carbo-Iron concentrations were 1, 3.2, 10, 32 and 100 mg/L. Exposure was performed in polystyrene multiwell plates with a nominal volume of 5 mL per well. Each well received 3 leaf discs, 5 mL of the respective test medium and one 38-day old *H. azteca* with a length of approximately 4 mm. Each treatment was replicated 30 times, and 5 additional wells were prepared without *H. azteca* to determine leaf mass loss due to abiotic or microbial decomposition or potential mass increase as a result of adsorption of Carbo-Iron onto the discs. The multiwell plates were incubated for 7 d at 23 ± 2 °C in the dark. At the termination of the experiment, test organisms and leaf discs were removed, dried and weighed as described above. The feeding rate was expressed in mg leaf disc per mg amphipod and day (Maltby et al., 2000). Replicates with dead *H. azteca* were excluded from evaluation.

2.3.3 42-d exposure

The 42-d chronic test in a water-sediment system was based on method 100.4 (US EPA, 2000) and performed with 12 replicates per treatment and control. The test started with 8-d old test organisms with a length of 2.1 ± 0.4 mm (mean \pm sd, n=20) and a mean individual fresh weight of 20 μ g. Test concentrations were 6.3, 12.5, 25, 50 and 100 mg/L and test conditions were as

described in section 2.3.1. During the first 21 d of exposure, each test vessel received 30 µL, and thereafter 50 µL TetraMin® suspension (50 g/L) three times per week. After 28 d, surviving organisms were counted on a light table. For each treatment and control, 4 replicates were sacrificed to determine length and weight of the test organisms. Deviating from the method 100.4 (US EPA, 2000) that describes water-only exposure for the following 14 d, *H. azteca* from the remaining 8 replicates were transferred to freshly prepared water-sediment systems and subjected to the same exposure conditions as during the first 28 d. At the termination of the test after 42 d, survival, weight and length of adult *H. azteca* were quantified and the number of juveniles was determined. Adult male *H. azteca* were identified by the presence of enlarged gnathopods, while presence of eggs or juveniles in the brood pouch were indicative for adult females.

2.3.4 56-d exposure

For the 56-d chronic test in a water-sediment system, 30-d old *H. azteca* with a length of 3.6 ± 0.4 mm (mean \pm sd, n=20) and a mean individual fresh weight of 38 µg were used. For each treatment and control, 6 replicates were used. At test start, three precopula pairs together with two male and two female amphipods (judged on their morphology) were introduced in each replicate ensuring a balanced sex ratio among replicates and treatments. The introduction of precopula pairs ensured that these were also present in the visually opaque Carbo-Iron suspension. *H. azteca* were fed three times per week with 50 µL TetraMin® suspension (50 g/L). Adult test organisms were transferred to new test vessels after 28 and 42 d of exposure. The offspring was collected and counted after 28, 42 and 56 d into glass beakers filled with culture medium, and used for the subsequent assessment of its sensitivity. The introduction of precopula pairs ensured that these were also present in the visually opaque Carbo-Iron suspension (section 2.3.5). Further endpoints (survival, length, weight, gender) were assessed as described in section 2.3.3.

2.3.5 Acute toxicity tests with juveniles collected from exposed parental organisms

Since the number of juveniles collected from the 56-d chronic toxicity test (section 2.3.4) was limited, only one replicate with 10 organisms could be used per treatment and control. At the start of these acute tests, juveniles had a body length ≤ 2 mm.

2.4 Determination of particle characteristics

Particle size was measured by dynamic light scattering (DLS) using a Zetasizer Nano ZS (Malvern Instruments, Germany). Particle diameters were determined in the Carbo-Iron stock suspensions and in all test concentrations during the acute toxicity test and the 42-d chronic test, as well as in the lowest, median and highest test concentration during the 56-d chronic test. Additionally,

samples from controls with and without CMC were analyzed to check for potential presence of particles ≤ 500 nm. Details on sampling procedures and particle size measurements are available in section 2 of the SI.

2.5 Evaluation of particle uptake via microscopic methods

Test organisms were sampled at the end of the acute toxicity test for analysis of Carbo-Iron distribution in the body. They were stored in a mixture of 2.5% glutaraldehyde and 3.7% formaldehyde in phosphate buffered saline (PBS) at 4°C. Scanning electron microscopy (SEM) and energy dispersive X-ray microanalysis (EDX) were performed using a Philips FEG-ESEM XL 30 (FEI Eindhoven, The Netherlands). Individual detection parameters are shown in Fig. 4, details for sample preparation and analysis are available in section 3 of the SI.

2.6 Statistical analysis

Statistical analyses were carried out using R Version 3.2.1 (R Development Core Team, 2011) and extension packages (Fox and Weisberg, 2011; Hothorn et al., 2008; Konietzschke, 2012; Lemon, 2006; Ritz and Streibig, 2005). Statistical analysis by null hypothesis significance testing was based on replicate means; non-normally distributed proportional data were arcsine-transformed before analysis. For comparison of differences between control and dispersant (CMC) control, the two-sided Welch two-sample t-test was used. Homogeneity of variances (Levene test) and normal distribution (visual examination of residual distribution and Shapiro-Wilk test) were checked. If the requirements for parametric testing were fulfilled, ANOVA and Dunnett's two-sided post-hoc test were performed, while Kruskal-Wallis with subsequent Wilcoxon ranks sum tests were used as non-parametric alternative. For all tests, a significance level of $p \leq 0.05$ was used (OECD, 2006). Treatments were compared to the dispersant control. Additionally to hypothesis testing, models were fitted to the data to calculate effective concentrations. For the endpoint mortality, 2-parameter log-normal models were established and Carbo-Iron concentrations causing 20% and 50% mortality (LC_{20} and LC_{50}) were determined where data were appropriate. For sublethal endpoints (weight, length, number of offspring and feeding activity), 3-parameter models were employed to determine concentrations leading to 20% and 50% effect (EC_{20} and EC_{50}) using the dispersant control as reference. In some cases, LC_{50} and EC_{50} were beyond the investigated concentration range. To allow comparison of effects among the tests, LC_{20} and EC_{20} are reported.

3. Results & Discussion

3.1 Particle characteristics

In the stock suspensions, measured particle diameters were between 322 ± 6 nm and 395 ± 12 nm (Fig. 2; detailed results are shown in Tab. S1 to S3). In all samples from control and dispersant control, no particles < 500 nm were detected. Test suspensions at concentrations ≥ 12.5 mg/L Carbo-Iron were stable for 3 d and measured diameters were between 315.1 ± 9 nm and 575 ± 35 nm. As a general trend the polydispersity index was increasing over time. The main reason for this is most likely the precipitation of Carbo-Iron from the water that results in reduced particle concentration in the water phase as also described by Dabrunz et al. (2011). Moreover, fine particles from the sediment mixed with Carbo-Iron particles contributed further to a broader particle size distribution increasing the polydispersity indices. With increasing Carbo-Iron concentration this effect was less pronounced. Analysis of test suspensions with 6.3 mg/L Carbo-Iron sampled on d 7 after test initiation did not yield reliable results and measurement was discontinued. While test suspensions with Carbo-Iron concentrations ≥ 50 mg/L were nearly opaque after preparation, they became noticeably clearer ≥ 7 d after test initiation.

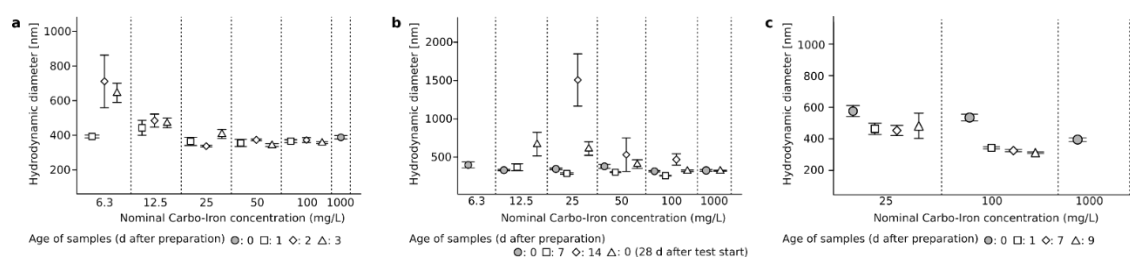


Fig. 2: Hydrodynamic particle diameters measured with DLS in Carbo-Iron suspensions from (a) the acute test, (b) the 42-d exposure and (c) the 56-d exposure with *H. azteca*. The investigated test concentrations were between 6.3 and 100 mg/L, additionally stock suspensions ($C_{\text{Carbo-Iron}}=1000$ mg/L) were sampled and analyzed. In the 42-d exposure, test organisms were transferred to freshly prepared suspensions after 28 d.

3.2 Acute toxicity test with previously unexposed organisms

The exposure of 8-d old *H. azteca* to Carbo-Iron for 10 d in a water-sediment system lead to a weak but non-significant increase in mortality at a Carbo-Iron concentration of 100 mg/L (Fig. 3a). Individual weight (Fig. 3b) and length (Fig. 3c) were significantly lower in *H. azteca* exposed to 100 mg/L Carbo-Iron compared to the dispersant control, and EC_{20} values were 58.3 and 89.1 mg/L, respectively (Tab. 1). Detailed results are provided in Tab. S5.

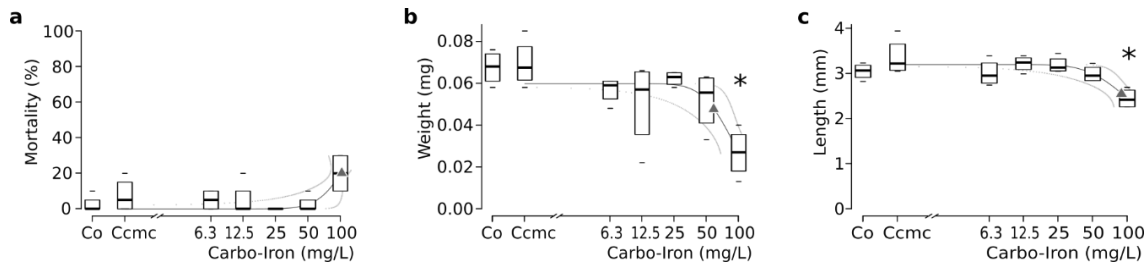


Fig. 3: Mortality (a), individual dry weight (b) and length (c) after 10 d exposure of *H. azteca* to aged Carbo-Iron in a water-sediment system (n=4). Co: control, Ccmc: control with the dispersant carboxymethyl cellulose (CMC, 20 mg/L); asterisks indicate a significant difference to Ccmc (ANOVA, two-sided Dunnett test). Data are presented as boxplots, the boxes represent the upper and lower quartile. Dashes outside the boxes are minimum and maximum values, dashes in each box are the median. The concentration-response model fitted to the respective data set is drawn as a solid curve; gray dots around this curve represent the lower and upper 95% confidence intervals. Triangles on the curves are EC₂₀ and EC₅₀ (weight, length) or LC₂₀ and LC₅₀ (mortality).

Microscopic analysis of *H. azteca* after 10 d of exposure showed only few particles associated with the outer surface of the amphipods (Fig. 4a). Particle-like structures were observed in the gut of the organisms (Fig. 4b and c), and presence of iron in these structures was detected with EDX (Fig. 4d). Based on these observations, the particles were assumed to be Carbo-Iron. Iron was distributed widely through the gut (Fig. 4e) as well as silicon, a component of kaolin and sand in the sediment (Fig. 4f). No Carbo-Iron was detected in tissues surrounding the gut.

The results from the acute toxicity test suggest that *H. azteca* ingest Carbo-Iron, which negatively influences growth parameters (weight and length).

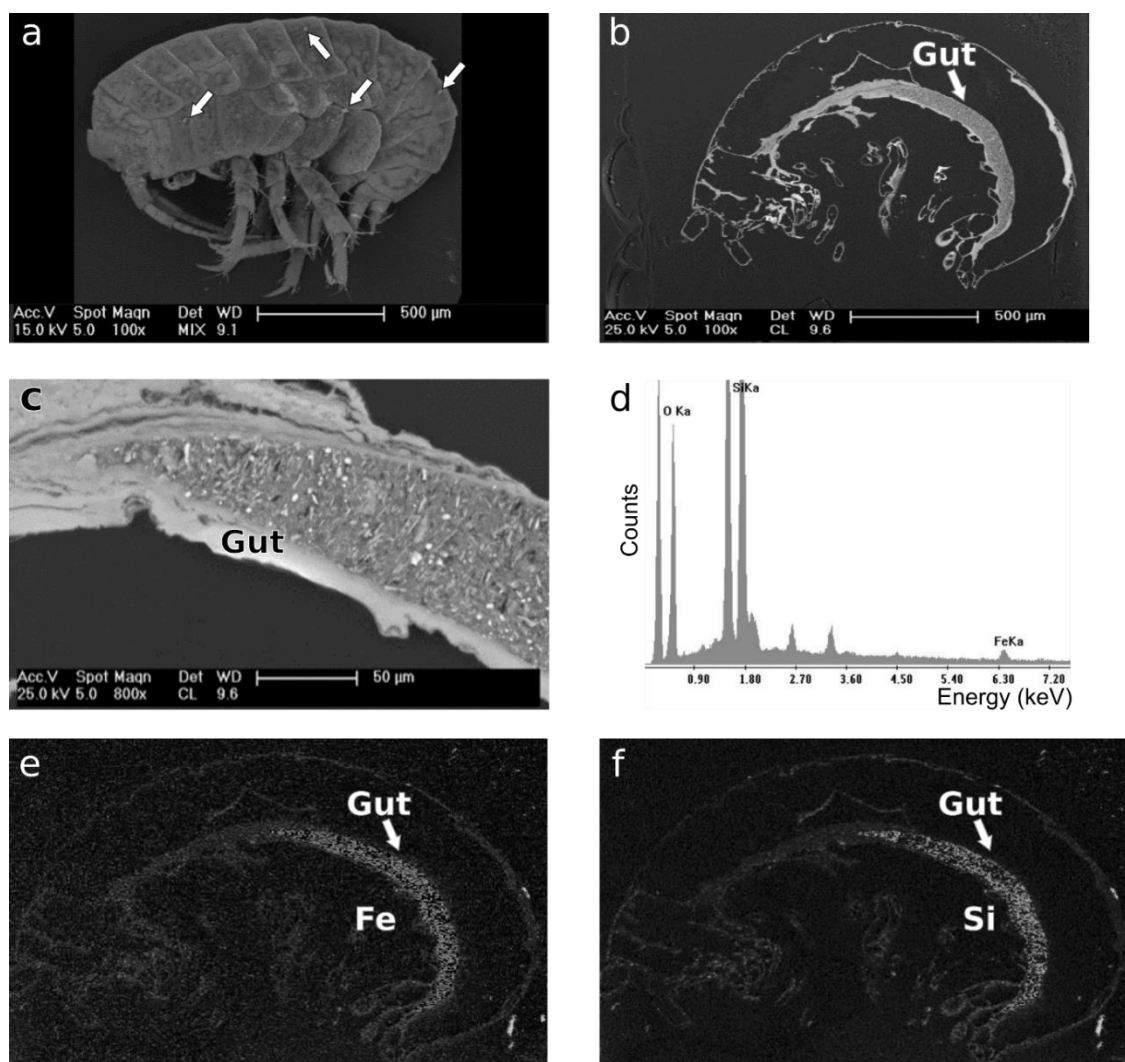


Fig. 4: (a) Scanning electron micrographs of *H. azteca* after exposure to aged Carbo-Iron (100 mg/L) show adherence of few agglomerated particles (white spots indicated by arrows) to the body surface. (b, c) Lateral cut (ultrathin section) through *H. azteca* shows particles (white spots) in the gut. (d) The EDX-spectrum of the area around these spots indicates presence of iron. (e, f) EDX elemental mapping shows distribution of iron (e) and silicon (f) as white spots in the gut of *H. azteca*. Detection parameters of SEM are provided in the caption of the respective image (Acc. V.: beam accelerating voltage [V], spot: spot size [nm], Magn.: magnification, DET: detector, MIX: signals from secondary electron detector and the back-scattered electron detector were mixed, CL: signals from cathode luminescence detector, WD: working distance [mm]).

3.3 Feeding activity test

After 7 d of exposure, all amphipods in the Carbo-Iron treatments and the control survived, and only 1 organism died in the dispersant control. In the control and dispersant control, feeding rates (mean \pm sd) were 0.279 ± 0.092 and 0.288 ± 0.115 mg leaf/mg amphipod/d, respectively (Fig. 5, detailed results in Tab. S6). In the highest test concentration, feeding rate (0.106 ± 0.074 mg leaf/mg

amphipod/d) was significantly reduced to 63% of the value in the dispersant control; EC_{20} was 33.8 mg/L (Tab. 1). Based on the nominal test concentrations, total mass of Carbo-Iron in the 5 mL test suspension in each replicate was 0.5 mg at the highest test concentration. Uptake of Carbo-Iron by the amphipods (at 100 mg/L max. 0.5 mg in 7 d, i.e. max. 0.07 mg/d, if the amphipods would have ingested all Carbo-Iron) might have led to a reduced percentage of usable organic matter in the ingested material. In addition, Carbo-Iron sedimented on leaf material might have reduced palatability of the leaves and, thus, food intake.

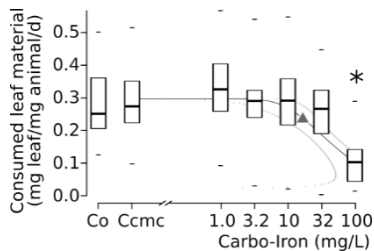


Fig. 5: Mean feeding rate of *H. azteca* during 7 d exposure to aged Carbo-Iron. Co: control, Ccmc: control with the dispersant carboxymethyl cellulose (CMC, 20 mg/L); the asterisk indicates a significant difference to Ccmc (ANOVA, two-sided Dunnett test, $p=0.05$). For a detailed description of symbols refer to Fig. 3.

3.4 42-d Exposure

No significant difference in mortality of *H. azteca* between controls and treatments was observed in the first 28 d of exposure (Fig. 6a, details in Tab. S7). Similar to the observations in the acute toxicity test, length and weight decreased slightly with increasing Carbo-Iron concentrations (Fig. 6c and e, details in Tab. S8 and S9). However, these effects were not significant.

After transfer to fresh Carbo-Iron suspensions and further 14 d of exposure, mortality was significantly increased at 100 mg/L (Fig. 6b). Weight and length of the organisms were significantly lower at 100 mg/L compared to the dispersant control (Fig. 6d and f). An LC_{20} of 57 mg/L and an EC_{20} of 82 mg/L for weight were derived (Tab. 1).

The mean number of offspring in the control was significantly higher than in the dispersant control (Fig. 6g, details in Tab. S10). Reasons for this difference could not be identified, as the measured physico-chemical parameters were in a very similar range throughout the exposure (section 7 in the SI). In the two highest test concentrations, Carbo-Iron led to a reduced number of juveniles; this effect was significant at 100 mg/L and the EC_{20} was 37.8 mg/L. The number of offspring per female followed a similar trend as total offspring per vessel (details are shown in Tab. S11).

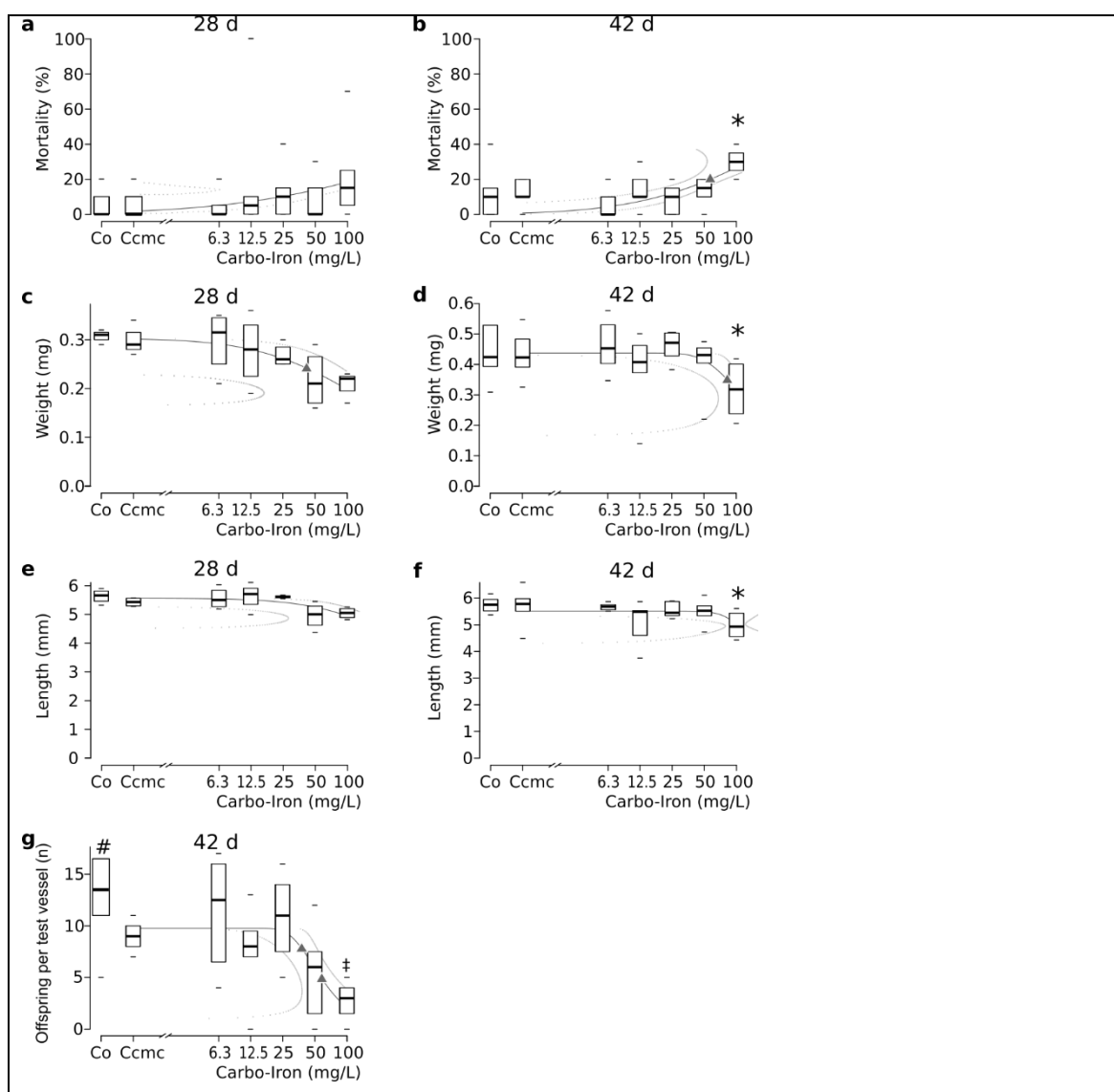


Fig. 6: 42 d Exposure of *H. azteca* to aged Carbo-Iron in a water-sediment system. Mortality (a, b), individual dry weight (c, d) and length (e, f) after 28 d (a, c, e) and 42 d (b, d, f, g). After 28 d of exposure, no *H. azteca* were found in one replicate with 12.5 mg/L Carbo-Iron. Since the reasons for this finding were unclear, data (i.e. 100% mortality in this replicate) were included in statistical analysis. Offspring was collected from the test vessels at test end (d 42) (g). Co: control, Ccmc: control with the dispersant carboxymethyl cellulose (CMC, 20 mg/L). Significant differences to Ccmc are indicated by: # (Welch two sample t-test); * (ANOVA, two-sided Dunnett test) and ‡ (Kruskal-Wallis rank sum test, Wilcoxon rank sum test). For a detailed description of symbols refer to Fig. 3.

3.5 56-d Exposure

Similar to the 42-d chronic test, no significant effects of Carbo-Iron on survival of *H. azteca* were observed after 28 d of exposure (Fig. 7a, details in Tab. S13). This second chronic test started with sexually mature amphipods and, thus, offspring was already present after 28 d of exposure. On d

28, there was a tendency towards a reduced number of offspring in the highest test concentration, but this effect was not significant (Fig. 7d, details in Tab. S16). Considering the turbidity of the Carbo-Iron suspensions and the layer of precipitated particles on the surface of the sediment, possible effects on reproduction could have been elicited by impairment of visual or tactile behavior during precopula pair formation. However, upon transfer of the test organisms to fresh test suspensions on d 28 and d 42, adult *H. azteca* in amplexus were observed in the controls and in all test concentrations (Tab. S18); no significant difference between treatments and controls was detected. Thus, effects of Carbo-Iron on reproduction are most likely not triggered by an influence of the nanomaterial on the formation of precopula pairs

After 42 d of exposure, mortality of adult *H. azteca* at 50 and 100 mg/L was significantly increased compared to the dispersant control (Fig. 7b). The cumulative number of offspring was significantly reduced in all test concentrations ≥ 12.5 mg/L (Fig. 7e), no juveniles were found at 100 mg/L (Tab. S16). For the endpoint offspring, an EC₂₀ of 8.7 mg/L was derived, which was considerably below the EC₂₀ of 37.8 mg/L obtained for the same endpoint and exposure time in the 42-d chronic test (Tab. 1). This difference is probably mainly due to the start of the 56-d chronic test with older test organisms leading to a higher number of offspring with lower variation among replicates and, thus, increasing the statistical power.

After 56 d, effects on the investigated endpoints became more pronounced. A significant increase in cumulative mortality (Kruskal-Wallis rank sum test; Wilcoxon rank sum test) was observed at 25, 50 and 100 mg/L (Fig. 7c). Survival of male *H. azteca* was significantly lower at ≥ 50 mg/L than in the dispersant control (Tab. S19). At 100 mg/L Carbo-Iron, none of the surviving adult organisms was male. The cumulative number of offspring (Fig. 7f) at ≥ 12.5 mg/L was significantly lower than in the dispersant control. Growth was significantly reduced at Carbo-Iron concentrations ≥ 50 mg/L (Fig. 7 g and h, details in Tab. S14 and S15).

The LC₂₀ values obtained after 28, 42 and 56 d (51, 21 and 9 mg/L, respectively) illustrate a clearly increasing toxicity of Carbo-Iron with increasing exposure duration. EC₂₀ values for the cumulative number of offspring and growth of *H. azteca* show a similar trend (Tab. 1).

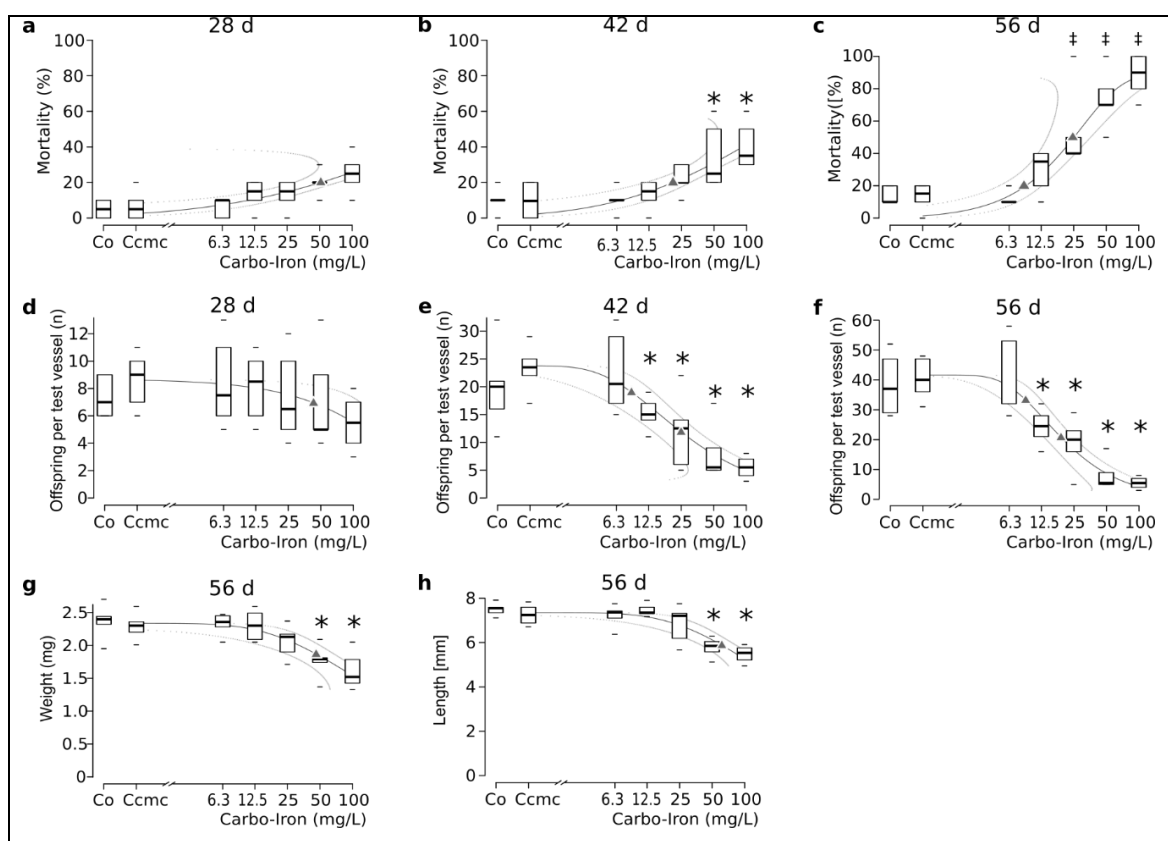


Fig. 7: 56-d Exposure of *H. azteca* to aged Carbo-Iron in a water sediment system. Mortality (a, b, c), cumulative offspring collected from test vessels (d, e, f), individual dry weight (g) and length (h) observed after 28 d (a, d), 42 d (b, e) and 56 d (c, f, g, h). Co: control, Ccmc: control with the dispersant carboxymethyl cellulose (CMC, 20 mg/L). Significant differences to Ccmc are indicated by: * (ANOVA, two sided Dunnett test) and ‡ (Kruskal-Wallis rank sum test, Wilcoxon rank sum test). For a detailed description of symbols refer to Fig. 3.

3.6 Acute toxicity tests with juveniles collected from exposed parental organisms

The acute toxicity tests with offspring from the amphipods exposed in the 56-d chronic test showed increasing mortality with increasing Carbo-Iron concentrations their parent generation had been exposed to (Fig. 8, detailed results in Fig. S1). The LC_{20} values for juveniles collected on d 28 from the test concentrations 6.3, 12.5 and 25 mg/L were 94.5, 46.6 and 26.9 mg/L, respectively. In addition, sensitivity of the offspring increased with increasing exposure duration of the parental organisms. For example, LC_{20} values of 46.6, 9.6 and 7.1 mg/L respectively, were derived for juveniles collected after 28, 42 and 56 d from 12.5 mg/L of Carbo-Iron (Tab. S20). Juveniles collected from 25 mg/L Carbo-Iron on d 42 and 56 of the chronic test appeared to be in poor conditions. With 30 and 40%, respectively, mortality was already high in the dispersant control. In the presence of Carbo-Iron concentrations of 6.3 – 100 mg/L, all juvenile amphipods died.

3.7 General discussion

In summary, survival of *H. azteca* was not influenced by Carbo-Iron in the 7 d feeding activity test, but mortality was slightly (yet not significantly) increased after 10 d exposure in the acute toxicity test. In the chronic tests, an exposure time of 28 d intensified the concentration-dependent mortality, yet again this effect was not statistically significant. Only after transfer of the organisms to freshly prepared test suspensions and exposure for further 14 d, mortality was significantly increased at ≥ 50 mg/L (Fig. 6 and Fig. 7). An additional transfer of the test organisms to freshly prepared test suspensions and a further elongation of the experimental duration by 14 d during the 56-d chronic test, led to a significantly increased mortality at ≥ 25 mg/L. The increasing sensitivity of *H. azteca* with increasing exposure time in combination with repeated transfer to fresh Carbo-Iron suspensions is clearly discernable in the continuous decrease of LC₂₀ and EC₂₀ values (Fig. 8 and Tab. S19). Iron concentrations (sum of Fe²⁺ and Fe³⁺) measured in controls and treatments were similar (≤ 0.28 mg/L) over all treatments. As this is including the controls, it is likely that most of the iron is leaching from the constituents of the artificial sediment rather than from Carbo-Iron. In a 10-d exposure, a Fe³⁺ concentration of 0.34 mg/L caused no mortality in *H. azteca* (Tab. S4). Furthermore, Borgmann et al. (2005) report an LC₅₀ > 1.0 mg/L after 7 d of exposure. Thus, a significant contribution of iron leaching from Carbo-Iron to the effects observed in the current study is unlikely.

The presence of Carbo-Iron in the gut of the amphipods but not in any other part of their body suggests that (1) ingestion is the major route of uptake, and (2) that Carbo-Iron is not transferred from the intestinal tract to the surrounding tissue. *H. azteca* ingests food and particles < 65 μ m (Environment Canada, 1997). The sediment used in the test systems contained 20% kaolin (mean grain-size: 2 μ m, according to the manufacturer) and 75% quartz sand (mean grain-size: 160 μ m, according to the manufacturer). *H. azteca* in the controls consumed food mixed with kaolin, while organisms in the treatments additionally consumed Carbo-Iron particles. Similar to kaolin, Carbo-Iron does not have any nutritive value. To compensate for the lower nutrient content of the ingested material in the presence of Carbo-Iron, increased feeding rates would have been necessary. However, feeding rate of the amphipods exposed to 100 mg/L Carbo-Iron decreased to 63% of the value in the dispersant control as shown in the feeding activity test. Due to the need to prolong gut transit time for exploiting the food, nutrient-poor food, as in this case Carbo-Iron, might move slower through the gut than nutrient-rich food (Tirelli and Mayzaud, 2005). This would slow down excretion of the food and, hence, result in reduced ingestion (i.e. reduced feeding rates) and, consequently, a reduced provision with nutrients. Thus, a reduced uptake of nutrients is likely to be the main reason leading to reduced survival and growth of *H. azteca* exposed to Carbo-Iron. The

binding of nutrients from the test media by activated carbon (Bundschuh et al., 2011), the main component of Carbo-Iron, and subsequent excretion of Carbo-Iron (with the bound nutrients) could have contributed to the assumed nutrient depletion and, hence, to the toxicity of Carbo-Iron to *H. azteca*. Energy reserves are passed from the parental generation to the eggs and used during the development (Dutra et al., 2007). In juvenile amphipods collected during the 56-d exposure, sensitivity to Carbo-Iron increased with the test concentrations the parental amphipods were exposed to, and the exposure time of the parental generation. The poor condition of the juveniles resulted most likely from the limited provision of the parental *H. azteca* with nutrients. Additionally, these juveniles were exposed to Carbo-Iron already in the marsupium, potentially adding to their increased sensitivity. Juveniles collected from test vessels with 25 mg/L Carbo-Iron were unable to recover from their persisting poor condition.

In both chronic toxicity tests, the ratio of male to female *H. azteca* in the Carbo-Iron treatments was reduced due to lower survival of male *H. azteca* (Tab. S12 and S19). Possible reasons for the higher sensitivity of the male amphipods could be related to their mating behavior. Dutra et al. (2007) described high energy costs and depletion of energy reserves due to mate guarding in males for the genus *Hyalella*, and Robinson and Doyle (1985) reported reduced feeding rates for males of the amphipod *Gammarus lawrencianus* in precopula. While the aforementioned reduced uptake of nutrients due to presence of Carbo-Iron in the gut would lead to limited energy reserves in both sexes of *H. azteca*, mate guarding would deplete the energy reserves in males even further, leading to the death of male *H. azteca*.

Higher crustaceans are important groundwater organisms and were shown to be more sensitive to some contaminants than lower crustaceans (Schäfers et al., 2001). Thus, the findings of the present study, especially the increasing sensitivity of juveniles collected from exposed parental *H. azteca*, are highly relevant for assessing a potential environmental risk of Carbo-Iron. The increasing sensitivity of juveniles collected from exposed parental *H. azteca* calls for attention when it comes to test selection for risk assessment. In a recent pilot study, 110 kg of Carbo-Iron in a suspension with $c_{\text{Carbo-Iron}} = 15$ g/L were applied into groundwater (Mackenzie et al., 2016). Assuming low flow rates in the range of cm/d, as is typical for many aquifers (Hancock et al., 2005), dilution of the Carbo-Iron suspension with groundwater could be a slow process. Even after dilution by a factor of 1000, local concentrations in the aquifer would be higher than the effect concentrations determined in the present study. In this context, it has to be noted that in aquifers, which are subject to remediation, concentrations of the actual pollutants may clearly exceed their toxicity thresholds in groundwater organisms. In the aforementioned pilot study with Carbo-Iron (Mackenzie et al., 2016), tetrachloroethene was measured in concentrations up to 120 mg/L in the

hot spot area, while Richter et al. (1983) determined an LC₅₀ value of 9 mg/L for the crustacean *Daphnia magna*. Thus, the presence of amphipods or other metazoan organisms in such a highly contaminated aquifer is unlikely. In a risk assessment of Carbo-Iron, it has to be carefully considered that Carbo-Iron is used for remediation of groundwater bodies, which are contaminated with persistent hydrocarbons and therefore do not represent a suitable habitat for many organisms.

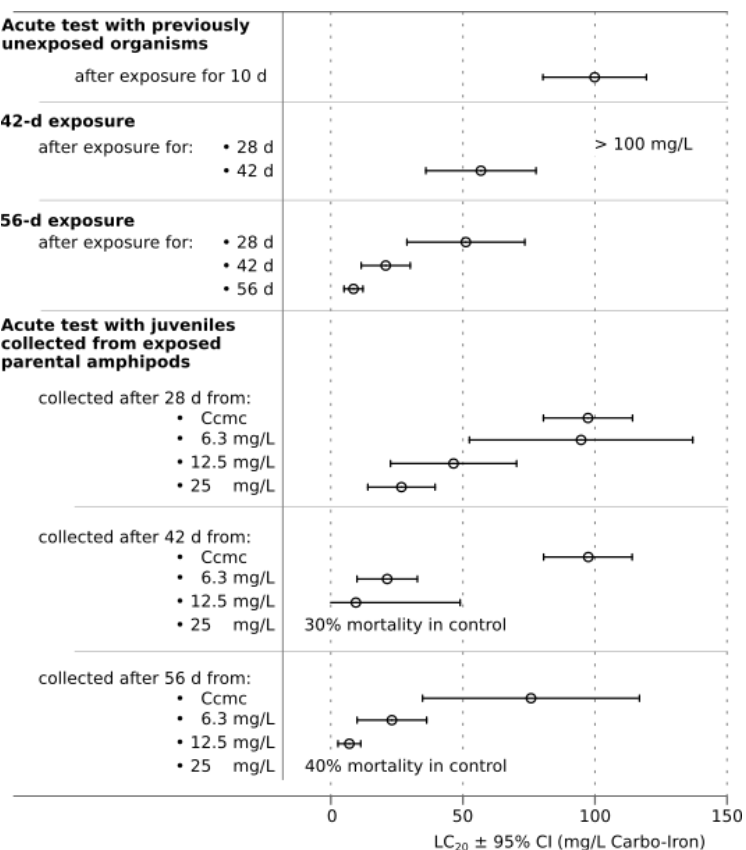


Fig. 8: Comparison of LC₂₀ values (± CI) derived in the toxicity tests with *H. azteca*. The acute test with previously unexposed organisms and both chronic tests were performed independently. The acute toxicity tests with offspring from exposed parental organisms were performed with juveniles collected from dispersant control (Ccmc) and Carbo-Iron treatments from the 56 d exposure on d 28, 42 and 56. In the tests with juveniles collected from 25 mg/L after 42 d and 56 d, mortality in Ccmc was ≥30% and LC₂₀ could not be calculated. Differences between LC₂₀ are considered significant, if CIs do not overlap. More detailed data are available in Tab. S19.

Tab. 1: Overview of EC₂₀ values (not including LC₂₀ values given in Fig. 8) derived in the toxicity tests with *H. azteca*.

Test system	Endpoint	EC ₂₀ (mg/L)	
		Time (95% confidence intervals)	
Feeding activity	Feeding rate	7 d	33.8 (21.7 - 45.9)
Acute test	Length	10 d	89.1 (64.2 - 113.9)
	Weight	10 d	58.3 (30 - 86.7)
42-d exposure	Number of offspring	42 d	37.8 (23.1 - 52.5)
	Offspring per female	42 d	34.5 (18.6 - 50.4)
	Weight	28 d	41.6 (0 - 89.1)
	Weight	42 d	82.4 (53.5 - 111.2)
	Length	28 d	> 100.0
	Length	42 d	> 100.0
56-d exposure	Number of offspring	28 d	42.8 (0 - 117.6)
	Number of offspring	42 d	8.7 (3.5 - 14)
	Number of offspring	56 d	9.4 (4.9 - 13.9)
	Offspring per female	56 d	9.0 (5.5 - 12.5)
	Length	56 d	61.7 (39.9 - 83.4)
	Weight	56 d	46.1 (24.6 - 67.6)

Acknowledgements

The authors thank Dr. Steffen Bleyl for the review of this manuscript and valuable input. The present work was funded by the German Ministry of Education and Research (project numbers 03X0082 A, B, C and F). The sole responsibility for the content of this publication lies with the authors.

References

- Baun, A., Hartmann, N.B., Grieger, K., Kusk, K.O., 2008. Ecotoxicity of engineered nanoparticles to aquatic invertebrates: a brief review and recommendations for future toxicity testing. *Ecotoxicology* 17, 387–95.
- Bleyl, S., Kopinke, F.-D., Mackenzie, K., 2012. Carbo-Iron®—Synthesis and stabilization of Fe(0)-doped colloidal activated carbon for in situ groundwater treatment. *Chemical Engineering Journal* 191, 588–595. DOI: 10.1016/j.cej.2012.03.021
- Borgmann, U., 1996. Systematic analysis of aqueous ion requirements of *Hyalella azteca*: A standard artificial medium including the essential bromide ion. *Archives of Environmental Contamination and Toxicology*. 30, 356–363. DOI: 10.1007/BF00212294
- Borgmann, U., Couillard, Y., Doyle, P., Dixon, D.G., 2005. Toxicity of sixty-three metals and metalloids to *Hyalella azteca* at two levels of water hardness. *Environmental Toxicology and Chemistry* 24, 641–652. DOI: 10.1897/04-177R.1
- Bundschuh, M., Seitz, F., Rosenfeldt, R.R., Schulz, R., 2012. Titanium dioxide nanoparticles increase sensitivity in the next generation of the water flea *Daphnia magna*. *PLoS ONE* 7, e48956. DOI: 10.1371/journal.pone.0048956
- Bundschuh, M., Zubrod, J.P., Seitz, F., Newman, M.C., Schulz, R., 2010. Mercury-contaminated sediments affect amphipod feeding. *Archives of Environmental Contamination and Toxicology*. 60, 437–443. DOI: 10.1007/s00244-010-9566-6
- Bundschuh, M., Zubrod, J.P., Seitz, F., Stang, C., Schulz, R., 2011. Ecotoxicological evaluation of three tertiary wastewater treatment techniques via meta-analysis and feeding bioassays using *Gammarus fossarum*. *Journal of Hazardous Materials* 192, 772–778. DOI: 10.1016/j.jhazmat.2011.05.079
- Dabrunz, A., Duester, L., Prasse, C., Seitz, F., Rosenfeldt, R., Schilde, C., Schaumann, G.E., Schulz, R., 2011. Biological surface coating and molting inhibition as mechanisms of tio2 nanoparticle toxicity in *Daphnia magna*. *PLoS ONE* 6, e20112. DOI: 10.1371/journal.pone.0020112
- Danielopol, D.L., Griebler, C., 2008. Changing paradigms in groundwater ecology—from the “living fossils” tradition to the “new groundwater ecology”. *International Review of Hydrobiology* 93, 565–577.
- Dimitriou, E., Karaouzas, I., Sarantakos, K., Zacharias, I., Bogdanos, K., Diapoulis, A., 2008. Groundwater risk assessment at a heavily industrialised catchment and the associated impacts on a peri-urban wetland. *Journal of Environmental Management* 88, 526–538. DOI: 10.1016/j.jenvman.2007.03.019
- Doig, L.E., Liber, K., 2010. An assessment of *Hyalella azteca* burrowing activity under laboratory sediment toxicity testing conditions. *Chemosphere* 81, 261–265. DOI: 10.1016/j.chemosphere.2010.05.054
- Dutra, B.K., Castiglioni, D.S., Santos, R.B., Bond-Buckup, G., Oliveira, G.T., 2007. Seasonal variations of the energy metabolism of two sympatric species of *Hyalella* (Crustacea, Amphipoda, Dogielinotidae) in the southern Brazilian highlands. *Comparative Biochemistry and Physiology Part A: Molecular & Integrative Physiology*, Includes papers presented in the session “Water Transport” at the Society of

-
- Experimental Biology's Annual Meeting at the University of Kent, Canterbury, UK, April 2nd–7th 2006
148, 239–247. DOI: 10.1016/j.cbpa.2007.04.013
- Environment Canada, 1997. EPS1/RM/33 Biological Test Method: Test for survival and growth in sediment using the freshwater amphipod "*Hyalella azteca*". Environment Canada, Ottawa, Ontario, Canada.
- Fatta, D., Naoum, D., Loizidou, M., 2002. Integrated environmental monitoring and simulation system for use as a management decision support tool in urban areas. *Journal of Environmental Management* 64, 333–343.
- Fox, J., Weisberg, S., 2011. An R Companion to Applied Regression, Second. ed. Sage, Thousand Oaks CA.
- Hahn, H.J., Fuchs, A., 2009. Distribution patterns of groundwater communities across aquifer types in south-western Germany. *Freshwater Biology* 54, 848–860. DOI: 10.1111/j.1365-2427.2008.02132.x
- Hancock, P.J., Boulton, A.J., Humphreys, W.F., 2005. Aquifers and hyporheic zones: Towards an ecological understanding of groundwater. *Hydrogeology Journal* 13, 98–111. DOI: 10.1007/s10040-004-0421-6
- Hothorn, T., Bretz, F., Westfall, P., 2008. Simultaneous inference in general parametric models. *Biometrical Journal* 50, 346–363. DOI: 10.1002/bimj.200810425
- Johnson, R.L., Nurmi, J.T., O'Brien Johnson, G.S., Fan, D., O'Brien Johnson, R.L., Shi, Z., Salter-Blanc, A.J., Tratnyek, P.G., Lowry, G.V., 2013. Field-scale transport and transformation of carboxymethylcellulose-stabilized nano zero-valent iron. *Environmental Science & Technology* 47, 1573–1580. DOI: 10.1021/es304564q
- Konietschke, F., 2012. nparcomp: Perform multiple comparisons and compute simultaneous confidence intervals for the nonparametric relative contrast effects.
- Lemon, J., 2006. Plotrix: a package in the red light district of R. *R-News* 6, 8–12.
- Mackenzie, K., Bleyl, S., Georgi, A., Kopinke, F.-D., 2012. Carbo-Iron - An Fe/AC composite - As alternative to nano-iron for groundwater treatment. *Water Research* 46, 3817–3826. DOI: 10.1016/j.watres.2012.04.013
- Mackenzie, K., Bleyl, S., Kopinke, F.-D., Doose, H., Bruns, J., 2016. Carbo-Iron as improvement of the nanoiron technology: From laboratory design to the field test. *Science of the Total Environment* DOI: 10.1016/j.scitotenv.2015.07.107
- Maltby, L., Clayton, S.A., Yu, H., McLoughlin, N., Wood, R.M., Yin, D., 2000. Using single-species toxicity tests, community-level responses, and toxicity identification evaluations to investigate effluent impacts. *Environmental Toxicology and Chemistry* 19, 151–157. DOI: 10.1002/etc.5620190118
- OECD, 2006. OECD series on testing and assessment. Number 54. Current approaches in the statistical analysis of ecotoxicity data: A guidance to application. (No. ENV/JM/MONO(2006)18). Organisation for Economic Co-operation and Development, Paris, France.
- OECD, 2004. OECD guideline for testing of chemicals. 219. Sediment-water chironomid toxicity test using spiked water. Organisation for Economic Co-operation and Development, Paris, France.
-

- Poynton, H.C., Lazorchak, J.M., Impellitteri, C.A., Blalock, B., Smith, M.E., Struewing, K., Unrine, J., Roose, D., 2013. Toxicity and transcriptomic analysis in *Hyalella azteca* suggests increased exposure and susceptibility of epibenthic organisms to zinc oxide nanoparticles. *Environmental Science & Technology* 47, 9453–9460. DOI: 10.1021/es401396t
- R Development Core Team, 2011. R: A Language and Environment for Statistical Computing. Vienna, Austria.
- Rail, C.D., 1989. Groundwater contamination: Sources, control, and preventive measures.
- Richter, J.E., Peterson, S.F., Kleiner, C.F., 1983. Acute and chronic toxicity of some chlorinated benzenes, chlorinated ethanes, and tetrachloroethylene to *Daphnia magna*. *Archives of Environmental Contamination and Toxicology*. 12, 679–684. DOI: 10.1007/BF01060751
- Ritz, C., Streibig, J.C., 2005. Bioassay Analysis using R. *Journal of Statistical Software* 12.
- Robinson, B.W., Robinson, B.W., Doyle, R.W., 1985. Trade-off between male reproduction (amplexus) and growth in the amphipod *Gammarus lawrencianus*. *Biology Bulletins* 168, 482–488. DOI: 10.2307/1541528
- Schäfers, C., Wenzel, A., Lukow, T., Sehr, I., Egert, E., 2001. Ökotoxikologische Prüfung von Pflanzenschutzmitteln hinsichtlich ihres Potentials zur Grundwassergefährdung. *UBA Texte* 76.
- Seitz, F., Bundschuh, M., Rosenfeldt, R.R., Schulz, R., 2013. Nanoparticle toxicity in *Daphnia magna* reproduction studies: The importance of test design. *Aquatic Toxicology* 126, 163–168. DOI: 10.1016/j.aquatox.2012.10.015
- Tirelli, V., Mayzaud, P., 2005. Relationship between functional response and gut transit time in the calanoid copepod *Acartia clausi*: role of food quantity and quality. *Journal of Plankton Research* 27, 557–568. DOI: 10.1093/plankt/fbi031
- US EPA, 2000. 600/R-99/064 Methods for measuring the toxicity and bioaccumulation of sediment-associated contaminants with freshwater invertebrates. Washington, D.C., USA.
- Weil, M., Meißner, T., Busch, W., Springer, A., Kühnel, D., Schulz, R., Duis, K., 2015. The oxidized state of the nanocomposite Carbo-Iron® causes no adverse effects on growth, survival and differential gene expression in zebrafish. *Science of the Total Environment* 530–531, 198–208. DOI: 10.1016/j.scitotenv.2015.05.087
- Xu, P., Zeng, G.M., Huang, D.L., Feng, C.L., Hu, S., Zhao, M.H., Lai, C., Wei, Z., Huang, C., Xie, G.X., Liu, Z.F., 2012. Use of iron oxide nanomaterials in wastewater treatment: A review. *Science of the Total Environment* 424, 1–10. DOI: 10.1016/j.scitotenv.2012.02.023
- Yin, K., Lo, I.M.C., Dong, H., Rao, P., Mak, M.S.H., 2012. Lab-scale simulation of the fate and transport of nano zero-valent iron in subsurface environments: Aggregation, sedimentation, and contaminant desorption. *Journal of Hazardous Materials* 227–228, 118–125. DOI: 10.1016/j.jhazmat.2012.05.019

Appendix C.2:

Supplemental information to:

Oxidized Carbo-Iron causes reduced reproduction and lower tolerance of juveniles in the amphipod *Hyalella azteca*

Mirco Weil^a, Tobias Meißner^b, Armin Springer^c, Mirco Bundschuh^{d, e}, Lydia Hübler^a
Ralf Schulz^e, Karen Duis^a

^a ECT Oekotoxikologie GmbH, Böttgerstrasse 2-14, 65439 Flörsheim, Germany
m.weil@ect.de; lydia.huebler@gmail.com; k-duis@ect.de

^b Fraunhofer Institute for Ceramic Technologies and Systems, Winterbergstrasse 28, 01277
Dresden, Germany
tmeiss@gmx.net

^c Dresden University of Technology, Budapesterstrasse 27, 01069 Dresden, Germany
armin.springer@nano.tu-dresden.de

^d Department of Aquatic Sciences and Assessment, Swedish University of Agricultural Sciences,
Uppsala, Sweden
mirco.bundschuh@slu.se

^e Institute for Environmental Sciences, University of Koblenz-Landau, Forststrasse 7, 76829
Landau, Germany
schulz@uni-landau.de

Corresponding author: Mirco Weil, ECT Oekotoxikologie GmbH, Böttgerstrasse 2-14, 65439
Flörsheim, Germany, m.weil@ect.de, +49 6145 956466

1. Development of *H. azteca*

For choosing suitable developmental stages of *H. azteca* for the toxicity tests, observations on development were performed. A synchronized culture with 250 organisms (F0 generation) was prepared in a vessel with a 3 cm quartz sand layer and 2 L test medium. From this culture, 10 organisms were removed 10, 20, 30, 40, 50 and 80 d after the assumed day of hatch and body length was measured under a dissecting microscope. The number of precopula pairs and presence of juveniles (F1 generation) in the brood pouch or the culture medium was evaluated daily.

The development of the culture of *H. azteca* used in the present study was generally in good agreement with previous descriptions (Geisler 1944; March 1978; Othman and Pascoe 2001), although occurrence of first offspring was delayed by 5 d compared to descriptions in US EPA (2000). Approximately 23 d after hatch, precopula pairs were observed (Fig. 1). Juveniles were present in the brood pouch of females starting 42 d after hatch of F0 generation, and 45 d after hatch of the F0, the juveniles were released into the culture medium. The numbers of fecund females and of offspring per female increased over time and were highest approx. 70 d after hatch.

2. Particle characteristics

Samples (20 mL) were taken from the vertical center of the water column in the test vessels and stored in polypropylene vials. On the same day, the samples were sent by overnight express to the analysis laboratory and analyzed upon arrival, i.e. less than 24 h after sampling. The influence of overnight transport on particle size distribution had previously been evaluated and was found to be negligible (Weil et al. 2015). Before analysis, samples from control and test suspensions were divided into 2 subsamples. For determination of the size of suspended Carbo-Iron particles, stock suspensions (1 g/L Carbo-Iron with 200 mg/L CMC) were diluted to $c_{\text{particle}} = 50 \text{ mg/L}$, while the samples from test suspensions were analysed without dilution. Particle size was measured by dynamic light scattering (DLS) in 10 mm disposable optical polystyrene cuvettes using a Zetasizer Nano ZS (Malvern Instruments, Germany). As described in ISO (2008), the cumulant method was used for determination of the mean hydrodynamic particle diameter and the polydispersity index. In the stock suspensions with 1000 mg/L Carbo-Iron, measured particle diameters were $392 \pm 10 \text{ nm}$ in the acute test, 326 ± 11 and $322 \pm 6 \text{ nm}$ in the 42-d exposure, and $395 \pm 12 \text{ nm}$ in the 56-d exposure (Tab. S1 to S3.). In all samples from control and dispersant control, no particles $\leq 500 \text{ nm}$ were detected.

Measured particle diameters in test suspensions with a Carbo-Iron concentration 12.5 mg/L were stable for 3 d with 383 ± 14 , 392 ± 64 and $395 \pm 12 \text{ nm}$ at test start, after 1 and 2 days, respectively

(Fig 2a). In test suspensions with 25, 50 and 100 mg/L Carbo-Iron, measured particle sizes 345 ± 11 , 379 ± 16 and 315 ± 9 nm on test start and 286 ± 9 , 302 ± 7 and 258 ± 4 nm on d 7. The decreasing particle size indicates sedimentation of agglomerates. In samples from d 14, larger particle diameters and high polydispersity index PI (≥ 0.6) were measured (Tab. S2). This indicates a low particle concentration in the suspensions, suggesting nearly complete precipitation of Carbo-Iron from the water phase and an increasing influence from sediment constituents. This observation was confirmed by visual check of the test vessels. While test suspensions with Carbo-Iron concentrations ≥ 50 mg/L were nearly opaque after preparation, they became noticeably clearer 7 to 8 d after the start of exposure. Upon transfer of the test organisms into new water-sediment test systems 28 d after the start of the experiment, particle sizes in suspensions with 50 and 100 mg/L Carbo-Iron were in a similar size range as at test start. Larger particle diameters in the test suspensions with lower test concentrations were probably related to less time between preparation of fresh suspensions and sampling, giving less time for particle agglomerates to settle. The 56-d exposure was performed under the same conditions as the 42-d exposure and analysis of test suspensions was focused on 25 and 100 mg/L Carbo-Iron. The initial particle size at test start was 575 ± 35 at 25 mg/L and 535 ± 22 nm at 100 mg/L. In the 42-d exposure, size of particles in suspension decreased to 482 ± 80 and 313 ± 5 nm in the test concentrations 25 and 100 mg/L, respectively, and PI values increased over time (Tab. S3).

Tab. S1: Mean hydrodynamic particle diameters (x_{DLS}) \pm sd (samples were divided in 2 subsamples and each subsample was measured 3 times with dynamic light scattering) and PI in stock and test suspensions in the acute toxicity test. Before measurement, samples from stock suspensions were diluted by factor 20. All samples were transferred to the analysis laboratory and measured upon arrival (18 – 24 h after sampling).

Carbo-Iron (mg/L)	x_{DLS} [nm] (PI)			
	d 0	d 1	d 2	d 3
6.3	-	393 \pm 8 (0.42)	711 \pm 152 (0.71)	645 \pm 56 (0.60)
12.5	-	443 \pm 43 (0.43)	485 \pm 37 (0.57)	472 \pm 28 (0.53)
25	-	365 \pm 24 (0.34)	337 \pm 5 (0.28)	408 \pm 26 (0.45)
50	-	356 \pm 21 (0.31)	374 \pm 4 (0.34)	343 \pm 8 (0.29)
100	-	366 \pm 8 (0.28)	373 \pm 14 (0.29)	358 \pm 6 (0.27)
Stock suspension (1000 mg/L)	491 \pm 10 (0.39)	-	-	-

Tab. S2: Mean hydrodynamic particle diameters (x_{DLS}) \pm sd (samples were divided in 2 subsamples and each subsample was measured 3 times with dynamic light scattering) and polydispersity index (PI) in stock and test suspensions in the 42-d exposure. Samples on d 28 were taken from freshly prepared stock and test suspensions (see section 2.5.2 for details). Before measurement, samples from stock suspensions were diluted by factor 20. All samples were transferred to the analysis laboratory and measured upon arrival (18 – 24 h after sampling).

Carbo-Iron (mg/L)	x_{DLS} [nm] (PI)			
	d 0	d 7	d 14	d 28
6.3	397 \pm 39 (0.45)	-	-	1280 \pm 355 (0.82)
12.5	329 \pm 8 (0.33)	368 \pm 46 (0.49)	-	669 \pm 153 (0.70)
25	345 \pm 11 (0.35)	286 \pm 9 (0.36)	1507 \pm 342 (0.83)	612 \pm 89 (0.63)
50	379 \pm 26 (0.44)	302 \pm 7 (0.33)	531 \pm 220 (0.60)	409 \pm 57 (0.45)
100	315 \pm 9 (0.26)	258 \pm 4 (0.29)	468 \pm 74 (0.61)	320 \pm 10 (0.42)
Stock suspension (1000 mg/L)	326 \pm 11 (0.31)	-	-	322 \pm 6 (0.28)

Tab. S3: Mean hydrodynamic particle diameters (x_{DLS}) \pm sd (samples were divided in 2 subsamples and each subsample was measured 3 times with dynamic light scattering) and polydispersity index (PI) in stock and test suspensions in the 56-d exposure. Before measurement, samples from stock suspensions were diluted by factor 20. All samples were transferred to the analysis laboratory and measured upon arrival (18 – 24 h after sampling).

Carbo-Iron (mg/L)	x_{DLS} [nm]			
	(PI)			
	d 0	d 1	d 7	d 9
6.3	657 \pm 37 (0.59)	882 \pm 302 (0.75)	1078 \pm 136 (0.77)	-
25	575 \pm 35 (0.54)	463 \pm 36 (0.46)	453 \pm 32 (0.53)	482 \pm 80 (0.53)
100	535 \pm 22 (0.46)	343 \pm 7 (0.26)	325 \pm 7 (0.25)	313 \pm 5 (0.23)
Stock suspension (1000 mg/L)	395 \pm 12 (0.39)	-	-	-

2.1 Evaluation of particle uptake via microscopic methods

Test organisms were sampled at the end of the acute toxicity test for analysis of Carbo-Iron distribution in the body. They were stored in a mixture of 2.5% glutaraldehyde and 3.7% formaldehyde in phosphate buffered saline (PBS) at 4°C. For scanning electron microscopy (SEM), samples were washed with PBS, dehydrated in a graduated series of acetone and critical point dried (CPD 030, BAL-TEC, Germany). Samples were mounted on SEM steps and carbon coated under vacuum. Analysis was performed using a Philips FEG-ESEM XL 30 (FEI Eindhoven, The Netherlands) with a secondary electron detector. Individual detection parameters are shown in the corresponding figures in section 3.

For SEM of the block face, fixed samples were washed with PBS, post-fixed with 2% osmium tetroxyde, dehydrated in a graduated series of acetone (including a contrast enhancing step with 1% uranyl acetate in 50% acetone) and infiltrated with pure epoxy resin (Spurr, 1969) at room temperature. After polymerisation at 60°C for 72 h samples were milled to appropriate shape (Leica EM Trimm, Leica Microsystems, Germany) equipped with a diamond mill (Diatome AG, Switzerland). A Leica EM UCT 6 ultramicrotome equipped with a Diatome diamond knife was used to prepare a flat surface of the block face of the samples. Samples were mounted on SEM steps and carbon coated under vacuum. They were analysed using a Philips FEG-ESEM XL 30 with a

backscatter electron detector and a cathode luminescence detector. Individual detection parameters are shown in the data bars of the respective figures in section 3.

Samples prepared for SEM were analyzed with regard to chemical elements by energy dispersive X-ray microanalysis (EDX). EDX-analysis and element mapping was performed with a Philips FEG-ESEM XL 30 equipped with an EDAX detecting unit and EDAX software (EDAX Inc., U.S.A.).

2.2 Acute toxicity test with FeCl₃

Tab. S4: Mean values \pm sd for survival determined in the 10-d acute toxicity test with *H. azteca* and FeCl₃. Exposure was initiated with 10 organisms per replicate and eight replicates per treatment. All other test parameters can be derived from section 2.3.1 of the manuscript.

Nominal FeCl ₃ concentration (mg/L)	Nominal Fe ³⁺ concentration (mg/L)	n	Survival (% of the introduced organisms)
Control	0.0	8	97.5 \pm 4.6
1	0.34	8	97.5 \pm 4.6
10	3.44	8	76.2 \pm 13.0

2.3 Acute toxicity test with Carbo-Iron

Physico-chemical parameters measured during exposure were (mean \pm sd, minimum and maximum values in parenthesis): temperature $23.6 \pm 0.1^\circ\text{C}$ (22.6 - 24.1 $^\circ\text{C}$, n=490), oxygen concentration 8.0 ± 0.3 mg/L (6.7 – 9.1 mg/L, n=35), total ammonium 2.2 ± 0.1 mg/L (0.0 – 6.2 mg/L, n=35); pH values were between 7.3 and 7.5 (n=35).

Tab. S5: Mean values \pm sd for survival, weight and length determined in the 10-d acute toxicity test with *H. azteca*.

Carbo-Iron (mg/L)	n	Survival (% of the introduced organisms)	Fresh individual weight (mg)	Length (mm)
Control	4	97.5 ± 5.0	0.068 ± 0.008	3.05 ± 0.18
Dispersant control	4	92.5 ± 9.6	0.070 ± 0.011	3.36 ± 0.41
6.3	4	95.0 ± 5.8	0.057 ± 0.006	3.01 ± 0.29
12.5	4	95.0 ± 10.0	0.051 ± 0.021	3.22 ± 0.17
25.0	4	100.0 ± 0.0	0.062 ± 0.003	3.19 ± 0.18
50.0	4	97.5 ± 5.0	0.052 ± 0.014	2.99 ± 0.18
100.0	4	80.0 ± 11.5	0.027 ± 0.012	2.45 ± 0.22

2.4 Feeding activity test with Carbo-Iron

Tab. S6: Mean values \pm sd for survival, weight of *H. azteca*, loss of leaf disc and feeding rate determined in the 7-d feeding activity test with *H. azteca*.

Carbo-Iron (mg/L)	Survival (% of the introduced organisms)	Dry weight <i>H.</i> <i>azteca</i> at test end (mg)	Loss of leaf disc weight (mg)	Feeding rate (mg leaf disc / mg amphipod / day)
Control	100.0	0.696 \pm 0.259	1.51 \pm 0.09	0.279 \pm 0.092
Dispersant control	96.7	0.662 \pm 0.261	1.51 \pm 0.04	0.288 \pm 0.115
1.0	100.0	0.579 \pm 0.222	1.56 \pm 0.08	0.321 \pm 0.111
3.2	100.0	0.565 \pm 0.219	1.51 \pm 0.17	0.282 \pm 0.103
10.0	100.0	0.678 \pm 0.225	1.44 \pm 0.10	0.287 \pm 0.117
32.0	100.0	0.545 \pm 0.222	1.31 \pm 0.11	0.253 \pm 0.109
100.0	100.0	0.439 \pm 0.172	1.20 \pm 0.09	0.106 \pm 0.074

2.5 42-d exposure with Carbo-Iron

Physico-chemical parameters (mean \pm sd, minimum and maximum values in parenthesis) measured during 42 d of exposure were: temperature $23.1 \pm 0.08^\circ\text{C}$ (21.7 – 24.1 $^\circ\text{C}$, n=2024), oxygen concentration 7.7 ± 0.3 mg/L (6.2 – 9.2 mg/L, n=131), total ammonium 2.2 ± 0.1 mg/L (0.2 – 6.2 mg/L, n=145); pH values were between 7.2 and 7.8 (n=126).

Tab. S7: Mean survival \pm sd with 95% confidence interval of *H. azteca* after 28 d and 42 d in the 42-d exposure.

Carbo-Iron (mg/L)	Day	n	Survival (% of the introduced organisms)	
			Mean \pm sd	95% confidence interval
Control	28	12	95.0 \pm 6.7	91.5 - 98.5
Dispersant control	28	12	95.0 \pm 6.7	91.5 - 98.5
6.3	28	12	96.7 \pm 6.5	93.3 - 100.0
12.5	28	12	87.5 \pm 28.0	73.0 - 102.0
25.0	28	12	90.0 \pm 12.1	83.7 - 96.3
50.0	28	12	92.5 \pm 10.6	87.0 - 98.0
100.0	28	12	78.3 \pm 24.4	65.7 - 91.0
Control	42	8	88.8 \pm 13.6	79.7 - 97.8
Dispersant control	42	8	87.5 \pm 7.1	82.8 - 92.2
6.3	42	8	95.0 \pm 7.6	89.9 - 100.1
12.5	42	^A 7	85.7 \pm 9.8	78.5 - 92.9
25.0	42	8	91.3 \pm 8.3	85.7 - 96.8
50.0	42	8	86.3 \pm 7.4	81.3 - 91.2
100.0	42	8	70.0 \pm 7.6	64.9 - 75.1

^A: After 28 d of exposure no *H. azteca* were found in one replicate with 12.5 mg/L Carbo-Iron. Thus, an additional replicate was used to evaluate endpoints (survival, length, weight) after 28 d and the remaining 7 replicates were used to continue the exposure until d 42.

Tab. S8: Mean length \pm sd with 95% confidence interval (mm) of *H. azteca* after 28 d and 42 d in the 42-d exposure.

Carbo-Iron (mg/L)	Day	n	Length (mm)	
			Mean \pm sd	95% confidence interval
Control	28	4	5.64 \pm 0.24	5.35 - 5.92
Dispersant control	28	4	5.43 \pm 0.15	5.25 - 5.61
6.3	28	4	5.56 \pm 0.37	5.12 - 5.99
12.5	28	4	5.63 \pm 0.47	5.08 - 6.18
25.0	28	4	5.61 \pm 0.05	5.55 - 5.67
50.0	28	4	4.96 \pm 0.46	4.42 - 5.49
100.0	28	4	5.05 \pm 0.19	4.82 - 5.27
Control	42	8	5.75 \pm 0.28	5.56 - 5.94
Dispersant control	42	8	5.70 \pm 0.61	5.30 - 6.11
6.3	42	8	5.67 \pm 0.13	5.59 - 5.76
12.5	42	^A 7	5.05 \pm 0.76	4.50 - 5.61
25.0	42	8	5.56 \pm 0.28	5.37 - 5.74
50.0	42	8	5.50 \pm 0.40	5.23 - 5.77
100.0	42	8	4.99 \pm 0.48	4.66 - 5.31

^A: After 28 d of exposure no *H. azteca* were found in one replicate with 12.5 mg/L Carbo-Iron. Thus, an additional replicate was used to evaluate endpoints (survival, length, weight) after 28 d and the remaining 7 replicates were used to continue the exposure until d 42.

Tab. S9: Mean fresh individual weight \pm sd with 95% confidence interval (mg) of *H. azteca* after 28 d and 42 d in the 42-d exposure.

Carbo-Iron (mg/L)	Day	n	Fresh weight (mg)	
			Mean \pm sd	95% confidence interval
Control	28	4	0.31 \pm 0.01	0.29 - 0.32
Dispersant control	28	4	0.30 \pm 0.03	0.26 - 0.33
6.3	28	4	0.30 \pm 0.06	0.22 - 0.37
12.5	28	4	0.28 \pm 0.07	0.19 - 0.36
25.0	28	4	0.27 \pm 0.02	0.24 - 0.30
50.0	28	4	0.22 \pm 0.06	0.15 - 0.29
100.0	28	4	0.21 \pm 0.03	0.18 - 0.24
Control	42	8	0.46 \pm 0.11	0.38 - 0.53
Dispersant control	42	8	0.43 \pm 0.07	0.39 - 0.48
6.3	42	8	0.46 \pm 0.08	0.41 - 0.52
12.5	42	^A 7	0.39 \pm 0.12	0.30 - 0.48
25.0	42	8	0.46 \pm 0.05	0.43 - 0.49
50.0	42	8	0.41 \pm 0.08	0.35 - 0.46
100.0	42	8	0.32 \pm 0.09	0.26 - 0.38

^A: After 28 d of exposure no *H. azteca* were found in one replicate with 12.5 mg/L Carbo-Iron. Four replicates were used to evaluate endpoints (survival, length, weight) after 28 d and the remaining 7 replicates were used to continue the exposure until d 42.

Tab. S10: Numbers of juveniles collected from the test vessels after 28 d and 42 d in the 42-d exposure (means \pm sd with 95% confidence interval).

Carbo-Iron (mg/L)	Day	n	Number of juveniles	
			Mean \pm sd	95% confidence interval
Control	42	8	13.1 \pm 4.3	10.2 - 16.0
Dispersant control	42	8	9.0 \pm 1.3	8.1 - 9.9
6.3	42	8	11.4 \pm 5.3	7.8 - 14.9
12.5	42	^A 7	7.7 \pm 4.1	4.7 - 10.7
25.0	42	8	10.8 \pm 4.0	8.1 - 13.4
50.0	42	8	5.3 \pm 4.2	2.5 - 8.0
100.0	42	8	2.8 \pm 1.8	1.6 - 3.9

^A: After 28 d of exposure no *H. azteca* were found in one replicate with 12.5 mg/L Carbo-Iron. Four replicates were used to evaluate endpoints (survival, length, weight) after 28 d and the remaining 7 replicates were used to continue the exposure until d 42.

Tab. S11: Numbers of juveniles per surviving female collected from test vessels after 28 d and 42 d in the 42-d exposure (means \pm sd with 95% confidence interval).

Carbo-Iron (mg/L)	Day	n	Number of juveniles	
			Mean \pm sd	95% confidence interval
Control	42	8	2.9 \pm 0.9	2.3 - 3.5
Dispersant control	42	8	2.0 \pm 0.2	1.8 - 2.1
6.3	42	8	2.3 \pm 1.0	1.6 - 3.0
12.5	42	^A 7	1.9 \pm 1.1	1.1 - 2.7
25.0	42	8	2.1 \pm 0.6	1.7 - 2.5
50.0	42	8	1.0 \pm 0.8	0.5 - 1.5
100.0	42	8	0.7 \pm 0.5	0.4 - 1.0

^A: After 28 d of exposure no *H. azteca* were found in one replicate with 12.5 mg/L Carbo-Iron. Four replicates were used to evaluate endpoints (survival, length, weight) after 28 d and the remaining 7 replicates were used to continue the exposure until d 42.

Tab. S12: Mean sex ratios (males / female) \pm sd determined on d 42 in the 42-d exposure.

Carbo-Iron (mg/L)	Sex ratio (mean \pm sd)
Control	1.0 \pm 0.1
Dispersant control	0.9 \pm 0.2
6.3	0.9 \pm 0.2
12.5	1.0 \pm 0.3
25.0	0.9 \pm 0.4
50.0	0.8 \pm 0.2
100.0	0.7 \pm 0.3

2.6 56 d exposure with Carbo-Iron

Physico-chemical parameters measured during 56 d of exposure were: temperature $23.1 \pm 0.1^\circ\text{C}$ ($21.7 - 24.1^\circ\text{C}$, $n=2024$), oxygen concentration 7.7 ± 0.3 mg/L ($6.2 - 9.2$ mg/L, $n=131$), total ammonium 2.2 ± 0.1 mg/L ($0.2 - 6.2$ mg/L, $n=145$); pH values were between 7.2 and 7.8 ($n=126$).

Tab. S13: Survival \pm sd and 95% confidence intervals after 28, 42 and 56 d in the 56-d exposure.

Carbo-Iron (mg/L)	Day	n	Survival (% of introduced organisms)	
			Mean \pm sd	95% confidence interval
Control	28	6	95.0 ± 5.5	90.5 - 99.5
Dispersant control	28	6	93.3 ± 8.2	86.6 - 100.1
6.3	28	6	93.3 ± 5.2	89.1 - 97.6
12.5	28	6	86.7 ± 8.2	79.9 - 93.4
25.0	28	6	86.7 ± 8.2	79.9 - 93.4
50.0	28	6	80.0 ± 6.3	74.8 - 85.2
100.0	28	6	75.0 ± 10.5	66.4 - 83.6
Control	42	6	90.0 ± 6.3	84.8 - 95.2
Dispersant control	42	6	90.0 ± 8.9	82.6 - 97.4
6.3	42	6	90.0 ± 6.3	84.8 - 95.2
12.5	42	6	86.7 ± 8.2	79.9 - 93.4
25.0	42	6	78.3 ± 7.5	72.1 - 84.5
50.0	42	6	66.7 ± 17.5	52.3 - 81.1
100.0	42	6	60.0 ± 12.6	49.6 - 70.4
Control	56	6	86.7 ± 5.2	49.6 - 70.4
Dispersant control	56	6	86.7 ± 8.2	49.6 - 70.4
6.3	56	6	88.3 ± 4.1	49.6 - 70.4
12.5	56	6	70.0 ± 12.6	49.6 - 70.4
25.0	56	6	48.3 ± 24.0	49.6 - 70.4
50.0	56	6	26.7 ± 16.3	49.6 - 70.4
100.0	56	6	11.7 ± 11.7	49.6 - 70.4

Tab. S14: Mean length \pm sd and 95% confidence interval (mm) of *H. azteca* after 56 d in the 56-d exposure. Due to high mortality, the number of replicates in test concentrations \geq 25 mg/L is lower.

Carbo-Iron (mg/L)	n	Length (mm)	
		Mean \pm sd	95% confidence interval
Control	6	7.5 \pm 0.3	7.3 - 7.7
Dispersant control	6	7.3 \pm 0.4	6.9 - 7.6
6.3	6	7.2 \pm 0.5	6.8 - 7.6
12.5	6	7.4 \pm 0.3	7.2 - 7.7
25.0	5	6.8 \pm 0.9	6.0 - 7.7
50.0	5	5.8 \pm 0.5	5.4 - 6.2
100.0	4	5.5 \pm 0.4	5.0 - 6.0

Tab. S15: Mean fresh individual weight \pm sd and 95% confidence interval (mg) of *H. azteca* after 56 d in the 56-d exposure. Due to high mortality, the number of replicates in test concentrations \geq 25 mg/L is lower.

Carbo-Iron (mg/L)	n	Fresh individual weight (mg)	
		Mean \pm sd	95% confidence interval
Control	6	2.37 \pm 0.24	2.17 - 2.57
Dispersant control	6	2.29 \pm 0.19	2.13 - 2.45
6.3	6	2.33 \pm 0.15	2.20 - 2.45
12.5	6	2.30 \pm 0.23	2.12 - 2.49
25.0	5	2.06 \pm 0.26	1.81 - 2.30
50.0	5	1.76 \pm 0.26	1.51 - 2.01
100.0	4	1.61 \pm 0.31	1.24 - 1.97

Appendix C.2:

Tab. S16: Juveniles collected per replicate [n] in the 56-d exposure.

Carbo-Iron (mg/L)	Day	n	Number of juveniles	
			Mean \pm sd	95% confidence interval
Control	28	6	8.3 \pm 3.4	5.5 - 11.2
Dispersant control	28	6	8.7 \pm 1.9	7.1 - 10.2
6.3	28	6	8.3 \pm 3.1	5.8 - 10.9
12.5	28	6	8.2 \pm 2.3	6.3 - 10.1
25.0	28	6	7.3 \pm 3.1	4.8 - 9.9
50.0	28	6	6.8 \pm 3.5	4.0 - 9.7
100.0	28	6	5.5 \pm 1.9	4.0 - 7.0
Control	42	6	11.7 \pm 4.4	8.0 - 15.3
Dispersant control	42	6	14.7 \pm 2.3	12.7 - 16.6
6.3	42	6	14.0 \pm 6.0	9.1 - 18.9
12.5	42	6	7.0 \pm 3.7	4.0 - 10.0
25.0	42	6	4.7 \pm 3.6	1.7 - 7.6
50.0	42	6	1.0 \pm 1.7	-0.4 - 2.4
100.0	42	6	0.0	-
Control	56	6	18.3 \pm 7.7	12.0 - 24.7
Dispersant control	56	6	17.0 \pm 3.5	14.2 - 19.8
6.3	56	6	18.7 \pm 5.5	14.1 - 23.2
12.5	56	6	9.2 \pm 3.5	6.3 - 12.1
25.0	56	6	6.8 \pm 4.7	3.0 - 10.7
50.0	56	6	0.0	-
100.0	56	6	0.0	-

Tab. S17: Juveniles per female (n) in the 56-d exposure. Exposure of individual replicates was not terminated during the test and sex of surviving mobile *H. azteca* could not be determined with certainty on d 28 and d 42. Thus, data are available only for the test end on d 56.

Carbo-Iron (mg/L)	Day	n	Number of juveniles per female	
			Mean \pm sd	95% confidence interval
Control	56	6	4.3 \pm 2.0	2.7 - 5.9
Dispersant control	56	6	4.0 \pm 1.0	3.1 - 4.8
6.3	56	6	4.4 \pm 1.6	3.1 - 5.8
12.5	56	6	2.4 \pm 1.0	1.6 - 3.1
25	56	5	2.3 \pm 1.4	1.0 - 3.7
50	56	5	0.0	-
100	56	4	0.0	-

Tab. S18: *H. azteca* in amplexus in the 56-d exposure.

Carbo-Iron (mg/L)	Day	n	<i>H. azteca</i> in amplexus (% of surviving organisms)	
			Mean \pm sd	95% confidence interval
Control	28	6	17.6 \pm 5.6	13.0 - 22.2
Dispersant control	28	6	21.6 \pm 6.6	16.1 - 27.0
6.3	28	6	19.8 \pm 4.9	15.8 - 23.8
12.5	28	6	17.0 \pm 5.0	12.9 - 21.1
25.0	28	6	25.1 \pm 4.5	21.4 - 28.8
50.0	28	6	20.7 \pm 5.8	15.9 - 25.4
100.0	28	6	11.5 \pm 5.9	6.6 - 16.4
Control	42	6	18.8 \pm 6.5	13.5 - 24.1
Dispersant control	42	6	17.0 \pm 9.3	9.3 - 24.7
6.3	42	6	16.5 \pm 5.5	12.0 - 21.1
12.5	42	6	21.2 \pm 4.6	17.3 - 25.0
25.0	42	6	25.7 \pm 2.5	23.7 - 27.7
50.0	42	6	24.8 \pm 2.7	22.5 - 27.0
100.0	42	6	23.1 \pm 10.2	14.8 - 31.5
Control	56	6	26.9 \pm 9.4	19.1 - 34.6
Dispersant control	56	6	25.5 \pm 9.6	17.6 - 33.4
6.3	56	6	24.5 \pm 4.5	20.9 - 28.2
12.5	56	6	23.2 \pm 8.6	16.1 - 30.3
25.0	56	6	0.0	-
50.0	56	6	0.0	-
100.0	56	6	0.0	-

Tab. S19: Mean sex ratios after 56 d in the 56-d exposure.

Carbo-Iron (mg/L)	Sex ratio [males / female]
Control	1.0 ± 0.2
Dispersant control	1.0 ± 0.1
6.3	1.1 ± 0.2
12.5	0.8 ± 0.2
25	0.6 ± 0.3
50	0.3 ± 0.3
100	0.0 (no males)

2.7 Acute toxicity tests with juveniles collected from exposed parental organisms

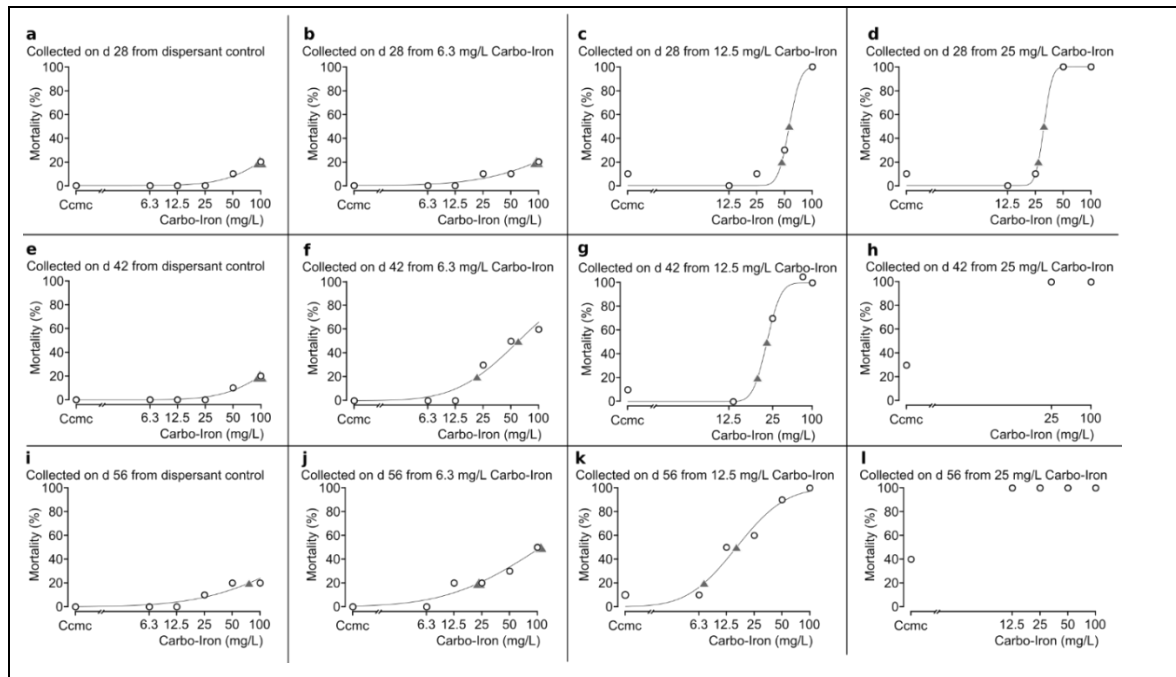


Fig. S1: Results from the acute toxicity tests with juvenile *H. azteca* collected from exposed parental organisms with a body length of approximately 2 mm. Test organisms were collected from the 56-d chronic toxicity test on d 28 (a-d), d 42 (e-h) and d 56 (i-l) from the dispersant control Ccmc (a, e, i) and Carbo-Iron test concentrations of 6.3 (b, f, j), 12.5 (c, g, k) and 25 mg/L (d, h, l).

The 2-parameter log-normal models were created using the R package *drc* (Ritz and Streibig 2005), and Carbo-Iron concentrations causing 20% and 50% mortality (LC_{20} and LC_{50}) were determined where data were appropriate. The concentration-response model fitted to the respective data set is drawn as a solid curve, triangles on the curves are LC_{20} and LC_{50} , respectively.

2.8 Summary of LC₂₀ values for the exposed *H. azteca*

Tab. S20: LC₂₀ values determined in the different tests with Carbo-Iron.

Test system	Time	LC ₂₀ [mg/L] (95% confidence intervals)	
Feeding activity test	7 d	no mortality in treatments	
Acute toxicity test with previously unexposed organisms	10 d	100 (80.4 - 119.6)	
42-d exposure	28 d	125.8 (-49.4 - 301)	
	42 d	56.9 (36.1 - 77.8)	
56-d exposure	28 d	51.3 (28.9 - 73.6)	
	42 d	20.9 (11.6 - 30.2)	
	56 d	8.7 (5.1 - 12.3)	
Acute toxicity tests with juveniles collected from exposed parental <i>H. azteca</i>			
Collected on d 28 from:	Dispersant control	10 d	97.5 (80.6 - 114.4)
	6.3 mg/L	10 d	94.9 (52.6 - 137.2)
	12.5 mg/L	10 d	46.6 (22.7 - 70.5)
	25.0 mg/L	10 d	26.9 (14.1 - 39.6)
Collected on d 42 from:	Dispersant control	10 d	97.5 (80.6 - 114.4)
	6.3 mg/L	10 d	21.4 (10 - 32.9)
	12.5 mg/L	10 d	9.6 (-29.9 - 49.1)
	25.0 mg/L	10 d	- ^A
Collected on d 56 from:	Dispersant control	10 d	75.8 (34.7 - 117)
	6.3 mg/L	10 d	23.2 (10.1 - 36.4)
	12.5 mg/L	10 d	7.1 (2.8 - 11.5)
	25.0 mg/L	10 d	- ^A

^A: 30% mortality in Ccmc, 100% mortality in all Carbo-Iron treatments.

Appendix D.1

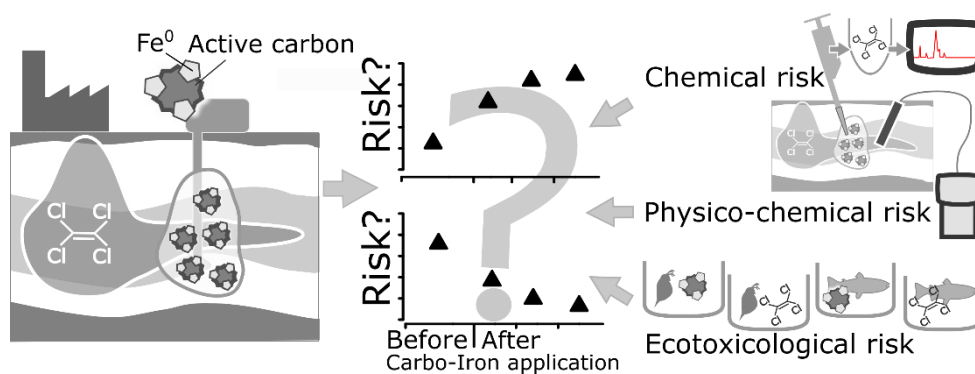
Environmental risk or benefit? Comprehensive risk assessment of groundwater treated with nano Fe⁰-based Carbo-Iron[®]

Mirco Weil, Katrin Mackenzie, Kaarina Foit, Dana Kühnel, Wibke Busch,
Mirco Bundschuh, Ralf Schulz, Karen Duis

Published in: Science of the Total Environment (2019),

Vol. 677, Pages: 156-166

Graphical abstract



Keywords

environmental risk assessment, nanoremediation, Fe⁰, groundwater treatment, chloroethenes

Highlights

- Environmental concentrations for the nFe⁰ agent Carbo-Iron derived from field study
- • Ecotoxicity data set for effects assessment was completed
- Standard risk assessment could be performed for a novel remediation agent
- Evaluation of benefit and risk of groundwater treatment for the environment
- Method applicable to identify environmental risks of other treatment techniques

Abstract

Groundwater is essential for the provision of drinking water in many areas around the world. The performance of the groundwater-bearing aquifer relies on the ecosystem services provided by groundwater-related organisms. Therefore, if remediation of contaminated groundwater is necessary, the remediation method has to be carefully selected to avoid risk-risk trade-offs that might impact these ecosystems. In the present study, the environmental risk of the *in situ* remediation agent Carbo-Iron was performed. Carbo-Iron[®] is a composite of zero valent nano-iron and active carbon. Existing ecotoxicity data were complemented by studies with *Daphnia magna* (crustacea), *Scenedesmus vacuolatus* (algae), *Chironomus riparius* (insecta) and nitrifying soil microorganisms. The predicted no effect concentration of 0.1 mg/L was derived from acute and chronic ecotoxicity studies. It was compared to measured and modelled environmental concentrations of Carbo-Iron applied in a groundwater contaminated with chlorohydrocarbons in a field study and risk ratios were derived. A comprehensive assessment approach was developed further based on existing strategies and used to identify changes of the environmental risk due to the remediation of the contaminated site with Carbo-Iron. With the data used in the present study, the total environmental risk decreased by approximately 50% in the heavily contaminated zones after the application of Carbo-Iron. Thus, based on the results of the present study, the benefit of remediation with Carbo-Iron seems to outweigh its negative effects on the environment.

1. Introduction

Groundwater constitutes more than 97% of the world's unfrozen fresh water and is the major source for drinking water in most developed and many developing nations (Gibert et al., 1994). Thereby, the groundwater-bearing aquifers are an important habitat for highly specialized and endemic species (Danielopol, 1989; Danielopol and Griebler, 2008). which provide important ecosystem services and play a critical role in carbon and nutrient cycling (Swartjes, 2011) and improve the water quality (Danielopol, 1989; Hahn, 2009). As a consequence of the unique and central properties of groundwater, the remediation of contaminated sites (e.g. in abandoned industrial sites) needs to be environmentally compatible.

Thus, the environmental risks of a remedial agent need to be assessed prior to the application into an aquifer. Obviously, a remediation method is only suitable, if the environmental risk after application is lower than before the start of the treatment (Lemming et al., 2010). Existing risk assessment strategies are implemented in several supporting tools which consider the remediation efficiency, treatment time, costs and the potential harm of the remedial method in comparison with alternative methods (Khadam and Kaluarachchi, 2003; Li et al., 2014; Ren et al., 2017; Tartakovsky, 2013; Yang et al., 2012). However, despite the high importance of groundwater for the environment, these tools often focus on the human health risk, whereas the environmental risk is only rarely considered (Wang et al., 2016).

For the treatment of groundwater contaminated with halogenated hydrocarbons, the Fe⁰-based remediation agent Carbo-Iron[®] was developed. It is a colloidal composite of nano Fe⁰ structures embedded in active carbon (AC) particles (Bleyl et al., 2012; Mackenzie et al., 2016, 2012). In several pilot studies, Carbo-Iron was applied for treating aquifers polluted by chlorohydrocarbons and the application of particles at a site mainly contaminated by tetrachloroethene (PCE) has recently been described (Mackenzie et al., 2016). Though nano Fe⁰-based groundwater remediation methods are promising, it is necessary to assess their potential harm to the environment and inform decision makers about possible risks (Grieger et al., 2010). In order to provide a comprehensive environmental risk-benefit analysis of Carbo-Iron, the present study comprises of three main aspects: 1) an effects assessment for Carbo-Iron, 2) an environmental risk assessment for Carbo-Iron, 3) a site-specific environmental risk assessment for the treated groundwater, considering all pollutant concentrations before and after application of Carbo-Iron.

Since previous ecotoxicity data for Carbo-Iron (Hjorth et al., 2017; Nguyen et al., 2018; Weil et al., 2016, 2015) were not sufficient for an environmental risk assessment, further ecotoxicity tests were performed. A predicted environmental concentration (PEC) of Carbo-Iron was estimated based on

available data from a field study and compared to the predicted no effect concentration (PNEC) derived in this manuscript, providing a first estimation of the environmental risk of Carbo-Iron. The Triad approach for comparison of environmental risks of sediments (Chapman, 1990) was applied which was already refined for a general use in risk assessment (Dagnino et al., 2008; Jensen and Pedersen, 2006; Weeks and Comber, 2005), and a specific use for risk assessment in groundwater (Crévecoeur et al., 2011). In the present study, we further modified this approach to evaluate the risk caused by the application of the remediation agent Carbo-Iron into an aquifer during a field study.

2. Material and Methods

2.1 Effect assessment for Carbo-Iron

Active Carbo-Iron rapidly alters chemically by the target reaction with halogenated hydrocarbons and by oxidation reactions with water. This ageing process of the material in groundwater is unavoidable and starts immediately after injection. Therefore, all toxicity tests were performed with aged Carbo-Iron, which means that the originally zero-valent iron was treated in slightly acidic deoxygenated water leading to formation of Fe^{2+} and, by further reaction with dissolved oxygen, to Fe^{3+} . This way, the ageing process of Carbo-Iron in the aquifer was simulated. Henceforth, the term Carbo-Iron is used for aged Carbo-Iron, consisting mainly of FeOOH , Fe_3O_4 and less Fe_2O_3 embedded in the AC with an iron content of approx. 22% (w/w)

The characteristics of Carbo-Iron particles in aqueous media were extensively examined in previous studies with *Danio rerio* (Weil et al., 2015) and *Hyaella azteca* (Weil et al., 2016). In these studies, particle diameters measured in the stock suspensions varied only marginally. In the present study, the same methods for preparation of stock and test suspensions were used (see SI section 1.1.1). Briefly, stock suspensions were prepared by homogenizing Carbo-Iron with an ultrasonic probe (Hielscher UP200S, Teltow, Germany) in deionized water. Test suspensions were prepared by dilution of the stock suspension with the culture medium for the respective test organisms. As stabilizing additive, carboxymethyl cellulose (CMC; 70,000 g/mol and a range in substitution degree from 0.65 to 0.9, which correspond to a concentration of carboxylic groups of 2.8 to 3.9 mval/g, respectively; Antisol FL 30, Wolff Cellulosics) was used in the stock and test suspensions with 20% w/w relative to the highest used test concentration to prevent rapid sedimentation of Carbo-Iron. CMC was also used as particle stabilizer for Carbo-Iron suspensions during injection into the groundwater. In each toxicity test, a control group in culture medium was included. Additionally, a CMC dispersant control group with culture medium and CMC at the same concentration as in the test suspensions was used in all tests except the test with *Scenedesmus vacuolatus*. Supplemental

to the tests described here, a nitrogen-transformation test was performed as a sensitive indicator for effects on soil-inhabiting microorganisms (see SI section 1.1.5 for method description).

2.1.1 Toxicity tests with *Daphnia magna*

The 48-h acute toxicity test with *D. magna* (Crustacea, Branchiopoda, Cladocera) was based on OECD (2004a), extended by a 5-d post-exposure period. Daphnids were exposed to Carbo-Iron concentrations between 0.562 and 100 mg/L. For each treatment and control, 4 replicates with 5 daphnids each were used. During the 48-h exposure, no food was provided. Immobility was evaluated after 48 h of exposure. Then, daphnids were transferred to M7 medium without Carbo-Iron and CMC and fed daily with 4.0×10^5 cells/mL (1.67 mg C/L) of a suspension of batch-cultured green algae (*Desmodesmus subspicatus*). During a post-exposure period of 5 d, immobility was assessed daily.

The *D. magna* chronic reproduction test was based on OECD (2008). For each treatment and control, 10 replicates with 1 daphnid each were used; the investigated Carbo-Iron concentrations were between 0.1 and 10 mg/L. During the 21 d exposure, daphnids were fed three times per week with green algae (*D. subspicatus*, 9.6×10^5 cells/mL corresponding to 4.0 mg C/L). Three times weekly, the survival of adult daphnids and number of living offspring per animal per day were assessed, and test solutions were renewed. This interval of the test media renewal coincides with the finding of a previous study with *Hyalella azteca*, where Carbo-Iron suspensions with concentrations up to 100 mg/L were stable for approx. 3 d after start of the exposure (Weil et al., 2016). To verify this assumption, Carbo-Iron concentrations in the test suspensions with 3.16 and 31.6 mg/L were measured after 24, 48 and 72 h with the dynamic light scattering-based method described in Weil et al (2015). Further details on exposure conditions are described in SI section 1.1.2.

2.1.2 Algal growth inhibition test

The algal growth inhibition test with *Scenedesmus vacuolatus* (Chlorophyta, Chlorophyceae, Sphaeropleales) was performed with Carbo-Iron and with active carbon (AC; Norit® SA Super, Cabot, USA; milled to $d_{50} = 0.8 \mu\text{m}$). This pure AC powder is used as a basis for the preparation of Carbo-Iron and was applied in the algae test to investigate whether effects were a result of the reduced light intensity due to shading by the particles. Carbo-Iron test concentrations were between 16 - 62.5 mg/L and the test concentrations for AC (15 – 43.5 mg/L) correspond to the content of AC of the tested Carbo-Iron concentrations. The test suspensions were prepared by

adding 0.8 mL of algae suspension (cell density 7-9.5 in 10-fold concentrated culture medium) to 7.2 mL of a respective Carbo-Iron or AC suspension. Aeration of the test suspensions kept the algae cells as well as the Carbo-Iron particles in suspension and no precipitates were observed during the exposure. Light intensity was measured at the beginning of exposure in each culture tube of the lowest and highest investigated test concentration with Carbo-Iron and AC, respectively.

The effect of Carbo-Iron and AC on algal growth based on cell numbers could not be measured in a cell counter or under the microscope, because Carbo-Iron and AC particles had a similar size as the algal cells after cell division. Further, effects on photosynthesis could not be quantified, because the particles interfered with the measurement of fluorescence. For these reasons, the parameter cell volume was used as alternative to assess effects on algal growth (Faust et al., 1992). Cell volume was measured after an exposure duration of 16 h, when cells had increased in volume, but not yet divided. The cell diameter at this time point was 6-15 μm and a clear distinction from the particles ($< 5 \mu\text{m}$) was possible. Further information on exposure conditions is provided in SI section 1.1.3. Additionally, the toxicity of PCE to *S. vacuolatus* was investigated, details are provided in SI sections 1.1.3 and 2.3.3.

2.1.3 Sediment-water test with *Chironomus riparius*

The sediment-water toxicity test was performed according to OECD (2004) with *C. riparius* (Arthropoda, Insecta, Diptera). This test organism was chosen for its relevance for particle suspensions with limited stability, since Carbo-Iron precipitated to the sediment surface would remain available for the sediment-dwelling larvae. Test vessels with artificial sediment and medium M4 were prepared. Immediately after addition of Carbo-Iron test suspensions to the water phase of the water-sediment systems, first instar larvae were introduced to the test vessels (10 organisms per vessel). For each treatment and control, 8 replicates were used. Test vessels were incubated at $20 \pm 2^\circ\text{C}$ with slight aeration and a photoperiod of 16 h light and 8 h dark. During the 28 d exposure, the emergence and development rate were evaluated (for further details, see SI section 1.1.4).

2.1.4 Statistical analysis

Statistical analyses were carried out using R Version 3.3.0 (R Development Core Team, 2011). Statistical analysis by null hypothesis significance testing was based on replicate means; proportional data were arcsine-transformed before analysis. For comparison of differences between control and dispersant control, the two-sided Welch two-sample t-test was used. If the requirements for parametric testing (homogeneity of variances and normal distribution) were

fulfilled, ANOVA and Dunnett's two-sided post-hoc test were performed, while the Kruskal-Wallis test with subsequent Wilcoxon ranks sum test were used as non-parametric alternative. For all tests, a significance level of $p \leq 0.05$ was used (OECD, 2006). Treatments were compared to the dispersant (CMC) control. Where appropriate, the log-normal model with 3 parameters was fitted to the data to calculate effective concentrations (Ritz and Streibig, 2005).

2.2 Assessment of the environmental risk of aged Carbo-Iron

2.2.1 Exposure assessment for Carbo-Iron

The relevant release of Carbo-Iron into the environment is not, as for many industrial chemicals, via diffuse routes over the whole product life cycle. Instead, Carbo-Iron release is intended and immediate, i.e. a major portion of the produced amounts is pumped into contaminated groundwater. Thus, the present study focuses on the exposure to Carbo-Iron in the area close to the treated site. Carbo-Iron was used in a pilot study for remediation of groundwater contaminated with chlorohydrocarbons (Mackenzie et al., 2016). The contaminated site (Figure 1) was a former military area with a chemical cleaning facility that caused groundwater pollution by chlorohydrocarbons, mainly tetrachloroethene (PCE). Several sampling ports were used to monitor concentrations of the pollutants before and during treatment with Carbo-Iron (see section 2.3.2). Based on the measured PCE concentrations, the site was subdivided in four contamination zones (I – IV, Figure 1A). The groundwater flow velocities were between 30 cm/day in the southern part of the site and of 6 cm/day in the northern part. For remediation of the site, Carbo-Iron suspensions (10 g/L) were prepared by dispersion of dry Carbo-Iron into deoxygenized tap water using a high-speed homogenizer. CMC (the same as described in section 2.1) at a concentration of 2 g/L was used as colloid stabilizer. The first injection campaign with 20 kg of Carbo-Iron was applied in two injection ports (IP1 and IP3; Figure 1A) and was designed to build a fence-like reactive barrier in the aquifer. In a second injection campaign Carbo-Iron was applied in a two-dimensional injection pattern (Mackenzie et al., 2016). For the present study, only data from the first campaign are used to exploit the rare opportunity of a localized remediation of groundwater with a very uniform distribution of the remediation agent Carbo-Iron. Groundwater conditions are often highly complex and the added complexity of the two-dimensional injection pattern using 15 injection ports would have impeded the attribution of the observed effects to the remediation.

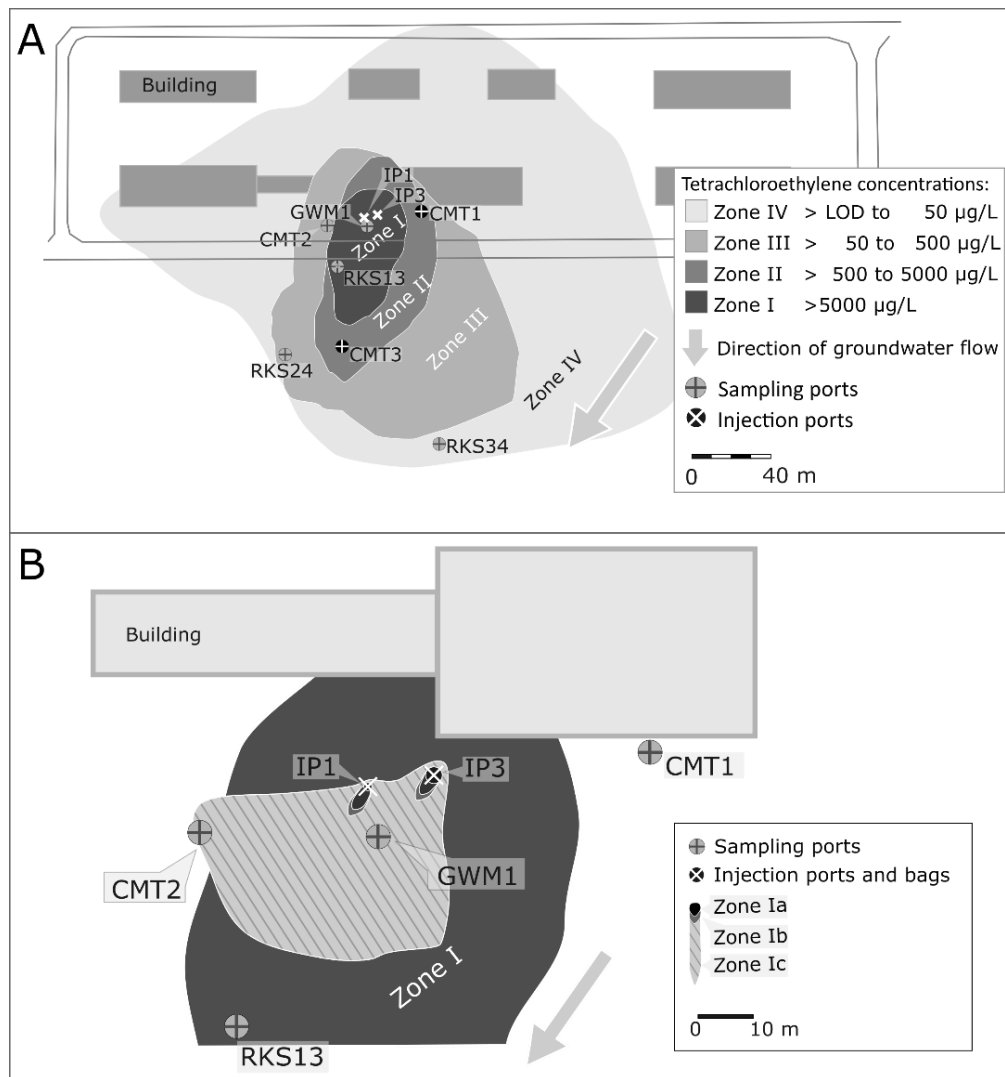


Figure 1: Site treated with Carbo-Iron in the pilot study of Mackenzie et al. (2016). Groundwater monitoring well (GWM1) with a sampling depth of 8 m below ground level; continuous monitoring well with multichannel-tubing (CMT1, CMT2, CMT3) with seven ports in depths between 6 and 25 m below ground level; window sampling tube (RKS 13, RKS 24, RKS 34) with two sampling ports at approx. 6.5 and 8 m below ground level. **A**: Overview of the area and allocation of zones based on measured concentrations of PCE above analytical limit of detection (LOD=0.5 µg/L). **B**: Distribution of Carbo-Iron after injection in zone I. Subdivisions Ia, Ib, and Ic indicate the calculated Carbo-Iron concentrations (Table 1) based on data from the column studies (SI section 2.1).

Before termination of the monitoring period, sediment samples were taken by direct push from zone I and analysed for its Carbo-Iron content (see SI section 2.2.2). Concentrations of Carbo-Iron in the wells were not measured with common analytical methods, since the Carbo-Iron constituents would be unnoticeable at the high natural background values of iron and carbon. Therefore, concentrations (Table 1) and distribution of Carbo-Iron in the groundwater (Figure 1B) were estimated based on information on the time-dependent distribution pattern of Carbo-Iron from soil

column studies with various standard and natural porous materials (such as Dorsilit and sediment from the site; see SI section 3.1) using columns with different lengths (Batka and Hofmann, 2016).

Table 1: Estimated concentrations of Carbo-Iron in the distribution zones (Figure 1). Carbo-Iron concentrations were estimated based on data from soil column studies (SI section 2.1).

Contamination zone	Sampling well	Distance from Carbo-Iron injection (m)	Estimated mean Carbo-Iron concentration (mg/L)
Ia	-	0 – 1.3	650
Ib	-	1.3 – 1.9	475
Ic	GWM1	1.9 – 12.9	1.3
I	RKS13	0 to approx. 20	0.5
	CMT2	approx. 20	1.3*
II	CMT3	approx. 40	0
	RKS24	approx. 80	0
III	RKS24	approx. 80	0
IV	RKS34	approx. 100	0
II	CMT1	5 to approx. 20 (Opposite to direction of groundwater flow)	0

*: Sampling well CMT2 is in zone II but bordering to zone Ic. For a conservative risk assessment approach, the Carbo-Iron concentration was based on concentrations estimated for zone Ic.

2.2.2 Derivation of a PNEC, environmental risk assessment for Carbo-Iron

A predicted no effect concentration (PNEC) for Carbo-Iron was derived based on the effect concentrations generated in the present study, and by Weil et al. (2016, 2015) and Hjorth et al. (2017). The PNEC value was then calculated as the quotient of the most sensitive endpoint and the related assessment factor. The latter was selected depending on the availability of results from (a) acute and chronic tests, and (b) trophic/functional groups algae, crustaceans, fish as recommended for the risk characterisation of chemicals (ECHA, 2017, 2008). The risk quotient (i.e. PEC/PNEC ratio) indicates the degree of risk expected to be caused by Carbo-Iron in the treated aquifer. A risk quotient below 1 is generally considered acceptable (ECHA, 2016).

2.3 Site-specific risk-benefit analysis

2.3.1 Theoretical impact of Carbo-Iron on the relevant pollutants

The desired remedial effect of Carbo-Iron is promoted by two mechanisms: (a) after Carbo-Iron is introduced into the groundwater, the sorption capacity of the AC component in Carbo-Iron increases the retention time of the pollutants, i.e. the migration of PCE through the groundwater slows down by a calculated factor of approx. 30 compared to migration before Carbo-Iron

treatment (Georgi et al., 2015). This leads to a rapid decrease of the PCE concentrations in zone I.

(b) The chemical degradation of the pollution induced by the Fe⁰-component of Carbo-Iron leads to an additional decrease of the pollutant concentration.

2.3.2 Exposure assessment for the relevant pollutants

In the field study (Mackenzie et al., 2016), Carbo-Iron was applied to an aquifer polluted by chlorohydrocarbons (see section 2.2.1), mainly by PCE at concentrations up to 120 mg/L. In groundwater samples from wells distributed over the contaminated area (Figure 1 and Table 1), chemical analysis was performed for trichloroethene and PCE. Additionally, transformation products of the reduction by Carbo-Iron, 1,1-dichloroethene, 1,2-dichloroethene (cis and trans), ethane and ethene (as a sum parameter) and vinyl chloride, were analysed. Furthermore, the redox potential and total organic carbon (Table S16), pH and iron concentration (Table S 17) and oxygen concentration (Table S18) were measured. In the present study, data for day 0 (i.e. before Carbo-Iron injection) and days 9, 31, 58, 93 and 190 after application of Carbo-Iron into the groundwater were evaluated. For the contamination zones I to IV, the wells GWM1, RKS13, CMT2, CMT3, RKS24 and RKS34 were selected based on the availability of continuous data for chemical analysis. To evaluate groundwater dynamics that are independent from the application of Carbo-Iron, the sampling well CMT1 (located in a distance of approx. 10 m from the injection points in opposite direction of the groundwater flow) was included. For all calculations, the median value per well and sampling day was used.

2.3.3 Derivation of PNECs for the relevant pollutants / chlorinated hydrocarbons

For the determination of PNECs for the analysed pollutants, effect data for at least three trophic/functional groups (algae, crustaceans and fish) were retrieved from ECHA registrations dossiers (echa.europa.eu), the ECOTOX database (<http://cfpub.epa.gov/ecotox/>) and the QSAR Toolbox platform (<https://www.qsartoolbox.org/>, Dimitrov et al., 2016) that retrieves data from the Aquatic OASIS and Aquatic Japan databases. This database search was extended by a literature search using the name of each substance in combination with the trophic/functional group or representative species in these groups. In the case of multiple data for one trophic/functional group, the lowest relevant and reliable (criteria were e.g. guideline test, accompanying chemical analysis) value was chosen. PNEC values were then calculated as described for Carbo-Iron in section 2.2.2.

2.3.4 Triad-based risk-benefit analysis

General aspects

The Triad approach was developed for the quality assessment of sediments (Chapman, 1990; Critto et al., 2007; Long and Chapman, 1985) and integrates data on (1) the concentrations of the contaminants compared to target values (chemical component), (2) alterations in biodiversity of the local community compared to a reference site (ecological component) and (3) potential adverse effects of the contaminants on environmental organisms (ecotoxicological component). Dagnino et al. (2008) further developed the approach for the assessment of contaminated sites and calculated risk indices for each component. To assess the environmental risk before and after the application of Carbo-Iron, the approach of Dagnino et al. (2008) was used with the following modifications:

- (1) The chemical component of the assessment integrates concentrations of the relevant pollutants (section 2.3.2) before and after treatment with Carbo-Iron. Carbo-Iron concentrations were not considered, because the calculation of risk indices requires target values lacking for Carbo-Iron.
- (2) The ecotoxicological component covers data for the relevant pollutants as well as for Carbo-Iron. Instead of ecotoxicity tests with groundwater samples, data from single-substance standard ecotoxicity tests were used. This was done because groundwater samples, usually with low oxygen concentrations, do not provide suitable conditions for the commonly used test organisms. An adjustment of groundwater samples to the requirements of these test organisms would most likely have an impact on the pollutant concentration (e.g. stripping of volatile compounds by aeration of the samples). Moreover, a culture of aquifer-inhabiting organisms in the laboratory is often problematic and standard test guidelines as recommended for risk assessment are not available for groundwater organisms.
- (3) The ecological component was excluded from analysis. The determination of the ecological status of a groundwater is extremely difficult, as observations on biodiversity cannot be performed directly in the aquifer. Sampling of the aquifer fauna is not only time-consuming but in most cases incomplete due to the patchy distribution (Hahn, 2006; Steube et al., 2009), and standardized sampling protocols are lacking (Stein et al., 2010). Additionally, the ecological component requires an appropriate reference site with minimal anthropogenic pollution but similar fauna and physico-chemical parameters (Dagnino et al., 2008; Jensen and Pedersen, 2006). For groundwater, selection of a reference site is complicated because of the aforementioned patchy distribution of fauna in groundwater and a high number of

endemic species (Stein et al., 2010). Furthermore, in case of highly contaminated groundwater, it is very likely that the abundance of organisms is poor, or organisms are completely absent which makes it impossible to calculate a risk index for the ecological component.

- (4) A physico-chemical component was introduced, as suggested by Crévecoeur et al. (2011). Changes in physico-chemical parameters due to the injection of Carbo-Iron may increase the environmental risk for the groundwater fauna. The physico-chemical component includes parameters that are very likely to change after application of Carbo-Iron into the groundwater including redox potential, conductivity and pH.

Chemical component

Risk indices were calculated for each sampling well and day in three steps: (1) risk quotients (RQ) were calculated as quotients of the mean measured concentrations of the relevant pollutants per day and well and the respective target values, (2) chemical toxic pressure (cTP) for each sampling well per day was then calculated as sum of the risk quotients for all 6 pollutants, (3) chemical risk indices (cRI) were calculated (Eq. 1 to Eq. 3) depending on the cTP value in comparison to two defined threshold values (Th' and Th'') representing two levels of risk.

The target values for vinyl chloride, 1,1-dichloroethene, 1,2-dichloroethene (cis and trans), trichloroethene and tetrachloroethene of 5, 5.8, 20, 500 and 40 µg/L were generally taken from Swartjes (1999), who derived intervention values for the assessment of groundwater. These values are based on potential risks to humans and ecosystems and should, if exceeded, trigger a remediation of the site (Swartjes, 1999). For ethane and ethene, no quality standards for groundwater were identified, and a maximum permissible concentration of 8500 µg/L in surface water was only available for ethene (Crommentuijn et al., 2000). This value was used as target value for the sum parameter ethane/ethene.

If any measured value for a parameter was above the respective target value, the TP was > 1 and a risk for the environment was expected. A TP below Th' will lead to calculated RI between 0 and a predefined level of risk α ; a TP between Th' and Th'' will lead to a risk index between α and 1. Above Th'', the risk index acquires the maximum value of 1. It should be pointed out that the value for Th'' in the present study is higher than the value selected by Dagnino et al. (2008) who compared negative effects of the deposition of contaminated soils on xenobiotic compounds and applied Th'=1 and Th''=10. With these thresholds Dagnino et al. (2008) derived cRI ≤ 0.75 and a differentiation of the investigated soils was possible. In the present study, Th'=1 was chosen, too. However, due the high pollutant concentrations in groundwater samples from zone I, several RQ

were in the range of 1000, leading to similarly high TP values. Thus, a $Th''=10$ would have led to cRI and eRI above the maximum value of 1 in several cases and identification of a positive or negative influence of Carbo-Iron on these components would have been impossible. Thus, to detect changes in the risk under the influence of Carbo-Iron, $Th''=1000$ was chosen for the calculation of cRI and eRI.

$$\text{If } TP_{well, day} \leq Th' \quad RI = \frac{TP}{Th'} \times \alpha \quad (\text{Eq. 1})$$

$$\text{If } Th' < TP_{well, day} \leq Th'' \quad RI = \alpha + \frac{TP - Th'}{Th'' - Th'} \times (1 - \alpha) \quad (\text{Eq. 2})$$

$$\text{If } TP_{well, day} > Th'' \quad RI = 1 \quad (\text{Eq. 3})$$

Ecotoxicity component

Ecotoxicity risk quotients were calculated as quotients of the concentrations of the relevant pollutants (see section 2.3.2) measured in groundwater samples and the PNEC for the respective compound as target values. Toxic pressure (eTP) for each sampling well per day was then calculated as sum of the risk quotients. This differs from the method described by Dagnino et al. (2008), who used the mean of all risk quotients (instead of the sum) when evaluating the toxicity of contaminated sediments based on ecotoxicity tests with sediment samples. In the present study, additive effects of the pollutants are covered in the risk assessment by using the sum of the eRQs. Risk indices (eRI) were calculated as described in Eq. 4 to Eq. 6 with the threshold values $Th'=1$ and $Th''=1000$. For the ecotoxicity component, a TP below Th' will lead to an RI of 0 and TP values between Th' and Th'' will lead to a risk index between 0 and 1. Above Th'' , the risk index acquires the maximum value of 1 for all three components.

$$\text{If } TP_{well, day} \leq Th' \quad RI = 0 \quad (\text{Eq. 4})$$

$$\text{If } Th' < TP_{well, day} \leq Th'' \quad RI = \frac{TP - Th'}{Th'' - Th'} \quad (\text{Eq. 5})$$

$$\text{If } TP_{well, day} > Th'' \quad RI = 1 \quad (\text{Eq. 6})$$

Physico-chemical component

The passage of groundwater through the reactive barrier of Carbo-Iron can potentially change physico-chemical characteristics of the groundwater. While a potential ecotoxicological risk due to exposure of organisms to Carbo-Iron is locally limited by the mobility and distribution of Carbo-Iron in the aquifer, extreme physico-chemical parameters in the groundwater could lead to an increased risk beyond this area. During the field study (Mackenzie et al., 2016), physico-chemical parameters were measured in the groundwater samples. In the present study, only conductivity, pH and redox potential were considered. Data for total organic carbon (Table S16), iron concentration (Table S17) and oxygen concentrations (Table S18) could not be attributed to Carbo-Iron application and were thus not included. For each of the relevant physico-chemical parameters per day and sampling well, a risk index was calculated as described in the following and the mean value of these risk indices was used as the physico-chemical risk index per well and day (pRI).

The target values of 2500 $\mu\text{S}/\text{cm}$ for the parameter conductivity was taken from the EU directive on the quality of water for human consumption (European Communities, 1998). Since only a maximum but no minimum target value was available, the risk index was calculated in two steps (1) the quotient of measured data and target value for each day and well was calculated and (2) these values were used as TP to calculate a RI for conductivity as described in Eq. 1 to Eq. 3. For pH and redox potential, however, optimum ranges were defined and used to directly derive a risk index for the two parameters. For pH, the calculation of the risk index followed the description of Crévecoeur et al. (2011; see Eq. 7 to Eq. 9) in the target range of pH 6.5 to 9.0 (US EPA, 1999). For the redox potential, no target values could be identified in literature. However, due to the high potential of Carbo-Iron to affect this parameter, its observation was considered necessary. In low-oxygen groundwater, the redox potential ranges usually between -300 and 0 mV (Grenthe et al., 1992). However, due to the high permeability of sandy sediments and the low distance to the ground level, the aquifer of the field study was also markedly influenced by precipitation events and groundwater samples frequently showed relatively high oxygen concentrations carried in by rainwater (Table S18). Therefore, redox potentials representative for surface waters ranging between 0 and 500 mV were additionally considered (Pepper and Gentry, 2015; Søndergaard, 2009; Williams and Fraústo da Silva, 2006). Combining both, the target range for the parameter redox potential was set to -300 to 500 mV. This range is in accordance with live-promoting ranges mentioned in the comprehensive review on redox potentials by Husson (2013). Measured values beyond the range of -300 to 500 mV result in a risk index of 1, values from -300 to -225 and from 375 to 500 mV are attributed to a risk index of 0.5, values between -225 and 375 mV are attributed to a risk index of 0.

$$\text{If } pH_{well, day} < 6.5 \quad pRI_{pH, well, day} = 1 - (0.0085 \times e^{0.7032 \times pH_{well, day}}) \quad (\text{Eq. 7})$$

$$\text{If } 6.5 \leq pH_{well, day} \leq 9 \quad pRI_{pH, well, day} = 1 - (-0.163 + 0.1381 \times pH_{well, day}) \quad (\text{Eq. 8})$$

$$\text{If } pH_{well, day} > 9 \quad RI_{pH, well, day} = 1 - (2.163 - 0.1481 \times pH_{well, day}) \quad (\text{Eq. 9})$$

Environmental risk

To integrate the risk indices for the chemical, ecotoxicological and physico-chemical components, the environmental risk was calculated as described by Dagnino et al. (2008) as the mean value of the three risk indices (Eq. 10).

$$EnvRI = \frac{cRI + eRI + pRI}{3} \quad (\text{Eq. 10})$$

3. Results & Discussion

3.1 Effect assessment for Carbo-Iron

In the additionally performed nitrogen-transformation test, no effects were observed in the investigated test concentrations up to 2828 mg Carbo-Iron/kg soil dw (see SI section 2.3.5 and Table S9 for results). In the algae test with *S. vacuolatus* and PCE, a LC_{50} = 25.6 mg/L was determined (see SI section 2.3.3 and Table S7 for the results).

3.1.1 Toxicity tests with *Daphnia magna*

The stability of the test suspensions decreased over time and was independent from the nominal Carbo-Iron concentrations. After exposure for 24, 48 and 72 h to 3.16 and 31.6 mg/L, measured concentrations decreased to 93, 87 and 81% of the nominal concentrations, respectively. Despite these deviations from the desired test concentrations, all exposure concentrations are given as nominal values.

Between 50 and 70% of the *D. magna* were immobile after 48-h exposure to Carbo-Iron at concentrations between 10 and 56.2 mg/L (Figure 2A and Table S1). However, in the highest test concentration only 30% of the *D. magna* were immobile. A 48-h LC_{50} of 33.5 mg/L was determined (Table S2). After the 5-d post-exposure period in the culture medium without Carbo-Iron, mean immobility was at least 90% in all test concentrations ≥ 10 mg/L (Figure 2B), and for the postexposure a LC_{50} of 3.4 mg/L was derived (Table S2).

In the 21-d chronic test, no mortality was recorded at concentrations ≤ 3.2 mg/L while exposure of *D. magna* to 10 mg/L Carbo-Iron reduced the survival to 70% (Table S3). The reproduction rate was significantly lower compared to the CMC control at the two highest test concentrations of 3.16 and 10 mg/L (Figure 2C and Table S3) and an EC₁₀ of 2.0 mg/L (Table S4) was calculated.

While approx. 90% of the daphnids were immobile at 10 mg/L after the post-exposure period in the acute toxicity test, only 30% of the introduced daphnids were immobile in the chronic toxicity test at the same test concentration. In both tests, the same method was used for the preparation of the Carbo-Iron suspensions. However, as required by OECD (2012) daphnids were not fed during the 48-h exposure in the acute toxicity test, while food was provided every second day starting on d 0 in the chronic test. Potentially, daphnids in the acute test ingested more Carbo-Iron than the algae-fed daphnids in the chronic test. During the post-exposure phase after the acute toxicity test, this reduced food uptake could not be compensated for. In a previous study with Carbo-Iron and the crustacean *Hyaella azteca* (Weil et al., 2016), effects on survival of adults and offspring were related to presence of Carbo-Iron in the gut, a reduced feeding rate, and an assumed decreased gut clearing time that most likely led to nutrient depletion. The general gut physiology of the pelagic cladoceran *D. magna* and the epi-benthic malacostracan *H. azteca* is similar: It is composed of oesophagus, midgut and hindgut with setae that allow the separation between food particles and liquid compounds (Ceccaldi, 1989). Likely, similar increases of gut transit times and food uptake rates as probably caused by Carbo-Iron in *H. azteca* are the reason for the delayed mortality of *D. magna* observed in the post exposure of the acute toxicity test.

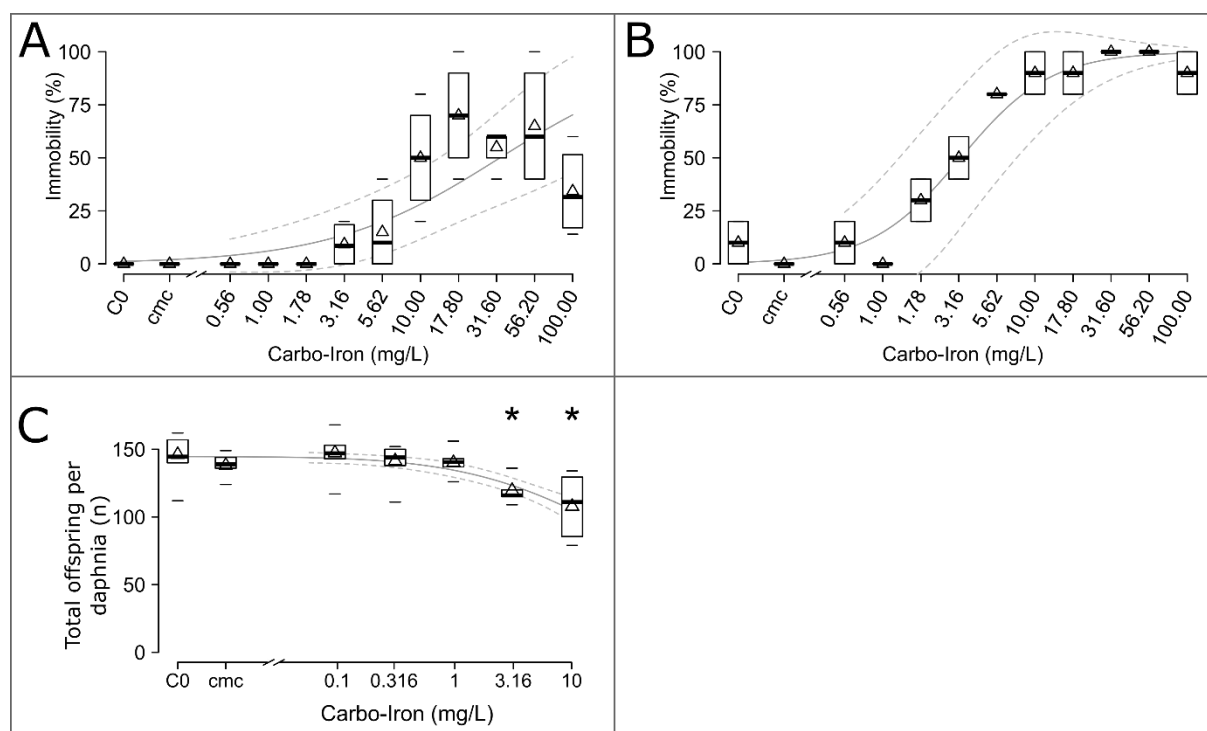


Figure 2: Results of the toxicity tests with *D. magna* and Carbo-Iron. In the acute test, immobility ($n=4$) was assessed after 48 h exposure (A). Subsequently, *Daphnia* were transferred to culture medium without Carbo-Iron and mortality was assessed after 5 d post-exposure (B). In the chronic test (C) total number of living offspring per *Daphnia* ($7 \leq n \leq 10$) was determined during 21 d of exposure. In all tests, negative controls with culture medium (C0) and CMC controls with 20 mg/L CMC (cmc) were investigated. *: Significant difference from the CMC control (Wilcoxon ranks sum test, $p \leq 0.05$). Triangles are mean values; boxes represent the upper and lower quartile of the data, horizontal dashes represent extreme values outside this range.

3.1.2 Algal growth inhibition test

In the algae growth inhibition test with *S. vacuolatus* the endpoint cell volume inhibition was measured after 16 h exposure to Carbo-Iron and AC, respectively. In all Carbo-Iron treatments, significant inhibition of cell volumes was found in comparison to the control (Figure 3). The observed effects on cell volume in the Carbo-Iron treatments were comparable to those observed in the AC treatments, considering the mass difference of approx. 1.2 between Carbo-Iron and active carbon with $EC_{10}=7.2$ and 6.4 mg/L, respectively (Table S6).

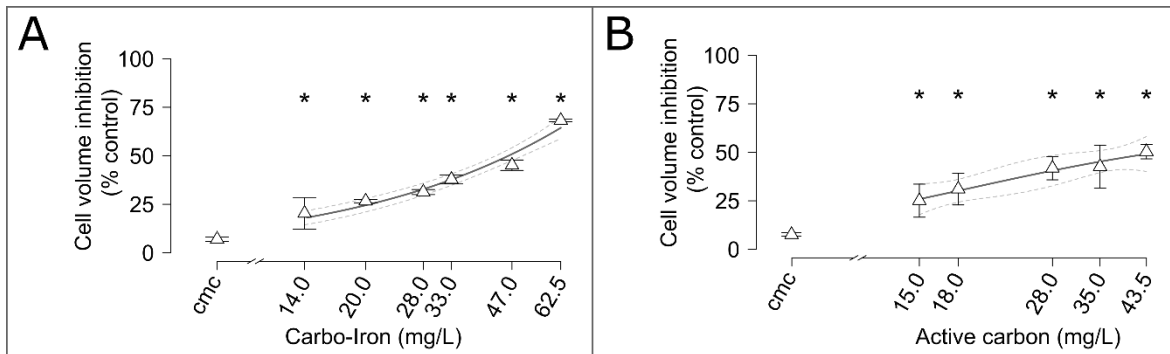


Figure 3: Cell volume inhibition (mean \pm sd; n=3) in *S. vacuolatus* after 16 h exposure to Carbo-Iron (A) and AC (B). In all tests, negative controls with culture medium (C0) and CMC controls with 20 mg/L CMC (cmc) were investigated. Cell volume inhibition was normalized to the control values. *: Significant difference to the CMC control (ANOVA followed by two-sided Dunnett's test, $p \leq 0.05$).

In order to evaluate the effect of shading by the particles, the light intensity at the beginning of the exposure was measured in selected test vessels (SI section 2.3.2). Light intensities decreased with increasing Carbo-Iron and AC content (Table S5). Light intensities in Carbo-Iron treatments were significantly higher than in the corresponding AC treatment (Fig. S3). The shading effects observed in the tests with Carbo-Iron and AC are potentially the main reason for the observed effects on algae. Similar effects were reported for CNT-exposed green algae (Schwab et al., 2011). However, the binding of nutrients from the test media by AC (Bundschuh et al., 2011) could additionally have caused nutrient depletion in the culture medium and thus contributed to the observed toxicity.

3.1.3 Sediment-water test with *Chironomus riparius*

Carbo-Iron suspensions were initially homogeneously grey in concentrations < 56.2 mg/L and nearly opaque at test concentrations ≥ 56.2 mg/L. The test suspensions became visibly clearer approx. 10 d after start of exposure and black precipitate was visible on the sediments, indicating nearly complete sedimentation of the particles in all treatments. Emergence of *C. riparius* was not affected by Carbo-Iron and reached a similarly high value of 89% in the highest test concentration as in the CMC control with 90% (Table S8). For development rate, a significant increase was observed in the CMC control compared to the control with 0.057 and 0.061 d^{-1} , respectively; Figure 4, Table S8). Positive effects of α -cellulose as organic material (i.e. nutrient) on the growth of *Chironomus tentans* were observed by Lacey et al. (2009) in a 10-d exposure. Due to the similar chemical structure of α -cellulose and CMC it is likely that CMC had a positive effect on the development of the midge larvae. However, while all Carbo-Iron treatments had the same CMC content, exposure to Carbo-Iron minimized the positive effect of CMC and a significantly lower development rate of

0.056 d⁻¹ was observed in the highest test concentration of 100 mg/L Carbo-Iron in comparison to 0.061 d⁻¹ in the CMC control.

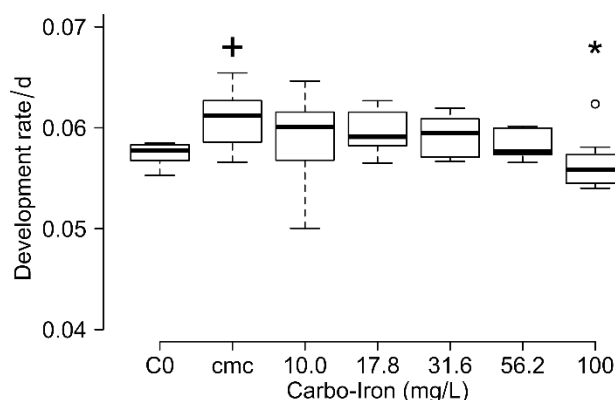


Figure 4: Development rate of *C. riparius* (n=8) during the 28-d exposure to Carbo-Iron in the water-sediment test. Triangles are mean values, boxes represent the upper and lower quartile of the data, whiskers extend to minimum and maximum values within a 1.5 quartile distance, circles represent extreme values outside this range. +: significant difference to the control (C0, two-sided t-test, $p \leq 0.05$); *: significant difference from the CMC control (cmc, two-sided Dunnett's test, $p \leq 0.05$).

3.2 Assessment of the environmental risk of aged Carbo-Iron

The results from the ecotoxicity studies with aged Carbo-Iron are summarized in Table S10. The most sensitive effect concentration observed in the chronic ecotoxicity tests was the NOEC of 1.0 mg/L derived in the 21-d study with *D. magna*. Since results of chronic studies with all three trophic levels are available, an assessment factor of 10 was used and a PNEC of 0.1 mg/L was derived for Carbo-Iron. This PNEC is relatively high when compared to PNEC values obtained for nano-Ag (0.02 µg/L), nano-ZnO (1 µg/L), fullerenes (4 µg/L), nano-TiO₂ (16 µg/L) and carbo-nano tubes (CNT; 56 µg/L) (Coll et al., 2016).

At the pilot study site, the estimated environmental concentration of Carbo-Iron in the area close to the injection points (zone Ia: 650 mg/L, see Table 1), exceeds the PNEC by a factor of 6500. The risk quotients decrease with increasing distance to the injection point to 4750 (zone Ib), 13 (zone Ic, sampling well GWM1) and 5 (zone I, sampling well RKS13, approx. 10 m from injection points). The estimated migration of Carbo-Iron through the aquifer is supported by the detection of Carbo-Iron particles in samples from GWM1 on days 30, 57, 92 and 139 after injection, and in samples from CMT2 on day 139 after injection (Fig. S1). The detection method used for this analysis is described in SI section 2.2 and was developed recently. However, the quantification of Carbo-Iron with this method is currently not possible. A further indication of the transport of Carbo-Iron is provided by the observed change in redox potential (Table S16), and Carbo-Iron can be assumed to

considerably influence the aquifer for approx. 200 d after the first injection. Based on the estimated transport data for Carbo-Iron from the column studies (SI section 2.1), a distribution of Carbo-Iron beyond zone I is unlikely. Hence, the risk quotients in zones II, III and IV can be assumed to be below 1 indicating no risk due to Carbo-Iron application.

3.3 Site-specific risk-benefit analysis

The pilot study site was highly polluted with chlorohydrocarbons (Table S11) and the potential benefit or a possible risk/risk trade-off of the Carbo-Iron treatment was assessed. For this assessment, available ecotoxicity data for the most relevant hydrocarbons polluting the pilot study site were evaluated to derive PNEC values (Table S13) and used in a Triad-based environmental risk assessment. Due to the lack of target values, Carbo-Iron was not included in the calculation of the cRI. However, it was included as a pollutant, equal to the chlorohydrocarbons, for the calculations of the eRI. The calculations of the risk indices were performed with exposure data collected during the 1st application of Carbo-Iron (Mackenzie et al., 2016, see sections 2.2 and 2.3).

In Figure 5, the results of the site-specific environmental risk assessment are shown for the contamination zones I to IV as defined in Figure 1 and Table 1. The physico-chemical risk (Tables S19 and S20) was relatively stable in all contamination zones during the 190 d after Carbo-Iron injection. Increased risk indices due to a reduced redox potential are visible in zone II (CMT2) on d 190 and zone III (RKS24) on d 31 and d 58. The slightly increased physico-chemical risk in zone II (well CMT1) on d 93 was caused by an increased conductivity and a lower pH than on the sampling days before (Table S19). These observations of increased physico-chemical risk indices are very likely related to the application of Carbo-Iron into the aquifer. The effect on redox potential can be assumed to be temporary, caused by the reaction of Carbo-Iron with the pollutants and the oxygen in the groundwater, i.e. ceasing with loss of reactivity of Carbo-Iron. Yet, with the available data it is not possible to verify these assumptions. The desired remedial effect of Carbo-Iron is discernible in the decreasing chemical and ecotoxicological risk indices in all groundwater samples investigated (Figure 5 and Tables S9 and S12) during the first 58 d after Carbo-Iron injection. This effect is most pronounced in samples from the contamination zones Ic and I (wells GWM1 and RKS13). Obviously, the amount of Carbo-Iron applied into the aquifer during the first injection campaign was not sufficient to completely remediate the contamination with chlorohydrocarbons, which was not the intention of the study by Mackenzie et al. (2016). The chemical (Table S11 and S12) and ecotoxicological (Tables S14 and S15) risks increase again after 58 d (Figure 5), possibly due to inflow of chlorohydrocarbon-contaminated groundwater from the non-treated area upstream of the injection wells and depletion of reactive Carbo-Iron. However, on d 190 in zones Ic (GWM1), I

(RKS13) and III (RKS24), a strong decline of the chemical and ecotoxicological risk occurred compared to d 93. This was mainly caused by a drop of measured concentrations of PCE and trichloroethene (Table S11), maybe as a result of precipitation event. In most zones investigated, the eRI and cRI reached similar but lower values on d 190 than before application of Carbo-Iron. The calculated environmental risk (Table 2) integrates all three risk indices and its highest value is usually observed on d 0 during the 190 d of monitoring. Yet, in zone II (CMT2), the eRI increased on d 93 and d 190 above any previous values and the environmental risk is higher than before the application of Carbo-Iron. On these days, concentrations of ethane, ethene and 1,1-dichloroethene and 1,2-dichloroethene reached their maximum value, after steadily increasing from 0 mg/L on d 0 (Table S11). Similar increasing concentrations are observable for all zones investigated. The measured concentrations exceed the relatively low PNEC values of 1,1-dichloroethene and 1,2-dichloroethene and this represents the main reason for the increased eRI in zone II. The presence of these transformation products and simultaneous absence of vinyl chloride corresponds to the spectrum of PCE degradation by Carbo-Iron and thus indicates proper functioning of the remediation (Mackenzie et al., 2012). Yet, the increased risk is not desirable. In the present study, effects of Carbo-Iron on the pollutants beyond d 190 were not considered and the fate of the transformation products was not examined. However, Vogel et al. (2018) observed in a field study that 600 days after treatment with Carbo-Iron microorganisms in the groundwater grow on the AC component of Carbo-Iron and biogenic dehalogenation of halogenated alkenes occurs. Thus, in the long term, further decreasing values for the eRI and cRI are expected when an exhaustive remediation with Carbo-Iron is envisaged.

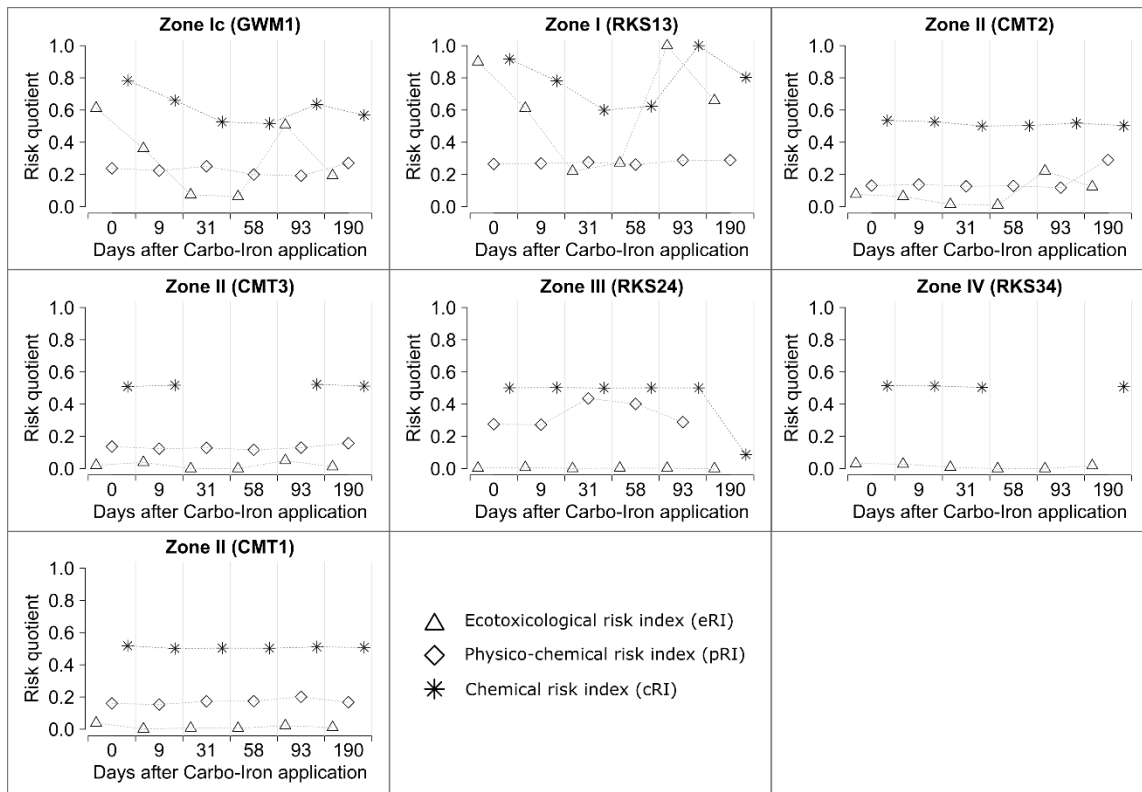


Figure 5: Comparison of the calculated risk indices for groundwater contaminated with chlorohydrocarbons during the first 190 d after treatment with Carbo-Iron using a TRIAD-based approach. No data points available for days with no measurement data.

Table 2: Environmental risk for groundwater contaminated with chlorohydrocarbons integrating the risk indices for the chemical, ecotoxicological and physico-chemical component.

Contamination zone (Sampling well)	Days after Carbo-Iron injection					
	0	9	31	58	93	190
Zone Ic (GWM1)	0.545	0.4152	0.2846	0.260	0.445	0.344
Zone I (RKS13)	0.694	0.554	0.365	0.386	0.763	0.583
Zone II (CMT2)	0.248	0.243	0.214	0.214	0.287	0.306
Zone II (CMT3)	0.222	0.223	- ^A	- ^A	0.234	0.227
Zone III (RKS24)	0.2606	0.260	0.312	0.302	0.264	NA
Zone IV (RKS34)	- ^B	- ^B	- ^B	- ^B	- ^B	- ^B
Zone II (CMT1)	0.239	0.219	0.228	0.227	0.245	0.229

^A: No data for the determination of the cRI available, the environmental risk could not be calculated;

^B: No data for the determination of the pRI available, the environmental risk could not be calculated.

4. Conclusion

With the crustacea *D. magna* a NOEC of 1 mg/L was determined, a similar range as the NOEC of 6.3 mg/L determined in a study with the crustacean *Hyalella azteca*, likely associated to reduced nutrient uptake and negative effects on the energy budget. The effect of Carbo-Iron on the algae *S. vacuolatus* however is probably caused by shading of the algae by the particles, reducing light intensity required for photosynthesis.

Estimated concentrations of Carbo-Iron were exceeding the PNEC in the areas close to the injection, but decreasing rapidly with increasing distance to injection wells. Carbo-Iron successfully reduced the concentrations of the investigated pollutants while the presence of Carbo-Iron and the increasing concentrations of the transformation products were usually not leading to environmental risks exceeding the levels before the remediation was initiated. However, in the single occurrence of increased risk, increasing concentrations of the transformation product dichloroethene was identified as the responsible compound. Pre-existing natural attenuation is not negatively affected by the presence of Carbo-Iron in the groundwater and very likely reduces the concentrations of the transformation products in the time period exceeding the monitored time in the present study. With the data analysed in the present study, the benefit of applying Carbo-Iron into the groundwater outweighs the potential negative effects on the environment and a risk/risk-trade-off is considered as very unlikely.

In case of remediation of contaminated groundwater, the best available option has to be chosen. The procedure described for environmental risk assessment in the present manuscript is not limited to Carbo-Iron; it is suitable to support decisions on other remediation methods as well. With sufficient data, the Triad-based approach presented in the current study can be used to compare the potential environmental risks of other remedial agents, whether they are based on nano zero-valent iron or on other *in situ* treatment methods.

Acknowledgements

The authors wish to thank Dr. Johannes Bruns and Golder Associates for permission to use the raw data obtained during the field experiment with Carbo-Iron and Oliver Frank and Frederique Sans Piche for generating the data on *Scenedesmus vacuolatus*. Further, we thank Dr. Tobias Meißner and Diana Meinel for the measurement of Carbo-Iron concentrations in the tests with *D. magna*. Parts of the present work were funded by the German Ministry of Education and Research (project numbers 03X0082 A and F). The sole responsibility for the content of this publication lies with the authors.

References

- Batka, V.M., Hofmann, T., 2016. Stability, mobility, delivery and fate of optimized nps under field relevant conditions. Deliverable 4.2 of Project Nr.: 309517 EU, 7th FP, NMP.2012.1.2 „Taking nanotechnological remediation processes from lab scale to end user applications for the restoration of a clean environment“.
- Bleyl, S., Kopinke, F.-D., Mackenzie, K., 2012. Carbo-Iron®—Synthesis and stabilization of Fe(0)-doped colloidal activated carbon for in situ groundwater treatment. *Chemical Engineering Journal* 191, 588–595. DOI: 10.1016/j.cej.2012.03.021
- Bundschuh, M., Zubrod, J.P., Seitz, F., Stang, C., Schulz, R., 2011. Ecotoxicological evaluation of three tertiary wastewater treatment techniques via meta-analysis and feeding bioassays using *Gammarus fossarum*. *Journal of Hazardous Materials* 192, 772–778. DOI: 10.1016/j.jhazmat.2011.05.079
- Ceccaldi, H., 1989. Anatomy and physiology of digestive tract of crustaceans decapods reared in aquaculture. Presented at the Advances in Tropical Aquaculture, Workshop at Tahiti, French Polynesia, 20 Feb - 4 Mar 1989.
- Chapman, P.M., 1990. The sediment quality triad approach to determining pollution-induced degradation. *Science of the Total Environment* 97, 815–825. DOI: 10.1016/0048-9697(90)90277-2
- Coll, C., Notter, D., Gottschalk, F., Sun, T., Som, C., Nowack, B., 2016. Probabilistic environmental risk assessment of five nanomaterials (nano-TiO₂, nano-Ag, nano-ZnO, CNT, and fullerenes). *Nanotoxicology* 10, 436–444. DOI: 10.3109/17435390.2015.1073812
- Crévecoeur, S., Debacker, V., Joaquim-Justo, C., Gobert, S., Scippo, M.-L., Dejonghe, W., Martin, P., Thomé, J.-P., 2011. Groundwater quality assessment of one former industrial site in Belgium using a TRIAD-like approach. *Environmental Pollution* 159, 2461–2466. DOI: 10.1016/j.envpol.2011.06.026
- Critto, A., Torresan, S., Semenzin, E., Giove, S., Mesman, M., Schouten, A.J., Rutgers, M., Marcomini, A., 2007. Development of a site-specific ecological risk assessment for contaminated sites: Part I. A multi-criteria based system for the selection of ecotoxicological tests and ecological observations. *Science of the Total Environment* 379, 16–33. DOI: 10.1016/j.scitotenv.2007.02.035
- Crommentuijn, T., Sijm, D., de Bruijn, J., van Leeuwen, K., van de Plassche, E., 2000. Maximum permissible and negligible concentrations for some organic substances and pesticides. *Journal of Environmental Management* 58, 297–312. DOI: 10.1006/jema.2000.0334
- Dagnino, A., Sforzini, S., Dondero, F., Fenoglio, S., Bona, E., Jensen, J., Viarengo, A., 2008. A weight-of-evidence approach for the integration of environmental “triad” data to assess ecological risk and biological vulnerability. *Integrated Environmental Assessment and Management* 4, 314–326. DOI: 10.1897/IEAM_2007-067.1
- Danielopol, D.L., 1989. Groundwater Fauna Associated with Riverine Aquifers. *J. North Am. Benthol. Soc.* 8, 18–35.
- Danielopol, D.L., Griebler, C., 2008. Changing Paradigms in Groundwater Ecology—from the ‘Living Fossils’ Tradition to the “New Groundwater Ecology.” *International Review of Hydrobiology* 93, 565–577.
-

-
- Dimitrov, S.D., Diderich, R., Sobanski, T., Pavlov, T.S., Chankov, G.V., Chapkanov, A.S., Karakolev, Y.H., Temelkov, S.G., Vasilev, R.A., Gerova, K.D., Kuseva, C.D., Todorova, N.D., Mehmed, A.M., Rasenberg, M., Mekenyan, O.G., 2016. QSAR Toolbox – workflow and major functionalities. *SAR and QSAR in Environmental Research* 27, 203–219. DOI: 10.1080/1062936X.2015.1136680
- ECHA, 2017. Guidance on information requirements and chemical safety assessment. Chapter R.7.b: Endpoint specific guidance. European Chemicals Agency.
- ECHA, 2016. Guidance on information requirements and chemical safety assessment - Part E: Risk Characterisation.
- ECHA, 2008. Guidance on information requirements and chemical safety assessment - Chapter R.10: Characterisation of dose [concentration]-response for environment.
- European Communities, 1998. Council Directive 98/83/EC on the quality of water intended for human consumption.
- Faust, M., Altenburger, R., Bodeker, W., Grimme, L.H., 1992. Algentoxizitätstests mit synchronisierten Kulturen., in: Steinhauser, K.G., Hansen, P.D. (Eds.), *Bioassays with unicellular algae*, Biologische Testverfahren. Fischer, Stuttgart/New York, pp. 311–321.
- Fu, F., Dionysiou, D.D., Liu, H., 2014. The use of zero-valent iron for groundwater remediation and wastewater treatment: A review. *Journal of Hazardous Materials* 267, 194–205. DOI: 10.1016/j.jhazmat.2013.12.062
- Georgi, A., Schierz, A., Mackenzie, K., Kopinke, F.-D., 2015. Colloidal activated carbon for in-situ groundwater remediation — Transport characteristics and adsorption of organic compounds in water-saturated sediment columns. *Journal of Contaminant Hydrology* 179, 76–88. DOI: 10.1016/j.jconhyd.2015.05.002
- Gibert, J., Danielopol, D., Stanford, J.A., 1994. Groundwater ecology. Academic Press.
- Grenthe, I., Stumm, W., Laaksoharju, M., Nilsson, A.C., Wikberg, P., 1992. Redox potentials and redox reactions in deep groundwater systems. *Chemical Geology* 98, 131–150. DOI: 10.1016/0009-2541(92)90095-M
- Grieger, K.D., Fjordbøge, A., Hartmann, N.B., Eriksson, E., Bjerg, P.L., Baun, A., 2010. Environmental benefits and risks of zero-valent iron nanoparticles (nZVI) for in situ remediation: Risk mitigation or trade-off? *Journal of Contaminant Hydrology* 118, 165–183. DOI: 10.1016/j.jconhyd.2010.07.011
- Hahn, H.J., 2009. A proposal for an extended typology of groundwater habitats. *Hydrogeology Journal* 17, 77–81. DOI: 10.1007/s10040-008-0363-5
- Hahn, H.J., 2006. The GW-Fauna-Index: A first approach to a quantitative ecological assessment of groundwater habitats. *Limnologica* 36, 119–137. DOI: 10.1016/j.limno.2006.02.001
- Hjorth, R., Coutris, C., Nguyen, N.H.A., Sevcu, A., Gallego-Urrea, J.A., Baun, A., Joner, E.J., 2017. Ecotoxicity testing and environmental risk assessment of iron nanomaterials for sub-surface remediation – Recommendations from the FP7 project NanoRem. *Chemosphere* 182, 525–531. DOI: 10.1016/j.chemosphere.2017.05.060
-

- Husson, O., 2013. Redox potential (Eh) and pH as drivers of soil/plant/microorganism systems: a transdisciplinary overview pointing to integrative opportunities for agronomy. *Plant and Soil* 362, 389–417. DOI: 10.1007/s11104-012-1429-7
- Jensen, J., Pedersen, M.B., 2006. Ecological risk assessment of contaminated soil. *Reviews of Environmental Contamination and Toxicology* 186, 73–105.
- Khadam, I.M., Kaluarachchi, J.J., 2003. Multi-criteria decision analysis with probabilistic risk assessment for the management of contaminated ground water. *Environmental Impact Assessment Review* 23, 683–721. DOI: 10.1016/S0195-9255(03)00117-3
- Kuppusamy, S., Palanisami, T., Megharaj, M., Venkateswarlu, K., Naidu, R., 2016. In-situ remediation approaches for the management of contaminated sites: a comprehensive overview, in: Voogt, P. de (Ed.), *Reviews of Environmental Contamination and Toxicology*. 236, pp. 1–115. DOI: 10.1007/978-3-319-20013-2_1
- Lacey, R., Watzin, M.C., McIntosh, A.W., 2009. Sediment organic matter content as a confounding factor in toxicity tests with *Chironomus tentans*. *Environmental Toxicology and Chemistry* 18, 231–236. DOI: 10.1002/etc.5620180219
- Lemming, G., Hauschild, M.Z., Bjerg, P.L., 2010. Life cycle assessment of soil and groundwater remediation technologies: literature review. *The International Journal of Life Cycle Assessment* 15, 115. DOI: 10.1007/s11367-009-0129-x
- Li, J., He, L., Lu, H., Fan, X., 2014. Stochastic goal programming based groundwater remediation management under human-health-risk uncertainty. *Journal of Hazardous Materials* 279, 257–267. DOI: 10.1016/j.jhazmat.2014.06.082
- Long, E.R., Chapman, P.M., 1985. A Sediment Quality Triad: Measures of sediment contamination, toxicity and infaunal community composition in Puget Sound. *Marine Pollution Bulletin* 16, 405–415. DOI: 10.1016/0025-326X(85)90290-5
- Mackenzie, K., Bleyl, S., Kopinke, F.-D., Doose, H., Bruns, J., 2016. Carbo-Iron as improvement of the nanoiron technology: From laboratory design to the field test. *Science of the Total Environment* DOI: 10.1016/j.scitotenv.2015.07.107
- Mackenzie, K., Bleyl, S., Schierz, A., Georgi, A., 2012. In-situ generation of sorption and reaction barriers using colloidal sorbents and sorbent-carried nano-iron, in: Dey, T. (Ed.), *Nanotechnology for Water Purification*. Brown Walker Press, pp. 71–88.
- Nguyen, N.H.A., Von Moos, N.R., Slaveykova, V.I., Mackenzie, K., Meckenstock, R.U., Thümmler, S., Bosch, J., Ševců, A., 2018. Biological effects of four iron-containing nanoremediation materials on the green alga *Chlamydomonas* sp. *Ecotoxicology and Environmental Safety* 154, 36–44. DOI: 10.1016/j.ecoenv.2018.02.027
- OECD, 2008. OECD guideline for testing of chemicals. 211. *Daphnia magna* reproduction test. Organisation for Economic Co-operation and Development, Paris, France.
-

-
- OECD, 2006. OECD series on testing and assessment. Number 54. Current approaches in the statistical analysis of ecotoxicity data: A guidance to application. (No. ENV/JM/MONO(2006)18). Organisation for Economic Co-operation and Development, Paris, France.
- OECD, 2004a. OECD guideline for testing of chemicals. 202. *Daphnia* sp., acute immobilisation test. Organisation for Economic Co-operation and Development, Paris, France.
- OECD, 2004b. OECD guideline for testing of chemicals. 219. Sediment-water chironomid toxicity test using spiked water. Organisation for Economic Co-operation and Development, Paris, France.
- Pepper, I.L., Gentry, T.J., 2015. Chapter 4 - Earth Environments, in: Pepper, I.L., Gerba, C.P., Gentry, T.J. (Eds.), *Environmental Microbiology* (Third Edition). Academic Press, San Diego, pp. 59–88. DOI: 10.1016/B978-0-12-394626-3.00004-1
- R Development Core Team, 2011. R: A language and environment for statistical computing. Vienna, Austria.
- Ren, L., He, L., Lu, H., Li, J., 2017. Rough-interval-based multicriteria decision analysis for remediation of 1,1-dichloroethane contaminated groundwater. *Chemosphere* 168, 244–253. DOI: 10.1016/j.chemosphere.2016.10.042
- Ritz, C., Streibig, J.C., 2005. Bioassay analysis using R. *Journal of Statistical Software* 12. DOI: 10.18637/jss.v012.i05
- Schwab, F., Bucheli, T.D., Lukhele, L.P., Magrez, A., Nowack, B., Sigg, L., Knauer, K., 2011. Are carbon nanotube effects on green algae caused by shading and agglomeration? *Environmental Science & Technology* 45, 6136–6144. DOI: 10.1021/es200506b
- Søndergaard, M., 2009. Redox Potential, in: Likens, G.E. (Ed.), *Encyclopedia of Inland Waters*. Academic Press, Oxford, pp. 852–859. DOI: 10.1016/B978-012370626-3.00115-0
- Stein, H., Kellermann, C., Schmidt, S.I., Brielmann, H., Steube, C., Berkhoff, S.E., Fuchs, A., Hahn, H.J., Thulin, B., Griebler, C., 2010. The potential use of fauna and bacteria as ecological indicators for the assessment of groundwater quality. *Journal of Environmental Monitoring* 12, 242–254. DOI: 10.1039/B913484K
- Steube, C., Richter, S., Griebler, C., 2009. First attempts towards an integrative concept for the ecological assessment of groundwater ecosystems. *Hydrogeology Journal* 17, 23–35. DOI: 10.1007/s10040-008-0346-6
- Swartjes, F.A., 1999. Risk-based assessment of soil and groundwater quality in the netherlands: standards and remediation urgency. *Risk Analysis* 19, 1235–1249. DOI: 10.1023/A:1007003332488
- Swartjes, Frank A. (Ed.), 2011. Dealing with contaminated sites - from theory towards practical application. Springer, Dordrecht, Heidelberg, London, New York.
- Tartakovsky, D.M., 2013. Assessment and management of risk in subsurface hydrology: A review and perspective. *Advances in Water Resources*, 35th Year Anniversary Issue 51, 247–260. DOI: 10.1016/j.advwatres.2012.04.007
- USEPA. 1999. National Recommended Water Quality Criteria. Office of Water. EPA 822-Z-99-001. April 1999.
-

- Vogel, M., Nijenhuis, I., Lloyd, J., Boothman, C., Pöritz, M., Mackenzie, K., 2018. Combined chemical and microbiological degradation of tetrachloroethene during the application of Carbo-Iron at a contaminated field site. *Science of the Total Environment* 628–629, 1027–1036. DOI: 10.1016/j.scitotenv.2018.01.310
- Wang, Z., He, L., Lu, H., Ren, L., Xu, Z., 2016. Network environmental analysis based ecological risk assessment of a naphthalene-contaminated groundwater ecosystem under varying remedial schemes. *Journal of Hydrology* 543, Part B, 612–624. DOI: 10.1016/j.jhydrol.2016.10.034
- Weeks, J.M., Comber, S.D.W., 2005. Ecological risk assessment of contaminated soil. *Mineral. Mag.* 69, 601–613. DOI: 10.1180/0026461056950274
- Weil, M., Meißner, T., Busch, W., Springer, A., Kühnel, D., Schulz, R., Duis, K., 2015. The oxidized state of the nanocomposite Carbo-Iron® causes no adverse effects on growth, survival and differential gene expression in zebrafish. *Science of the Total Environment* 530–531, 198–208. DOI: 10.1016/j.scitotenv.2015.05.087
- Weil, M., Meißner, T., Springer, A., Bundschuh, M., Hübler, L., Schulz, R., Duis, K., 2016. Oxidized Carbo-Iron causes reduced reproduction and lower tolerance of juveniles in the amphipod *Hyalella azteca*. *Aquatic Toxicology* 181, 94–103. DOI: 10.1016/j.aquatox.2016.10.028
- Williams, R.J.P., Fraústo da Silva, J.J.R., 2006. Chapter 2 - Basic Chemistry of the Ecosystem, in: Williams, R.J.P., Fraústo da Silva, J.J.R. (Eds.), *The Chemistry of Evolution*. Elsevier Science Ltd, Amsterdam, pp. 35–76. DOI: 10.1016/B978-044452115-6/50045-2
- Yang, A.L., Huang, G.H., Qin, X.S., Fan, Y.R., 2012. Evaluation of remedial options for a benzene-contaminated site through a simulation-based fuzzy-MCDA approach. *Journal of Hazardous Materials* 213–214, 421–433. DOI: 10.1016/j.jhazmat.2012.02.027

Appendix D.2

Supplemental information to:

Environmental risk or benefit? Comprehensive risk assessment of groundwater treated with nano Fe₀-based Carbo-Iron®

Mirco Weil^a, Katrin Mackenzie^b, Kaarina Foit^c, Dana Kühnel^d, Wibke Busch^d, Mirco Bundschuh^{e, f},
Ralf Schulz^f, Karen Duis^a

^a ECT Oekotoxikologie GmbH, Böttgerstrasse 2-14, 65439 Flörsheim, Germany
m.weil@ect.de; k-duis@ect.de

^b Helmholtz Centre for Environmental Research – UFZ, Department of Environmental Engineering,
Permoser Strasse 15, 04318 Leipzig, Germany
katrin.mackenzie@ufz.de

^c Helmholtz Centre for Environmental Research – UFZ, Department of System Ecotoxicology,
Permoser Strasse 15, 04318 Leipzig, Germany
kaarina.foit@ufz.de

^d Helmholtz Centre for Environmental Research – UFZ, Department of Bioanalytical Ecotoxicology,
Permoser Strasse 15, 04318 Leipzig, Germany
dana.kuehnel@ufz.de

^e Department of Aquatic Sciences and Assessment, Swedish University of Agricultural Sciences,
Uppsala, Sweden

^f Institute for Environmental Sciences, University of Koblenz-Landau, Forststrasse 7, 76829
Landau, Germany
bundschuh@uni-landau.de
schulz@uni-landau.de

Corresponding author: Mirco Weil, ECT Oekotoxikologie GmbH, Böttgerstrasse 2-14, 65439
Flörsheim, Germany, m.weil@ect.de, +49 6145 956411

1. Material and Methods

1.1 Effects assessment

1.1.1 Preparation of Carbo-Iron suspensions

The toxicity tests were performed with aged Carbo-Iron, which means that the originally zero-valent iron was oxidized to Fe^{2+} and, mainly, Fe^{3+} . Aged Carbo-Iron was provided by the producers Mackenzie and colleagues (for further details on composition and other particle characteristics see Bleyl et al., 2012; Mackenzie et al., 2012 and 2016); its iron content was approx. 22% (w/w).

Stock suspensions were prepared as described by Weil et al. (2015). As stabilizing additive, 2 g carboxymethyl cellulose (CMC; Antisol® FL 30, Sigma-Aldrich, Germany) were added to 1 L of 0.1 mM NaOH. The CMC solution was stirred overnight at room temperature, subsequently filtered through a 0.4 μm filter (MN GF-5, Macherey-Nagel, Germany) and stored for a maximum of 7 d at 4°C. Before use, it was diluted with deionized water to 200 mg CMC/L. Carbo-Iron stock suspensions (1 g/L) with 200 mg/L CMC (i.e. 20% w/w relative to Carbo-Iron) were prepared by adding 100 mg Carbo-Iron to 100 mL CMC solution. The suspensions were placed on ice and treated with an ultrasonic probe (Hielscher UP200S, Germany, 14 mm probe diameter) at approx. 80 W for 7 min. If volumes > 100 mL were needed, this procedure was repeated and the obtained suspensions were pooled until sufficient volume was prepared. Carbo-Iron stock suspensions were used within 2 h after preparation.

The suspension stability is a crucial requirement for the particle injection in porous matrices to prevent agglomeration, because it limits particle transport in water-saturated sediments and can lead to pore clogging. Therefore, static sedimentation experiments were performed in the filed study (Mackenzie et al. 2016) with freshly dispersed suspensions in closed vessels under inert atmosphere; an aliquot of the particle suspension was sampled at a pre-defined height (1 or 4 cm below the water table) and analysed for the particle concentration (Batka and Hofmann, 2016). A small fraction (< 10 wt-%) precipitated quickly within the first 30 min. The remaining suspension showed a high stability over several hours. Estimates using Stokes law and assuming a mean density of water-filled composite particles of $\delta \approx 2 \text{ g/cm}^3$ means that Carbo-Iron is present under the chosen conditions predominantly as non-agglomerated individual particles.

1.1.2 Toxicity tests with *Daphnia magna*

Tests were performed with *D. magna*, clone B (obtained from Bayer CropScience, Monheim, Germany). Culture and test medium Elendt M7 was prepared according to OECD (2004). *D. magna*

were cultured in 2 L glass beakers containing 20 daphnids in 1.8 L M7. The medium was renewed twice weekly, offspring was discarded daily. After three weeks in culture, daphnids were discarded and replaced with neonates. Daphnids were fed daily with a suspension of batch-cultured green algae (*Desmodesmus subspicatus*, 4.0×10^5 cells/mL, 1.67 mg C/L). The culture and the tests were performed at a temperature of $20 \pm 0.5^\circ\text{C}$ and a photoperiod of 16:8 h (light:dark).

1.1.3 Acute toxicity test

The 48 h acute toxicity test with *D. magna* was conducted according to OECD (2004). For each concentration level and the control, 4 replicates with 5 daphnids each were used in a static test. The following concentrations of aged Carbo-Iron were tested: 0.56, 1, 1.8, 3.2, 5.6, 10, 32, 56 and 100 mg/L. The test containers were 100-mL glass beakers filled with 40 mL of the test suspension. During exposure, daphnids were not fed. Immobility was evaluated after 48 h. As an extension of the standard acute toxicity test, 48-h-exposed daphnids were transferred into M7 medium and the immobility was observed over a post-exposure time of 5 days.

1.1.4 Reproduction test

The *D. magna* reproduction test was conducted according to OECD test guideline 211 (OECD, 2008). The semi-static test was started with 10 replicates of one neonate aged less than 24 h. Test organisms were exposed for 21 days to the following concentrations of Carbo-Iron: control, 0.32, 1, 3.2 and 10 mg/L. The test containers were 100-mL glass beakers filled with 50 mL of test solution. Daphnids were fed three times per week with a suspension of batch-cultured green algae (*D. subspicatus*, 9.6×10^5 cells/mL corresponding to 4.0 mg C/L). Three times weekly, survival and offspring production were assessed and test solutions were renewed.

1.1.5 Algae growth inhibition test

Cultures of the unicellular freshwater chlorophyte *Scenedesmus vacuolatus* (strain 211-15) were grown photoautotrophically at $28 \pm 0.5^\circ\text{C}$ in a sterile inorganic medium (pH 6.4) according to Grimme and Boardmann (1972). A 14:10-h light:dark synchronizing growth regime was applied and monitored daily as described in Altenburger et al. (1990). Aeration of the cultures ensured input of carbon dioxide and constant mixing.

The concentration-dependent changes of algae cell volume were assessed after 16 h of exposure to Carbo-Iron as well as after exposure to AC at test concentrations of 0, 15, 20, 25, 45 and 65 mg/L. Culture volumes were 8 mL, to 7.2 mL of the respective Carbo-Iron concentration 0.8 mL of algae suspension (cell density 7-9.5 in 10-fold concentrated GB medium) were added. Sterilized, water-saturated air, enriched with CO₂ (1.5-2.0%, v/v) was used to aerate the cultures, keeping the cells in suspension. The cultures were illuminated by a combination of two types of white fluorescent

tubes (Osram L36W/41 Interna, Osram L36W/II Daylight, Osram, Berlin) with an intensity of 13-18 W/m² (22-33 klux) and a photon flux density of about 400 μmol photons*m⁻²*s⁻¹ at the surface of the tubes. The standard cell density was 1 * 10⁶/mL. For each tube, the initial light intensity within the algal suspension was monitored using a quantum sensor (Li-Cor, USA, LI-189 light meter). Measurements were taken in the center of each tube, 2 cm below the surface of the suspension. Cell volume was measured using a Multisizer 3 Coulter Counter (Beckman Coulter GmbH). Cell volume inhibition was calculated using equation S1, with CellVol_{exp} the cell volume measured after exposure to a given concentration and \bar{x} (CellVol_{ctrl}) the average cell volume measured in the controls.

$$\text{Inhibition}_{\text{cell volume}} (\%) = 100 - \frac{100 * \text{cell volume}_{\text{treatment}}}{\bar{x} (\text{cell volume}_{\text{control}})} \quad (\text{Eq. S1})$$

In the test with tetrachloroethene, the endpoint cell number was investigated. For this endpoint, the number of cells was counted after 24 h of exposure in a cell counter Multisizer 3 Coulter Counter (Beckman Coulter GmbH). One ml of algae suspension was diluted in 10 ml of Isoton II solution before the measurement. By using the cell number/mL growth inhibition was calculated using equation S2 and S3.

$$\text{Increase}_{\text{cell number}} = \frac{\text{cell number}_{t24} - \text{cell number}_{t0}}{\text{cell number}_{t0}} \quad (\text{Eq. S2})$$

$$\% \text{ Inhibition} = \frac{\text{increase}_{\text{cell number control}} - \text{increase}_{\text{cell number sample}}}{\text{increase}_{\text{cell number control}}} * 100 \quad (\text{Eq. S3})$$

1.1.6 Sediment-water test with *Chironomus riparius*

C. riparius were cultured in glass dishes with approx. 1 L of M4 and quartz sand as substrate (3 cm height) at 20 ± 2°C with a 12:12 h photoperiod. Two days before start of the exposure, < 24 h old eggs were removed from the culture, and kept in fresh M4 supplemented with green algae at 20 ± 2°C with slight aeration.

The sediment-water toxicity test was performed according to OECD (2004). Test medium M4 was prepared as described by (Elendt and Bias, 1990)). Artificial sediment according to OECD (2004) with 75% quartz sand (Quarzwerte Frechen, Germany), 20% kaolin (Chinafill 100, Ziegler, Germany) and 5% peat (Thomafloer, Germany) was prepared approx. one week before use, and preconditioned at 23 ± 2°C with aeration. Two days prior to the start of the exposure, glass beakers with screw caps and a total volume of 500 mL were filled with 80 ± 1 g (w.w.) of artificial sediment. Subsequently,

180 mL of M4 were added to each vessel. Test vessels were then incubated at $20 \pm 2^\circ\text{C}$ with slight aeration until test start. Immediately before introduction of *C. riparius* larvae, Carbo-Iron stock suspension (1 g/L of Carbo-Iron and 200 mg/L of CMC) and CMC solution (200 mg/L) were mixed in the necessary ratios to achieve 10-fold nominal test concentrations in a final volume of 20 mL. These mixtures were then added to the respective test vessels to prepare Carbo-Iron concentrations of 1.0, 3.2, 10.0, 31.6 and 100 mg/L in the water-phase of the water-sediment systems. In all Carbo-Iron test suspensions, the final CMC concentration was 20 mg/L. A control (M4) and a dispersant control (20 mg/L CMC in M4) were included in the test. For each Carbo-Iron concentration and control, eight biological and two technical replicates were prepared for assessment of (a) the biological endpoints and (b) measurement of the physico-chemical parameters (oxygen, temperature, pH, ammonia) and particle size, respectively.

Test vessels were incubated for 28 d at $20 \pm 2^\circ\text{C}$ with slight aeration and a photoperiod of 16 h light and 8 h dark. Food (ground TetraMin flakes in suspension, 50 g/L) was added three times per week; the amount was adapted to the development of the larvae and the number of remaining larvae in each test vessel (2004b). Hatched imagos were collected and counted daily, and sex was determined based on the presence of bushy antenna. The mean development rate \bar{x} was calculated by the formula (Eq. S4) provided in the OECD guideline (OECD, 2004b)

$$\bar{x} = \sum_{i=1}^m \frac{f_i x_i}{n_e} \quad (\text{Eq. S4})$$

with:

- i: index of inspection interval;
- m: maximum number of inspection intervals;
- f_i : number of midges emerged in the inspection interval i;
- n_e : total number of midges emerged at the end of the experiment;
- x_i : development rate of midges emerged in interval i (Eq.S5)

$$x_i = \frac{1}{\left(\text{day}_i - \frac{l_i}{2}\right)} \quad (\text{Eq. S5})$$

with:

day_i: day of inspection interval i;

l_i: length of inspection interval i.

1.1.7 Nitrogen-transformation test

The nitrogen-transformation test is a sensitive indicator for effects on soil-inhabiting microorganisms and thus relevant for the environmental exposure occurring after application of Carbo-Iron into groundwater. The test was performed according to OECD (2000). In the transformation test with soil microorganisms, sieved, fresh soil (LUFA type 2.3, *Landwirtschaftliche Untersuchungs- und Forschungsanstalt*, Speyer, Germany) was used. Water content of the soil was $8.2 \pm 0.1\%$ relative to the dry weight (dw) and water capacity was 25 g water/100 g soil dry weight (dw). Before use in the test, ground dried lucerne (*Medicago sativa*, *Raiffeisen Waren-Zentrale Rhein-Main eG*, *Kraftfutterwerk Schierstein*, Wiesbaden, Germany) was added (5 g/kg soil dw). Due to bacterial activity in the soil, nitrogen-containing structures such as the nitrogen-rich alfalfa powder are usually metabolized to nitrate.

The soil for the test concentrations was spiked either by application of Carbo-Iron suspended in CMC solution (concentration range: 500 - 2500 mg Carbo-Iron/kg soil dw) or by mixing the Carbo-Iron powder into the soil (707 - 2828 mg Carbo-Iron/kg soil dw). This way, a potential influence of the distribution of Carbo-Iron in the soil depending on the spiking method or an influence of the ultrasonic treatment on Carbo-Iron prior to the application via suspensions and should be investigated. CMC concentration in the treatments spiked with suspensions and in the CMC control was 17.1 mg CMC/kg soil dw. Soil without addition of Carbo-Iron was used as control, and soil with addition of CMC solution as additional control for application of Carbo-Iron in suspensions. Final humidity in all test soils was adjusted with deionized water to 45% of the maximum water holding capacity. Each treatment was tested with four replicates.

For each treatments and control, 4 replicates were used. The 28 d-exposure was performed at $20 \pm 2^\circ\text{C}$ in the dark. During the exposure, all test vessels were weighed weekly and any weight loss due to evaporation of water was compensated by addition of deionized water. Soil samples (20 g dw) were removed from each test vessel at test start (day 0) and on days 7 and 28. Nitrate was

extracted by mixing the samples with 100 mL of 0.01 M CaCl₂ and incubating at room temperature on a shaker with 150 rpm for 60 min. Immediately after incubation, samples were poured over a cellulose filter (Schleicher & Schüll 595 ½, VWR International GmbH, Darmstadt, Germany) and nitrate concentrations were quantified photometrically (LCK 339, Hach Lange GmbH, Berlin, Germany).

2. Results

2.1 Column experiments and estimation of $L_{T,50}$, $L_{T,63.5}$ and $L_{T,99.9}$

The standard sediment used in the column tests was quartz sand Dorsilit 8 (fraction 0.3–0.8 mm, Gebr. Dorfner GmbH Co, Hirschau, Germany). Additionally, sediment from the site (reference well outside the contaminated area) was taken by direct push from 6 to 7 m below ground, dried and sieved. $L_{T,50}$, $L_{T,63.5}$ and $L_{T,99.9}$ values were calculated according to Eq.S6 (Batka and Hofmann, 2016). Measuring travel distances of particles in the aquifer is tedious and, in some cases, simply impossible. However, commonly one can predict particle transport by using the breakthrough behaviour of particles in column experiments (Laumann et al., 2013). The predicted travel distance L_T [m] for CMC-stabilized Carbo-Iron at which 50, 63.5 and 99.9% of the particle mass was removed by the aquifer sediment ($c/c_0 = 0.5$; 0.365 and 0.001 for $L_{T,50}$, $L_{T,63.5}$ and $L_{T,99.9}$, respectively) was calculated using the column properties (d_c and n_e), η_0 and α according to (Elimelech et al., 2013):

$$L_T = -\frac{2d_c}{3(1-n_e)\alpha\eta_0} \ln\left(\frac{c}{c_0}\right) \quad (\text{Eq. S6})$$

with

d_c : average particle diameter of the sediment (mm)

c/c_0 : ratio of the particle concentration at the outlet and inlet of the column

n_e : effective porosity (-)

α : attachment efficiency (-)

η_0 : single-collector contact efficiency (-)

2.2 Investigation of Carbo-Iron mobility and measurements of particle occurrence

The transport behaviour of Carbo-Iron in porous media has been studied using columns (D.I and D.II) with bed lengths of $L = 0.25$ m to 1 m and the method described in SI section 3.2.1. The breakthrough performance of the column beds packed with various porous media, such as the model quartz sand Dorsilit 8 (fraction 0.3–0.8 mm, Gebr. Dorfner GmbH Co, Hirschau, Germany) and aquifer material from the field site, was evaluated using standard model groundwater (according to US EPA (2002) standard soft, medium hard and hard water) and real samples from the site. For targeted particle deposition under confined conditions, harmonized balancing of particle concentration and suspension stabilizer content was found to be the key factor for particle migration. Based on sedimentation experiments, long-term-stable Carbo-Iron suspensions for 10 g/L particle concentration were received when adding CMC in concentrations above 10 w/w% referred to the particle concentration – in the present case above 1 g/L. These long-term stable suspensions show a high subsurface mobility which makes them suitable for the generation of broad treatment zones for plume control. Migration of Carbo-Iron through the aquifer is supported by the detection of Carbo-Iron particles in samples from GWM1 on sampling days 30, 57, 92 and 139 after injection after injection (Fig. S1).

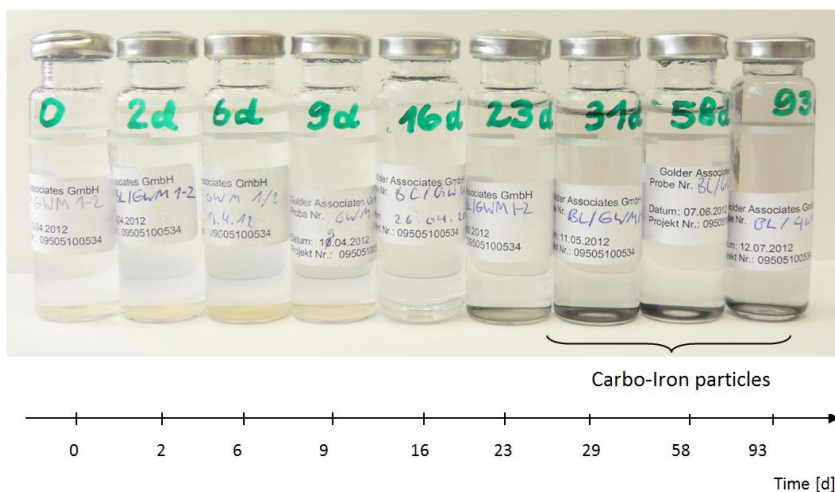


Fig. S 1: Suspended Carbo-Iron in water samples from GWM1 indicate particle migration from the injection ports.

2.2.1 C/Fe-content of Carbo-Iron as fingerprint

Soil samples were analysed in order to obtain more information on the subsurface distribution of the reactive particles. To date no reliable methods were available for the carbon-based particle differentiation from natural background in groundwater. For Carbo-Iron the possibility of using the

specific elemental composition Fe-C as finger print exists. Since both elements are ubiquitous in soil and groundwater, it is not sufficient for Carbo-Iron detection to simply quantify the element concentrations. We used the $c_{\text{Fe,total}}/c_{\text{POC}}$ ratio and compared reference points and Carbo-Iron-affected sediments. Figure S2 shows a marked difference in the element ratio for background sediment ($c_{\text{Fe,total}}/c_{\text{POC}} \approx 1$) and Carbo-Iron-loaded sediments ($c_{\text{Fe,total}}/c_{\text{POC}} \leq 0.5$). Original Carbo-Iron samples showed similar element finger printing. However, reliable quantification of a Carbo-Iron loading was not possible for this method.

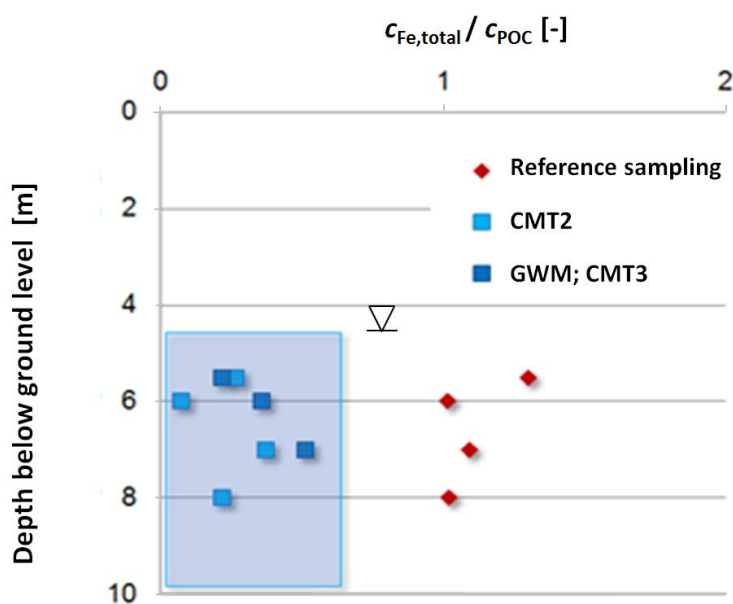


Fig. S 2: The ratio $c_{\text{Fe,total}}/c_{\text{POC}}$ for sample taken at the measuring points CMT2 and GWM (with depth profile) at the site of the field study.

2.2.2 Incineration temperature as Carbo-Iron fingerprint

Before termination of the monitoring period in the field study (Mackenzie et al., 2016), sediment samples were taken by direct push from zone I and analysed for their Carbo-Iron content. A method was developed for Carbo-Iron analysis in complex sediment matrices which is based on temperature-programmed oxidation (TPO) and quantification of temperature-resolved CO_2 peaks. Carbo-Iron-associated TPO peaks could be separated from other (iron-free) AC-based peaks due to a peak shift to a lower incineration temperature which is caused by iron-catalysed oxidation.

2.3 Effects assessment for Carbo-Iron

2.3.1 Toxicity tests with *Daphnia magna*

Acute test

At the beginning and after 48 d of exposure, physico-chemical parameters were measured in the test media of the control and of all test concentrations. Mean values (min-max) for the parameters pH, oxygen saturation, conductivity and temperature were 6.4 (5.8-7.6), 81 (72-92) %, 0.6 (0.56-0.7) mS/cm and 20.9 (20.2-22.6) °C, respectively. Hence, the validity criteria according to the test guideline (OECD, 2004a) were met.

Table S1: Results of the 48-h acute toxicity test with *D. magna*. According to the test guideline (OECD, 2004a), exposure is terminated and immobility is assessed after 48 h exposure (d 2). In the present study, test organisms were transferred to culture medium after 48 h and immobility was assessed for a post-exposure period of 5 d (d 5).

Treatment	Carbo-Iron (mg/L)	CMC (mg/L)	Mean immobility ± sd (%; n=4)	
			d 2	d 5
C0	0	0	0.0 ± 0.0	10.0 ± 5.0
C0cmc	0	20	0.0 ± 0.0	0.0 ± 0.0
C1	0.56	20	0.0 ± 21.2	10.0 ± 0.0
C2	1.0	20	0.0 ± 19.1	0.0 ± 25.8
C3	1.78	20	0.0 ± 25.8	30.0 ± 10.0
C4	3.16	20	9.3 ± 30.0	50.0 ± 14.1
C5	5.62	20	15.0 ± 14.1	80.0 ± 14.1
C6	10.0	20	50.0 ± 0.0	90.0 ± 14.1
C7	17.8	20	70.0 ± 14.1	90.0 ± 0.0
C8	31.6	20	55.0 ± 14.1	100.0 ± 14.1
C9	56.2	20	65.0 ± 0.0	100.0 ± 0.0
C10	100.0	20	34.3 ± 0.0	90.0 ± 10.8

Table S2: Lethal concentrations determined by 3 parametric log-normal modelling (lower limit: 0) in the acute toxicity test with *D. magna* after 48 h exposure (d2) and in the post-exposure period (d 5).

	Effect concentration (mg/L) (95% confidence intervals)	
	d 2	d 5
LC ₁₀	2.31 (0.0 - 5.97)	0.64 (0.0 - 1.71)
LC ₂₀	5.79 (0.0 - 12.43)	1.13 (0.0 - 2.67)
LC ₅₀	33.51 (0.0 - 70.52)	3.37 (0.15 - 6.59)

Chronic test

At the beginning and at 3 weekly intervals during the test run of 21 days, physico-chemical parameters were measured in the test media of the control and of all test concentrations. Mean values (min-max) for the parameters pH, oxygen concentration, conductivity and temperature were 7.7 (7.4-8.5), 8.1 (6.7-10) mg/L, 0.6 (0.54-0.67) mS/cm and 20.5 (19.2-21.8) °C, respectively. Hence, the validity criteria according to the test guideline (OECD, 2012) were met.

Table S3: Survival and number of offspring (mean \pm standard deviation, n=7 – 10) in the 21-d chronic toxicity test with *D. magna*. *: Significant difference from the CMC control (Wilcoxon ranks sum test, $p \leq 0.05$).

Treatment	Carbo-Iron (mg/L)	CMC (mg/L)	Survival (%)	Total number of living offspring \pm sd
C0	0.0	0	100	146 \pm 13
C0cmc	0.0	20	100	138 \pm 8
C1	0.1	20	100	147 \pm 13
C2	0.3	20	100	141 \pm 12
C3	1.0	20	100	140 \pm 8
C4	3.2	20	100	120 \pm 8 *
C5	10.0	20	70	108 \pm 24 *

The coefficient of variation for the control reproductive output was 9.2% and is in accordance with the criteria of $\leq 25\%$ in the OECD test guideline (OECD, 2012). The validity criteria (mortality of parent animals $\leq 20\%$ and number of living offspring ≥ 60) of the test guideline (OECD, 2012) were met.

Table S4: Effect concentrations for reproduction determined with 3 parametric log-normal modelling (lower limit: 0) for the chronic toxicity test with *D. magna*.

	Effect concentration (mg/L)] (95% confidence intervals)
EC ₁₀	2.02 (0.66 - 3.38)
EC ₂₀	5.73 (3.17 - 8.29)
EC ₅₀	42.23 (4.00 - 80.45)

2.3.2 Algae growth inhibition test with Carbo-Iron and active carbon

Algae cultures were monitored constantly for temperature (28°C) and light-dark cycle (14:10-h) to ensure synchronized growth. Aeration of the cultures ensured input of carbon as source of algae growth as well as a constant mixing regime. At start and end of the test the pH of the algae suspensions was checked. The pH varied within the acceptable range between 6.4 – 7.

Table S5: Light intensities (mean \pm sd, n=4) in exposure suspensions containing algae and Carbon-Iron or activated carbon, respectively. (b, c, d, e) Significant differences from the CMC control (Anova followed by Tukey HSD post-hoc test, $p \leq 0.05$).

Treatment	Carbo-Iron (mg/L)	Activated carbon (mg/L)	CMC (mg/L)	Light intensity ($\mu\text{mol m}^{-2} \text{s}^{-1}$) median (upper, lower quartile, n=4)
Control	0.0	0.0	20	235 (251.3, 229)
AC1	0.0	15.9	20	124.5 (130.2, 119.6)
CI1	19.78	0.0	20	152.8 (148.2, 155)
AC2	0.0	43.5	20	44.4 (46.7, 39.5)
CI2	62.5	0.0	20	62.9 (64.4, 59.8)

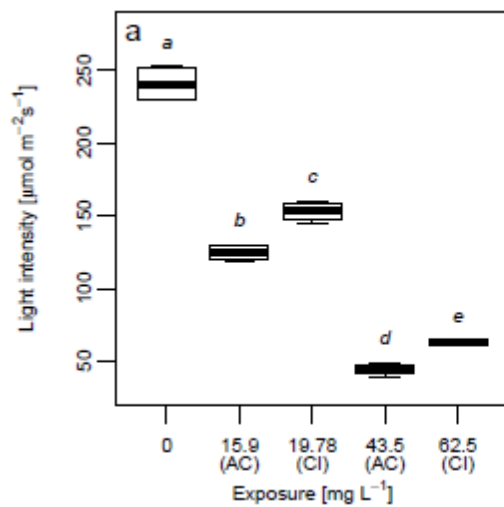


Fig. S 3: Light intensities at the beginning of the exposure to active carbon (AC) and Carbo-Iron (CI) in algae suspension in the test vessels. Anova followed by Tukey HSD post-hoc test were used to test differences in light intensity and cell volume inhibition between the different treatments.

In particle free test medium, light intensity of 235 μmol photo active radiation photons (PAR) $\text{m}^{-2} \text{s}^{-1}$ was measured. A significant difference of light intensity was found between two treatments with similar masses of active carbon (15.9 mg/L active carbon and 19.78 mg/L Carbo-Iron), with average values of 124.5 and 153 μmol PAR photons $\text{m}^{-2} \text{s}^{-1}$, respectively. A significant difference of light

intensities was also found between the active carbon 43.5 and Carbo-Iron treatment 62.5 (p-value: 0.016), with averages values of 44.4 and 62.9 $\mu\text{mol PAR photons m}^{-2} \text{s}^{-1}$, respectively.

Table S6: Effect concentrations for reproduction determined with 3 parametric log-normal modelling (lower limit: 0) for *S. vacuolatus* after exposure to Carbo-Iron and active carbon, respectively.

		Effect concentration (mg/L)] (95% confidence intervals)
Carbo-Iron	EC ₁₀	7.22 (0.00 - 30.12)
	EC ₂₀	15.84 (0.00 - 68.02)
	EC ₅₀	46.04 (0.00 - 205.1)
Active carbon	EC ₁₀	6.39 (0.50 - 12.29)
	EC ₂₀	11.52 (0.00 - 23.17)
	EC ₅₀	45.95 (0.00 - 255.8)

2.3.3 Algae growth inhibition test with tetrachloroethene

Algae cultures were monitored constantly for temperature (28°C) and light-dark cycle (14:10-h) to ensure synchronized growth. Aeration of the cultures ensured input of carbon as source of algae growth as well as a constant mixing regime. At start and end of the test the pH of the algae suspensions was checked. The pH varied within the acceptable range between 6.4 – 7.

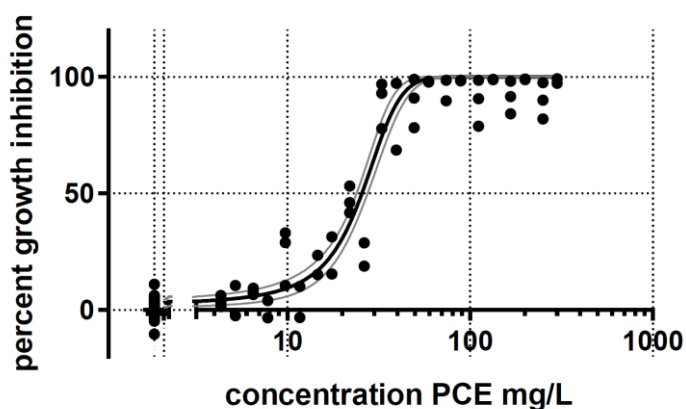


Fig. S 4: Effect of tetrachloroethene on growth of the algae *Scenedesmus vacuolatus* after 24 h of exposure.

Table S7: Results (mean \pm sd, n=3) of growth inhibition test with *Scenedesmus vacuolatus* after exposure to tetrachoroethene.

Treatment	PCE (mg/L)	Growth inhibition (%)
Control	0.0	0.0 \pm 3.6
PCE	4.3	3.5 \pm 2.4
PCE	5.2	4.0 \pm 9.2
PCE	6.5	7.9 \pm 1.4
PCE	7.8	0.3 \pm 5.2
PCE	9.8	24.2 \pm 12.0
PCE	11.7	3.5 \pm 9.4
PCE	14.6	20.6 \pm 4.7
PCE	17.6	23.4 \pm 11.3
PCE	21.9	47.0 \pm 5.8
PCE	26.3	23.8 \pm 7.1
PCE	32.9	89.2 \pm 10.1
PCE	39.5	82.9 \pm 20.2
PCE	49.4	89.3 \pm 10.4
PCE	59.3	98.0 \pm 0.2
PCE	74.1	94.2 \pm 6.3
PCE	88.9	98.5 \pm 0.2
PCE	111.1	89.3 \pm 9.9
PCE	133.3	98.9 \pm 0.1
PCE	166.7	91.3 \pm 7.1
PCE	200.0	98.9 \pm 0.1
PCE	250.0	89.8 \pm 7.8
PCE	300.0	98.2 \pm 1.4

2.3.4 Sediment-water test with *Chironomus riparius*

During the 28 d of exposure mean values (min-max) in the test media for the physico-chemical parameters pH, oxygen concentration, hardness, NH₄⁺-N and temperature were 7.8 (7.7-8.1), 7.8 (7.4-8.8) mg/L, 296 (271-339) mg/L CaCO₃, 0.83 (0.75-1.12) mg/L and 19.9 (19.5-20.4) °C, respectively.

In the formulated sediment, measured pH was 7.0 to 7.1, dry weight (dw) was 66.7% of wet weight. The total organic carbon content of the sediment was 2.54 wt-% dw.

Table S8: Results (mean \pm sd, n=8) of the water-sediment test with *Chironomus riparius* after 28 d exposure to Carbo-Iron. *: Significant difference from the CMC control (cmc, two-sided Dunnett's test, $p \leq 0.05$).

Treatment	Carbo-Iron (mg/L)	CMC (mg/L)	Emergence (%)	Development rate (d ⁻¹)
C0	0.0	0	94.3 \pm 9.8	0.057 \pm 0.001
C0cmc	0.0	20	90.0 \pm 13.1	0.061 \pm 0.003
C1	10.0	20	93.8 \pm 9.2	0.059 \pm 0.005
C2	17.8	20	90.0 \pm 12.6	0.060 \pm 0.002
C3	31.6	20	91.3 \pm 9.9	0.059 \pm 0.002
C4	56.2	20	91.7 \pm 7.5	0.058 \pm 0.001
C5	100.0	20	88.8 \pm 17.3	0.056 \pm 0.003 *

The validity criteria (pH was between 6.8 and 7.9, desired: 6 – 9; oxygen concentration was $\geq 68\%$, desired $\geq 60\%$; temperature difference between successive days was $\leq 0.5^\circ\text{C}$, desired: less than $\pm 1^\circ\text{C}$; emergence in control and cmc control was 94 and 90%, respectively, desired: $\geq 70\%$) of the test guideline (OECD, 2012) were met. However, 1 adult emerged in the negative controls and in the cmc controls, respectively, after day 23. In the guideline desired: emergence concluded after day 23. This deviation from the validity criterion was supposed to have a low impact on the validity of the study, since emergence of the controls was within validity limits before day 23 of the exposure.

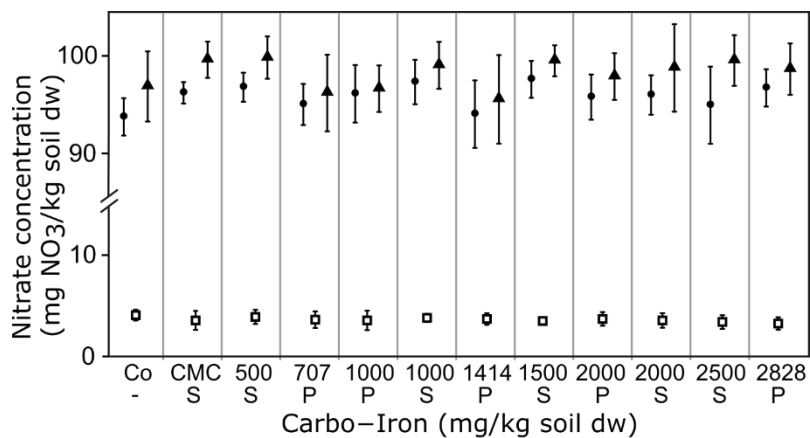
2.3.5 Nitrogen-transformation test

During the 28-d exposure, nitrate concentrations were measured on d 0, d 7 and d 28 in soil samples. Exposure to Carbo-Iron, as powder or suspension, had no effect on the nitrogen transformation of the microbial community in the soil: the pattern of nitrogen transformation was similar in all 10 different Carbo-Iron treatments and the controls. The initial nitrate concentrations of 93.6 - 97.7 mg/kg dw decreased to 3.3 - 4.1 mg/kg dw on d 7 (Figure 7 and table S1). This decline is typical for nitrogen-transformation tests and is caused by rapid metabolization of nitrate present in the soil. Between d 7 and d 28, nitrate concentrations increased again to a similar range as at the start of the experiment (95.3 and 99.4 mg/kg dw). This increase can be explained by metabolization of other nitrogen sources, mainly the added alfalfa powder, that are transformed to nitrate. The mean variation of nitrate concentrations in the controls was 2.3%, 12.0% and 4.2% on d 0, d 7 and d 28, respectively (i.e. below the maximum validity criterion of 15% described in OECD 2000). A NOEC of ≥ 2828 mg/kg dw was derived. Similarly, Hjorth et al. (2017) observed no effects in acute toxicity tests with the aquatic microorganisms *Aliivibrio fischeri* after exposure for 15 minutes to

Carbo-Iron test concentration up to 100 mg/L nor for the aquatic 6-h exposure with *Escherichia coli* up to 1000 mg/L.

Table S9: Results (mean \pm sd, n=4) of the 28-d nitrogen-transformation test with Carbo-Iron. Carbo-Iron application was performed either in suspension (S) or as powder (P). All concentrations refer to soil dry weight (dw). CMC concentration in the treatments spiked with suspensions and in the CMC control was 17.1 mg CMC/kg soil dw (i.e. 20 mg CMC/kg soil f.w.).

Treatment	Appli- cation	Carbo-Iron (mg/kg dw)	CMC (mg/kg dw)	Nitrate (mg NO ₃ ⁻ / kg dw)		
				d 0	d 7	d 28
C0	none	0	0.0	93.6 \pm 1.8	4.1 \pm 0.5	96.6 \pm 3.5
C0cmc	none	0	17.1	96.0 \pm 1.1	3.6 \pm 0.9	99.2 \pm 1.8
C1	S	500	17.1	96.5 \pm 1.4	3.9 \pm 0.7	99.4 \pm 2.0
C1	P	707	0.0	94.8 \pm 2.0	3.7 \pm 0.8	96.0 \pm 3.8
C2	P	1000	0.0	95.9 \pm 2.8	3.6 \pm 1.0	96.4 \pm 2.3
C2	S	1000	17.1	97.0 \pm 2.2	3.8 \pm 0.4	98.7 \pm 2.3
C3	P	1414	0.0	93.9 \pm 3.3	3.7 \pm 0.6	95.3 \pm 4.4
C3	S	1500	17.1	97.3 \pm 1.8	3.5 \pm 0.3	99.1 \pm 1.5
C4	P	2000	0.0	95.6 \pm 2.2	3.7 \pm 0.7	97.6 \pm 2.3
C4	S	2000	17.1	95.8 \pm 1.9	3.6 \pm 0.7	98.4 \pm 4.3
C5	S	2500	17.1	94.8 \pm 3.8	3.4 \pm 0.7	99.2 \pm 2.5
C5	P	2828	0.0	96.5 \pm 1.8	3.3 \pm 0.6	98.3 \pm 2.5



Nitrate measurements (d after test start): ● 0 d; □ 7 d; ▲ 28 d

Figure 1: Nitrate concentrations in the 28-d nitrogen transformation test on d 0, d 7 and d 28 after the start of exposure. Carbo-Iron was either added to soil as powder (P) or applied in suspension (S). Co: control; CMC: test soil with carboxymethyl cellulose.

The validity criteria (variation between replicates in the negative control and cmc control was 3.4 and 1.1%, desired \leq 15%) of the test guideline (OECD, 2000) were met.

2.4 Substance-specific assessment of the environmental risk

Table S 10: Summary of ecotoxicity data for Carbo-Iron.

Functional/trophic group	Species	Exposure time	Effect data	Endpoint	Source
Acute data					
Algae	<i>Raphidocelis subcapitata</i>	48 h	NOEC ≥ 100	Growth	A
Algae	<i>Chlamydomonas sp.</i>	48 h	NOEC ≥ 100	Growth	A
Algae	<i>Scenedesmus vacuolatus</i>	16 h	EC ₅₀ = 46.04	Growth	B
Bacteria	<i>Aliivibrio fischeri</i>	15 min	NOEC ≥ 100	Luminescence inhibition	A
Bacteria	<i>Escherichia coli</i>	6h / 24 h	NOEC ≥ 100	Growth	A
Crustacea	<i>Daphnia magna</i>	48 h	NOEC ≥ 100	Immobility	A
Annelida	<i>Lumbriculus variegatus</i>	96 h	NOEC ≥ 100	Survival	A
Chronic data					
Algae	<i>Scenedesmus vacuolatus</i>	16 h	EC ₁₀ = 7.22	Cell volume	B
Bacteria	N-transforming soil microorganisms	28 d	NOEC ≥ 2828 mg/kg dw	Nitrate formation	B
Insecta	<i>Chironomus riparius</i>	28 d	NOEC = 56.2	Development rate:	B
Crustacea	<i>Daphnia magna</i>	21 d	NOEC = 1.0	Reproduction	B
Crustacea	<i>Hyalella azteca</i>	56 d	NOEC: 6.3	Reproduction	C
Fish	<i>Danio rerio</i>	28 d	NOEC ≥ 25	Growth	D

^A: Hjorth et al. (2017); ^B: present study; ^C: Weil et al. (2016); ^D: Weil et al. (2015).

2.5 Site-specific comparative risk assessment

2.5.1 Chemical component

Table S11: Measured concentrations ($\mu\text{g/L}$) and minimum (min) and maximum (max) concentrations of the pollutants in samples from the respective sampling wells before (d0) and for 190 d after injection of Carbo-Iron into the aquifer. If samples from more than one sampling depth were analysed ($n>1$), the mean value was calculated. Chemical analysis in groundwater from the sampling wells was performed for the following pollutants: 1,1-dichloroethylene and 1,2-dichloroethylene (cis and trans) as sum parameter (DCEs), trichloroethylene (TCE) and tetrachloroethylene (PCE). Additionally, groundwater samples were analysed for the potentially occurring transformation products of treatment with Carbo-Iron, ethane and ethane (as a sum parameter) and vinyl chloride (VC). For each substance and day, the chemical risk quotient (cRQ) was calculated as the quotient of the concentration and the target value.

Well	Substance	Day	Concentration ($\mu\text{g/L}$)	min	max	n	Target value ($\mu\text{g/L}$)	cRQ
GWM1	DCEs	0	0.00	0.00	0.00	2	5.8	0.000
GWM1	DCEs	9	7.25	4.83	9.67	2	5.8	1.250
GWM1	DCEs	31	2.68	1.54	3.81	2	5.8	0.461
GWM1	DCEs	58	1.00	0.70	1.30	2	5.8	0.172
GWM1	DCEs	93	6.21	4.20	8.22	2	5.8	1.071
GWM1	DCEs	190	15.78	15.78	15.78	1	5.8	2.721
GWM1	Ethane+Ethene	0	0.00	0.00	0.00	2	8500	0.000
GWM1	Ethane+Ethene	9	455.00	444.00	466.00	2	8500	0.054
GWM1	Ethane+Ethene	31	473.25	369.60	576.90	2	8500	0.056
GWM1	Ethane+Ethene	58	1484.40	1151.40	1817.40	2	8500	0.175
GWM1	Ethane+Ethene	93	20342.46	9905.56	30779.37	2	8500	2.393
GWM1	Ethane+Ethene	190	3599.37	3599.37	3599.37	1	8500	0.423
GWM1	PCE	0	22647.50	21401.00	23894.00	2	40	566.188
GWM1	PCE	9	12719.00	9235.49	16202.50	2	40	317.975
GWM1	PCE	31	2114.75	1966.31	2263.19	2	40	52.869
GWM1	PCE	58	1318.50	1117.00	1520.00	2	40	32.963
GWM1	PCE	93	10745.22	7646.35	13844.08	2	40	268.630
GWM1	PCE	190	5359.86	5359.86	5359.86	1	40	133.997
GWM1	TCE	0	526.50	509.00	544.00	2	500	1.053
GWM1	TCE	9	227.09	197.26	256.92	2	500	0.454
GWM1	TCE	31	24.27	22.67	25.87	2	500	0.049
GWM1	TCE	58	13.15	12.70	13.60	2	500	0.026
GWM1	TCE	93	67.68	59.25	76.11	2	500	0.135

Table S11: continued.

Well	Substance	Day	Concentration (µg/L)	min	max	n	Target value (µg/L)	cRQ
GWM1	TCE	190	178.95	178.95	178.95	1	500	0.358
GWM1	VC	0	0.00	0.00	0.00	2	5	0.000
GWM1	VC	9	0.00	0.00	0.00	2	5	0.000
GWM1	VC	31	0.00	0.00	0.00	2	5	0.000
GWM1	VC	58	0.00	0.00	0.00	2	5	0.000
GWM1	VC	93	0.00	0.00	0.00	2	5	0.000
GWM1	VC	190	0.00	0.00	0.00	1	5	0.000
RKS13	DCEs	0	0.00	0.00	0.00	2	5.8	0.000
RKS13	DCEs	9	7.51	6.16	8.87	2	5.8	1.295
RKS13	DCEs	31	3.05	2.05	4.05	2	5.8	0.526
RKS13	DCEs	58	4.85	4.70	5.00	2	5.8	0.836
RKS13	DCEs	93	7.16	0.73	13.58	2	5.8	1.234
RKS13	DCEs	190	0.00	0.00	0.00	1	5.8	0.000
RKS13	Ethane+Ethene	0	0.00	0.00	0.00	2	8500	0.000
RKS13	Ethane+Ethene	9	0.00	0.00	0.00	2	8500	0.000
RKS13	Ethane+Ethene	31	0.00	0.00	0.00	2	8500	0.000
RKS13	Ethane+Ethene	58	0.00	0.00	0.00	2	8500	0.000
RKS13	Ethane+Ethene	93	0.00	0.00	0.00	2	8500	0.000
RKS13	Ethane+Ethene	190	0.00	0.00	0.00	1	8500	0.000
RKS13	PCE	0	33218.19	19933.97	46502.41	2	40	830.455
RKS13	PCE	9	22425.11	21953.06	22897.16	2	40	560.628
RKS13	PCE	31	7955.84	7696.15	8215.53	2	40	198.896
RKS13	PCE	58	9892.50	6641.00	13144.00	2	40	247.313
RKS13	PCE	93	45166.38	37877.80	52454.97	2	40	1129.160
RKS13	PCE	190	24192.34	24192.34	24192.34	1	40	604.809
RKS13	TCE	0	1167.20	898.81	1435.59	2	500	2.334
RKS13	TCE	9	405.43	366.75	444.10	2	500	0.811
RKS13	TCE	31	174.99	165.40	184.58	2	500	0.350
RKS13	TCE	58	224.30	194.60	254.00	2	500	0.449
RKS13	TCE	93	368.38	111.23	625.53	2	500	0.737
RKS13	TCE	190	261.48	261.48	261.48	1	500	0.523
RKS13	VC	0	0.00	0.00	0.00	2	5	0.000
RKS13	VC	9	0.00	0.00	0.00	2	5	0.000

Table S11: continued.

Well	Substance	Day	Concentration (µg/L)	min	max	n	Target value (µg/L)	cRQ
RKS13	VC	31	0.00	0.00	0.00	2	5	0.000
RKS13	VC	58	0.00	0.00	0.00	2	5	0.000
RKS13	VC	93	0.00	0.00	0.00	2	5	0.000
RKS13	VC	190	0.00	0.00	0.00	1	5	0.000
CMT2	DCEs	0	0.00	0.00	0.00	6	5.8	0.000
CMT2	DCEs	9	1.80	1.08	2.52	2	5.8	0.311
CMT2	DCEs	31	0.72	0.00	1.43	2	5.8	0.124
CMT2	DCEs	58	0.65	0.00	1.30	2	5.8	0.112
CMT2	DCEs	93	13.81	0.00	70.68	7	5.8	2.381
CMT2	DCEs	190	0.00	0.00	0.00	7	5.8	0.000
CMT2	Ethane+Ethene	0	0.00	0.00	0.00	6	8500	0.000
CMT2	Ethane+Ethene	9	411.74	338.40	485.08	2	8500	0.048
CMT2	Ethane+Ethene	31	1207.30	1207.30	1207.30	1	8500	0.142
CMT2	Ethane+Ethene	58	320.15	184.00	456.30	2	8500	0.038
CMT2	Ethane+Ethene	93	18534.10	251.59	112758.73	7	8500	2.180
CMT2	Ethane+Ethene	190	11895.08	112.38	35139.52	7	8500	1.399
CMT2	PCE	0	2901.00	379.00	10238.00	6	40	72.525
CMT2	PCE	9	2205.72	585.71	3825.74	2	40	55.143
CMT2	PCE	31	120.15	76.69	163.61	2	40	3.004
CMT2	PCE	58	308.50	88.00	529.00	2	40	7.713
CMT2	PCE	93	1381.00	33.78	4325.09	7	40	34.525
CMT2	PCE	190	230.11	37.84	610.76	7	40	5.753
CMT2	TCE	0	89.17	19.00	282.00	6	500	0.178
CMT2	TCE	9	56.39	27.22	85.56	2	500	0.113
CMT2	TCE	31	4.10	2.18	6.02	2	500	0.008
CMT2	TCE	58	6.60	2.00	11.20	2	500	0.013
CMT2	TCE	93	30.84	2.02	101.56	7	500	0.062
CMT2	TCE	190	10.95	5.12	21.44	7	500	0.022
CMT2	VC	0	0.00	0.00	0.00	6	5	0.000
CMT2	VC	9	0.00	0.00	0.00	2	5	0.000
CMT2	VC	31	0.00	0.00	0.00	2	5	0.000
CMT2	VC	58	0.00	0.00	0.00	2	5	0.000
CMT2	VC	93	0.00	0.00	0.00	7	5	0.000

Table S11: continued.

Well	Substance	Day	Concentration (µg/L)	min	max	n	Target value (µg/L)	cRQ
CMT2	VC	190	0.00	0.00	0.00	7	5	0.000
CMT3	DCEs	0	0.00	0.00	0.00	2	5.8	0.000
CMT3	DCEs	9	0.00	0.00	0.00	1	5.8	0.000
CMT3	DCEs	93	17.05	0.57	30.63	7	5.8	2.940
CMT3	DCEs	190	119.99	0.00	406.12	7	5.8	20.687
CMT3	Ethane+Ethene	0	0.00	0.00	0.00	2	8500	0.000
CMT3	Ethane+Ethene	9	0.00	0.00	0.00	1	8500	0.000
CMT3	Ethane+Ethene	93	327.28	0.00	652.70	7	8500	0.039
CMT3	Ethane+Ethene	190	484.01	0.00	747.62	7	8500	0.057
CMT3	PCE	0	791.00	540.00	1042.00	2	40	19.775
CMT3	PCE	9	1473.23	1473.23	1473.23	1	40	36.831
CMT3	PCE	93	1752.12	159.79	5124.61	7	40	43.803
CMT3	PCE	190	196.79	4.44	509.97	7	40	4.920
CMT3	TCE	0	17.50	9.00	26.00	2	500	0.035
CMT3	TCE	9	36.71	36.71	36.71	1	500	0.073
CMT3	TCE	93	69.12	7.96	144.01	7	500	0.138
CMT3	TCE	190	22.97	1.14	75.88	7	500	0.046
CMT3	VC	0	0.00	0.00	0.00	2	5	0.000
CMT3	VC	9	0.00	0.00	0.00	1	5	0.000
CMT3	VC	93	0.00	0.00	0.00	7	5	0.000
CMT3	VC	190	0.00	0.00	0.00	7	5	0.000
RKS24	DCEs	0	0.00	0.00	0.00	2	5.8	0.000
RKS24	DCEs	9	0.00	0.00	0.00	2	5.8	0.000
RKS24	DCEs	31	0.00	0.00	0.00	2	5.8	0.000
RKS24	DCEs	58	0.00	0.00	0.00	2	5.8	0.000
RKS24	DCEs	93	0.00	0.00	0.00	2	5.8	0.000
RKS24	DCEs	190	0.00	0.00	0.00	1	5.8	0.000
RKS24	Ethane+Ethene	0	0.00	0.00	0.00	2	8500	0.000
RKS24	Ethane+Ethene	9	0.00	0.00	0.00	2	8500	0.000
RKS24	Ethane+Ethene	31	0.00	0.00	0.00	2	8500	0.000
RKS24	Ethane+Ethene	58	0.00	0.00	0.00	2	8500	0.000
RKS24	Ethane+Ethene	93	0.00	0.00	0.00	2	8500	0.000
RKS24	Ethane+Ethene	190	0.00	0.00	0.00	1	8500	0.000

Appendix D.2

Table S11: continued.

Well	Substance	Day	Concentration (µg/L)	min	max	n	Target value (µg/L)	cRQ
RKS24	PCE	0	153.63	147.91	159.35	2	40	3.841
RKS24	PCE	9	299.51	108.22	490.80	2	40	7.488
RKS24	PCE	31	68.36	55.57	81.16	2	40	1.709
RKS24	PCE	58	151.50	70.00	233.00	2	40	3.788
RKS24	PCE	93	115.06	105.21	124.91	2	40	2.876
RKS24	PCE	190	6.92	6.92	6.92	1	40	0.173
RKS24	TCE	0	1.51	1.38	1.64	2	500	0.003
RKS24	TCE	9	5.38	0.95	9.81	2	500	0.011
RKS24	TCE	31	0.55	0.44	0.66	2	500	0.001
RKS24	TCE	58	1.70	0.50	2.90	2	500	0.003
RKS24	TCE	93	0.97	0.96	0.99	2	500	0.002
RKS24	TCE	190	0.39	0.39	0.39	1	500	0.001
RKS24	VC	0	0.00	0.00	0.00	2	5	0.000
RKS24	VC	9	0.00	0.00	0.00	2	5	0.000
RKS24	VC	31	0.00	0.00	0.00	2	5	0.000
RKS24	VC	58	0.00	0.00	0.00	2	5	0.000
RKS24	VC	93	0.00	0.00	0.00	2	5	0.000
RKS24	VC	190	0.00	0.00	0.00	1	5	0.000
RKS34	DCEs	0	0.00	0.00	0.00	1	5.8	0.000
RKS34	DCEs	9	0.00	0.00	0.00	2	5.8	0.000
RKS34	DCEs	31	0.00	0.00	0.00	1	5.8	0.000
RKS34	DCEs	190	0.73	0.73	0.73	1	5.8	0.125
RKS34	Ethane+Ethene	0	0.00	0.00	0.00	1	8500	0.000
RKS34	Ethane+Ethene	9	0.00	0.00	0.00	2	8500	0.000
RKS34	Ethane+Ethene	31	0.00	0.00	0.00	1	8500	0.000
RKS34	Ethane+Ethene	190	0.00	0.00	0.00	1	8500	0.000
RKS34	PCE	0	1190.00	1190.00	1190.00	1	40	29.750
RKS34	PCE	9	1085.11	990.34	1179.87	2	40	27.128
RKS34	PCE	31	340.09	340.09	340.09	1	40	8.502
RKS34	PCE	190	701.75	701.75	701.75	1	40	17.544
RKS34	TCE	0	15.00	15.00	15.00	1	500	0.030
RKS34	TCE	9	7.52	6.57	8.46	2	500	0.015
RKS34	TCE	31	3.01	3.01	3.01	1	500	0.006

Table S11: continued.

Well	Substance	Day	Concentration (µg/L)	min	max	n	Target value (µg/L)	cRQ
RKS34	TCE	190	4.22	4.22	4.22	1	500	0.008
RKS34	VC	0	0.00	0.00	0.00	1	5	0.000
RKS34	VC	9	0.00	0.00	0.00	2	5	0.000
RKS34	VC	31	0.00	0.00	0.00	1	5	0.000
RKS34	VC	190	0.00	0.00	0.00	1	5	0.000
CMT1	DCEs	0	0.00	0.00	0.00	3	5.8	0.000
CMT1	DCEs	9	0.63	0.00	1.25	2	5.8	0.108
CMT1	DCEs	31	2.03	0.00	4.05	2	5.8	0.349
CMT1	DCEs	58	0.00	0.00	0.00	2	5.8	0.000
CMT1	DCEs	93	12.64	0.00	30.10	7	5.8	2.180
CMT1	DCEs	190	36.43	0.00	149.29	7	5.8	6.281
CMT1	Ethane+Ethene	0	0.00	0.00	0.00	3	8500	0.000
CMT1	Ethane+Ethene	9	0.00	0.00	0.00	2	8500	0.000
CMT1	Ethane+Ethene	31	0.00	0.00	0.00	2	8500	0.000
CMT1	Ethane+Ethene	58	0.00	0.00	0.00	2	8500	0.000
CMT1	Ethane+Ethene	93	43.78	0.00	276.50	7	8500	0.005
CMT1	Ethane+Ethene	190	131.69	0.00	513.89	7	8500	0.015
CMT1	PCE	0	1471.33	1024.00	1746.00	3	40	36.783
CMT1	PCE	9	109.68	9.00	210.36	2	40	2.742
CMT1	PCE	31	310.10	124.49	495.72	2	40	7.753
CMT1	PCE	58	245.00	231.00	259.00	2	40	6.125
CMT1	PCE	93	842.11	74.11	2820.36	7	40	21.053
CMT1	PCE	190	381.69	115.44	1222.34	7	40	9.542
CMT1	TCE	0	31.33	21.00	40.00	3	500	0.063
CMT1	TCE	9	3.97	1.74	6.20	2	500	0.008
CMT1	TCE	31	2.30	0.69	3.90	2	500	0.005
CMT1	TCE	58	1.10	0.30	1.90	2	500	0.002
CMT1	TCE	93	11.98	2.23	31.33	7	500	0.024
CMT1	TCE	190	14.87	1.27	36.63	7	500	0.030
CMT1	VC	0	0.00	0.00	0.00	3	5	0.000
CMT1	VC	9	0.00	0.00	0.00	2	5	0.000
CMT1	VC	31	0.00	0.00	0.00	2	5	0.000
CMT1	VC	58	0.00	0.00	0.00	2	5	0.000

Table S11: continued.

Well	Substance	Day	Concentration (µg/L)	min	max	n	Target value (µg/L)	cRQ
CMT1	VC	93	0.00	0.00	0.00	4	5	0.000
CMT1	VC	190	0.00	0.00	0.00	4	5	0.000

Table S 12: Calculated values for toxic pressure (cTP) and risk indices (cRI) for the ecotoxicity component of the triad before the injection of Carbo-Iron into the aquifer (d0) and for the first 190 d after the injection.

Well	Contamination zone	cTP for the following days after Carbo-Iron injection						cRI for the following days after Carbo-Iron injection					
		0	9	31	58	93	190	0	9	31	58	93	190
GWM1	Ic	567.24	319.73	53.43	33.34	272.23	137.50	0.78	0.66	0.53	0.52	0.64	0.57
RKS13	I	832.79	562.73	199.77	248.60	1131.13	605.33	0.92	0.78	0.60	0.62	1.00	0.80
CMT2	II	72.70	55.62	3.28	7.88	39.15	7.17	0.54	0.53	0.50	0.50	0.52	0.50
CMT3	II	19.81	36.90	-	-	46.92	25.71	0.51	0.52	-	-	0.52	0.51
RKS24	III	3.84	7.50	1.71	3.79	2.88	0.17	0.50	0.50	0.50	0.50	0.50	0.09
RKS34	IV	29.78	27.14	8.51	-	-	17.68	0.51	0.51	0.50	-	-	0.51
CMT1	-	36.85	2.86	8.11	6.13	23.26	15.87	0.52	0.50	0.50	0.50	0.51	0.51

2.5.2 Ecotoxicity component

Table S 13: Ecotoxicity data and predicted no effect concentrations (PNEC) for the relevant pollutants at the pilot site treated with Carbo-Iron. For each pollutant, effect data (EC: effective concentrations for a specified endpoint, LC: lethal concentrations, NOEC: no observed effect concentrations) were categorized to a trophic / functional group. Due to the lack of experimental data, effect data for two trophic / functional groups for ethene were estimated with computer models (calc. NOEC). Depending on the exposure duration (Exp.) and the availability of data for several functional groups, assessment factors (AF) were applied to the most sensitive effect concentration for each pollutant (bold values), and predicted no effect concentrations (PNEC) were derived.

Substance/ Trophic / functional group	Species	Exp.	Effect concentrations (mg/L), endpoint and source			AF	PNEC (mg/L)
Ethene#							
Acute data							
Algae	<i>Selenastrum capricornutum</i>	72 h	NOEC = 13.9	Growth	A		
Crustacea	<i>Daphnia</i> sp.	16 h	calc. NOEC = 37.4	Mortality	A		
Chronic data							
Higher plants	<i>Nuphar lutea</i>	30 d	NOEC = 5	Reproduction	B	50	0.1
Fish	-	28 d	calc. NOEC = 13	Mortality	A		
Vinyl chloride							
Acute data							
Algae	<i>Raphidocelis subcapitata</i>	48 h	LC ₅₀ = 5.15	Growth	C		
Fish	<i>Danio rerio</i>	96 h	LC ₅₀ = 210	Mortality	D		
Fish	<i>Danio rerio</i>	96 h	NOEC = 128	Mortality	B		
Chronic data							
Algae	<i>Raphidocelis subcapitata</i>	48 h	NOEC = 2.5	Growth	C	100	0.025
Crustacea	<i>Daphnia magna</i>	10 d	NOEC ≥ 0.01	Reproduction	E		
1,1-Dichloroethene							
Acute data							
Algae	<i>Chlamydomonas reinhardtii</i>	72 h	EC ₅₀ = 9.12	Growth	B		
Crustacea	<i>Daphnia magna</i>	48 h	LC ₅₀ = 11.6	Mortality	B		
Fish	<i>Oryzias latipes</i>	48 h	LC ₅₀ = 19.8	Mortality	F		
Chronic data							
Algae	<i>Chlamydomonas reinhardtii</i>	72 h	EC₁₀ = 3.94	Growth	B	100	0.039

Appendix D.2

Table S 13: continued.

Substance/ Trophic / functional group	Species	Exp.	Effect concentrations (mg/L), endpoint and source			AF	PNEC (mg/L)
1,2-Dichloroethene*							
Acute data							
Algae	<i>Raphidocelis subcapitata</i>	72 h	NOEC = 74.0	Growth	G		
Crustacea	<i>Daphnia magna</i>	21 d	NOEC = 4.5	Reproduction	G	100	0.045
Fish	<i>Oryzias latipes</i>	96 h	LC ₅₀ = 67.0	Mortality	G		
Trichloroethylene							
Acute data							
Algae	<i>Chlamydomonas reinhardtii</i>	72 h	EC ₅₀ = 36.5	Growth	H		
Crustacea	<i>Daphnia magna</i>	48 h	EC ₅₀ = 20.8	Immobility	H		
Fish	<i>Jordanella floridae</i>	96 h	LC ₅₀ = 28.3	Mortality	H		
Chronic data							
Algae	<i>Chlamydomonas reinhardtii</i>	72 h	EC ₁₀ = 12.3	Growth	H		
Fish	<i>Jordanella floridae</i>	10 d	NOEC = 5.76	Larval survival	H	50	0.115
Tetrachloroethylene							
Acute data							
Algae	<i>Chlamydomonas reinhardtii</i>	72 h	EC ₁₀ = 1.77	Growth	i		
Crustacea	<i>Daphnia magna</i>	48 h	EC ₅₀ = 8.5	Immobility	i		
Fish	<i>Oncorhynchus mykiss</i>	96 h	5	Mortality	i		
Chronic data							
Algae	<i>Chlamydomonas reinhardtii</i>	72 h	EC ₁₀ = 1.77	Growth	i		
Crustacea	<i>Daphnia magna</i>	21 d	NOEC = 0.51	Reproduction	B, i	10	0.051
Fish	<i>Pimephales promelas</i>	32 d	NOEC = 0.5	Growth	B		

Table S 13: continued.

Substance/ Trophic / functional group	Species	Exp.	Effect concentrations (mg/L), endpoint and source		AF	PNEC (mg/L)
Carbo-Iron						
Acute data						
Bacteria	<i>Aliivibrio fischeri</i>	15 min	NOEC ≥ 100	Luminescence inhibition	J	
Bacteria	<i>Escherichia coli</i>	6h / 24 h	NOEC ≥ 100	Growth	J	
Algae	<i>Raphidocelis subcapitata</i>	48 h	NOEC ≥ 100	Growth	J	
Algae	<i>Chlamydomonas sp.</i>	48 h	NOEC ≥ 100	Growth	J	
Algae	<i>Scenedesmus vacuolatus</i>	16 h	EC ₅₀ = 46.04	Growth		
Crustacea	<i>Daphnia magna</i>	48 h	NOEC ≥ 100	Immobility	J	
Clitellata	<i>Lumbriculus variegatus</i>	96 h	NOEC ≥ 100	Survival	J	
Chronic data						
Algae	<i>Scenedesmus vacuolatus</i>	16 h	EC ₁₀ = 7.22	Cell volume	K	
Insecta	<i>Chironomus riparius</i>	28 d	NOEC = 56.2	Development rate:	K	
Crustacea	<i>Daphnia magna</i>	21 d	NOEC = 1.0	Reproduction	K	10
Crustacea	<i>Hyalella azteca</i>	56 d	NOEC: 6.3	Reproduction	L	0.1
Fish	<i>Danio rerio</i>	28 d	NOEC ≥ 25	Growth	M	

^A: ECHA registration data (<https://echa.europa.eu/registration-dossier/-/registered-dossier/16094/6/2/2>); ^B: ECOTOX database; ^C: Nam & An (2010); ^D: ECHA registration data (<https://echa.europa.eu/registration-dossier/-/registered-dossier/16163/6/2/2>); ^E: Houde et al. (2015); ^F: Aquatic OASIS database; ^G: Aquatic Japan; ^H: Risk Assessment Report Trichloroethylene (EU, 2004); ^I: ECHA registration data (<https://echa.europa.eu/registration-dossier/-/registered-dossier/14303/6/2/2>); ^J: Hjorth et al. (2017); ^K: this manuscript; ^L: Weil et al. (2016); ^M: Weil et al. (2015); [#]: ethane and ethene were evaluated as sum parameter and data for ethene are used here since these effect concentrations were lower than for ethane; ^{*}: cis- and trans-dichloroethene were analysed as sum parameter. Since effect concentrations for trans-isomer were lower, they were used for deriving a PNEC.

Table S 14: Estimated (Carbo-Iron) and measured (all other substances) concentrations in samples from the respective sampling wells before (d0) and for 190 d after injection of Carbo-Iron into the aquifer. If samples from more than one sampling depth were analysed (n>1), the mean value was calculated. For each substance and day, the ecotoxicological risk quotient (eRQ) was calculated as the quotient of the mean and the predicted no effect concentration (PNEC).

Well	Substance	Day	Concentration (mg/L)	n	PNEC (mg/L)	eRQ
GWM1	Carbo-Iron	0	0.00E+00	1	0.1	0.00E+00
GWM1	Carbo-Iron	9	1.30E+00	1	0.1	1.30E+01
GWM1	Carbo-Iron	31	1.30E+00	1	0.1	1.30E+01
GWM1	Carbo-Iron	58	1.30E+00	1	0.1	1.30E+01
GWM1	Carbo-Iron	93	1.30E+00	1	0.1	1.30E+01
GWM1	Carbo-Iron	190	1.30E+00	1	0.1	1.30E+01

Table S 14: continued.

Well	Substance	Day	Concentration (mg/L)	n	PNEC (mg/L)	eRQ
GWM1	DCEs	0	0.00E+00	2	0.045	0.00E+00
GWM1	DCEs	9	7.25E-03	2	0.045	1.61E-01
GWM1	DCEs	31	2.68E-03	2	0.045	5.94E-02
GWM1	DCEs	58	1.00E-03	2	0.045	2.22E-02
GWM1	DCEs	93	6.21E-03	2	0.045	1.38E-01
GWM1	DCEs	190	1.58E-02	1	0.045	3.51E-01
GWM1	Ethane+Ethene	0	0.00E+00	2	0.1	0.00E+00
GWM1	Ethane+Ethene	9	4.55E-01	2	0.1	4.55E+00
GWM1	Ethane+Ethene	31	4.73E-01	2	0.1	4.73E+00
GWM1	Ethane+Ethene	58	1.48E+00	2	0.1	1.48E+01
GWM1	Ethane+Ethene	93	2.03E+01	2	0.1	2.03E+02
GWM1	Ethane+Ethene	190	3.60E+00	1	0.1	3.60E+01
GWM1	PCE	0	2.26E+01	2	0.037	6.12E+02
GWM1	PCE	9	1.27E+01	2	0.037	3.44E+02
GWM1	PCE	31	2.11E+00	2	0.037	5.72E+01
GWM1	PCE	58	1.32E+00	2	0.037	3.56E+01
GWM1	PCE	93	1.07E+01	2	0.037	2.90E+02
GWM1	PCE	190	5.36E+00	1	0.037	1.45E+02
GWM1	TCE	0	5.27E-01	2	0.576	9.14E-01
GWM1	TCE	9	2.27E-01	2	0.576	3.94E-01
GWM1	TCE	31	2.43E-02	2	0.576	4.21E-02
GWM1	TCE	58	1.32E-02	2	0.576	2.28E-02
GWM1	TCE	93	6.77E-02	2	0.576	1.17E-01
GWM1	TCE	190	1.79E-01	1	0.576	3.11E-01
GWM1	VC	0	0.00E+00	2	1.28	0.00E+00
GWM1	VC	9	0.00E+00	2	1.28	0.00E+00
GWM1	VC	31	0.00E+00	2	1.28	0.00E+00
GWM1	VC	58	0.00E+00	2	1.28	0.00E+00
GWM1	VC	93	0.00E+00	2	1.28	0.00E+00
GWM1	VC	190	0.00E+00	1	1.28	0.00E+00
RKS13	Carbo-Iron	0	0.00E+00	1	0.1	0.00E+00
RKS13	Carbo-Iron	9	5.00E-01	1	0.1	5.00E+00
RKS13	Carbo-Iron	31	5.00E-01	1	0.1	5.00E+00
RKS13	Carbo-Iron	58	5.00E-01	1	0.1	5.00E+00
RKS13	Carbo-Iron	93	5.00E-01	1	0.1	5.00E+00
RKS13	Carbo-Iron	190	5.00E-01	1	0.1	5.00E+00
RKS13	DCEs	0	0.00E+00	2	0.045	0.00E+00
RKS13	DCEs	9	7.51E-03	2	0.045	1.67E-01
RKS13	DCEs	31	3.05E-03	2	0.045	6.77E-02
RKS13	DCEs	58	4.85E-03	2	0.045	1.08E-01
RKS13	DCEs	93	7.16E-03	2	0.045	1.59E-01
RKS13	DCEs	190	0.00E+00	1	0.045	0.00E+00

Table S 14: continued.

Well	Substance	Day	Concentration (mg/L)	n	PNEC (mg/L)	eRQ
RKS13	Ethane+Ethene	0	0.00E+00	2	0.1	0.00E+00
RKS13	Ethane+Ethene	9	0.00E+00	2	0.1	0.00E+00
RKS13	Ethane+Ethene	31	0.00E+00	2	0.1	0.00E+00
RKS13	Ethane+Ethene	58	0.00E+00	2	0.1	0.00E+00
RKS13	Ethane+Ethene	93	0.00E+00	2	0.1	0.00E+00
RKS13	Ethane+Ethene	190	0.00E+00	1	0.1	0.00E+00
RKS13	PCE	0	3.32E+01	2	0.037	8.98E+02
RKS13	PCE	9	2.24E+01	2	0.037	6.06E+02
RKS13	PCE	31	7.96E+00	2	0.037	2.15E+02
RKS13	PCE	58	9.89E+00	2	0.037	2.67E+02
RKS13	PCE	93	4.52E+01	2	0.037	1.22E+03
RKS13	PCE	190	2.42E+01	1	0.037	6.54E+02
RKS13	TCE	0	1.17E+00	2	0.576	2.03E+00
RKS13	TCE	9	4.05E-01	2	0.576	7.04E-01
RKS13	TCE	31	1.75E-01	2	0.576	3.04E-01
RKS13	TCE	58	2.24E-01	2	0.576	3.89E-01
RKS13	TCE	93	3.68E-01	2	0.576	6.40E-01
RKS13	TCE	190	2.61E-01	1	0.576	4.54E-01
RKS13	VC	0	0.00E+00	2	1.28	0.00E+00
RKS13	VC	9	0.00E+00	2	1.28	0.00E+00
RKS13	VC	31	0.00E+00	2	1.28	0.00E+00
RKS13	VC	58	0.00E+00	2	1.28	0.00E+00
RKS13	VC	93	0.00E+00	2	1.28	0.00E+00
RKS13	VC	190	0.00E+00	1	1.28	0.00E+00
CMT2	Carbo-Iron	0	0.00E+00	1	0.1	0.00E+00
CMT2	Carbo-Iron	9	0.00E+00	1	0.1	1.30E+01
CMT2	Carbo-Iron	31	0.00E+00	1	0.1	1.30E+01
CMT2	Carbo-Iron	58	0.00E+00	1	0.1	1.30E+01
CMT2	Carbo-Iron	93	0.00E+00	1	0.1	1.30E+01
CMT2	Carbo-Iron	190	0.00E+00	1	0.1	1.30E+01
CMT2	DCEs	0	0.00E+00	6	0.045	0.00E+00
CMT2	DCEs	9	1.80E-03	2	0.045	4.01E-02
CMT2	DCEs	31	7.17E-04	2	0.045	1.59E-02
CMT2	DCEs	58	6.50E-04	2	0.045	1.44E-02
CMT2	DCEs	93	1.38E-02	7	0.045	3.07E-01
CMT2	DCEs	190	0.00E+00	7	0.045	0.00E+00
CMT2	Ethane+Ethene	0	0.00E+00	6	0.1	0.00E+00
CMT2	Ethane+Ethene	9	4.12E-01	2	0.1	4.12E+00
CMT2	Ethane+Ethene	31	1.21E+00	1	0.1	1.21E+01
CMT2	Ethane+Ethene	58	3.20E-01	2	0.1	3.20E+00
CMT2	Ethane+Ethene	93	1.85E+01	7	0.1	1.85E+02
CMT2	Ethane+Ethene	190	1.19E+01	7	0.1	1.19E+02

Table S 14: continued.

Well	Substance	Day	Concentration (mg/L)	n	PNEC (mg/L)	eRQ
CMT2	PCE	0	2.90E+00	6	0.037	7.84E+01
CMT2	PCE	9	2.21E+00	2	0.037	5.96E+01
CMT2	PCE	31	1.20E-01	2	0.037	3.25E+00
CMT2	PCE	58	3.09E-01	2	0.037	8.34E+00
CMT2	PCE	93	1.38E+00	7	0.037	3.73E+01
CMT2	PCE	190	2.30E-01	7	0.037	6.22E+00
CMT2	TCE	0	8.92E-02	6	0.576	1.55E-01
CMT2	TCE	9	5.64E-02	2	0.576	9.79E-02
CMT2	TCE	31	4.10E-03	2	0.576	7.11E-03
CMT2	TCE	58	6.60E-03	2	0.576	1.15E-02
CMT2	TCE	93	3.08E-02	7	0.576	5.35E-02
CMT2	TCE	190	1.09E-02	7	0.576	1.90E-02
CMT2	VC	0	0.00E+00	6	1.28	0.00E+00
CMT2	VC	9	0.00E+00	2	1.28	0.00E+00
CMT2	VC	31	0.00E+00	2	1.28	0.00E+00
CMT2	VC	58	0.00E+00	2	1.28	0.00E+00
CMT2	VC	93	0.00E+00	7	1.28	0.00E+00
CMT2	VC	190	0.00E+00	7	1.28	0.00E+00
CMT3	Carbo-Iron	0	0.00E+00	1	0.1	0.00E+00
CMT3	Carbo-Iron	9	0.00E+00	1	0.1	0.00E+00
CMT3	Carbo-Iron	31	0.00E+00	1	0.1	0.00E+00
CMT3	Carbo-Iron	58	0.00E+00	1	0.1	0.00E+00
CMT3	Carbo-Iron	93	0.00E+00	1	0.1	0.00E+00
CMT3	Carbo-Iron	190	0.00E+00	1	0.1	0.00E+00
CMT3	DCEs	0	0.00E+00	2	0.045	0.00E+00
CMT3	DCEs	9	0.00E+00	1	0.045	0.00E+00
CMT3	DCEs	93	1.71E-02	7	0.045	3.79E-01
CMT3	DCEs	190	1.20E-01	7	0.045	2.67E+00
CMT3	Ethane+Ethene	0	0.00E+00	2	0.1	0.00E+00
CMT3	Ethane+Ethene	9	0.00E+00	1	0.1	0.00E+00
CMT3	Ethane+Ethene	93	3.27E-01	7	0.1	3.27E+00
CMT3	Ethane+Ethene	190	4.84E-01	7	0.1	4.84E+00
CMT3	PCE	0	7.91E-01	2	0.037	2.14E+01
CMT3	PCE	9	1.47E+00	1	0.037	3.98E+01
CMT3	PCE	93	1.75E+00	7	0.037	4.74E+01
CMT3	PCE	190	1.97E-01	7	0.037	5.32E+00
CMT3	TCE	0	1.75E-02	2	0.576	3.04E-02
CMT3	TCE	9	3.67E-02	1	0.576	6.37E-02
CMT3	TCE	93	6.91E-02	7	0.576	1.20E-01
CMT3	TCE	190	2.30E-02	7	0.576	3.99E-02

Table S 14: continued.

Well	Substance	Day	Concentration (mg/L)	n	PNEC (mg/L)	eRQ
CMT3	VC	0	0.00E+00	2	1.28	0.00E+00
CMT3	VC	9	0.00E+00	1	1.28	0.00E+00
CMT3	VC	93	0.00E+00	7	1.28	0.00E+00
CMT3	VC	190	0.00E+00	7	1.28	0.00E+00
RKS24	Carbo-Iron	0	0.00E+00	1	0.1	0.00E+00
RKS24	Carbo-Iron	9	0.00E+00	1	0.1	0.00E+00
RKS24	Carbo-Iron	31	0.00E+00	1	0.1	0.00E+00
RKS24	Carbo-Iron	58	0.00E+00	1	0.1	0.00E+00
RKS24	Carbo-Iron	93	0.00E+00	1	0.1	0.00E+00
RKS24	Carbo-Iron	190	0.00E+00	1	0.1	0.00E+00
RKS24	DCEs	0	0.00E+00	2	0.045	0.00E+00
RKS24	DCEs	9	0.00E+00	2	0.045	0.00E+00
RKS24	DCEs	31	0.00E+00	2	0.045	0.00E+00
RKS24	DCEs	58	0.00E+00	2	0.045	0.00E+00
RKS24	DCEs	93	0.00E+00	2	0.045	0.00E+00
RKS24	DCEs	190	0.00E+00	1	0.045	0.00E+00
RKS24	Ethane+Ethene	0	0.00E+00	2	0.1	0.00E+00
RKS24	Ethane+Ethene	9	0.00E+00	2	0.1	0.00E+00
RKS24	Ethane+Ethene	31	0.00E+00	2	0.1	0.00E+00
RKS24	Ethane+Ethene	58	0.00E+00	2	0.1	0.00E+00
RKS24	Ethane+Ethene	93	0.00E+00	2	0.1	0.00E+00
RKS24	Ethane+Ethene	190	0.00E+00	1	0.1	0.00E+00
RKS24	PCE	0	1.54E-01	2	0.037	4.15E+00
RKS24	PCE	9	3.00E-01	2	0.037	8.09E+00
RKS24	PCE	31	6.84E-02	2	0.037	1.85E+00
RKS24	PCE	58	1.52E-01	2	0.037	4.09E+00
RKS24	PCE	93	1.15E-01	2	0.037	3.11E+00
RKS24	PCE	190	6.92E-03	1	0.037	1.87E-01
RKS24	TCE	0	1.51E-03	2	0.576	2.63E-03
RKS24	TCE	9	5.38E-03	2	0.576	9.34E-03
RKS24	TCE	31	5.49E-04	2	0.576	9.53E-04
RKS24	TCE	58	1.70E-03	2	0.576	2.95E-03
RKS24	TCE	93	9.73E-04	2	0.576	1.69E-03
RKS24	TCE	190	3.87E-04	1	0.576	6.71E-04
RKS24	VC	0	0.00E+00	2	1.28	0.00E+00
RKS24	VC	9	0.00E+00	2	1.28	0.00E+00
RKS24	VC	31	0.00E+00	2	1.28	0.00E+00
RKS24	VC	58	0.00E+00	2	1.28	0.00E+00
RKS24	VC	93	0.00E+00	2	1.28	0.00E+00
RKS24	VC	190	0.00E+00	1	1.28	0.00E+00

Table S 14: continued.

Well	Substance	Day	Concentration (mg/L)	n	PNEC (mg/L)	eRQ
RKS34	Carbo-Iron	0	0.00E+00	1	0.1	0.00E+00
RKS34	Carbo-Iron	9	0.00E+00	1	0.1	0.00E+00
RKS34	Carbo-Iron	31	0.00E+00	1	0.1	0.00E+00
RKS34	Carbo-Iron	58	0.00E+00	1	0.1	0.00E+00
RKS34	Carbo-Iron	93	0.00E+00	1	0.1	0.00E+00
RKS34	Carbo-Iron	190	0.00E+00	1	0.1	0.00E+00
RKS34	DCEs	0	0.00E+00	1	0.045	0.00E+00
RKS34	DCEs	9	0.00E+00	2	0.045	0.00E+00
RKS34	DCEs	31	0.00E+00	1	0.045	0.00E+00
RKS34	DCEs	190	7.25E-04	1	0.045	1.61E-02
RKS34	Ethane+Ethene	0	0.00E+00	1	0.1	0.00E+00
RKS34	Ethane+Ethene	9	0.00E+00	2	0.1	0.00E+00
RKS34	Ethane+Ethene	31	0.00E+00	1	0.1	0.00E+00
RKS34	Ethane+Ethene	190	0.00E+00	1	0.1	0.00E+00
RKS34	PCE	0	1.19E+00	1	0.037	3.22E+01
RKS34	PCE	9	1.09E+00	2	0.037	2.93E+01
RKS34	PCE	31	3.40E-01	1	0.037	9.19E+00
RKS34	PCE	190	7.02E-01	1	0.037	1.90E+01
RKS34	TCE	0	1.50E-02	1	0.576	2.60E-02
RKS34	TCE	9	7.52E-03	2	0.576	1.30E-02
RKS34	TCE	31	3.01E-03	1	0.576	5.22E-03
RKS34	TCE	190	4.22E-03	1	0.576	7.32E-03
RKS34	VC	0	0.00E+00	1	1.28	0.00E+00
RKS34	VC	9	0.00E+00	2	1.28	0.00E+00
RKS34	VC	31	0.00E+00	1	1.28	0.00E+00
RKS34	VC	190	0.00E+00	1	1.28	0.00E+00
CMT1	Carbo-Iron	0	0.00E+00	1	0.1	0.00E+00
CMT1	Carbo-Iron	9	0.00E+00	1	0.1	0.00E+00
CMT1	Carbo-Iron	31	0.00E+00	1	0.1	0.00E+00
CMT1	Carbo-Iron	58	0.00E+00	1	0.1	0.00E+00
CMT1	Carbo-Iron	93	0.00E+00	1	0.1	0.00E+00
CMT1	Carbo-Iron	190	0.00E+00	1	0.1	0.00E+00
CMT1	DCEs	0	0.00E+00	3	0.045	0.00E+00
CMT1	DCEs	9	6.25E-04	2	0.045	1.39E-02
CMT1	DCEs	31	2.03E-03	2	0.045	4.50E-02
CMT1	DCEs	58	0.00E+00	2	0.045	0.00E+00
CMT1	DCEs	93	1.26E-02	7	0.045	2.81E-01
CMT1	DCEs	190	3.64E-02	7	0.045	8.10E-01

Table S 14: continued.

Well	Substance	Day	Concentration (mg/L)	n	PNEC (mg/L)	eRQ
CMT1	Ethane+Ethene	0	0.00E+00	3	0.1	0.00E+00
CMT1	Ethane+Ethene	9	0.00E+00	2	0.1	0.00E+00
CMT1	Ethane+Ethene	31	0.00E+00	2	0.1	0.00E+00
CMT1	Ethane+Ethene	58	0.00E+00	2	0.1	0.00E+00
CMT1	Ethane+Ethene	93	4.38E-02	7	0.1	4.38E-01
CMT1	Ethane+Ethene	190	1.32E-01	7	0.1	1.32E+00
CMT1	PCE	0	1.47E+00	3	0.037	3.98E+01
CMT1	PCE	9	1.10E-01	2	0.037	2.96E+00
CMT1	PCE	31	3.10E-01	2	0.037	8.38E+00
CMT1	PCE	58	2.45E-01	2	0.037	6.62E+00
CMT1	PCE	93	8.42E-01	7	0.037	2.28E+01
CMT1	PCE	190	3.82E-01	7	0.037	1.03E+01
CMT1	TCE	0	3.13E-02	3	0.576	5.44E-02
CMT1	TCE	9	3.97E-03	2	0.576	6.89E-03
CMT1	TCE	31	2.30E-03	2	0.576	3.99E-03
CMT1	TCE	58	1.10E-03	2	0.576	1.91E-03
CMT1	TCE	93	1.20E-02	7	0.576	2.08E-02
CMT1	TCE	190	1.49E-02	7	0.576	2.58E-02
CMT1	VC	0	0.00E+00	3	1.28	0.00E+00
CMT1	VC	9	0.00E+00	2	1.28	0.00E+00
CMT1	VC	31	0.00E+00	2	1.28	0.00E+00
CMT1	VC	58	0.00E+00	2	1.28	0.00E+00
CMT1	VC	93	0.00E+00	4	1.28	0.00E+00
CMT1	VC	190	0.00E+00	4	1.28	0.00E+00

Table S 15: Calculated values for toxic pressure (eTP) and risk indices (eRI) for the ecotoxicity component of the triad before the injection of Carbo-Iron into the aquifer (d0) and for the first 190 d after the injection.

Well	Contamination zone	eTP for the following days after Carbo-Iron injection						eRI for the following days after Carbo-Iron injection					
		0	9	31	58	93	190	0	9	31	58	93	190
GWM1	Ic	613.01	361.86	74.99	63.52	507.09	194.52	0.613	0.361	0.074	0.063	0.507	0.194
RKS13	I	899.82	611.95	220.39	272.86	1226.51	659.30	0.900	0.612	0.220	0.272	1.000	0.659
CMT2	II	78.56	63.87	15.34	11.57	223.03	125.19	0.078	0.063	0.014	0.011	0.222	0.124
CMT3	II	21.41	39.88	0.00	0.00	51.13	12.87	0.020	0.039	0.000	0.000	0.050	0.012
RKS24	III	4.15	8.10	1.85	4.10	3.11	0.19	0.003	0.007	0.001	0.003	0.002	0.000
RKS34	IV	32.19	29.34	9.20	0.00	0.00	18.99	0.031	0.028	0.008	0.000	0.000	0.018
CMT1	-	39.82	2.99	8.43	6.62	23.50	12.47	0.039	0.002	0.007	0.006	0.023	0.011

2.5.3 Physico-chemical component

Table S 16: Physico-chemical parameters total organic carbon (TOC) and redox potential measured in the sampling wells over 190 d after application of Carbo-Iron in the aquifer. Parameters were measured in various sampling depths described in section 2.2.1 in the main part of the manuscript and range from 6 m below ground level (rectangle) to 25 m (descending indicated by circle, triangle, +, x, and diamond).

Well	TOC (mg/L)	Redox potential (mV)
GWM1	<p>TOC (mg/L) vs Days after Carbo-Iron injection for GWM1. The y-axis ranges from 0 to 15. The x-axis ranges from 0 to 190. Data points are shown for days 0, 16, and 93. At day 0, TOC is approximately 3.5 mg/L. At day 16, it is approximately 2 mg/L. At day 93, it is approximately 15 mg/L.</p>	<p>Redox potential (mV) vs Days after Carbo-Iron injection for GWM1. The y-axis ranges from 0 to 800. The x-axis ranges from 0 to 190. Data points are shown for days 0, 2, 6, 9, 16, 23, 31, 58, 93, 140, and 190. The redox potential starts at approximately 250 mV at day 0, peaks at approximately 750 mV at day 58, and then fluctuates between 50 and 250 mV for the remainder of the period.</p>
RKS13	<p>TOC (mg/L) vs Days after Carbo-Iron injection for RKS13. The y-axis ranges from 0.0 to 1.5. The x-axis ranges from 0 to 190. Data points are shown for days 0, 16, and 93. At day 0, TOC is approximately 0.0 mg/L. At day 16, it is approximately 1.1 mg/L. At day 93, it is approximately 1.6 mg/L.</p>	<p>Redox potential (mV) vs Days after Carbo-Iron injection for RKS13. The y-axis ranges from 0 to 800. The x-axis ranges from 0 to 190. Data points are shown for days 0, 2, 6, 9, 16, 23, 31, 58, 93, 140, and 190. The redox potential starts at approximately 350 mV at day 0, peaks at approximately 750 mV at day 58, and then fluctuates between 50 and 350 mV for the remainder of the period.</p>
CMT2	<p>TOC (mg/L) vs Days after Carbo-Iron injection for CMT2. The y-axis ranges from 0 to 15. The x-axis ranges from 0 to 190. Data points are shown for days 0, 16, and 93. At day 0, TOC is approximately 15 mg/L (x), 8 mg/L (triangle), 4 mg/L (diamond), 3 mg/L (circle), and 2 mg/L (square). At day 16, it is approximately 2 mg/L (circle). At day 93, it is approximately 4 mg/L (x), 2 mg/L (diamond), and 1 mg/L (square).</p>	<p>Redox potential (mV) vs Days after Carbo-Iron injection for CMT2. The y-axis ranges from 0 to 500. The x-axis ranges from 0 to 190. Data points are shown for days 0, 2, 6, 9, 16, 23, 31, 58, 93, 140, and 190. The redox potential starts at approximately 50 mV at day 0, peaks at approximately 420 mV at day 140, and then drops to approximately 40 mV at day 190.</p>

Table S 16: continued.

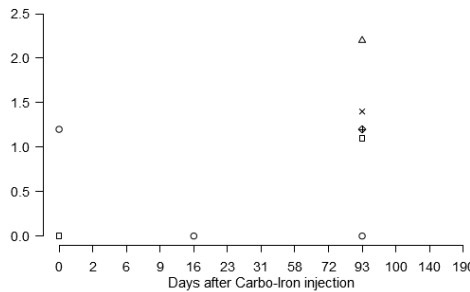
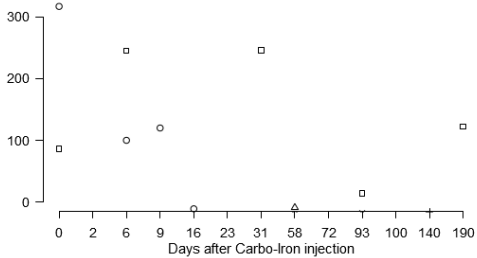
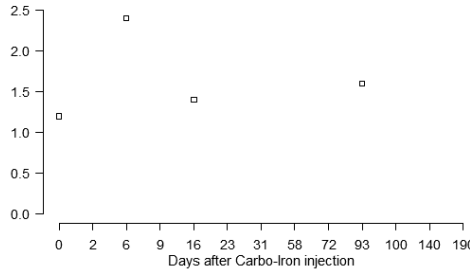
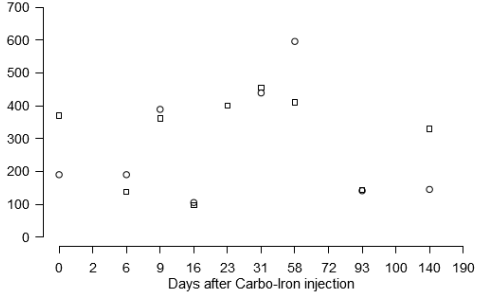
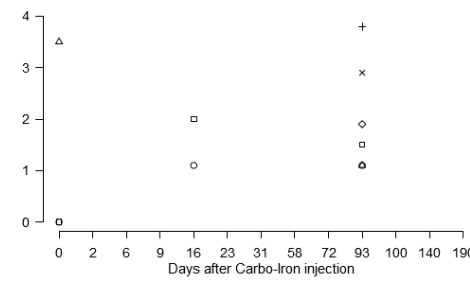
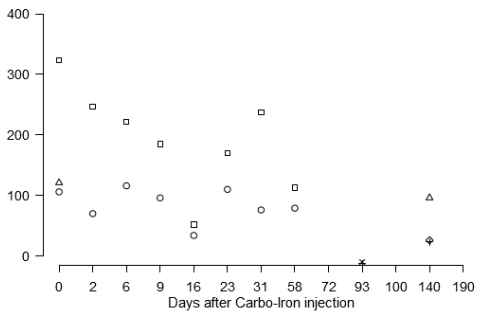
Well	TOC (mg/L)	Redox potential (mV)
CMT3		
RKS24		
RKS34	NA	NA
CMT1		

Table S 17: Physico-chemical parameters pH and iron (Fe) measured in the sampling wells over 190 d after application of Carbo-Iron in the aquifer. Parameters were measured in various sampling depths described in section 2.2.1 in the main part of the manuscript and range from 6 m below ground level (rectangle) to 25 m (descending indicated by circle, triangle, +, x, and diamond)

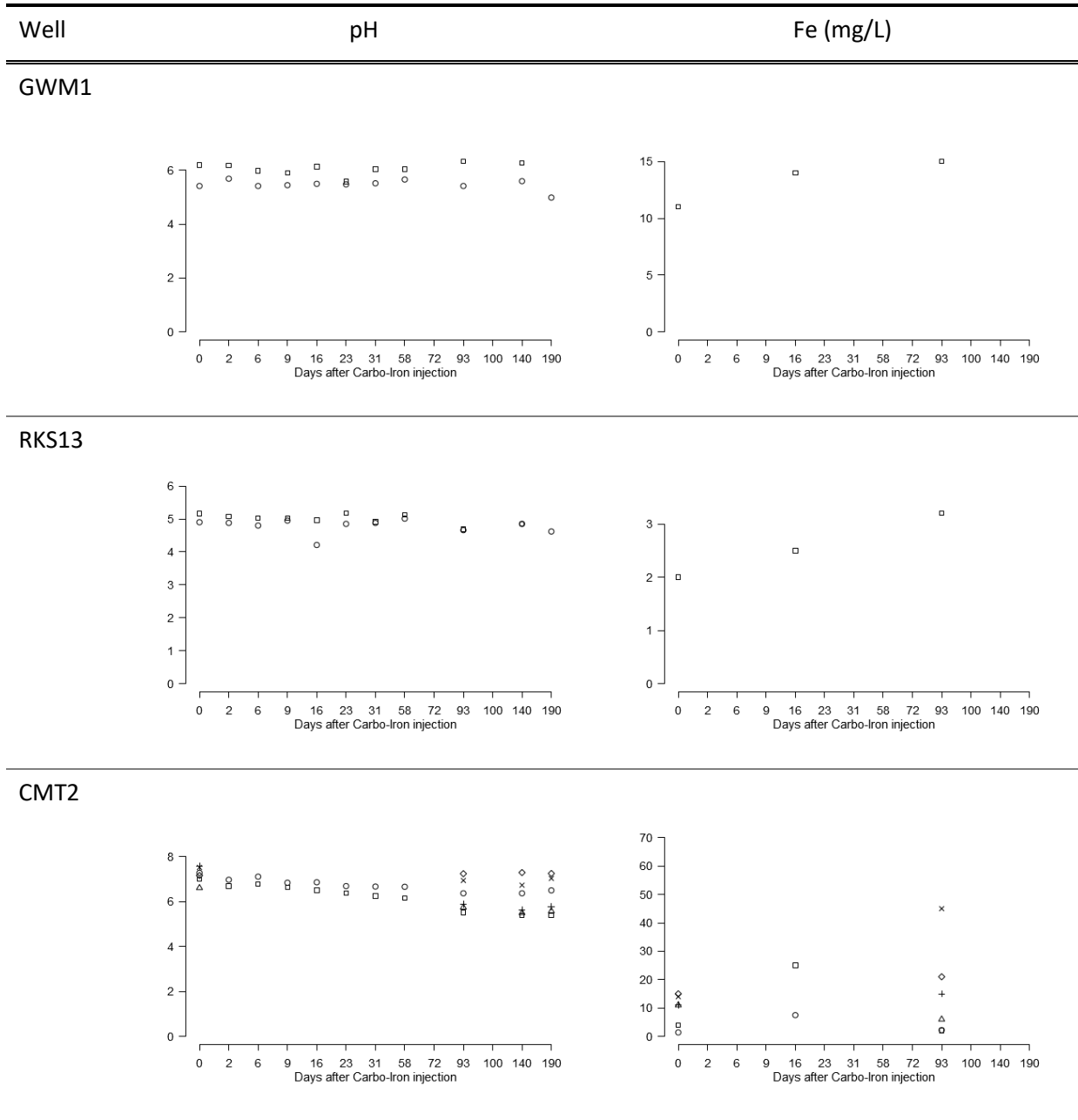


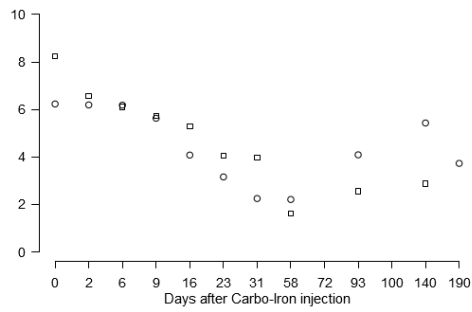
Table S 17: continued.

Well	pH	Fe (mg/L)
CMT3	<p>Scatter plot showing pH values for well CMT3 over 190 days. The y-axis ranges from 0 to 8. Data points are scattered between approximately 4.5 and 7.5.</p>	<p>Scatter plot showing Fe (mg/L) values for well CMT3 over 190 days. The y-axis ranges from 0 to 80. Most data points are below 20 mg/L, with a notable spike to approximately 80 mg/L at day 93.</p>
RKS24	<p>Scatter plot showing pH values for well RKS24 over 190 days. The y-axis ranges from 0 to 7. Data points are clustered between 4 and 6.</p>	<p>Scatter plot showing Fe (mg/L) values for well RKS24 over 190 days. The y-axis ranges from 0 to 15. Data points are mostly below 5 mg/L, with a peak of about 14 mg/L at day 16.</p>
RKS34	NA	NA
CMT1	<p>Scatter plot showing pH values for well CMT1 over 190 days. The y-axis ranges from 0 to 8. Data points are mostly between 5 and 7.</p>	<p>Scatter plot showing Fe (mg/L) values for well CMT1 over 190 days. The y-axis ranges from 0 to 40. Data points are scattered, with a peak of about 33 mg/L at day 16.</p>

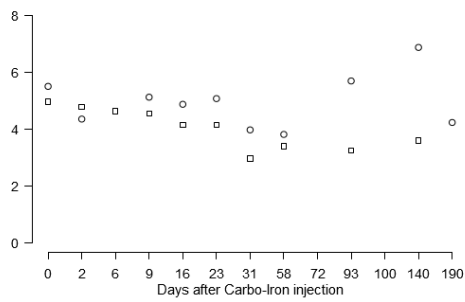
Table S 18: Physico-chemical parameter oxygen concentration measured in the sampling wells over 190 d after application of Carbo-Iron in the aquifer. Parameters were measured in various sampling depths described in section 2.2.1 in the main part of the manuscript and range from 6 m below ground level (rectangle) to 25 m (descending indicated by circle, triangle, +, x, and diamond)

Well	Oxygen (mg/L)
------	---------------

GWM1



RKS13



CMT2

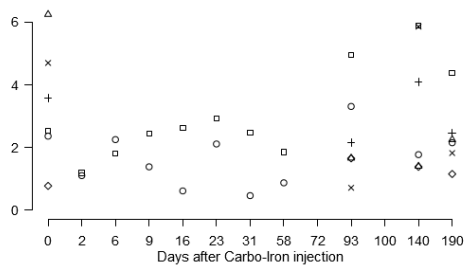
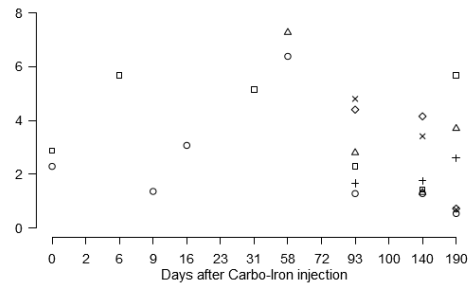


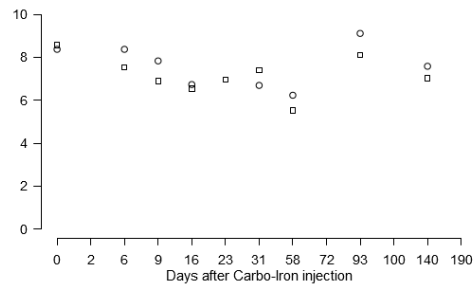
Table S 18: continued

Well	Oxygen (mg/L)
------	---------------

CMT3



RKS24



RKS34 NA

CMT1

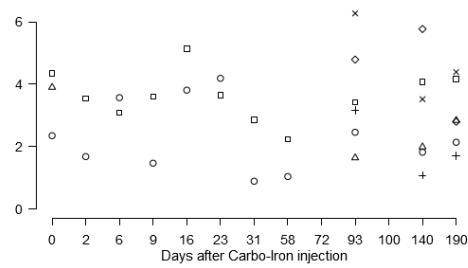


Table S 19: Values for selected physico-chemical parameters measured in groundwater samples. In all cases, samples from more at least two sampling depths were analysed ($n>1$). The risk index for each parameter (RI_{param}) was calculated as described in the main section of this manuscript.

Well	Parameter	Day	mean	min	max	n	RI_{param}
GWM1	conductivity ($\mu\text{S}/\text{cm}$)	0	552	276	827	2	2.21E-01
GWM1	conductivity ($\mu\text{S}/\text{cm}$)	9	335	297	373	2	1.34E-01
GWM1	conductivity ($\mu\text{S}/\text{cm}$)	31	621	523	718	2	2.48E-01
GWM1	conductivity ($\mu\text{S}/\text{cm}$)	58	298	292	304	2	1.19E-01
GWM1	conductivity ($\mu\text{S}/\text{cm}$)	93	263	249	277	2	1.05E-01
GWM1	conductivity ($\mu\text{S}/\text{cm}$)	190	242	242	242	1	9.68E-02
GWM1	pH	0	5.8	5.4	6.2	2	4.94E-01
GWM1	pH	9	5.7	5.5	5.9	2	5.39E-01
GWM1	pH	31	5.8	5.5	6.0	2	5.05E-01
GWM1	pH	58	5.9	5.7	6.0	2	4.80E-01
GWM1	pH	93	5.9	5.4	6.3	2	4.71E-01
GWM1	pH	190	5.0	5.0	5.0	1	7.16E-01
GWM1	Redox (mV)	0	268.5	267.0	270.0	2	0.00E+00
GWM1	Redox (mV)	9	216.0	175.0	257.0	2	0.00E+00
GWM1	Redox (mV)	31	-163.5	-268.0	-59.0	2	0.00E+00
GWM1	Redox (mV)	58	34.0	34.0	34.0	1	0.00E+00
GWM1	Redox (mV)	93	42.0	33.0	51.0	2	0.00E+00
GWM1	Redox (mV)	190	238.0	238.0	238.0	1	0.00E+00
RKS13	conductivity ($\mu\text{S}/\text{cm}$)	0	218	213	223	2	8.72E-02
RKS13	conductivity ($\mu\text{S}/\text{cm}$)	9	226	214	237	2	9.02E-02
RKS13	conductivity ($\mu\text{S}/\text{cm}$)	31	236	224	248	2	9.44E-02
RKS13	conductivity ($\mu\text{S}/\text{cm}$)	58	210	207	212	2	8.38E-02
RKS13	conductivity ($\mu\text{S}/\text{cm}$)	93	233	210	255	2	9.30E-02
RKS13	conductivity ($\mu\text{S}/\text{cm}$)	190	215	215	215	1	8.60E-02
RKS13	pH	0	5.0	4.9	5.2	2	7.08E-01
RKS13	pH	9	5.0	5.0	5.0	2	7.17E-01
RKS13	pH	31	4.9	4.9	4.9	2	7.34E-01
RKS13	pH	58	5.1	5.0	5.1	2	7.01E-01
RKS13	pH	93	4.7	4.7	4.7	2	7.72E-01
RKS13	pH	190	4.6	4.6	4.6	1	7.81E-01
RKS13	Redox (mV)	0	347.5	334.0	361.0	2	0.00E+00
RKS13	Redox (mV)	9	372.5	371.0	374.0	2	0.00E+00
RKS13	Redox (mV)	31	354.5	269.0	440.0	2	0.00E+00
RKS13	Redox (mV)	58	123.0	123.0	123.0	1	0.00E+00
RKS13	Redox (mV)	93	51.0	50.0	52.0	2	0.00E+00
RKS13	Redox (mV)	190	310.0	310.0	310.0	1	0.00E+00

Table S 19: continued.

Well	Parameter	Day	mean	min	max	n	RI _{param}
CMT2	conductivity (μS/cm)	0	584	342	860	6	2.22E-01
CMT2	conductivity (μS/cm)	9	447	423	471	2	1.79E-01
CMT2	conductivity (μS/cm)	31	434	361	507	2	1.74E-01
CMT2	conductivity (μS/cm)	58	383	313	453	2	1.53E-01
CMT2	conductivity (μS/cm)	93	408	219	719	7	1.39E-01
CMT2	conductivity (μS/cm)	190	394	190	762	7	1.43E-01
CMT2	pH	0	7.2	6.6	7.6	6	9.94E-02
CMT2	pH	9	6.7	6.6	6.8	2	1.67E-01
CMT2	pH	31	6.5	6.2	6.7	2	2.07E-01
CMT2	pH	58	6.4	6.2	6.7	2	2.34E-01
CMT2	pH	93	6.4	5.5	7.4	7	2.17E-01
CMT2	pH	190	6.4	5.4	7.4	7	2.28E-01
CMT2	Redox (mV)	0	9.0	-54.0	67.0	5	0.00E+00
CMT2	Redox (mV)	9	8.0	8.0	8.0	1	0.00E+00
CMT2	Redox (mV)	31	183.5	91.0	276.0	2	0.00E+00
CMT2	Redox (mV)	58	4.0	-63.0	48.0	3	0.00E+00
CMT2	Redox (mV)	93	-63.8	-189.0	55.0	6	0.00E+00
CMT2	Redox (mV)	190	-227.7	-305.0	-116.0	6	5.00E-01
CMT3	conductivity (μS/cm)	0	305	246	363	2	1.22E-01
CMT3	conductivity (μS/cm)	9	391	391	391	1	1.56E-01
CMT3	conductivity (μS/cm)	31	395	395	395	1	1.58E-01
CMT3	conductivity (μS/cm)	58	385	380	389	2	1.54E-01
CMT3	conductivity (μS/cm)	93	469	229	722	7	1.72E-01
CMT3	conductivity (μS/cm)	190	543	352	716	7	2.35E-01
CMT3	pH	0	6.3	5.2	7.4	2	2.89E-01
CMT3	pH	9	6.9	6.9	6.9	1	1.46E-01
CMT3	pH	31	6.4	6.4	6.4	1	2.29E-01
CMT3	pH	58	7.0	6.9	7.1	2	1.27E-01
CMT3	pH	93	6.8	6.0	7.8	7	1.50E-01
CMT3	pH	190	6.7	5.9	7.6	7	1.70E-01
CMT3	Redox (mV)	0	86.0	86.0	86.0	1	0.00E+00
CMT3	Redox (mV)	9	120.0	120.0	120.0	1	0.00E+00
CMT3	Redox (mV)	31	246.0	246.0	246.0	1	0.00E+00
CMT3	Redox (mV)	58	-14.5	-20.0	-9.0	2	0.00E+00
CMT3	Redox (mV)	93	-43.9	-83.0	14.0	7	0.00E+00
CMT3	Redox (mV)	190	-178.2	-295.0	-67.0	6	0.00E+00
RKS24	conductivity (μS/cm)	0	218	208	228	2	8.72E-02
RKS24	conductivity (μS/cm)	9	229	216	242	2	9.16E-02
RKS24	conductivity (μS/cm)	31	213	188	238	2	8.52E-02
RKS24	conductivity (μS/cm)	58	216	194	238	2	8.64E-02
RKS24	conductivity (μS/cm)	93	286	264	308	2	1.14E-01

Table S 19: continued.

Well	Parameter	Day	mean	min	max	n	Rl _{param}
RKS24	pH	0	4.9	4.8	5.0	2	7.40E-01
RKS24	pH	9	4.9	4.9	5.0	2	7.26E-01
RKS24	pH	31	5.0	4.9	5.1	2	7.21E-01
RKS24	pH	58	5.0	5.0	5.0	2	7.17E-01
RKS24	pH	93	4.8	4.6	5.0	2	7.52E-01
RKS24	Redox (mV)	0	190.0	190.0	190.0	1	0.00E+00
RKS24	Redox (mV)	9	375.0	361.0	389.0	2	0.00E+00
RKS24	Redox (mV)	31	447.0	439.0	455.0	2	5.00E-01
RKS24	Redox (mV)	93	142.0	141.0	143.0	2	0.00E+00
CMT1	conductivity (μS/cm)	0	228	157	270	3	1.03E-01
CMT1	conductivity (μS/cm)	9	204	151	256	2	8.14E-02
CMT1	conductivity (μS/cm)	31	204	145	262	2	8.14E-02
CMT1	conductivity (μS/cm)	58	205	150	260	2	8.20E-02
CMT1	conductivity (μS/cm)	93	277	134	374	7	1.04E-01
CMT1	conductivity (μS/cm)	190	325	136	692	7	1.04E-01
CMT1	pH	0	6.1	5.7	6.4	3	3.77E-01
CMT1	pH	9	6.1	6.1	6.2	2	3.78E-01
CMT1	pH	31	6.0	6.0	6.0	2	4.38E-01
CMT1	pH	58	6.0	5.9	6.1	2	4.40E-01
CMT1	pH	93	5.8	5.2	7.0	7	4.99E-01
CMT1	pH	190	6.1	5.1	7.0	7	3.99E-01
CMT1	Redox (mV)	0	113.5	106.0	121.0	2	0.00E+00
CMT1	Redox (mV)	9	140.5	96.0	185.0	2	0.00E+00
CMT1	Redox (mV)	31	156.5	76.0	237.0	2	0.00E+00
CMT1	Redox (mV)	58	96.0	79.0	113.0	2	0.00E+00
CMT1	Redox (mV)	93	-61.7	-156.0	-10.0	7	0.00E+00
CMT1	Redox (mV)	190	-152.0	-260.0	-88.0	7	0.00E+00

Table S 20: Calculated risk indices (pRI) for the physico-chemical component of the triad before the injection of Carbo-Iron into the aquifer (d0) and for the first 190 d after the injection.

Well	Contamination zone	pRI for the following days after Carbo-Iron injection					
		0	9	31	58	93	190
CMT1	-	0.16	0.15	0.17	0.17	0.20	0.17
GWM1	Ic	0.24	0.22	0.25	0.37	0.19	0.27
RKS13	I	0.27	0.27	0.28	0.43	0.29	0.29
CMT2	II	0.13	0.13	0.13	0.13	0.12	0.29
CMT3	II	0.13	0.12	0.13	0.12	0.13	0.16
RKS24	III	0.28	0.27	0.46	0.60	0.28	NA
RKS34	IV	NA	NA	NA	NA	NA	NA

References

- Batka, V.M., Hofmann, T., 2016. Stability, mobility, delivery and fate of optimized nps under field relevant conditions. Deliverable 4.2 of Project Nr.: 309517 EU, 7th FP, NMP.2012.1.2 „Taking nanotechnological remediation processes from lab scale to end user applications for the restoration of a clean environment“.
- Elenndt, B.-P., Bias, W.-R., 1990. Trace nutrient deficiency in *Daphnia magna* cultured in standard medium for toxicity testing. Effects of the optimization of culture conditions on life history parameters of *D. magna*. *Water Research* 24, 1157–1167. DOI: 10.1016/0043-1354(90)90180-E
- Elimelech, M., Gregory, J., Jia, X., 2013. Particle Deposition and Aggregation: Measurement, Modelling and Simulation. Butterworth-Heinemann.
- EU, 2004. Risk Assessment Report Trichloroethylene. United Kingdom.
- Hjorth, R., Coutris, C., Nguyen, N.H.A., Sevcu, A., Gallego-Urrea, J.A., Baun, A., Joner, E.J., 2017. Ecotoxicity testing and environmental risk assessment of iron nanomaterials for sub-surface remediation – Recommendations from the FP7 project NanoRem. *Chemosphere* 182, 525–531. DOI: 10.1016/j.chemosphere.2017.05.060
- Houde, M., Douville, M., Gagnon, P., Sproull, J., Cloutier, F., 2015. Exposure of *Daphnia magna* to trichloroethylene (TCE) and vinyl chloride (VC): Evaluation of gene transcription, cellular activity, and life-history parameters. *Ecotoxicology and Environmental Safety* 116, 10–18. DOI: 10.1016/j.ecoenv.2015.02.031
- Laumann, S., Micić, V., Lowry, G.V., Hofmann, T., 2013. Carbonate minerals in porous media decrease mobility of polyacrylic acid modified zero-valent iron nanoparticles used for groundwater remediation. *Environmental Pollution* 179, 53–60. DOI: 10.1016/j.envpol.2013.04.004
- Nam, S.-H., An, Y.-J., 2010. Assessing the ecotoxicity of vinyl chloride using green alga *P. subcapitata*, nematode *C. elegans*, and the SOS chromotest in a closed system without headspace. *Science of The Total Environment* 408, 3148–3152. DOI: 10.1016/j.scitotenv.2010.03.022
- OECD, 2012. OECD guideline for testing of chemicals. 211. *Daphnia magna* reproduction test. Organisation for Economic Co-operation and Development, Paris, France.
- OECD, 2004a. OECD guideline for testing of chemicals. 202. *Daphnia* sp., acute immobilisation test. Organisation for Economic Co-operation and Development, Paris, France.
- OECD, 2004b. OECD guideline for testing of chemicals. 219. Sediment-water chironomid toxicity test using spiked water. Organisation for Economic Co-operation and Development, Paris, France.
- OECD, 2000. OECD guideline for testing of chemicals. 216. Soil microorganisms: nitrogen transformation test. Organisation for Economic Co-operation and Development, Paris, France.
- US EPA, 2002. 821/R-02/012 Methods for Measuring the Acute Toxicity of Effluents and Receiving Waters to Freshwater and Marine Organisms. Washington, D.C., USA.
- Weil, M., Meißner, T., Busch, W., Springer, A., Kühnel, D., Schulz, R., Duis, K., 2015. The oxidized state of the nanocomposite Carbo-Iron® causes no adverse effects on growth, survival and differential gene

expression in zebrafish. *Science of The Total Environment* 530–531, 198–208. DOI: 10.1016/j.scitotenv.2015.05.087

Weil, M., Meißner, T., Springer, A., Bundschuh, M., Hübler, L., Schulz, R., Duis, K., 2016. Oxidized Carbo-Iron causes reduced reproduction and lower tolerance of juveniles in the amphipod *Hyalella azteca*. *Aquatic Toxicology* 181, 94–103. DOI: 10.1016/j.aquatox.2016.10.028

Curriculum vitae

Name: **Mirco Weil**
Geboren: 29. Januar 1980 in Gießen
Staatsangehörigkeit: deutsch

Ausbildung

1996 – 1999 Werner-von-Siemens-Schule Wetzlar. Abschluss: allgemeine Hochschulreife
2000 – 2005: Studium der Umwelthygienetechnik an der Fachhochschule Gießen
2005 – 2006: Diplomarbeit bei der ECT Oekotoxikologie GmbH:
"Untersuchung der schadstoffinduzierten differentiellen Expression ausgewählter Markergene in Zebrafischembryonen zur Entwicklung einer Alternative zu verlängerten und chronischen Fischtests"
seit Dez. 2010 Promotionsstudent an der Universität Landau, Institut für Umweltwissenschaften, Thema: "Assessment of the environmental risk and risk-benefit analysis of the nFe⁰-based groundwater remedial agent Carbo-Iron"

Berufspraxis

seit Juni 2006: Mitarbeiter der ECT Oekotoxikologie GmbH im Bereich aquatische Ökotoxikologie
Arbeitsschwerpunkte:

- Projektleiter in verschiedenen Forschungsprojekten
- Verantwortlicher für die Fischhaltung
- Toxizitäts- und Genexpressionsuntersuchungen an Fischembryonen
- Toxizitätstests mit Fischen und aquatischen Invertebraten

Berufliche Mitgliedschaften

seit Februar 2010 *Society of Environmental Toxicology and Chemistry (SETAC)*
2012 - 2015 *Student Advisory Council (SAC) der SETAC Europe*

List of publications

Peer-reviewed publications

- 2019** Weil, M., Falkenhain, A., Scheurer, M., Ryan, J., Coors, A. (2019). Uptake and effects of the beta-adrenergic agonist salbutamol in fish: supporting evidence for the fish plasma model". *Environmental Toxicology and Chemistry*. DOI: 10.1002/etc.4543
- Weil, M., Mackenzie, K., Foit, K., Kühnel, D., Busch, W., Bundschuh, M., Schulz, R., Duis, K. (2019). Environmental risk or benefit? Comprehensive risk assessment of groundwater treated with nano Fe⁰-based Carbo-Iron®. *Science of the Total Environment*. DOI: 10.1016/j.scitotenv.2019.04.360.
- 2017** Baudy, P., Zubrod, J.P., Kanschak, M., Weil, M., Schulz, R., Bundschuh, M. (2017). Does long-term fungicide exposure affect the reproductive performance of leaf-shredders? A partial life-cycle study using *Hyalella azteca*. *Environmental Pollution* 222, 458–464. DOI: 10.1016/j.envpol.2016.11.079.
- 2016** Weil, M., Meißner, T., Springer, A., Bundschuh, M., Hübler, L., Schulz, R., Duis, K. (2016). Oxidized Carbo-Iron causes reduced reproduction and lower tolerance of juveniles in the amphipod *Hyalella azteca*. *Aquatic Toxicology* 181, 94–103. DOI: 10.1016/j.aquatox.2016.10.028.
- 2015** Potthoff, A., Weil, M., Meißner, T., Kühnel, D. (2015). Towards sensible toxicity testing for nanomaterials: proposal for the specification of test design. *Science and Technology of Advanced Materials* 16, 065006. DOI: 10.1088/1468-6996/16/6/065006
- Weil, M., Meißner, T., Busch, W., Springer, A., Kühnel, D., Schulz, R., Duis, K. (2015). The oxidized state of the nanocomposite Carbo-Iron® causes no adverse effects on growth, survival and differential gene expression in zebrafish. *Science of The Total Environment* 530–531, 198–208. DOI: 10.1016/j.scitotenv.2015.05.087.
- 2013** Margot, J., Kienle, C., Magnet, A., Weil, M., Rossi, L., de Alencastro, L.F., Abegglen, C., Thonney, D., Chèvre, N., Schärer, M., Barry, D.A. (2013). Treatment of micropollutants in municipal wastewater: Ozone or powdered activated carbon? *Science of The Total Environment* 461–462, 480–498. DOI: 10.1016/j.scitotenv.2013.05.034
- 2010** Stalter, D., Magedeburg, A., Weil, M., Knacker, T., und Oehlmann, J. (2010). Toxication or detoxication? In vivo toxicity assessment of ozonation as advanced wastewater treatment with the rainbow trout. *Water Research* 44, 439-448. DOI: 10.1016/j.watres.2009.07.025
- 2009** Weil, M., Scholz, S., Zimmer, M., Sacher, F., und Duis, K. (2009). Gene expression analysis in zebrafish embryos: a potential approach to predict effect concentrations in the fish early life stage test. *Environmental Toxicology and Chemistry* 28, 1970-1978. DOI: 10.1897/08-627.1
-

Non-scientific articles

Zubrod, J., Jevtić, D., Melato, A., Agatz, A., Englert, D., Floehr, T., Knežević, V., Weil, M., Brinkmann, M. (2012). News from the SETAC Europe Student Advisory Council - September 2012. *Environmental Sciences Europe* 24, 27. DOI: 10.1186/2190-4715-24-27.

Zubrod, J., Jevtić, D., Melato, A., Englert, D., Weil, M., Brockmeier, E.K., Floehr, T., Knežević, V., A., Agatz, Brinkmann, M. (2013). News from the SETAC Europe Student Advisory Council - The 3rd Young Environmental Scientists (YES) Meeting at the Jagiellonian University, Poland. *Environmental Sciences Europe* 25, 16. DOI: 10.1186/2190-4715-25-16

Selected conference contributions

Coors, A., Weil, M., Falkenhain, A., Scheurer, M., Ryan, J. (2019). Effects and concentrations of the β 2-adrenergic agonists salbutamol in fish – do they confirm with the fish plasma model? SETAC Europe 29th Annual Meeting, Helsinki, Finland.

Weil, M., Coors, A. (2018). Preliminary results: Salbutamol in Fish-blood Plasma Concentrations and Effects. 5th iPiE Forum Meeting, Barcelona, Spain.

Baudy, P., Zubrod, J., Konschak, M., Weil, M., Schulz, R., Bundschuh, M. (2017). Chronic exposure towards field-relevant fungicide concentrations impairs reproduction in the amphipod leaf-shredder *Hyalella azteca*. SETAC Europe 27th Annual Meeting, Brussels, Belgium.

Simon, M., Schlechtriem, C., Egeler, P., Weil, M., Römbke, J., Karaoglan, B., Wiemann, A., Drost, W. (2017). PBT assessment of substances – Proposal of a trigger value for bioaccumulation in terrestrial oligochaetes. SETAC Europe 27th Annual Meeting, Brussels, Belgium.

Weil, M., Meißner, T., Springer, A., Duis, K. (2014). Increased sensitivity of second generation *Hyalella azteca* to the nanocomposite Carbo-Iron. SETAC Europe 24th Annual Meeting, Basel, Switzerland.

Weil, M., Meißner, T., Springer, A., Busch, W., Kühnel, D., Duis, K. (2014). The nanocomposite Carbo-Iron[®] shows no adverse effects on growth, survival and gene expression in zebrafish. Nanoparticles in soils and water: fate, transport and effects. Landau, Germany.

Weil, M., Meissner, T., Potthoff, A., Kühnel, D. (2014). Harmonisation of toxicity testing for nanomaterials: Proposal for decision trees. Nanosymposium, Antalya, Turkey.

Kühnel, D., Weil, M., Duis, K., Busch, W., Meißner, T., Springer, A., Scholz, S., Schmitt-Jansen, M., Mackenzie, K. (2014). Extensive ecotoxicological assessment of the nanocomposite Carbo-Iron[®] applied for groundwater remediation. Nanosymposium, Antalya, Turkey.

Meißner, T., Kühnel, D., Weil, D., Potthoff, A. (2014). Characterization of nanostructured materials for toxicological investigations demonstrated on the nanocomposite Carbo-Iron[®]. Nanosymposium, Antalya, Turkey.

Weil, M., Meissner, T., Kühnel, D., Duis, K. (2013). Erste Schritte zu einer einheitlichen ökotoxikologischen Bewertung von Fe-basierten Nanopartikeln und Nanokompositen. 17. SETAC-GLB Jahrestagung, Essen, Germany.

- Walter, M., Weil, M., Meißner, T., Springer, A., Duis, K. (2013). Acute and chronic effects of magnetite-based nanocomposites on invertebrates (*Hyalella azteca* and *Chironomus riparius*) and zebrafish embryos (*Danio rerio*). 3rd SETAC Young Environmental Scientists Meeting, Krakow, Poland.
- Weil, M., Meissner, T., Kühnel, D. (2013). Erste Schritte zur ökotoxikologischen Bewertung von Eisen-basierten Nanopartikeln und Nanokompositen. 3. Clustertreffen NanoCare/NanoNature, Frankfurt/Main, Germany.
- Weil, M., Walter, M., Duis, K. (2013). Toxizität, Aufnahme und Elimination des Nanokomposits Carbo-Iron® im Zebrabärbling und im Krebs *Hyalella azteca*. 3. Clustertreffen NanoCare/NanoNature, Frankfurt/Main, Germany.
- Weil, M., Kühnel, D., Meißner, T. (2012). NanoNature Workshop - Ökotoxikologische Untersuchung von Nanomaterialien. Jahrestagung der SETAC Gb und der GDCh, Leipzig, Germany.
- Weil, M., Busch, W., Kühnel, D., Meißner, T., Springer, A., Duis, K. (2012). Toxizität des Nanokomposits Carbo-Iron® auf den Zebrabärbling (*Danio rerio*). Poster, Jahrestagung der SETAC Gb und der GDCh, Leipzig, Germany.
- Weil, M., Hübler, L., Meißner, Potthoff, A., T., Springer, A., Gelinsky, M., Duis, K. (2012). Toxicity of the nanocomposite Carbo-Iron to *Danio rerio* and *Hyalella azteca*. 6th SETAC World Congress, Berlin, Germany.
- Weil, M., Duis, K., Potthoff, A., Gelinsky, M., Springer, A., Mackenzie, K., Scholz, S. (2011). Ecotoxicity of Carbo-Iron, a novel iron based nanocomposite, to aquatic organisms. 6th International Conference on the Environmental Effects of Nanoparticles and Nanomaterials, London, UK.
- Weil, M., Vorberg, L., Seltmann, K., Rooch, J., Kluever, N., Scholz, S., Yang, L., Legradi, J., Straehle, U., Sacher, F., Duis, K. (2011). Further development of a gene expression fish embryo test as a potential alternative to the fish early life stage test. 21st SETAC Europe Meeting., Milan, Italy.
- Weil, M., Duis, K., Potthoff, A., Gelinsky, M., Springer, A., Mackenzie, K., Scholz, S. (2010). Fe-NANOSIT - Ökotoxikologische Bewertung von Fe-basierten reaktiven Nanopartikeln und -kompositstrukturen: Akute und chronische Wirkungstests mit Organismen unterschiedlicher trophischer Ebenen. 4. Jahrestagung der GDCh und SETAC GLB, Dessau, Germany.
- Weil, M., Abegglen, C., Kienle, C., Thonney, D., Magnet, A., Schärer, M. (2010). Projekt MicroPoll – Überprüfung erweiterter Methoden zur Abwasserreinigung. 4 Jahrestagung der GDCh und SETAC GLB, Dessau, Germany.
- Weil, M., Duis, K., Sacher, F. and Scholz, S. (2006). Erfassung der differentiellen Genexpression in Zebrabärblingsembryonen: eine Alternative zu fish early life stage-Tests? 11th SETAC GLB Meeting, Landau (Pfalz), Germany.
- Weil, M., Duis, K., Sacher, F. and Scholz, S. (2005). Eignet sich die differentielle Genexpression in Zebrabärblingsembryonen zur Vorhersage verlängerter/chronischer Fischtoxizität? Erste Ergebnisse. 10th SETAC GLB Meeting September, Basel, Switzerland